The pathological role of synphilin-1 and the therapeutic potential of Hsp70 in models of Parkinson's disease using viral vectors

der Fakultät für Biologie
der EBERHARD KARLS UNIVERSITÄT TÜBINGEN

zur Erlangung des Grades eines Doktors
der Naturwissenschaften

von

Antje Krenz, geb. Elstner
aus Heilbad Heilgenstadt

vorgelegte

Dissertation

2010

Tag der mündlichen Prüfung:	04.12.2009
Dekan:	Prof. Dr. H.A. Mallot
1. Berichterstatter:	Prof. Dr. J.B. Schulz
2. Berichterstatter:	Prof. Dr. O. Rieß
3. Berichterstatterin:	Prof. Dr. C. Klein

Dedicated to my Husband

This study was conducted from January 2004 to December 2005 at the Hertie-Institute for Clinical Brain Research inTübingen and from January 2006 to December 2007 at the Department of Neurodegeneration and Restorative Research in Göttingen under supervision of Prof. Dr. J.B. Schulz and Dr. B.H. Falkenburger.

“A question that sometimes drives me hazy: am I or are the others crazy?”

Albert Einstein

CONTENTS

CONTENTS 6

ABBREVIATIONS 10

1. INTRODUCTION 12

1.1. Parkinson's disease 12
1.1.1. History 12
1.1.2. Clinical Picture 12
1.1.3. Prevalence and incidence 13
1.1.4. Diagnosis of PD 13
1.1.5. Pathological changes in PD 14

1.2. Pathogenesis of PD 15
1.2.1. Oxidative stress and mitochondrial dysfunction 16
1.2.2. Protein aggregation and impairment of the ubiquitin-proteasome system 18
1.2.3. Cell death mechanisms 19

1.3. PD genetics 20
1.3.1. α-synuclein 21
1.3.2. Synphilin-1 22

1.4. Therapeutic strategies 25
1.4.1. Pharmacotherapy 25
1.4.2. Surgical therapies 25

1.5. Experimental therapies 26
1.5.1. Neuroprotective therapies 26
1.5.2. Molecular chaperones 27
1.5.2.1. Heat shock proteins 29
1.5.3. Viral vector-mediated gene transfer 36
1.5.3.1. Adenoviral vectors (AdV) 37
1.5.3.2. Adeno-associated viral vectors (AAV) 39
1.5.3.3. Lentivirus (LV) 40

1.6. PD models 42
1.6.1. Cellular models of PD 42
1.6.2. Animal models of PD 43
1.6.2.1. Toxin-induced models 43
1.6.2.2. Genetically modified models 45

1.7. Objectives 47

2. METHODS 48

2.1. Molecular biology 48
2.1.1. Propagation and preparation of plasmid DNA 48
2.1.1.1. Bacteria culture conditions 48
2.1.1.2. Heat shock transformation 48
2.1.1.3. Plasmid mini preparation 49
2.1.1.4. Plasmid Midi, Maxi and Mega preparations 49
2.1.2. Isolation of genomic DNA from mouse tail biopsies 50
2.1.3. DNA precipitation 50
2.1.4. PCR 51
2.1.5. DNA restriction, electrophoresis, gel extraction 52

2.1.6. Cycle sequencing of PCR-amplified DNA ... 52
2.1.7. Quantitative real-time PCR (qPCR) ... 53
2.1.8. Plasmid construction ... 55
2.1.8.1. Cloning into pLV-plasmid ... 55
2.1.8.2. Cloning into pAAV-plasmid ... 56

2.2. Cell culture ... 57
2.2.1. Culture conditions, transient transfection ... 57
2.2.2. Viral Infection ... 58

2.3. Cell death assays ... 58
2.3.1. LDH release assay ... 58
2.3.2. Trypan blue exclusion assay ... 58
2.3.3. Caspase-3 activity (DEVD-cleavage assay) ... 59

2.4. Proteinbiochemie ... 59
2.4.1. Protein extraction ... 59
2.4.1.1. Preparation of cell culture lysates ... 59
2.4.1.2. Preparation of striatal brain tissue lysates ... 60
2.4.1.3. Determination of protein concentration ... 60
2.4.2. Western blot analysis ... 60
2.4.2.1. SDS-PAGE ... 60
2.4.2.2. Immuno blot ... 61

2.5. Viral vector preparation ... 62
2.5.1. Adenovirus production ... 62
2.5.2. Lentivirus production ... 62
2.5.3. Adeno-associated virus production ... 63

2.6. Animal work ... 64
2.6.1. Housing, strains and genotyping ... 64
2.6.1.1. Animal housing and strains ... 64
2.6.1.2. Genotyping ... 64
2.6.2. Surgery ... 65
2.6.2.1. Stereotaxical injections ... 65
2.6.2.2. Continuous minipump infusion of MPTP ... 65
2.6.3. Tissue preparation and processing ... 66
2.6.3.1. Paraffin sections ... 66
2.6.3.2. Cryosections ... 66
2.6.4. Behavior ... 66
2.6.5. Histology ... 67
2.6.5.1. General histology ... 67
2.6.5.2. Immunohistochemistry and immunocytochemistry ... 67
2.6.5.3. PK-digested paraffin-embedded tissue blot ... 69

2.7. Microscopy ... 69

2.8. Quantifications ... 70
2.8.1. Manual counting ... 70
2.8.2. Particle analysis ... 70
2.8.3. Stereology ... 70
2.8.4. Optical density ... 71

2.9. Statistics ... 71

2.10. Materials ... 71
2.10.1. Equipment ... 71
2.10.2. Chemicals and Biochemicals ... 73
2.10.3. Media, supplements and buffers for cell culture ... 75
2.10.4. Enzymes ... 75
2.10.5. Pharmaca and Narcotics ... 75

2.10.6. Kits 76
2.10.7. Antibodies 76
2.10.8. Cell lines 77

3. RESULTS 78

3.1. The (Thy1)-h[A30P]αSyn transgenic mouse model 78

3.2. Aggregate formation and toxicity by wild-type and R621C synphilin-1 via adenoviral gene transfer 80
3.2.1. Targeted transduction of the nigrostriatal system by stereotaxic AdV injection 81
3.2.2. Synphilin-1 induced aggregate formation 84
3.2.3. Synphilin-1 induced toxicity 87

3.3. No impairment of the ubiquitin proteasom system in A30PαSyn mice 88

3.4. Therapeutic approaches using the molecular chaperone HSP70 90
3.4.1. Hsp70 in cellular models of PD 90
3.4.1.1. Hsp70 inhibits MPP^+-induced toxicity in neuroblastoma cells 90
3.4.1.2. Hsp70 reduces α-synuclein–induced toxicity and aggregate load 94
3.4.2. Hsp70 in mouse models for PD 97
3.4.2.1. Lentiviral vector-mediated genetransfer to mouse models of PD 97
3.4.2.2. Lentiviral Hsp70 expression in the chronic MPTP mouse model 102
3.4.2.3. Lentiviral Hsp70 expression in the A30PαSyn transgenic mouse model 104
3.4.2.4. Evaluation of AAV-mediated gene transfer to improve overexpression of Hsp70 in A30PαSyn transgenic mice 107

4. DISCUSSION 110

4.1. Synphilin-1 induced aggregate formation and toxicity 110
4.1.1. Effects of AdV-EGFP control vector 110
4.1.2. WT synphilin-1 induces inclusion formation and toxicity 111
4.1.3. Effect of R621C mutant synphilin-1 on inclusion formation and toxicity 112
4.1.4. Differential interaction of synphilin-1 variants with α-synuclein in non-tg and A30PαSyn mice – a hypothesis 113

4.2. A30PαSyn/UbGFP reporter mice reveal no UPS impairment 115

4.3. The therapeutic potential of Hsp70 in several model systems of PD 117
4.3.1. Hsp70 inhibits MPP^+-induced toxicity in cell culture 117
4.3.2. Hsp70 reduces α-synuclein aggregation and toxicity in cell culture 119
4.3.3. The “chronic” MPTP mouse model for PD 119
4.3.4. Hsp70 expression in the “chronic” MPTP mouse model for PD 120
4.3.5. Hsp70 expression in the A30PαSyn transgenic mouse model for PD 121
4.3.6. Evaluation of Hsp70 as a therapeutic strategy 122
4.3.7. Comparison of cellular models with animal models 124
4.3.8. Comparison of MPP^+-based models with synuclein-based models 126

4.4. Evaluation of different viral vectors to model or to treat PD 126

5. ABSTRACT 129

6. REFERENCES 131

7. APPENDIX 150

7.1. Acknowledgements 150

7.2. Publications 151

7.3. Abstracts/Posters 151

CURRICULUM VITAE 152

Abbreviations

°C	degree centrigrade
6-OHDA	6-hydroxy dopamine
A30PαSyn	(Thy1)-h[A30P]α-syncuclein transgenic
AAV	Adeno-associated virus
Ac-DEVD-amc	acetyl-Asp-Glu-Val-Asp-amino-4-methylcoumarin
AD	Alzheimer's disease
AdV	Adenoviral
APS	ammonium persulfate
ATP	Adenosine triphosphate
bp	base pairs
BCIP	(5-Bromo-4-chloro-3-indolyl phosphate, toluidine salt
BSA	bovine serum albumin
cDNA	copy-DNA
cfu	colony forming units
CHAPS	3[(3Cholamidopropyl)dimethyl-ammonio]-propanesulfonic acid
CMV	cytomegalovirus immediate early promoter
CNS	central nervous system
DA	Dopamine
DAB	3,3'-Diaminobenzidine
DABCO	1,4-diazobicyclo-[2.2.2]-octane
DMSO	dimethylsulfoxide
DNA	desoxy ribonucleic acid
DTT	dithiothreitol
ECL	enhanced chemiluminescence
EDTA	ethylene diamine tetraacetic acid
EGFP	enhanced green fluorescent protein
EtOH	ethanol
FCS	fetal calf serum
GABA	γ-aminobutyric acid
GAPDH	Glycerinaldehyd-3-phosphat-Dehydrogenase
GDNF	Glial cell line-derived neurotrophic factor
GFAP	glial fibrillary acidic protein
GP	*globus pallidus*
GPe	*globus pallidus externum*
GPi	*globus pallidus internum*
GSH	glutathione
h	hour
HA	Hemagglutinin
HEPES	N-2-hydroxyethylpiperazin-N'-2-ethansulfonic acid
HRP	horseradish peroxidase
Hsp	Heat shock protein
i.p.	Intraperitoneal
kDa	kilo Dalton
LB	Luria broth
LV	Lentivirus
MAO-B	Monoamine oxidase-B
min	minute
MPP^+	1-Methyl-4-phenylpyridinium
MPTP	1-Methyl-4-phenyl-1,2,3,6-tetrahydropyridine
NBT	Nitro blue tetrazolium chloride
NGS	Normal goat serum
non-tg	non-transgenic (C57Bl/6-J)
NP-40	nonyl phenoxylpolyethoxylethanol.
o/n	over night
PAGE	polyacrylamide gel electrophoresis
PBS	phosphate-buffered saline
PCR	polymerase chain reaction
PD	Parkinson's disease
PET	paraffin embedded tissue
PFA	paraformaldehyde
PFU	plaque forming units
PK	Proteinase K
RNA	ribonucleic acid
RT	room temperature
SDS	sodium dodecylsulfate
sec	second
SN	Substantia nigra
SNc	Substantia nigra *pars compacta*
SOC	Super Optimal broth with Catabolite repression medium
STN	subthalamic nucleus
TAE	tris-acetate buffer
TBS	tris-buffered saline
TBS-T	TBS-tween
TE	tris-buffered EDTA
tg	transgenic
TH	Tyrosine hydroxylase
TH-IR	TH immunoreactive
T_m	melting temperature
Tris	Tris(hydroxymethyl)-aminomethan

UV	ultra violet
WB	western blotting
WPRE	woodchuck hepatitis virus posttranscriptional regulatory element
WT	wildtype
z-VAD-fmk	N-benzyloxycarbonyl-Val-Ala-Asp-fluoromethylketone

1. Introduction

1.1. Parkinson's disease

1.1.1. History

Parkinson's disease (PD) seems to have existed since ancient times. Descriptions of symptoms and treatments can be found in records of Erasistratos (300 BC), Galen von Pergamon (129-199 AD), Paracelsus (1493 - 1541), and in traditional medical systems from different parts of the world, including India, china and the Amazon basin (Garcia Ruiz 2004).
However, the British physician and pharmacist James Parkinson observed and described two of the three cardinal symptoms (tremor and akinesia, see below) in detail and assumed that these symptoms are attributed to a common origin in the brain. In 1817 he described the disease as a defined clinical picture for the first time in his monograph "An Essay on the Shaking Palsy" (Parkinson 2002). In his letters Wilhelm von Humboldt (1767 – 1835) precisely described the symptoms from a patient's point of view, although he interpreted the clinical signs as an accelerated aging process (Horowski *et al.* 1995). The disease was then known under the designation paralysis agitants; later it was named after J. Parkinson by Jean-Martin Charot (Haas 2001).

1.1.2. Clinical Picture

PD (also called idiopathic Parkinson syndrome) is a chronically progressive, neurodegenerative disease of the central nervous system, in which mainly voluntary and involuntary motor skills deteriorate (motor symptoms), but also speech and other functions including, thinking, mood and sensation (non-motor symptoms) (Jankovic 2008). It is the most common cause of a Parkinson syndrome, characterized by the four cardinal motor symptoms tremor, rigidity, brady-/akinesia and postural instability (Fahn 1988; Sian *et al.* 1999). Other, non-idiopathic Parkinson syndromes will be discussed below.
In PD, tremor is usually unilateral at onset in most cases, reaches maximum during rest and decreases with voluntary movement. Typically, the upper extremities are more affected than the lower ones. The term rigidity refers to stiffness and an increased tone of the muscles. Muscle strength is sustained; flexibility of the ankles is decreased, while the resistance increases. Movements are slowed (bradykinesia), diminished (hypokinesia) or, in cases of severe affection, completely abrogated (akinesia). An impairment of postural reflexes leads to gait and balance instability and an increased fall susceptibility (Dauer and Przedborski 2003).
Additional motor symptoms of PD comprise impairment of gait (shuffling, freezing), posture (camptocormia, dystonia), speech (hypophonia), swallowing and motor coordination performance, fatigue, reduced mimic (hypomimia) leading to a masked face and

micrographia (Deuschl and Goddemeier 1998; Lepoutre *et al.* 2006). Non-motor symptoms include disturbances in mood, cognition (slowed reaction time, dementia, dilution), sleep (somnolence, insomnia), autonomic control (dermatitis, urinary incontinence, weigth loss, nocturia) and sensation (reduction or loss of sense of smell, dizziness, pain, impaired proprioception) (Gupta and Bluhm 2004; Frank 2005; Ishihara and Brayne 2006; Lieberman 2006). Composition and severity of the symptoms is distinct for individual patients.

1.1.3. Prevalence and incidence

The mean age at onset of idiopathic PD is between 50 and 60. So called “juvenile” or early onset forms (before the age of 50) often point to inherited forms of the disease, which represent around 5 to 10% of all cases (see section 1.3).

The prevalence of idiopathic PD is age-related and increases with age from 100-200/100,000 overall to 2.2% above the age of 85. The incidence amounts of 10-20/100,000 per year. There is evidence that men are, in general, about 1.5 times more likely to develop Parkinson’s disease than women (Taylor *et al.* 2007). Since symptoms worsen over time, untreated patients show mortality, which is 1.5 to 3 times higher than for age-matched individuals. When L-Dopa treatment was established in the 1970s the mortality rate of PD patients decreased, and their quality of life increased. Nevertheless, several studies suggest that after 7-10 years of treatment the same severity of disability is reached again (Dauer and Przedborski 2003), and the longevity of PD patients seems to be reduced (Morgante *et al.* 2000).

1.1.4. Diagnosis of PD

As mentioned above the multitude of possible symptoms make it difficult to diagnose PD accurately. Patients are diagnosed with PD after occurrence of motor symptoms, if at least two cardinal symptoms are observed, and if symptoms respond well to L-Dopa treatment.

Despite constant improvements of clinical diagnostic criteria, only 75% of diagnosed PD cases are confirmed *post mortem* (Gelb *et al.* 1999), because no reliable test for definite diagnosis of PD during lifetime has been established to date (Riederer *et al.* 2000).

Functional imaging techniques including positron emission tomography (PET) and single photon emission computed tomography (SPECT) become more important in clinical (differential) diagnosis, because they complement diagnosis based on neurological examination and patient’s history. These techniques increased the accuracy of PD diagnosis up to more than 90% (Dethy and Hambye 2008).

1.1.5. Pathological changes in PD

A diagnosed PD can only be confirmed by the *post mortem* identification of the pathological hallmarks of PD in the in SNc.

One of these hallmarks is the loss of dopaminergic neurons in the SNc. The literal translation of the term “black substance” refers to the characteristic blackish-brown color of this structure. It is due to neuromelanin, a pigment generated during the metabolism of dopamine. Between the 5th and the 9th decade of life 5-6% of the dopaminergic neurons die per decade in the normal aging processes (Fearnley and Lees 1991). At the onset of PD symptoms, approximately 60% of the SNc dopaminergic neurons have been lost. With them, their axonal projections to the striatum are reduced and the degeneration of dopaminergic neurons of the SNc leads to a depletion of dopamine (DA) by approximately 80% in the putamen (Dauer and Przedborski 2003). If the dopamine content drops below a threshold of ~20%, the increase of the glutamatergic innervation of the cholinergic interneurons of the striatum shifts the balanced ratio between dopamine and acetylcholine to the latter one (Fig.1.1). The following physiological alterations in the activity of the neural circuits within the basal ganglia induce the manifestation of PD symptoms. The severity of the symptoms correlates with the reduction of the dopamine content (Bernheimer *et al.* 1973; Muller *et al.* 1999).

A decline in the thalamo-cortical activity leads to disturbances of the normal motor performance, which results in the PD symptoms bradykinesia and akinesia, while inhibition of nuclei in the brainstem is believed to cause gait and posture disturbances (Wichmann and DeLong 1993). Mental, autonomic and endocrine dysfunctions are proposed to be caused by extranigral alterations (Braak and Del Tredici 2008), since the degeneration process is not restricted to the SNc. Other pigment containing brain structures, which are affected to a different extent, include *locus coeruleus*, the ventral tegmental area, the *nucleus basalis Meynert*, the *thalamus*, *hypothalamus* and cortical areas (Gibb 1997).

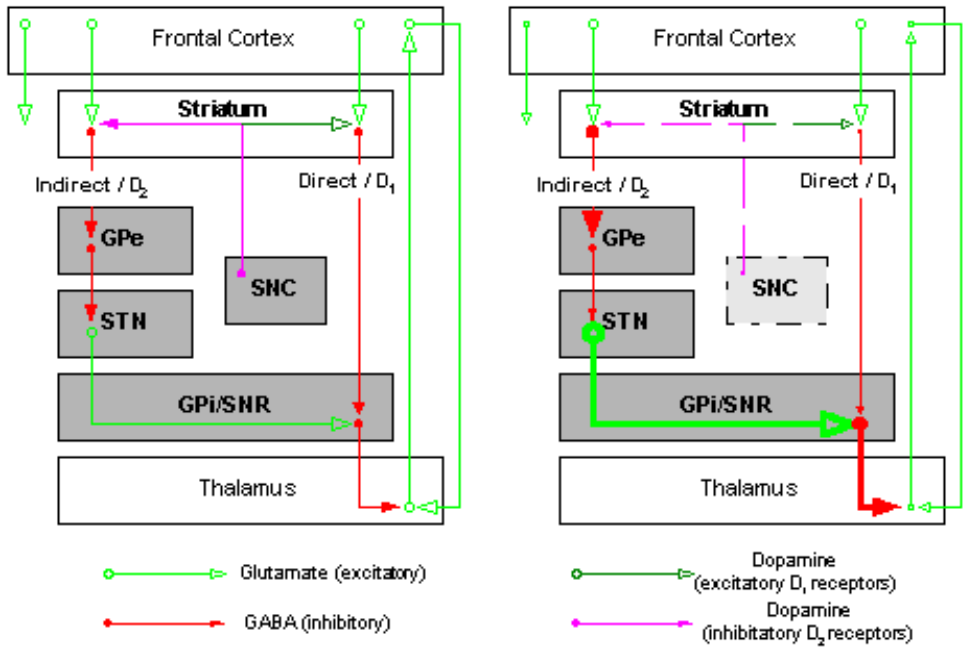

Fig.1.1 Schematic representation of the main connections in a basal ganglia-thalamocortical circuit. Left: Normal status: The two output routes ("indirect" and "direct") are in balance at the level of the output structures. Right: Proposed model in Parkinson's disease: Depletion of dopamine in the striatum leads to an imbalance in the two ouput routes and a suppression of thalamocortical activity. GP, globus pallidus; GPe, external segment of GP; GPi, internal segment of GP; SNR, pars recticulata of the substantia nigra; STN, subthalamus nucleus (online resource: Molson Medical Informatics Project http://sprojects.mmi.mcgill.ca/gait/parkinson/neurology.asp)

The second hallmark of PD is the presence of intracellular proteinaceous inclusions, so-called “Lewy Bodies” (LBs), which were described in 1912 for the first time and were named after their discoverer F.H. Lewy. LBs are spherical eosinophilic cytoplasmatic deposits with an diameter of more than 15 µm that consist of a dense granulovesicular core surrounded by a clear halo of 8-10 nm-wide radiating fibrils, the major component of which is α-synuclein (Duffy and Tennyson 1965; Pappolla 1986; Spillantini *et al.* 1997). Next to α-synuclein these LBs contain a variety of proteins including parkin (Shimura *et al.* 2001), ubiquitin (Lowe *et al.* 1988), ubiquitin carboxy-terminal hydrolase (UCH-L1) (Ardley *et al.* 2004), 2001 PINK1 (Muqit *et al.* 2006), cytoskeletal proteins (Schmidt *et al.* 1991; Ihara *et al.* 2003), and synphilin-1 (Wakabayashi *et al.* 2000).

1.2. Pathogenesis of PD

A variety of different pathological processes, including oxidative stress, inflammation, mitochondrial defects, excitotoxicity, apoptosis and genetic predisposition, was implicated in the pathogenesis of PD (Larkin 1999). Since a clear toxic, environmental or genetic etiology can be identified only in the minority of PD cases, a multifactorial genesis is currently

assumed, involving both genetic and environmental risk factors (Lorincz 2006). The function of recently discovered genes that can cause monogenic forms of the disorder, in combination with the cellular effects of toxins and environmental factors that lead to PD suggest that oxidative and nitrosative stress, the accumulation of aberrant or misfolded proteins, ubiquitin-proteasome system dysfunction and deficits in mitochondrial function are the most important pathways leading towards a PD pathology (Moore *et al.* 2005).

1.2.1. Oxidative stress and mitochondrial dysfunction

Compared to other brain structures the SNc is exposed to higher levels of oxidative stress, because the dopamine (DA) metabolism entails the formation of free radicals and other reactive oxygen species (ROS) including the superoxide anion ($O_2^{\bullet -}$), the hydroxyl radical (•OH) and hydrogen peroxide (H_2O_2). Free radicals are molecular species with unpaired highly reactive electrons on an otherwise open shell configuration (Coyle and Puttfarcken 1993), which rapidly react with cellular macromolecules, including membrane lipids, mitochondria, proteins and nucleic acids (Blandini *et al.* 2000). Oxidative modifications of amino acid residues or lipid peroxidation lead to dysfunction of membrane associated proteins (Bowling and Beal 1995), DNA damages induced by an increased 8-OH-2-desoxyguanosine proportion (Yoritaka *et al.* 1996), mitochondrial deficits (Allen *et al.* 1995), cell death (Halliwell 1992) and to the induction of apoptosis.

DA is metabolized to 3,4-dihydroxybenzoic acid (DOPAC) and homovanillic acid (HVA) by monoamine oxidase B (MAO-B) and catechol-O-methyltransferase (COMT), which leads to the formation of one molecule H_2O_2 per molecule DA. H_2O_2 is converted to highly reactive and cytotoxic hydroxyl radical if it reacts with reacts with Fe^{2+} ions via the Fenton reaction (Aisen et al. 1990). Since the SNc is enriched with iron compared to other brain structures and since elevated iron levels were observed in severely affected PD patients, the Fenton reaction might be involved in PD pathogenesis (Sofic et al. 1988; Dexter et al. 1989). Depletion of synaptic DA during the progression of PD triggers a compensatory increased DA turnover, which might exacerbate the oxidative stress by further increasing the generation of H_2O_2.

DA auto-oxidization in the presence of Fe^{2+} ions causes the generation of cytotoxic seminchinone. Semichinones decrease the synaptic transport of DA by inhibiting the dopamine transporter (DAT) and reduce the enzymatic activity of tyrosine hydroxylase (TH), which is involved in the DA biosynthesis. DA-quinone also participates in uncoupling processes of the respiratory chain, because it reduces the mitochondrial proton content (Berman and Hastings 1997; Kuhn et al. 1999). In the presents of hydroxyl radicals, semichinones can polymerize to non-degradable neuromelanin, which leads to the characteristic pigmentation of DA-ergic neurons in the SNc. The accumulation of

neuromelanin is proposed to inhibit cellular function and to enhance oxidative stress, because it leads to iron deposition and increases its proportion of the highly reactive iron species Fe^{2+} (Miller et al. 1990; Jenner 1998).

Cells have several defenses against the harmful effects of ROS. The main antioxidative systems consists of superoxide dismutase (SOD), glutathione peroxidase (GSH per) and glutathione reductase (GSH red) and the peroxisome-located catalase (CAT). SOD converts two superoxide anions into a molecule of hydrogen peroxide and one of oxygen, while catalase catalyzes the decomposition of hydrogen peroxide into water and oxygen in peroxisomes. Therefore mitochondrial and cytosolic H_2O_2 is mainly inactivated by GSH peroxidase. It reduces hydrogen peroxide to water via glutathione (GSH) oxidation (GSSH). Subsequently GSH is regenerated by GSH reductase in the presents of NADPH. Moreover, GSH peroxidase catalyzes the reduction of organic peroxides to non-toxic alcohols, and thereby prevents lipid membrane damaging chain reactions of radicals. Another antioxidative system includes ascorbic acid (vitamin C), α-tocopherol (vitamin E) and glutathione (GSH), which depends on the radical scavenger function of these substances (Schulz *et al.* 2000).

Since increased amounts of oxidative damaged lipids, proteins and DNA were found in the SNc of sporadic PD patients (Floor and Wetzel 1998; Jenner 2003) oxidative stress is considered to be a potential cause of the specific degeneration of dopaminergic neurons. Changes in the ROS detoxification systems observed in the SNc of PD patients also suggested that oxidative stress is involved in the pathogenesis of PD. Compared to age-matched control subjects the enzymatic activity of catalase and GSH peroxidase in PD patients are unaffected, while GSH levels are significantly decreased (Sian *et al.* 1994), which suggests that PD patients have a reduced H_2O_2 clearance capacity.

Another source of ROS is the oxidative phosphorylation of ADP to ATP via reduction of oxygen to water, which is facilitated by the protein complexes of the respiratory chain and takes place on the mitochondrial inner membrane. The amount of free radicals, which are normal byproducts of this multi-step redox process, can increase remarkably by dysfunctions of the electron transport chain (Nohl *et al.* 1978). The respiratory chain is sensitive to these radicals, which further exacerbates the dysfunction of the protein complexes and causes oxidative damage of mitochondrial DNA (Wallace 1992).

The first indication that deficits in mitochondrial function participate in the pathogenesis of PD originate from the fact that intoxication with the complex-I inhibitor 1-methyl-4-phenyl-1,2,3,6-tetrahydropyridine (MPTP) mimics clinical, biochemical, and neuropathological changes reminiscent of those occurring in idiopathic PD (Nicklas *et al.* 1987). Therefore, MPTP toxicity in mice became the most commonly used animal model of PD, see below. Later on, mitochondrial dysfunction, in particular, a decrease of the mitochondrial complex-I activity, was observed in PD (Schapira *et al.* 1989). Moreover, mutations in the genes encoding for

protein kinase 1 (PINK-1) (Valente *et al.* 2004) and DJ-1 (Bonifati *et al.* 2003), were identified to cause familial forms PD. Both proteins are implicated in mitochondrial function and oxidative stress. The cellular energy deficit resulting from mitochondrial dysfunction is supposed to increase the concentration of free cytosolic DA by disrupting its vesicular storage, which further increases the oxidative insult of the DA metabolism on cellular macromolecules. An increase in oxidative processes including the generation of toxic byproducts of the DA metabolism caused by mitochondria dysfunction and its consequence the cellular milieu in DA-ergic neurons is one of two mechanisms, which are mainly subjected to play a causative role in PD pathogenesis (Dauer and Przedborski 2003). The second one is protein misfolding and aggregation.

1.2.2. Protein aggregation and impairment of the ubiquitin-proteasome system

The presence of proteinaceous deposits, built-up by aggregated proteins is a characteristic of several age-related neurodegenerative disorders referred to as proteopathies, including PD (cytoplasmatic LBs), Alzheimer's disease (extracellular senile plaques) and HD (intranuclear huntingtin inclusions). Although these protein deposits vary in localization and protein composition, their common existence in age-related neurodegenerative diseases suggests that protein misfolding is involved in the pathology. An important cellular mechanism to handle “abnormal”, meaning misfolded, mutant or damaged proteins is the interplay between molecular chaperones and proteolysis.

The proteolytic ubiquitin-proteasome system (UPS) reduces the levels of soluble abnormal proteins (Voges *et al.* 1999; Pickart 2001; Hanna and Finley 2007). Ubiquitin (Ub) monomers are activated by the Ub-activating enzyme (E1) and transferred to an Ub-conjugating enzyme (E2). Target proteins are recognized by Ub protein ligases (E3), which mediate the transfer of Ub from the E2 enzyme to the target protein. The sequential addition of ubiquitin residues to target proteins forms poly-ubiquitin chains, which are required for recognition and degradation of the protein by the 26S proteasome in an ATP-dependent manner, leading to the generation of small peptide fragments. The remaining poly-Ub chains are recycled to free Ub monomers by de-ubiquitinating (DUB) enzymes, such as UCH-L1, for subsequent rounds of ubiquitination (Crews 2003). The 20S proteasom consists of a 19S cap particles and the 20S particles, which mediates the degradation of non-ubiquitinated proteins (Nandi *et al.* 2006).

Chaperones assist folding, refolding or degradation of misfolded polypeptides, prevent protein aggregation and are involved in the formation of proteinaceous inclusions, called aggresomes (Opazo *et al.* 2008). Aggresomes are formed at the centrosome in response to an overload of damaged proteins to protect the cell from potentially deleterious effects of these abnormal protein entities, if they cannot be eliminated via the UPS. Aggresomes are considered the equivalent in cell culture of LBs in the brain of PD patients (Kopito 2000; Junn

et al. 2002). Several lines of evidence suggest that protein mishandling and an impairment of the UPS might play a role in the pathogenesis of PD. Chaperones and components of the UPS, including UCH-L1, proteasomal subunits and ubiquitin are present in LBs in post mortem tissue of PD patients. Several gene mutations causing familial forms of PD encode for proteins that can impede proteasomal function, because they are degraded via the UPS (α-synuclein, Parkin, synphilin-1, mutated DJ-1) or because they are components of the degradation pathway (Parkin, UCHL1). A direct relation between the UPS and PD-related proteins was suggested by the interaction between α-synuclein and S6 proteasomal protein *in vitro* (Snyder et al. 2003). Moreover, structural and functional deficits at different steps in ubiquitin-mediated pathway were observed in the SNc of sporadic PD, too. Further implications of protein misfolding in PD and other aggregopathies emerges from a number of studies in which the pharmacological, transgenic or viral vector-induced expression of molecular chaperones have been shown to reduce neurodegeneration caused by overexpression of a variety of aggregating proteins, including α-synuclein, huntingtin, atixin-1, SOD1 (Warrick *et al.* 1999; Carmichael *et al.* 2000; Muchowski *et al.* 2000a; Cummings *et al.* 2001; Auluck *et al.* 2002; Takeuchi *et al.* 2002; Klucken *et al.* 2004c; Wyttenbach 2004).

1.2.3. Cell death mechanisms

Neuronal cell death in PD occurs by necrosis or apoptosis, or intermediates of these two distinct molecular death mechanisms.

Necrosis is defined as un-controlled lysis following extreme stress and irreversible injury of the cell. It can also be induced by secondary inflammatory tissue responses (Kerr *et al.* 1972). Cellular contents are released into the intracellular space, which damages neighboring cells and leads to inflammation (Leist and Jaattela 2001). Morphological signs of necrosis are vacuolization of the cytoplasm, mitochondrial swelling, dilatation of ER, and disruption of plasma membrane (Artal-Sanz and Tavernarakis 2005).

A cascaded activation of caspases leads to cleavage of substrates and culminates in the manifestation of the morphological characteristics of apoptosis including cell shrinkage and rounding, packaging of organelles, chromatin condensation (pyknosis) and fragmentation (karyorrhexis), membrane blebbing, and formation of apoptotic bodies, which are phagocytosed by the surrounding tissue (Hengartner 2001; Schulz 2006). The major biochemical sign of apoptosis is the activation caspases, aspartate-specific cysteine proteases (Thornberry 1998; Boatright and Salvesen 2003). Caspases are classified according to their activation mode in (i) “initiator” caspases, including caspase-2, 8, and 9, and (ii) “executioner” caspases, including caspase-3, 6, and 7 (Schulz *et al.* 1999; Beere 2005).

Two different mechanisms of caspase activation have been defined as the intrinsic and the extrinsic pathway. The extrinsic pathway is initiated by ligation of cell surface death receptors like TNF-R (Tumor necrosis factor receptor), Fas, and DR4/5 (Death Receptor 4/5) triggered by binding of their specific death ligands TNF, Fas-Ligand and TRAIL (TNF-related apoptosis-inducing ligand) (Wajant 2003). In contrast to that, the intrinsic pathway is induced by endogenous harms like hypoxia, DNA damage, heat shock, increased ROS or Ca^{2+} concentrations or mitochondrial damage (Kaufmann and Earnshaw 2000). It is mainly mediated by permeabilization of the mitochondrial outer membrane and release of pro-apoptotic factors from mitochondria to the cytosol. These factors are cytochrome c (Kluck *et al.* 1997; Yang *et al.* 1997), AIF (apoptosis inducing factor) (Susin *et al.* 1999) and smac/DIABOLO (second mitochondria-derived activator of caspase) (Du *et al.* 2000; Verhagen *et al.* 2000). This is followed by apoptosome formation and activation of pro-caspase 9 (Srinivasula *et al.* 1998; Zou *et al.* 1999).
Both pathways culminate in activation of executor caspases and cleavage of their target substrates. They are integrated by caspase-8 mediated cleavage and activation of Bid and JNK (C-jun-N-terminal kinases), which can affect mitochondrial membrane integrity (Chowdhury *et al.* 2006; Reich *et al.* 2008).
Besides apoptosis and necrosis two intermediated forms of cell death have been classified: (i) Apoptosis-like programmed cell death occurs via lysosomal substrate degradation independently from caspases and shows a less compact and complete chromatin condensation. (ii) Necrosis-like programmed cell death might be initiated by caspases, while caspase-mediated execution and chromatin condensation have not been described (Schulz 2006).

1.3. PD genetics

Studies investigating the concordance rate of PD in twin cohorts failed to unveil a role for hereditable factors in PD (Duvoisin 1977; Ward *et al.* 1983; Marttila *et al.* 1988). On the other hand, clinicians observed PD patients with affected relatives (Mulholland 1996) and described families that showed a Mendelian inheritance of PD (Bell and Clark 1926) already in very early studies. Nevertheless, PD was deemed to be a classic non-genetic disorder, because until the end of the last century, no distinct genetic locus responsible for rare familial cases had been identified. Since the late 1990s, genetic analysis of families revealed a number of loci and genes associated with either autosomal dominant, autosomal recessive or incomplete penetrated inherited forms of PD to play a causal role in PD (Tab.1.1). Familial PD is typically characterized by an early onset and a slowed progression of motor and cognitive symptoms and in some cases a lack of LB formation. Importantly, most of the

proteins encoded by these genes are involved in mitochondrial function or the UPS, mechanisms, which were suggested to dysfunction in PD (see section 1.2) and are found in LBs.

Locus	Chromosomal Localization	Gene product	Inheritance	Lewy body pathology	Specific clinical symptoms
PARK 1	4q21	α-Synuclein +	AD	Yes	Dementia
PARK 2	6q25.2-27	Parkin	AR	No	Early onset, L-Dopa-induced dyskinesias, improvement during sleep, foot dystonia
PARK 3	2p13	?	AD	Yes	Dementia
PARK 4	4q21	α-Synuclein *	AD	Yes	Dementia, postural tremor
PARK 5	4p14	UCH-L1	AD	No report	Not described
PARK 6	1p35-36	PINK-1	AR	No report	Early onset, tremor dominant
PARK 7	1p36	DJ-1	AR	No report	Early onset, dystonia, psychiatric alterations
PARK 8	12cen	LRRK2/Dardarin	AD	Yes/but also Tau pathology	Tremor, late onset
PARK 9	1p36	ATP13A2	AR		Kufor-Rakeb syndrome, very early onset
PARK 10	1p32	?	AD (?)	No report	Late onset
PARK 11	2q34	?	AD (?)	No report	Late onset
	5q23	Synphilin-1	Susceptibility	No report	Late onset
PARK 13	2p13	HtrA2/Omi	Susceptibility	No report	Late onset

Tab.1.1 Loci and genes associated with familial PD or implicated in PD1. Abbreviations: AD, autosomal dominant; AR, autosomal recessive; +: point mutations; *: triplication (modified from Schulz 2008).

1.3.1. α-synuclein

A G to A transition at position 157 in the PARK1 gene locus encoding for α-synuclein leading to an amino acid substitution from alanine to threonine was the first mutation linked to autosomal dominant familial aggregation of PD in an Italian American family of 400 members including more than 60 affected individuals (Polymeropoulos et al. 1997). Two other missense mutations were found in the α-synuclein gene; an A30P-mutation was identified in a German family (Kruger et al. 1998) and E46K mutation in a Spanish family (Zarranz et al. 2004). The PARK4 locus was associated with a gene triplication of the α-synuclein gene and was found to be causative for PD in an American family (Singleton et al. 2003).

Synucleins are a protein family small phospho-proteins including α-synuclein, β-synuclein and γ-synuclein, highly conserved in vertebrates (George 2002). α-synuclein is a 140-amino-acid-protein with a molecular weight of 15-20 kDa. It is abundantly expressed in presynaptic nerve terminals throughout the mammalian brain. Structurally, α-synuclein is composed of an N-terminal amphipathic region containing six imperfect repeats, in which all three point mutations are located, a hydrophobic central region, and an acidic C-terminal region. A non-amyloid-β component (NAC)-fragment was originally isolated from amyloid plaques in AD patients. It had been identified to be the major component of LBs in PD as well as a precursor peptide of amyloid plaques in AD (Irizarry et al. 1996; Kahle et al. 2000).

In cell culture, α-synuclein overexpression inhibited the activity of TH, which resulted in decrease in DA-synthesis (Perez et al. 2002). On the other hand, the absence of α-synuclein in a knock-out mouse model also inhibited synaptic DA-release, leading to striatal DA-deficits in these mice. Furthermore, α-synuclein was implicated in axonal (neurotransmitter) transport. Thus, α-synuclein had been suggested to regulate DA neurotransmission by binding to synaptic vesicles and stabilizing their protein-lipid-interaction mice (Abeliovich et al. 2000). However, the precise biological function of α-synuclein remains to be elucidated.

α-synuclein is natively unfolded, but depending on the surrounding milieu, it forms different secondary and tertiary structures, including α-helices and β-sheets, as well as mono- or oligomeric species or amyloid fibrils and aggregates of high molecular weight (Uversky 2003). The accumulation of soluble oligomeric species into so-called protofibrils is an intermediated step during formation of amyloid-like fibrillary aggregates, which are found in LBs. Several studies concerning the role of soluble protofibrils in PD pathogenesis implied the protofibrils rather then the fibrils to be the pathogenic entity. Compared to wildtype, the A53T as well as the A30P mutation increased the propensity of α-synuclein to self-aggregate into oligomers and LB-like fibrils in vitro. Later the same authors demonstrated that both mutations seem to stabilize the oligomeric forms. In a subsequent study, they have shown that DA inhibited the protofibril-to-fibril conversion leading to an accumulation of α-synuclein protofibrils (Conway et al. 1998; Conway et al. 2000; Conway et al. 2001). Furthermore, the mutations were found to induce the formation of annular protofibrils that resemble pore-like structures, which might affect cellular viability by disturbing the membrane integrity (Lashuel et al. 2002).

1.3.2. Synphilin-1

Synphilin-1 was named and implicated in PD according to its identification as an α-synuclein-interacting protein and as a component of LBs in patients with PD and other synucleinopathies. Synphilin-1 was found interact with α-synuclein in an yeast two-hybrid screen and in cellular model systems, where the co-expression of both proteins caused formation of cytoplasmatic inclusions (Engelender *et al.* 1999; Chung *et al.* 2001; Kawamata *et al.* 2001; O'Farrell *et al.* 2001; Lee *et al.* 2002a; Tanaka *et al.* 2004). Synphilin-1 is protein of 919 amino acids with a molecular weight of 100-120 kDa and consists of several domains, such as such as six ankyrin-like repeats, a coiled-coil domain and a putative ATP/GTP-binding motif (Engelender *et al.* 1999). The domains critical for the binding of synphilin-1 to its interaction partners are depicted in Fig.1.2.

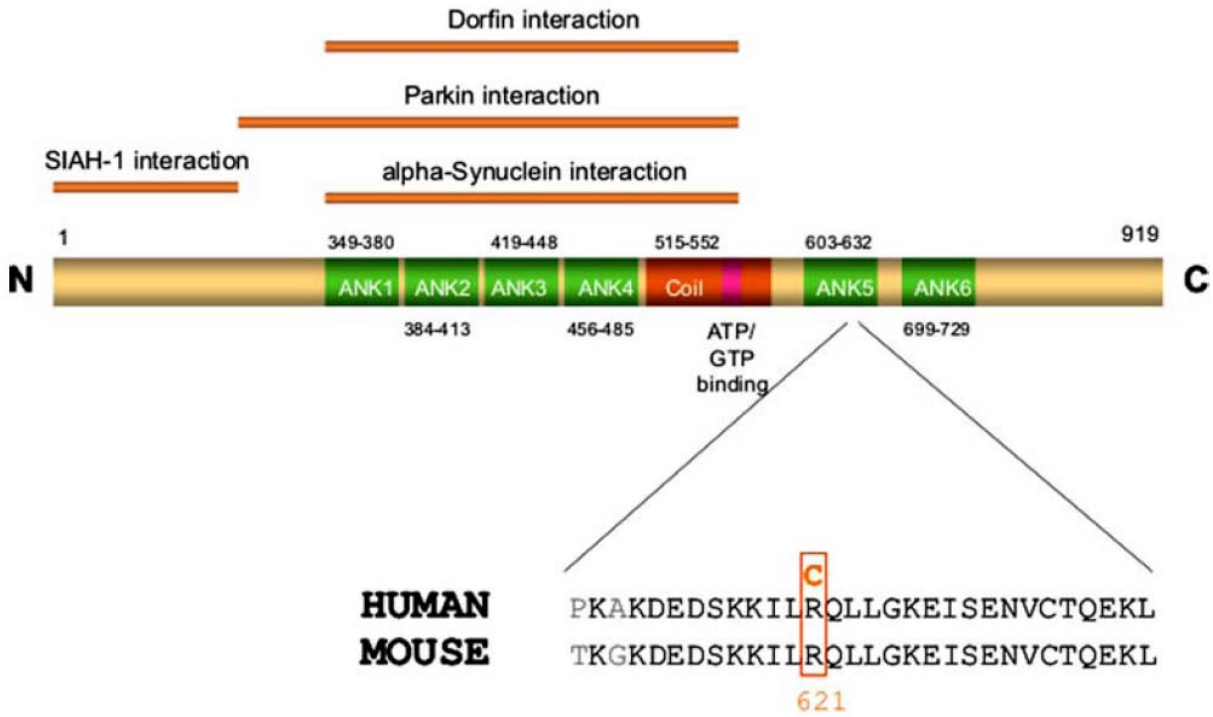

Fig.1.2 Schematic view of the synphilin-1 protein based on Swiss Prot #Q9Y6H5, including an interspecies comparison of the amino acid sequence of human and mouse synphilin-1 (red bars critical domains for interaction with alpha-synuclein, parkin, dorfin, and SIAH- 1, ANK ankyrin-repeat, Coil coiled-coil domain) taken from Krüger 2004.

In a recent study different domains had been linked to distinct forms of cellular protein accumulation. Consistent with other studies (see above) overexpression of synphilin-1 in HEK293 cells induced the formation of multiple small highly mobile aggregates, while proteasome or Hsp90 inhibition rapidly triggered their translocation into the aggresome, indicating that aggresome formation, but not aggregation of synphilin-1, is a cellular response to a dysfunction of the proteasome/chaperone machinery. Translocation to aggresomes required the ankyrin-like repeat domain (ANK1-ANK4), which is located upstream of the central coiled-coil-domain, a deletion of either the Coil domain or the ANK5/6 domain prevented formation of multiple aggregates, indicating that ANK1-ANK4 domain is necessary and sufficient for aggresome targeting, while both CC and ANK2 domains are necessary, and their combination is sufficient for formation of multiple aggregates (Zaarur *et al.* 2008).

Synphilin-1 is mainly expressed in neurons and co-localizes with α-synuclein at presynaptic nerve terminals (Ribeiro *et al.* 2002). There it binds to synaptic vesicles, which has been suggested to mediate synaptic functions including the release of DA attributed to α-synuclein (Nagano *et al.* 2003).

Synphilin-1 has been reported to interact with several E3-Ubiquitin-ligases and with the protein kinase LRRK2 involved in both autosomal dominant and sporadic PD (Smith *et al.* 2006; Szargel *et al.* 2007). Synphilin-1 is poly-ubiquitinated by the E3-ubiquitin-ligases parkin (Chung *et al.* 2001), SIAH-1 (Nagano *et al.* 2003), SIAH-2 (Liani *et al.* 2004) and Dorfin (Ito *et al.* 2003), all of which are components of LBs. The proteasome regulator NUB1, which

down-regulates the ubiquitin-like protein NEDD8 by targeting it to proteasomal degradation, was found to co-localize with synphilin-1 in LBs of PD patients and to physically interact with synphilin-1 through its NEDD8-binding site in cell culture. NUB1 suppressed the formation of synphilin-1-positive inclusions in HEK293 cells co-transfected with NUB1 and synphilin-1, suggesting that NUB1 regulates the proteasomal degradation of synphilin-1, too (Tanji *et al.* 2006).

Synphilin-1 was also identified as a substrate of GSK3beta (Glycogen synthase kinase 3 beta), which decreased the ubiquitination of synphilin-1 and led to a reduced SIAH-mediated degradation of synphilin-1. When synphilin-1 was less phosphorylated either by inhibition of GSK3beta or introducing a point mutation at the Ser 556 amino acid residue, which is the major GSK3beta phosphorylation site in synphilin-1, ubiquitination and inclusion body formation by SIAH were increased, while proteasome function was inhibited. Thus, the phosphorylation status of synphilin-1 was suggested to regulate proteasome function (Avraham *et al.* 2005). Synphilin-1 was further functionally linked to the proteasome based on its interaction with the 19S proteasome subunit S6 ATPase, which was identified as another component in 25% of the LBs in brains of sporadic PD patients. In cell culture overexpression of both S6 ATPase and synphilin-1 inhibited proteasome function and induced the formation of synphilin-1 inclusions (Marx *et al.* 2007). These data indicate that synphilin-1 might be not only a substrate, but a modulator of the ubiquitin-proteasome system, too.

Giaime *et al.* proposed that synphilin-1 has an anti-apoptotic function controlled by the C-terminal fragment which is generated through cleavage by caspase-3 (Giaime *et al.* 2006).

Recently, an alternative splice variant of synphilin-1, synphilin-1A has been described to bind to α-synuclein, too. It showed much higher propensity to aggregate as compared to synphilin-1. Moreover, synphilin-1A was present in LBs of both PD and DLBD patients, suggesting a role of synphilin-1A in the pathogenesis of α-synucleinopathies (Eyal *et al.* 2006).

A mutation in the synphilin-1 gene leading to a substitution from arginine (R) to cysteine (C) at position 621 (R621C) in PD patients was identified in an earlier study in our laboratory. *In vitro* assays assessing necrotic as well as apoptotic cell death have revealed a slightly increased vulnerability to cellular stress induced by the pan-kinase-inhibitor staurosporine of cells overexpressing mutant R621C compared with wildtype (WT) synphilin-1. Interestingly, the tendency to form intracellular inclusions in SH-SY5Y cells after proteasome inhibition was smaller with R621C than with WT synphilin-1 (Marx *et al.* 2003). In a subsequent study, the regulatory subunit of the 19S proteasom S6 ATPase was found to interact with synphilin-1 in a cellular model and to be a component of LB in brains of PD patients. Co-expression of synphilin-1 and S6 ATPase caused proteasomal inhibition followed by the formation intracellular inclusions, which stained positive for both proteins (Marx *et al.* 2007).

Although the identification of its domain structure and several interaction partners suggested a role of synphilin-1 in synaptic function, protein degradation and in the molecular mechanisms leading to neurodegeneration in PD, its physiological function has remained unclear.

1.4. Therapeutic strategies

1.4.1. Pharmacotherapy

To date, there is no causal treatment for PD.

Since the symptoms of PD are caused by degeneration of the synaptic terminals of the DA-ergic neurons of the SNc, which induces a deficit of DA in the striatum the current therapeutic strategy for a pharmacological symptomatic treatment of PD is to substitute DA by: (i) administration of DA precursors or agonists and (ii) inhibition of DA degradation.

The classical treatment remains medication with the dopamine precursor L-3,4-dihydroxyphenylalanine (L-DOPA). It went into clinical practice after being reported to improve akinesia in PD in a large study in the late 1960s (Cotzias 1968; Hornykiewicz 2002).

L-DOPA has to be combined with DOPA-decarboxylase blockers like carbidopa and benserazide to inhibit peripheral metabolization to DA and consecutive side effects. Thus a considerable amount of the drug can cross the blood brain barrier. It is then decarboxylated to DA in the brain. As the disease progresses, up to 80% of patients experience motor fluctuations within 5-10 years after disease onset. DA agonists can be used as an initial and adjunctive therapy in PD to delay these fluctuations. Unwanted side effects of DA agonists include cardiovascular and psychiatric complications, which limit their utility (Jankovic and Stacy 2007). Novel drug delivery systems for constant administration of L-Dopa and dopamine agonists via intratestinal, transcutaneous or subcutaneous infusion further reduce medication dosage dependent fluctuations (Schulz 2008).

MAO-B inhibitors, such as rasagiline and selegiline, increase concentrations of dopamine in the brain by blocking its reuptake from the synaptic cleft. This can slow motor decline, prolong “on” time and improve symptoms of PD. Since DA and are L-DOPA are metabolized by COMT, administration of COMT inhibitors in combination with L-DOPA decelerate the elimination half-life of L-DOPA, leading to decreased “off” time and increased “on” time and allow for a lower daily L-DOPA dosage.

1.4.2. Surgical therapies

In advanced stages of PD, when symptoms are no longer adequately controllable with medications, or if medications have severe side effects, surgery represents an alternative for

these patients. The common principle of these neurosurgical treatments is to mimic the inhibitory function of the SNc on its target regions, which become overactive due to the degeneration of the SNc by preventing them from firing either via electrothermal tissue ablation or using chronic, high frequency deep brain stimulation (DBS) (Kringelbach *et al.* 2007). Anatomic targets include the ventrointermediate thalamic nucleus (Vim), the *Globus pallidus internus* (GPi), and the *Nucleus subthalamicus* (STN). Lesioning techniques are irreversible invasive procedures, which surgically destroy cells of the GPi (pallidotomy), the Vim (thalamotomy), and the STN (subthalamotomy). Deep brain stimulation (DBS) is accomplished by implantation of electrodes in the target area and a battery-powered brain pacemaker called neurostimulator near the *clavicula*, which provides constant high frequency electrical stimulation. Although the underlying principles and mechanisms remain uncertain, DBS has shown remarkable therapeutic benefits. It is well tolerated and displays advantages such as the option to adjusting electrical stimulation for optimal control and minimal side effects (Walter and Vitek 2004).

Recently, three independent laboratories reported their autopsy-controlled findings after transplanting fetal nigral dopaminergic nerve cells, with the intention of replacing striatal dopamine in individuals who no longer respond to levodopa (Kordower *et al.* 2008; Li *et al.* 2008; Mendez *et al.* 2008). The long term clinical benefits were limited, while some of the grafts developed Lewy pathology (i) suggesting host-to-graft disease propagation and (ii) underscoring limitations of such an approach (Braak and Del Tredici 2008).

However, all medications or surgery techniques established to date represent a symptomatic rather than curative treatment of PD, because they do not stop or decelerate the progressive degeneration of nigrostriatal system.

1.5. Experimental therapies

1.5.1. Neuroprotective therapies

In order to stop or slow PD progression, treatments that protect the neurons of the SNc from cell death are needed. The monoamine oxidase inhibitors rasagiline and the complex I mitochondrial fortifier coenzyme Q10 are under clinical investigation for neuroprotective effects (Schulz 2008). To stop the progressive neurodegeneration, earlier studies focused on blocking executioner caspases of apoptotic cell death, but no sustained neuroprotection could be accomplished (Kermer *et al.* 1999; Perrelet *et al.* 2000; Rideout and Stefanis 2001). Thus several studies aimed on the maintenance of mitochondrial integrity by overexpression of anti-apoptotic members of the bcl-2 family of proteins (Azzouz *et al.* 2000; Malik *et al.* 2005; Wong *et al.* 2005). Although this approach was reported to be significantly more efficient than caspase inhibition, in long-term studies substantial neuronal cell loss was still

observed (Kim 2005; Malik *et al.* 2005). Neurotrophic factors, with the possible exception of glial cell line-derived neurotrophic factor (GDNF) were only sufficient to induce a shortly delayed neuronal degeneration (Cheng *et al.* 2002; van Adel *et al.* 2003). When our group investigated the role of the GDNF receptor RET (rearranged during transfection), in the MPTP model of PD, GDNF-mediated activation of RET did not protect neurons but rather stimulated axonal sprouting (Kowsky *et al.* 2007).

1.5.2. Molecular chaperones

By definition “molecular chaperones are a functional class of otherwise unrelated families of protein that assist the correct non-covalent assembly of other polypeptide-containing structures *in vivo,* but are not components of these assembled structures when they are performing their biological functions.” They do not provide steric information essential for correct assembly, but rather inhibit incorrect interactions, which can produce non-functional structures during protein self-assembly (Ellis and van der Vies 1991). Thus, molecular chaperones contribute to the cellular control of protein conformation, turnover, aggregation and toxicity in bacteria, plant and animal cells (Liberek *et al.* 2008). For example, molecular chaperones assist the correct non-covalent folding of newly synthesized proteins, facilitate translocation of proteins across membranes, help assemble and disassemble protein complexes, help present substrates for degradation, and suppress protein aggregation in different intracellular compartments. Additionally, chaperones are involved in the regulation of protein–protein interactions (Fig.1.3).

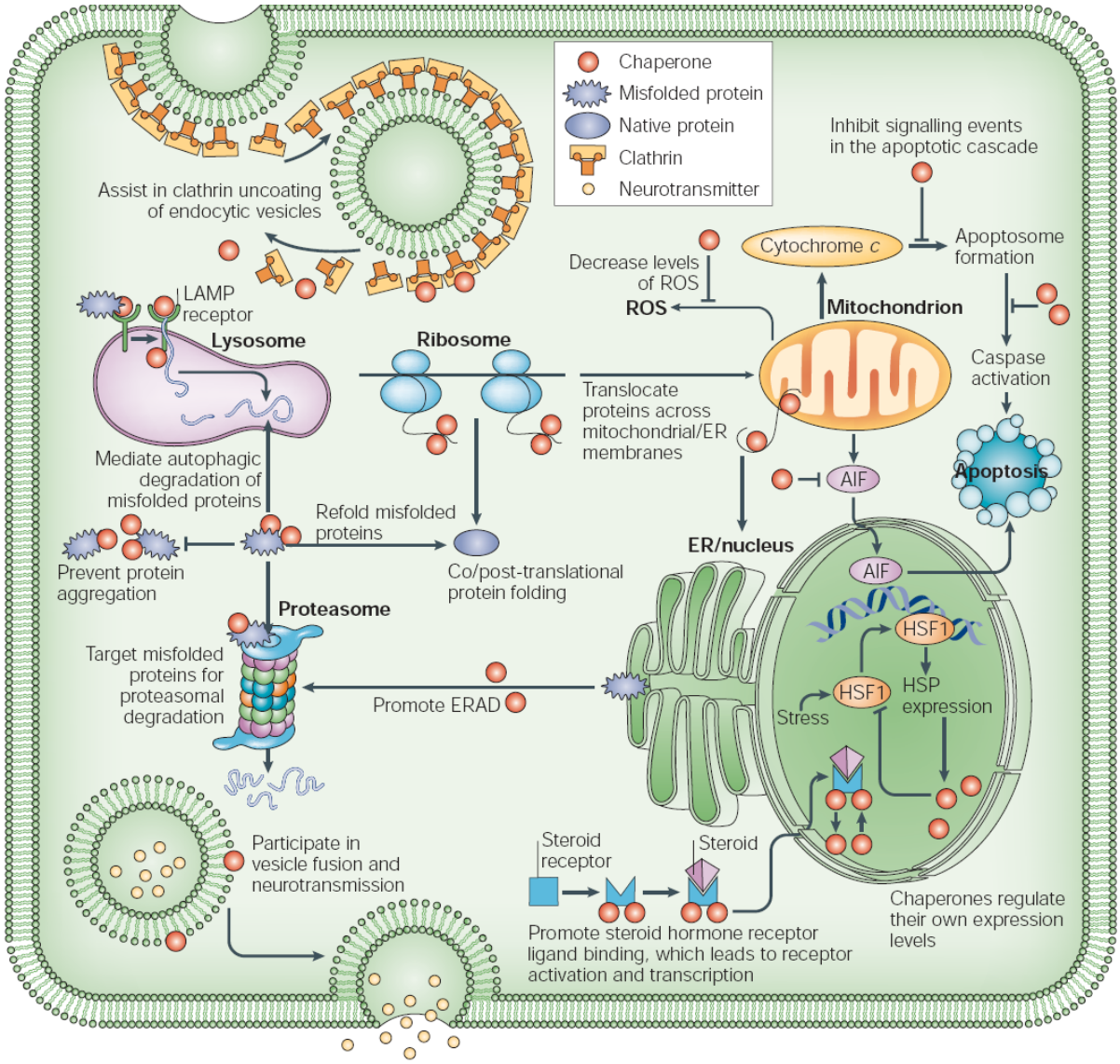

Fig.1.3 Molecular chaperones regulate several important cellular processes. It is well known that the molecular chaperones facilitate protein folding and prevent protein aggregation. However, molecular chaperones also regulate several other cellular processes, such as autophagy, vesicle fusion, signal transduction, apoptosis and proteasomal degradation. AIF, apoptosis inducing factor; ER, endoplasmic reticulum; ERAD, endoplasmic reticulum-associated degradation; HSF1, heat shock transcription factor 1; HSP, heat shock protein; LAMP, lysosomal-associated membrane protein; ROS, reactive oxygen species (taken from Muchowski and Wacker 2005).

Molecular chaperones function not only under normal conditions, but also to limit the damage to proteins caused by stresses such as heat shock. Heat-induced denaturation of proteins leads to an increased propensity to aggregate. Thus, many heat shock proteins act as molecular chaperones, but not all molecular chaperones are heat shock proteins (Ellis and van der Vies 1991).

1.5.2.1. Heat shock proteins

Heat shock proteins (Hsp) represent an evolutionary highly conserved subgroup of chaperones, which consists of different unrelated families. Hsp are categorized into six major families based on their molecular mass: small Hsp, Hsp40, Hsp60, Hsp70, Hsp90, and Hsp100.

Small Hsp (sHsp) are found in both prokaryotes and eukaryotes. Members of this diverse protein family are characterized by their low monomeric molecular mass of 15–43 kDa and the existence o so-called α-crystallin-domain, a conserved stretch of approximately 100 amino-acid residues (Haslbeck 2002; Haslbeck *et al.* 2005), which shows sequence similarity to the vertebrate eye lens protein α-crystallin. Alpha-crystallin prevents protein precipitation and cataract formation in the eye lens (Meehan *et al.* 2004). sHsp differ from other chaperones in that their activity is independent of ATP hydrolysis. Hsp27 is one of the small Hsp that are constitutively expressed at different levels in various cell types and tissues. Like other small heat shock proteins, Hsp27 is regulated at both the transcriptional and posttranslational levels (Ganea 2001). The expression of Hsp27 increases several-fold in response to stress. As a result of the activation of the p38 MAP kinase pathway (Landry *et al.* 1992; Rouse *et al.* 1994). Hsp27 is phosphorylated by MAPK-activated protein kinase 2, which changes the tertiary structure of Hsp27 and shifts the protein from large multimers to dimers and monomers (Rogalla *et al.* 1999). Up-regulation and phosphorylation of Hsp27 have been demonstrated to modify actin polymerization and reorganization (Lavoie *et al.* 1993; Rousseau *et al.* 1997).

Hsp40 and Hsp40-like proteins are a large family of chaperone proteins that are homologous to *E. coli* DnaJ protein. Based on their structures these proteins are classified into three subtypes. The common feature of the family is a conserved J domain, which is usually located at the amino terminus of proteins and is responsible for their association with Hsp70 (Cheetham and Caplan 1998; Fan *et al.* 2003). Human Hsp40, also known as Hdj1, belongs to subtype II that contain a unique Gly/Phe-rich region. Proteins of the Hsp40 family bind unfolded proteins, prevent their aggregation, and then deliver them to Hsp70 (Langer *et al.* 1992; Fan *et al.* 2003). Another major function of Hsp40 is to stimulate ATPase activity of Hsp70, which causes conformational change of the unfolded proteins (Liberek *et al.* 1991; Cyr *et al.* 1992). The Hsp40-Hsp70-unfolded protein complex further binds to the co-chaperones Hip, Hop and Hsp90 or components of the protein degradation machinery such as CHIP and BAG-1, which either leads to protein folding or degradation, respectively (Hohfeld *et al.* 2001).

Hsp60 was identified as a mitochondrial chaperone, which facilitates protein folding after import into the mitochondria (Jindal *et al.* 1989). A significant amount of Hsp60 is also present in the cytosol of many cells, induced by stress (Itoh *et al.* 2002; Gupta and Knowlton

2005), inflammatory and immune response (Deocaris *et al.* 2006; Lai *et al.* 2007). Chaperonins belong to the Hsp60 family and assist the folding of nascent, non-native polypeptides. They form large protein complexes, composed of two rings built-up by seven to nine subunits to build a barrel-like structure. Supported by co-chaperonins chaperonins undergo conformational changes, during the ATP-dependent folding reaction to bind unfolded or misfolded protein, encapsulate it within one of the cavities formed by the two rings, and release the protein back into the cytosol (Fenton and Horwich 2003).

Ubiquitously expressed Hsp70 are the largest and probably best-researched family of Hsp and are described below. Molecular chaperones of the 70 kDa heat shock protein family (Hsp70) function in a diverse set of processes, including protein folding, multimer association and dissociation, translocation of proteins across membranes, and the regulation of heat shock response (Hartl 1996; James *et al.* 1997).

The Hsp90 protein contains three functional domains, the ATP binding, protein binding and dimerizing domain, each of which plays a crucial role in the function of the protein (Csermely *et al.* 1998). Similar to Hsp70, Hsp90 is expressed constitutively under normal conditions to maintain protein homeostasis and is upregulated upon environmental stress. It interacts with unfolded proteins to prevent irreversible aggregation and catalyzes the refolding of their substrates in an ATP and co-chaperone dependent manner. Compared to Hsp70, Hsp90 tends to have a more limited subset of substrates, most of which are signaling molecules. Beyond its chaperone function Hsp90 is essential for the maturation and inactivation of nuclear hormones and other signaling molecules and plays a role in vesicle formation and protein trafficking (Nollen and Morimoto 2002; Pratt and Toft 2003; Young *et al.* 2003).

Proteins in the Hsp100/Clp family form large hexameric structures in the presence of ATP. Their chaperone function occurs by threading the substrate protein through a small 2 nm pore to unfold and thereby allow the substrate to fold correctly during a second folding reaction. Instead of that, other members of the Hsp100 family, like ClpA and ClpX, do not catalyze refolding reactions, but rather associate with the double-ringed tetradecameric serine protease ClpP to disrupt tagged and misfolded proteins (Maurizi and Xia 2004).

Hsp were discovered in the 1960s by coincidence in *D. melanogaster*, when the incubation temperature of fruit flies accidentally increased. Examination of the chromosomes revealed an elevated gene transcription of an unknown protein, which was indicated by a "puffing pattern" of the chromosomes (Ritossa 1996). Based on that finding the phenomenon was designated "Heat Shock Response" and the proteins were termed the "Heat Shock Proteins" (Hsp). Their expression is regulated by a group of transcription factors called heat shock factors (HSFs) (Wu 1995).

Besides increased temperatures, a variety of cell damaging stimuli including inflammation, infection, exposure to trace metals, noxious drugs, UV radiation, inhibitors of the cellular energy metabolism, nutrient withdrawal, ischemia, poly-glutamine expansion, death receptor ligation, chemotherapeutically induced DNA damage, hypoxia, reactive oxygen species (ROS), ER stresses, proteasom inhibition, and cytoskeletal perturbation have been demonstrated to induce the cellular stress or heat-shock response machinery (Kopecek *et al.* 2001; Nollen and Morimoto 2002).

To avert a pathological state cells react to these non-physiological conditions by the induction of pathways mediating either apoptotic cell death or survival, depending on their ability to preserve cellular function by protection or recovery from injurious events. Hsps take part in protective mechanisms because they first, facilitate proper folding of nascent proteins, second monitor for the presence of misfolded proteins and third, either disaggregate, refold and renature misfolded or abnormal proteins or target these abnormal protein species for degradation (Beere 2005; Liberek *et al.* 2008).

Hsp70

Heat shock proteins of the Hsp70 family share structural and biochemical similarities and range in size from 66 to 78 kDa. They are found in virtually all living organisms: DnaK, HscA (Hsc66), HscC (Hsc62) exist in prokaryotes. The four different Hsp70 family members expressed in eukaryotic organisms differ in their expression pattern, function and subcellular localization. Hsp70 (or Hsp72) is the classical stress-induced protein, which is up-regulated by and functions in response to cellular stress (see below).

Glucose regulated protein 78 (Grp78 or BiP) localizes in the endoplasmic reticulum (ER). It is up-regulated in response to starvation- or stress-induced accumulation of unfolded proteins in the ER. Grp78/BiP binds to unfolded proteins and prevents their transport. Moreover, Grp78/BiP-induction leads to upregulation of other chaperons to prevent aggregation of unfolded proteins (Ma and Hendershot 2001). This so-called “unfolded protein response” (UPR) was found to be downregulated in a familial form of Alzheimer’s disease, which increased the neuronal vulnerability to ER stress (Imaizumi *et al.* 2001).

In contrast to classical stress-induced heat-shock protein family members, the so-called heat-shock cognate proteins are constitutively expressed. Hsc70 is abundantly found in unstressed cells, where it plays an important role in protein biosynthesis (Dworniczak and Mirault 1987). It binds to nascent polypeptides to assist correct folding and is involved in the lysosomal protein degradation. It also exhibits an ATPase function and thereby catalyzes the ATP-dependent disassembly of clathrin-coated pits during vesicles transport. Based on its 85% homology with Hsp70 it was presumed that both proteins are functionally

interchangeable (Gething and Sambrook 1992), while a more recent study suggest differential cellular function (Goldfarb *et al.* 2006).

Another cognate, heat un-inducible Hsp70 family member is mortalin (mtHSP70/GRP7), which is located at various subcellular sites including mitochondria. Adapted from its chaperone, mitochondrial import and oxidative stress response functions, it was implicated in cellular aging processes. It has been shown to be involved in old age pathologies like AD and PD (Shi *et al.* 2008). Moreover, mortalin is a major target for oxidation and its overexpression is sufficient to expand the cellular life span (Yaguchi *et al.* 2007).

Hsp70 function

All Hsp70s are composed of three major functional domains to carry out the chaperones reaction cycle, which is regulated by the co-chaperones Hsp40 and Bag-1 and primarily facilitates initial folding of the nascent polypeptide chain: In the “open” ATP bound state of Hsp70 the N-terminal domain exhibits a weak ATPase activity. An α-helical C-terminal domain covers the substrate binding domain, which comprises a groove that binds peptides up to seven neutral, hydrophobic amino acid residues in length. Binding of a target protein to this domain stimulates an increase in the ATPase activity. This is followed by a conformational change of the substrate binding domain to its “closed” ADP bound state leading to tight binding of the peptide chain. In the presence of an interacting substrate ATP hydrolysis is further accelerated by the J-domain co-chaperone Hsp40. Moreover Hsp40 has been suggested to mediate substrate binding, too. Bag-1 acts as a nucleotide exchange factor and thereby facilitates substrate unloading from the chaperone by opening the binding pocket, which is needed to allow for a new reaction cycle. The newly synthesized protein is then released to fold on its own, or further processed by other chaperones (Ohtsuka and Hata 2000; Bukau *et al.* 2006).

Hsp70 protects cells from thermal or oxidative stress, because these stresses usually induce partial unfolding and possible aggregation. By binding to hydrophobic residues exposed during cellular stress (Brown 2007), Hsp70 prevents these partially-denatured proteins from aggregating, and facilitates their refolding. Hsp70 also binds to proteins during their transmembrane transport to stabilize their partially-folded state, which is required for the translocation process (Mayer and Bukau 2005).

As mentioned above, Hsp70 is involved in the degradation of defective or damaged proteins via the lysosome (autophagy) as well as via the ubiquitin proteasom system (see section 1.2.2).

The carboxyl terminus of Hsp70-interacting protein (CHIP), which was identified as a co-chaperone, seems to exhibit E3 ligase function. CHIP increases the folding capacity of

Hsp70 and regulates its chaperone activity (Ballinger et al. 1999) by promoting ubiquitinylation of Hsp70 substrates like the glucocorticoid receptor (Connell *et al.* 2001), Raf-1 protein kinase (Demand *et al.* 2001) cystic fibrosis transmembrane conductance regulator (Meacham et al. 2001), and ErbB2 (Zhou *et al.* 2003) and directing them to degradation through the proteasome. This suggests that regulation by CHIP shifts the function of Hsp70 from a refolding towards a degradation function.

Another consequence of exposure to cell damaging stimuli, in which Hsp70 have been shown to be protective, is induction of cell death mechanisms. Depending on several conditions (e.g. tissue type, severity of insult) cell death occurs by necrosis or apoptosis, or intermediates of these two distinct molecular death mechanisms.

Hsp70 promotes cell survival via its anti-apoptotic function at several levels of apoptotic signaling pathways. Within the extrinsic pathway Hsp70 suppresses the occurrence of pro-apoptotic kinase-mediated signaling including activation of JNK and cleavage of Bid (Park and Liu 2001; Gabai *et al.* 2002). Hsp70 has been shown to inhibit cytochrome c release from mitochondria (Mosser *et al.* 2000)and formation of the apoptosome out of cytochrome c, Apaf-1 and caspase 9 by binding to the caspase recruitment domain of Apaf-1 (Beere *et al.* 2000; Li *et al.* 2000; Saleh *et al.* 2000). Moreover, it enhances expression of the anti-apoptotic factor Bcl-2 (B-cell lymphoma protein 2) (Kelly *et al.* 2002) and inhibits caspase-3 (Mosser *et al.* 1997).

Hsp70 was also found to inhibit caspase-independent apoptotic mechanisms. By sequestration of AIF, Hsp70 decreased the nuclear translocation of AIF. This led to a reduction of AIF-induced DNA fragmentation and chromatin condensation (Susin *et al.* 2000; Matsumori *et al.* 2005). Moreover, Hsp70 inhibited lysosomal membrane permeabilization. Thereby, it prevented the release of cathepsins from the lysosomal lumen to the cytosol, where they might induce mitochondrial outer membrane permeabilization followed by the events of the apoptotic cascade described above (Nylandsted *et al.* 2004).

Chaperone-based therapeutic strategies in neurodegenerative diseases

Protein aggregates or inclusion bodies are distinctive for a variety of neurodegenerative disorders including AD, PD, FALS (familial amyotrophic lateral sclerosis) HD, and related poly-glutamine expansion diseases (Sherman and Goldberg 2001). All these structures are found to be associated with molecular chaperones and components of the UPS.

Neurodegenerative disease	Disease genes	Lesion	Main aggregate component	Co-localization of chaperones with lesions (human brain tissue)	References
Alzheimer's disease	*APP* Presenilin 1 Presenilin 2	Extracellular senile plaques	Aβ peptides (Aβ40, Aβ42)	HSP72 HSP28 αB-crystallin, HSP27 GRP78, HSP90	119 120 121 28
		Intracellular neurofibrillary tangles	Hyperphosphorylated tau	HSP27 HSP90	122 43
Parkinson's disease	α-synuclein Parkin *UCHL1* *PINK1* *DJ1*	Intracellular Lewy bodies	α-synuclein	HSP70, HSP40	50
Dementia with Lewy bodies		Intracellular Lewy bodies	α-synuclein	HSP90, HSP70, HSP60, HSP40, HSP27	47
Familial amyotropic lateral sclerosis	*SOD1*	Intracellular inclusions	Mutant SOD1	HSC70	123
Polyglutamine diseases		Cytoplasmic and nuclear inclusions			
Huntington's disease	*IT15* (huntingtin)		Mutant huntingtin		
Spinocerebellar ataxias (SCA1–3, 7)	ataxins		Mutant ataxin	HSP40, HSP70 HSP40	59 124
Spinal and bulbar muscular atrophy (SBMA)	Androgen receptor		Mutant adrogen receptor		

Tab.1.2 Protein misfolding diseases associated with molecular chaperones. Aβ, amyloid-β; *APP*, amyloid precursor protein; *DJ1*, Parkinson disease (autosomal recessive, early onset) 1; GRP78, glucose-regulated protein 78; HSC70, heat shock cognate 70, HSP, heat shock protein; *PINK1*, phosphatase and tensin induced putative kinase 1; *SOD1*, superoxide dismutase 1;*UCHL1*, ubiquitin carboxyl-terminal hydrolase L1 (taken from Wacker and Muchowski 2005).

This was interpreted as a sign of irreversible protein retention, following cellular incapacity to refold or degrade aggregated proteins properly.

These multiple protective functions characterize molecular chaperones as powerful inhibitors of neurodegeneration. This turns them into interesting therapeutic targets for aggregation-associated neurodegenerative disorders. Molecular chaperones have been proven to reduce toxicity and/or protein aggregation in a variety of experimental models for neurodegenerative proteopathies.

Chaperone-based therapeutic strategies in models of AD (Alzheimer's disease)

In cellular models of AD, transiently overexpressed APP (amyloid precursor protein) was bound by ER-localized chaperone BiP/GRP78 and thereby probably retained from β/γ-secretase cleavage, which resulted in reduced amyloid-β40/42 secretion in a stable cell line (Yang *et al.* 1998). Viral vector-mediated overexpression of Hsp70 rescued primary neurons from the toxic effects of intracellular Aβ-toxicity (Magrane *et al.* 2004). Hsp27 increased the proportion of non-phosphorylated tau and reduced tau hyperphosphorylation, which is the basis for tau release from its physiological mictrotubular location into neurofibrilarry tangles, the second neuropathological hallmark of AD and thereby inhibited tau-toxicity (Shimura *et al.* 2004). In a mouse model, inducible Hsp70 overexpression significantly reduced tau levels (Petrucelli *et al.* 2004). Interaction of Hsp70 and the E3-ligase CHIP assisted tau ubiquitylation and suppressed tau-mediated death in cell culture, although levels of insoluble

ubiquitilylated tau were increased, indicating the partition of soluble toxic protein species into an insoluble compartment as a cellular detoxifying process (Muchowski and Wacker 2005).

Chaperone-based therapeutic strategies in models of FALS

Hsp70 expression was also investigated in a nuclear micro-injection-mediated cellular model for FALS. Co-injection of an Hsp70 expression vector into primary motor neurons expressing toxic mutant was protective against SOD1 aggregation and toxicity. SOD1 (superoxid dismutase) is the main aggregate component found in FALS (Bruening *et al.* 1999). Combined overexpression of Hsp70 and Hsp40 suppressed aggregate formation in neuroblastoma-like cells expressing mutant SOD1 and reduced toxicity to an extent similar to Hsp70 alone (Takeuchi *et al.* 2002).

Chaperone-based therapeutic strategies polyQ disease models

The influence of chaperones on aggregation and toxicity of proteins bearing poly-glutamine (polyQ) expansions have been investigated in a variety of models for polyQ diseases. In cell culture, Hsp40 as well as Hsp70 overexpression inhibited the formation of polyQ inclusion bodies (Chai *et al.* 1999; Jana *et al.* 2000; Kobayashi and Sobue 2001). In one study the ability of Hsp70 to reduce Huntingtin-induced toxicity was mediated by suppression of caspase activity, independently from polyQ aggregation, indicating a dissociation of both phenomena (Zhou *et al.* 2001). In models for polyQ diseases in *Saccharomyces cerevisia* overexpression of the yeast homologues of Hsp70 shifted the formation of large detergent-insoluble into many small Huntingtin aggregates (Krobitsch and Lindquist 2000; Meriin *et al.* 2002). In *Drosophila melanogaster*, Hsp70 overexpression inhibited the polyQ-mediated neurodegenerative phenotype, but did not change the polyQ inclusion body burden (Warrick *et al.* 1998; Warrick *et al.* 1999; Gunawardena *et al.* 2003). Pharmacological activation of HSF1 reduced polyQ-induced compound eye degeneration and inclusion formation and lethality through induction of multiple molecular chaperone expression including Hsp70, Hsp40, and Hsp90 in a dose-dependent manner in a Drosophila model of SCA (Fujikake *et al.* 2008).

In one transgenic mouse model for the polyQ disorder Huntington's disease (HD), overexpression of Hsp70 at up to 15 times endogenous level was insufficient to improve the progressive neurological phenotype (Hansson *et al.* 2003) induced by expression of huntingtin with an expanded stretch of 150 glutamine repeats (Mangiarini *et al.* 1996). However, transgenic overexpression of Hsp70 in mouse model for SCA1 (spinocerebellar ataxia) ameliorated the behavioral and neuropathological phenotype in a gene dose dependent manner (Cummings *et al.* 2001), while it had not effect on inclusion bodies. An intracellular antibody (intrabody) who's binding to a unique epitope of human huntingtin is

enhanced by polyglutamine expansion had been shown to suppress neuropil aggregates and neurological symptoms in a mouse model for HD (Wang *et al.* 2008). Hsp70 overexpression combined with this intrabody improved survival of the HD flies to eclosion, prolonged adult life, reduced neurodegeneration in photoreceptors and slowed aggregation of mutant huntingtin in a combinational approach (McLear *et al.* 2008).

Chaperone-based therapeutic strategies in models of PD

In cell culture models of PD, overexpression of wt or mutant α-synuclein was not sufficient to cause robust inclusion body formation, while treatment with an additional stressor to the cell, such as iron (Hasegawa *et al.* 2004; Roberti *et al.* 2007), proteasome inhibition (McLean *et al.* 2001), MPP^+ (Lee *et al.* 2001), H_2O_2 (Jiang *et al.* 2007) or co-transfection with synphilin-1 triggered aggregation of α-synuclein in cell culture (McLean *et al.* 2001; Shin *et al.* 2005). In the latter model, Hsp70 overexpression remarkably decreased inclusion formation (McLean *et al.* 2002) and the proportion of detergent-insoluble, high molecular mass forms of α-synuclein (Klucken *et al.* 2004a). Consistent with their *in vitro* findings, the authors found a reduction of the same α-synuclein species in transgenic mice expressing α-synuclein, when they crossbred this mouse line with Hsp70-overexpressing mice. Moreover, Hsp70 facilitated a partial protection from α-synuclein-mediated cellular toxicity in that study (Klucken *et al.* 2004a).

Induction of Hsps by heat shock pre-conditioning (Freyaldenhoven and Ali 1997; Quigney *et al.* 2003; Donaire *et al.* 2005) or geldanamycin application, or Hsp overexpression (Fan *et al.* 2006) have been demonstrated to be protective against MPP^+-mediated in cell culture. Besides the protective effect, Fan *et al.* observed a reduction of MPP^+-induced α-synuclein aggregates.

In a *D. melanogaster* model for PD expression of wt or mutant α-synuclein in dopaminergic neurons caused neuronal loss and inclusion body formation. Co-expression of Hsp70 as well as pharmacological induction of Hsp70 by administration of geldanamycin (Auluck *et al.* 2002) resulted in suppression α-synuclein-induced toxicity, which was not accompanied by a changed inclusion body phenotype (Auluck *et al.* 2005). Elevation of the Hsp70 expression either induced by viral vector-mediated gene-transfer (Dong *et al.* 2005) or by intraventricular injection of geldanamycin (Shen *et al.* 2005) emerged to protective dopaminergic neurons in the SNc in the MPTP model of PD.

1.5.3. Viral vector-mediated gene transfer

Since early stages of PD are characterized by a localized neurodegeneration, mainly limited to the dopaminergic neurons of the SNc, gene transfer should be a useful tool deliver

therapeutic molecules to treat PD. Due to their evolution over millions of years viruses are capable to efficiently transfer genes to survive and replicate in mammalian hosts (Verma and Weitzman 2005). This makes viruses the most efficient method to transfer functional genes to the CNS at present. Besides direct *in vivo* gene therapy, *ex vivo* gene therapy is an additional option. It uses viral infection of various cells *in vitro*, which are then grafted into the PD brain (Dass *et al.* 2006). In an experimental primate model for PD GDNF-secreting human neural progenitor cells, which were generated using lentiviral vectors increase tyrosine hydroxylase and VMAT2 expression in MPTP-treated cynomolgus monkeys (Emborg *et al.* 2008).

Recombinant viral vectors such as herpes simplex virus (HSV), adenovirus (AdV), adeno-associated virus (AAV) and lentivirus (LV) have been engineered to transfer genes of interest into target tissues of the adult central nervous system (CNS) (Mandel *et al.* 2008). Viral vectors are also used for the expression of proteins known or suspected to play a role in PD to mimic PD pathology in animal models, which provides new insights in the underlying mechanisms of PD pathogenesis and helps to develop new therapeutic strategies.

1.5.3.1. Adenoviral vectors (AdV)

Recombinant AdV (rAdV) have the longest history of a successful application in the brain (Le Gal La Salle *et al.* 1993) and in animal models of PD (Choi-Lundberg *et al.* 1997; Barkats *et al.* 1998). Wild type AdV (wt-AdV) are medium-sized (90–100 nm), non-enveloped (naked) viruses of icosahedric shape composed of a nucleocapsid and a double-stranded linear DNA genome of 36-38 kb. The over 52 different serotypes cause receptor-mediated infections of the respiratory as well as gastrointestinal tract and conjunctivitis in humans (Modrow and Falke 1997).

Since mitotic and post-mitotic cells can be transduced by rAdV, both neurons and glia are tranduced in the CNS (Akli *et al.* 1993). The genome of wtAdV consists of two ITRs (inverted terminal repeat) that are required for replication, a packaging signal, early genes and late genes. AdV form episomes, because they cannot integrate into the genome (Harui *et al.* 1999; Hillgenberg *et al.* 2001).

The E1A early gene that is needed for viral growth and induction of late genes was deleted in first generation rAdV to generate safe replication-deficient viral vectors and to allow the insertion of therapeutic genes. For viral vector production the E1A gene product are supplied from another plasmid (Danthinne and Imperiale 2000). E1A-deleted first generation type 5 rAdV were successfully used in our laboratory to provide synergistic protective effects of XIAP (X-Chromosome-Linked Inhibitor of Apoptosis) and GDNF (glial cell line-derived neurotrophic factor) expressed under control of strong constitutive CMV promoter in the

MPTP mouse model of PD (Eberhardt *et al.* 2000). Second generation rAdV with E1A, E3/E4 genes deletion, were reported to be effective for the expression GDNF under the control of the cellular GFAP promoter in the 6-OHDA rat model of PD (Do Thi *et al.* 2004).

Expression levels of late viral genes might be reduced by the deletion of early genes, expression of these remaining wt genes induces strong host inflammatory response *in vivo* (Byrnes *et al.* 1996; Dewey *et al.* 1999; Lowenstein and Castro 2003).

rAdV have been successfully engineered to integrate into the genome by addition of a transposon to a helper-dependent (high capacity) rAdV with an increased frequency of integration and enhanced long-term gene expression (Yant *et al.* 2002). In so-called gutless high-capacity vectors only the ITRs are remaining, which is accompanied by the need of helper first generation AdV for viral vector production, only the inverted terminal repeats remain (Parks *et al.* 1996; Hardy *et al.* 1997; Szelid *et al.* 2002). Gutless AdV induce less toxicity, but their transduction efficiency seemed to be reduced, too (Lowenstein *et al.* 2002). Besides that, safety concerns are raised on the fact that removing all helper AdV from the final gutless AdV preparation is difficult and incomplete, and that even small but significant contamination with helper AdV can contribute to adverse inflammatory reactions (Puntel *et al.* 2006). Regardless of its internal genomic structure, there is an innate inflammatory response to AdV infection (Muruve 2004).

Based on their aptitude to induce high levels of transgene expression (Bohn *et al.* 1999; Gerdes *et al.* 2000) in neurons as well as in glia, AdV still are suitable for gene delivery at least in animal models for PD. Another important feature of AdV is their capability to be retrogradely transported to the *Substantia nigra pars compacta* (SNc) by nigrothalamic axons following injection into striatum (Le Gal La Salle *et al.* 1993; Soudais *et al.* 2000; Peltekian *et al.* 2002).

Our lab and others have been successfully used AdV to express transgenes in the SNc after intrastriatal injection of AdV (Eberhardt *et al.* 2000; Kitao *et al.* 2007; Krenz *et al.* 2009). Thus, adenoviral gene transfer to the SNc can be accomplished in a much less invasive way by injection of an AdV preparation to the striatum. In addition, AdV have been used to for efficient gene transfer in primary neuronal cell cultures (Simons *et al.* 1999; Kugler *et al.* 2001; von Coelln *et al.* 2001; Huang *et al.* 2008; Southgate *et al.* 2008) and hardly transfectable cell lines (Bonin *et al.* 2008; Sahara *et al.* 2008), which are both notorious to be hardly accessible by lipid based transfection methods, as well as in organotypic slice cultures (Ridoux *et al.* 1995; Mioduszewska *et al.* 2008). Moreover, a recombinant replication-deficient adenovirus containing (Ad-NURR1) was successfully used to express the NURR1 gene in neural stem cells (NSC) transplanted into 6-hydroxydopamine lesioned rats (Li *et al.* 2007).

Since the technical respectively safety issues appear to be conquerable, gutless AdV might be employed even in human PD therapy in the future (Mandel *et al.* 2008). AdV are produced by viral infection rather than transient transfection of the producer cells, which makes them further attractive for clinical use, because of the ease of scaling-up to clinical levels of vector (Kamen and Henry 2004).

1.5.3.2. Adeno-associated viral vectors (AAV)

WT adeno-associated virus (wt-AAV) is a small non-enveloped parvovirus (≈20 nm) with a broad tissue and cell type tropism for dividing and quiescent cells. It integrates into the host genome preferentially at a specific site on chromosome19. It requires co-infection of a helper virus to enter a lytic cycle for progeny production. Thus, AAV are classified as dependovirus (Kremer 2005).

The linear single-stranded DNA genome with a length of 4.7 kb consists of two non-overlapping open reading frames encoding for three capsid proteins (*cap*) and for four different proteins. These are necessary for virus replication, transcription of the viral genes and host genome integration (rep) flanked by ITRs. ITRs contribute to synthesis of the second DNA strand and to both integration of the AAV DNA into the host cell genome and rescue from it (Weitzman *et al.* 1994; Wang *et al.* 1995). They are required for efficient encapsidation of the AAV DNA and generation of AAV particles in wtAAV, too (Zhou and Muzyczka 1998).

The fact that wt-AAV is not known to be associated with any disease in humans or mammals, makes it an attractive tool for human gene therapy. In recombinant AAV (rAAV) both *rep* and *cap* genes have been deleted, while only the ITRs remain. The structural and packaging genes necessary for vector production are provided *in trans* by transfection of helper plasmids (Cao *et al.* 2000; Hauswirth *et al.* 2000). Thus, rAAV vectors used for gene therapy are devoid of 96% of their genome, which results in a transgene capacity of up to ~ 4.7 kb and one of the highest biosafety ranking among the viral vectors (Mandel *et al.* 2008). On the other hand, deletion of the wt *rep* gene impairs their propensity for the site-specific integration in the chromosomal DNA ending up mainly in an episomal form of the AAV DNA (Duan *et al.* 1998). Nevertheless, rAAV have been proven to mediate stable transgene expression for more than one year (Woo *et al.* 2005; Stieger *et al.* 2006). Ten different AAV serotypes (AAV1 – AAV9, and AAV-Rh10) have been identified at present, among which AAV1-, AAV2-, AAV5-, AAV8- and AAV10-derived viral vectors have been used for in the CNS (Mandel *et al.* 2008).

rAAV2, which has a purely neuronal tropism, is the best serotype for CNS studies (Burger *et al.* 2004). Since the cellular receptors, which mediate the up-take of AAV2 into a cell, are

differentially expressed in different brain regions, rAAV2 is more efficient in some areas such as GPi and SN than in others regions (Klein and Ackerman 2003; Burger *et al.* 2004).
A large proportion of the human population has circulating antibodies to AAV2 as well as other serotypes, which were capable of blocking rAAV transduction in the brain (Peden *et al.* 2004; Sanftner *et al.* 2004; Zaiss and Muruve 2008). Nevertheless, in a phase 1 trial of AAV-mediated expression of glutamic acid decarboxylase (*GAD*) in the STN, neither antibody responses to either the AAV vector or the expressed transgene, occurred during at least 12 month, demonstrating that AAV gene therapy is safe and well tolerated by patients with advanced PD. In this study enhanced activity of GAD, which catalysis the synthesis of the inhibitory neurotransmitter GABA, was capable to balance increased STN activity of PD patients (Kaplitt *et al.* 2007). Another phase I clinical safety trial using intrastriatal infusion of an AAV expression the human aromatic l-amino acid decarboxylase (hAADC) is underway. Preliminary non-blinded analysis of a first cohort of five patients, all of which showed good tolerance of the viral vector infusion, in the absence of controls revealed an average 30% increase in striatal 6-[^{18}F]-fluoro-L-dopa uptake capacity as a marker for DA synthesis, a modest improvement in the clinical symptoms (Eberling *et al.* 2008). Moreover, marrow stromal cells expressing TH after AAV-mediated gene transfer were successfully transplanted into the striatum in the 6-OHDA rat model demonstrating the therapeutic benefit of TH-engineered mesenchymal stem cells for PD (Lu *et al.* 2005). Beside these therapeutic approaches, AAV have been widely used as a tool for transgene delivery in neuroblastoma cells (Wang *et al.* 2005; Wang *et al.* 2006), mouse (Mochizuki *et al.* 2001; St Martin *et al.* 2007), rat (Bjorklund *et al.* 2000; Tian *et al.* 2007) and nonhuman primate models (Kirik *et al.* 2003; Sanftner *et al.* 2005; Bankiewicz *et al.* 2006; Stieger *et al.* 2006).

1.5.3.3. Lentivirus (LV)

Lentiviruses (LV) are complex enveloped single-stranded (+)-RNA viruses and represent a genus within the *retroviridae* family. Many wtLV induce slowly progressing chronic diseases, which is reflected by their designation (lentus = “slow” in Latin), while others are non-pathogenic (Modrow and Falke 1997). Since recombinant retroviruses have the longest history in general gene therapy and HIV is one of the best studied wt viruses, LV have been adapted as vectors for in vivo gene delivery (Naldini *et al.* 1996a). Retroviral genomes are composed of the three genes *gag,* which encodes the matrix, capsid and nucleocapsid proteins, *pol* encoding the viral enzymes protease, reverse transcriptase and integrase, and *env* encoding proteins of the virion envelope. LV have a more complex genome structure, because they additionally contain other regulatory genes such as *tat* and *rev*, as well as other accessory genes including *vif, vpr, vpu*, and *nef*. Reverse transcription of the RNA into

DNA begins prior to internalization and is finished in the cytoplasm. The nuclear import mechanism of this double-stranded proviral DNA in non-dividing cells, via a proteinaceous pre-integration complex facilitates transduction of post-mitotic, including neuronal cells, which distinguishes LV from other retroviruses. The lentiviral coding sequences are flanked by flanked by LTRs (long terminal repeats), which are necessary for integration, transcription and polyadenylation (Naldini *et al.* 1996a; Naldini and Verma 2000; Verma and Weitzman 2005).

Naldini and Trono established HIV-derived vectors in 1996 (Naldini *et al.* 1996b). The core and enzymatic components of these replication-deficient LV come from HIV-1, while the envelope is derived from a heterologous virus, most often vesicular stomatitis virus (VSV) due to the high stability and broad tropism of its G protein (Zhu *et al.* 1990). rLV are generated by co-expressing three viral transfection constructs: a packaging construct, the vector construct containing the LTRs, and a plasmid encoding the VSV-gene (Naldini *et al.* 1996b; Kim *et al.* 1998).

The vector construct, which typically contains the transgene cassette flanked by *cis*-acting elements necessary for its encapsidation, reverse transcription and integration, is the only genetic material entering the target cells (Salmon and Trono 2006).

In the first generation LV packaging system all HIV-1 genes besides the envelope are remaining. To further increase bio safety, two new generations of LV have been developed.

Packaging constructs of the second generation are additionally deleted in all viral auxiliary genes that are unnecessary for vector propagation (*vif, vpr, vpu,* and *nef*). The essential *tat* gene is supplied in a separate plasmid to produce the tat protein *in trans* (Dull *et al.* 1998). A third generation of LV, termed the self-inactivating (SIN) LV has lost the transcriptional capacity of the LTR to vastly reduce the risk to obtain replication competent recombinants and to avoid problems linked to promoter interference after the vector genome has integrated into the host (Zufferey *et al.* 1997; Miyoshi *et al.* 1998). Third generation LV packaging constructs comprise only *gag* and *pol*, while *rev* is provided on a fourth plasmid.

The fact that LV efficiently integrate into the genome (Mitchell *et al.* 2004; Sinn *et al.* 2005) in principle carries the risk of tumor formation. However, VSV-g pseudotyped LV almost exclusively transduce neurons (Naldini *et al.* 1996b; Blomer *et al.* 1997), which preferentially enter an apoptotic pathway rather re-entering the cell cycle (Klein and Ackerman 2003). Another barrier for clinical application of LV-mediated gene transfer is the development of innate and adaptive immune responses to the delivery vector and the therapeutic transgene. Thus, more research is warranted to develop strategies to overcome these obstacles (Follenzi *et al.* 2007). However, LV have been used to explore the neuropathological features of CNS diseases as well as to investigate new therapeutic strategies in different animal models of PD: GDNF-expressing LV conferred a significant protection of nigral DA in the 6-

OHDA model in mice, in the forebrain bundle axotomy in rats, and in the MPTP-model in monkeys (Bensadoun and Aebischer 2006). LV-mediated expression of GPX (glutathione peroxidase) was neuroprotective against the 6-hydroxydopamine in neuroblastoma cell culture as well as in the rats, demonstrating the relevance of antioxidative gene therapy for PD (Ridet *et al.* 2006). Besides that, LV gene transfer was used to develop genetic PD models in diverse animal species (Bensadoun and Aebischer 2006).

1.6. PD models

Models of PD are needed to understand the pathogenesis of the disease, as well as to test the novel therapeutic strategies. A good model should recapitulate both behavioral and neuropathological aspects of PD including dopaminergic cell loss and LB formation, which is not the case in most models at present. In principle, these features can be modeled in two different ways: (i) by exposure to toxins to induce the (selective) destruction of the nigrostriatal system or (ii) by overexpression of the genetically altered forms of proteins, which are involved in familial forms of PD.

1.6.1. Cellular models of PD

Cellular models of cell death and/or inclusion formation have often been used prior and in addition to animal models. Cultured cells are repeatedly accessible in high numbers, which allows rapid screening and comparison of many different conditions in the same experiment. Moreover, pharmacological or genetic manipulations in a large proportion of the cell population are easier to perform then in animal models, which allow the use of biochemical assays that are impossible on a single-cell basis. These pre-evaluations largely reduce the necessary number of animal experiments.

The most commonly used cellular models to study cell death in DA-ergic neurons employ 6-OHDA (6-hydroxydopamine) and MPP^+ (1-methyl-4-phenylpyridinium), which both induce oxidative stress followed by the formation of ROS (reactive oxygen species), inhibition of oxidative phosphorylation and cell death (see section 1.6.2.1). Since both neurotoxins are selectively taken up into the cell by the DAT (DA-transporter), these models require the use of DA-ergic cells lines like SHSY-5Y, PC12 or MN9D. Neuronal differentiation of these immortalized cell lines, which is needed for the induction of a DA-ergic phenotype characterized including DAT expression, can be achieved by retinoic acid treatment. Thus, toxin-induced effects in undifferentiated cells not displaying characteristics of dopaminergic neurons can only be acquired with very high toxin doses and might be rather unspecific. In the differentiated state, cells are often no longer easy to transfect to a large extent, making viral vector-mediated gene transfer necessary (Falkenburger and Schulz 2006).

Since mutations or gene multiplications of α-synuclein have been implied in PD, it was employed to induce the formation of LB-like inclusions. However, overexpression of wt or mutant α-synuclein alone was not sufficient to cause robust inclusion body formation (McLean *et al.* 2001). Thus, co-transfection with synphilin-1 (Chung *et al.* 2001; O'Farrell *et al.* 2001; Lee *et al.* 2002a; Tanaka *et al.* 2004) or treatment with an additional stressor to the cell, such as iron (Hasegawa *et al.* 2004; Roberti *et al.* 2007), proteasome inhibition (McLean *et al.* 2001), MPP^+ (Fan *et al.* 2006), or H_2O_2 (Jiang *et al.* 2007) have been commonly used.

1.6.2. Animal models of PD

To model PD as accurately as possible, besides neuropathological characteristic of PD (loss of dopaminergic neurons and aggregate formation in the SNc), animal models of PD should mimic behavioral features. Although PD does not exist in animals, different toxin-induced and transgenic models have been developed.

1.6.2.1. Toxin-induced models

Neurotoxin-based models producing selective degeneration of the nigrostriatal system include 6-hydroxydopamine (6-OHDA), 1-methyl-4-phenyl-1,2,3,6-tetrahydropyridine (MPTP), rotenone, and paraquat (N,N-dimethyl-4-4-bipiridinium) (Terzioglu and Galter 2008).

6-OHDA

After its initial application in sympathetic heart denervation, the hydroxylated analogue of DA 6-OHDA was already used to model PD associated with SNc dopaminergic neuronal death in the late 1960s (Ungerstedt 1968). 6-OHDA requires direct application into the brain, because it cannot cross the blood brain barrier. The specific toxicity of 6-OHDA for catecholaminergic neurons is due to its preferential uptake by DA and noradrenaline transporters (Terzioglu and Galter 2008). Cell death occurs after the cytosolic accumulation of 6-OHDA, which causes the formation of ROS and toxic quinones (Bove *et al.* 2005). Moreover, 6-OHDA has been demonstrated to impair enzyme activity of cellular anti-oxidants like glutathione and SOD in rat brains, which can further enhance destructive effects of oxidative stress (Schober 2004). When stereotaxically injected into the SNc, 6-OHDA causes an anterograde, while an intrastriatal infusion leads to retrograde degeneration of the whole nigrostriatal system with a DA depletion of up to 97% (Kirik *et al.* 1998; O'Neill *et al.* 2004). Unilateral lesion of nigrostriatal system of rats is the most widely used paradigm for behavioural studies of PD, because injection of DA receptor agonists or amphetamine causes quantifiable circling

behavior. Several other behavioral tasks for the evaluation of fine motor skill tasks and the cylinder test have been developed to further assess striatal DA depletion (Emborg 2004).

MPTP

In 1982s, several drug abusers developed an irreversible, rapidly progressing parkinsonian syndrome following the intravenous injection of an illicit preparation of 1-methyl-4-phenyl-4-propionpiperidine (MPPP), an analog of the narcotic meperidine (Demerol), contaminated with MPTP, which was inadvertently synthesized as a by-product of MPPP. Due to its lipophilic character, MPTP can easily pass cell membranes and the blood brain barrier. In the brain it is converted into the active toxic metabolite MPP^+ (1-methyl-4-phenyl-2,3-dihydropyridium ion) by the enzyme MAO-B (monoamine oxidase B) in non-dopaminergic cells like glia and serotoninergic neurons. MPP^+ is selectively taken up into DA-ergic neurons by the DA transporter (DAT). There it can be transported in to mitochondria and inhibits complex I of the mitochondrial respiratory chain. This causes ATP depletion and increased generation of ROS. In the cytosol both ROS and MPP^+ itself can damage essential cellular macromolecules including lipids, enzymes, and DNA, which might induce neurodegeneration.

Other cell death mechanisms including inflammation, the activation of excitatory amino acid receptors, apoptosis, and autophagia have been implicated in MPTP toxicity, too (Dawson 2000a; Beal 2001). The susceptibility to MPTP seems to depend (i) on MAO-B activity and (ii) on the capacity to sequester MPP+ into synaptic vesicles via VMAT (vesicular monoamine transporters) as cellular protective mechanism, which seems to rely on the ratio of DAT and VMAT. This might explain why rats are relatively resistant to MPTP, different mouse strains react very differently to the toxin, whereas humans are sensitive to MPTP intoxication at quite low doses. Depending on the regimen of MPTP administration in mice, systemic MPTP treatment has been reported to induce either loss of DA-ergic neurons in the SNc and striatal DA depletion alone, or in addition, motor symptoms including bradykinesia, rigidity and posture abnormalities (Sedelis *et al.* 2000).

Paraquat and rotenone

The herbicide paraquat, which has structural similarities to MPTP, is not selectively taken-up by DAT and thus does not accumulate in DA-ergic neurons after systemic administration, but it induces a modest, specific loss of DA-ergic neurons in the SNc (McCormack *et al.* 2002; Ossowska *et al.* 2006). Paraquat toxicity is mediated by redox cycling with cellular diaphorase such as nitric oxide synthase producing ROS.

Rotenone produced in the roots and stems of tropical *leguminosa* plants was widely used around the world as insecticide and piscicide. It affects mitochondrial function at the same

site as MPP^+ by inhibiting the transfer of electrons from complex I to ubiquinone in the mitochondrial electron transfer chain, but it is only mildly toxic for humans and highly unstable, with a short half-life in the environment. In rodents, particularly in rats, chronic infusion has been reported to produce a slowly progressing neurodegeneration of DA-ergic neurons associated with intracellular multiform α-synuclein immunoreactive (IR) aggregates, ocurrence of widespread oxidatively modified DJ-1, and proteasomal impairment (Betarbet *et al.* 2006). However, rotenone has limited usability, because of its low reproducibility and high numbers of drop-outs, caused by acute toxicity, unrelated to central nervous system involvement (Terzioglu and Galter 2008).

1.6.2.2. Genetically modified models

The identification of mutations in genes, which cause familial forms of PD, and susceptibility genes (see section 1.3) allowed to develop transgenic animal models to study mechanisms leading to disease.

Knock-out techniques are used to model recessively inherited loss-of-function mutations in Parkin, DJ-1 and PINK1, all of which cause early-onset PD.

To model the dominantly inherited gain-of-function mutations such as in α-synuclein and leucine-rich repeat kinase 2 (LRRK2), transgenic mice are made via introduction of extra copies of the gene are introduced into the mouse genome.

Transgenic mouse and fly models were created by the overexpression of either human wt or mutant α-synuclein (Feany and Bender 2000; Kahle *et al.* 2000; Masliah *et al.* 2000; van der Putten *et al.* 2000). While the fly model shows adult-onset loss of dopaminergic neurons and the formation of Lewy body-like inclusions (Feany and Bender 2000), the nigrostriatal dopaminergic projections were surprisingly resistant to α-synucleinopathy in transgenic mice, although they tended to be more vulnerable to neurotoxins (Dawson 2000b; Kahle *et al.* 2000; Masliah *et al.* 2000; van der Putten *et al.* 2000; Beal 2001). However, despite the lack of dopaminergic neuronal loss in transgenic mice, these models developed specific neuropathology including somatodendritic accumulation of the transgenic α-synuclein with neuritic distortions.

Thus, they are valuable and relevant to some aspects of synucleinopathies such as PD. First, they reproduce the vulnerability of certain neuronal populations to develop α-synuclein aggregates, which help to identify factors responsible for this predisposition. Furthermore, in some of the models, the occurrence of reduced striatal levels of TH and/or dopamine in the nigrostriatal dopaminergic projection (Richfield, 2002), cognitive decline and motor phenotypes, including impaired rotarod performance, grip strength or stride length, suggests

that the accumulation of α-synuclein can indeed disturb neuronal function significantly, even without inducing cell death. Thus, it was speculated that α-synuclein may induce dopaminergic dysfunction in the early phase of the pathogenic process, possibly leading to cell death at later stages.

Viral vector-mediated gene transfer for the site specific expression of transgenes represents an alternative approach to classical transgenesis. For example expression of α-synuclein using viral vectors induced nigrostriatal degeneration and formation of α-synuclein-positive deposits in rats and non-human primates. Interestingly, viral vector delivery of α-synuclein to the SNc in mice resulted in less α-synuclein pathology and cell loss than in rats and non-human primates (St Martin *et al.* 2007).

1.7. Objectives

PD is a bad disease. Causal treatment does not exist. Therefore it is important to better understand the pathogenesis and test new therapeutic strategies.

Based on the potential role of synphilin-1 in the pathogenesis of PD, it is of interest to elucidate its influence on aggregate formation and cellular viability. The goal of this project was the characterization of synphilin-1 expression in an animal model. We here used an adenoviral gene transfer to study the effects of wild-type (WT) and R621C synphilin-1 in DA neurons in mouse brain. To investigate not only the effects of synphilin-1 alone but also its interaction with synuclein, we investigated not only non-transgenic C57Bl/6 mice but also (Thy1)-h[A30P]αsynuclein transgenic (A30PαSyn) animals.

Proteasomal inhibition is thought to be involved in aggregate formation in neurodegenerative diseases like PD. To test the hypothesis that proteasomal function might be impaired early in the course of the disease, a reporter mouse line expressing Ub^{G76V}-GFP mice were crossbred with A30PαSyn.

As both cellular and animal models have their advantages and disadvantages, Hsp70 was tested both in cell culture and mouse models of PD. As a perfect model of PD does not exist, but both oxidative stress and protein misfolding appear to be important, we used both models based on the mitochondrial toxin MPP, and models based on overexpression of the aggregating protein alpha-synuclein.

Finally, we tested different viral vectors (AdV, LV, AAV) for their capabilities to mediate expression of a protein of interest such as Hsp70 in neuronal cells, specifically in dopaminergic neurons of the SNc *in vivo*.

2. Methods

2.1. Molecular biology

Recombinant DNA techniques were performed according to the protocols described in Molecular Cloning Laboratory Manual, 2nd edition (Sambrook, J. et al., 1989). Primer design and all major cloning steps were first simulated using the Vector NTI® software. Restriction endonucleases and DNA-modifying enzymes were used according to the manufacturer's instructions. Materials including instruments, chemicals, buffers, solutions, antibodies and primers are listed in section 2.10.

2.1.1. Propagation and preparation of plasmid DNA

Plasmids were propagated in DH-5α (Invitrogen GmbH, Karlsruhe), SURE chemicompetent (Stratagene, La Jolla, USA) or chemicompetent BD Fusion-Blue™ Competent Cells (BD Biosciences, Heidelberg) *E.coli* bacteria.

Buffers and Media for bacterial culture

LB-medium: 10 g/l tryptone, 5 g/l yeast extract, 5 g/l NaCl.
LB-plate: LB-medium, 2% (m/v) Agar.
SOC: 20 g/l trypton, 5 g/l yeast extract, 10 mM NaCl, 10 mM $MgCl_2$, 10 mM $MgSO_4$, 20 mM glucose

2.1.1.1. Bacteria culture conditions

All *E. coli* were cultured in LB-Ampicillin liquid or solid (LB-Amp agar plates) medium, at 37ºC. For liquid culture, bacteria were incubated by shaking at 200 rpm o/n.
Glycerolstocks for longterm storage were prepared by adding 150 µl sterile glycerol (100%) to 850 µl o/n culture in a 2 ml screw-cap vial. The vial was vortexed vigorously to ensure even mixing of the bacterial culture and the glycerol, frozen in a dry ice–ethanol bath and stored at –80°C.

2.1.1.2. Heat shock transformation

Heat shock transformations of DH-5α were performed according to manufacturer's instructions. Briefly, after thawing 50 µl bacteria suspension on ice, an appropriate amount of DNA (50-200 ng purified plasmid DNA or 1/10 of a BD In-Fusion™ Dry-Down PCR cloning reaction) was added. Next, cells were gently mixed by finger tapping and incubated on ice for 30 minutes. After a heat shocking in a water bath at 42°C for 45 sec, cells were placed on ice

for 2 min. Next cells were supplemented with 450 µl of SOC medium and incubated at 37°C for 60 min while shaking at 250 rpm. 50–500 µl of the suspension were then spread on LB-amp selective plates and incubated at 37°C o/n.

Sure Shot cells were transformed in a similar manner: 20 µl of bacteria suspension were pretreated by adding 4 µl β-Mercaptoethanol followed by 10 min incubation on ice. 1 µl of the AVV ligation reaction was added, the heat shock was carried out at 42°C for 30 sec. Cells were supplement with only 200 µl SOC medium, the whole suspension was spread on LB-amp plates.

The resulting single colonies were analyzed via colony PCR or used to inoculated LB liquid cultures.

2.1.1.3. Plasmid mini preparation

Buffers for plasmid mini preparation

Resuspension buffer: 50 mM Tris-HCl; 10 mM EDTA; 100 µg/ml RNaseA; pH 8,0
Lysis buffer: 200 mM NaOH; 1% SDS
Neutralization buffer: 3.0 M potassium acetate, pH 5.5

An alkaline lysis method (modified according to Sambrook and Russel, 2001) was used to extract the plasmid DNA from transformed cells.

Three ml of LB-amp medium were inoculated with a single colony picked from a freshly streaked selective LB-Amp agar plate and incubated by shaking at 200 rpm at 37°C. One ml o/n culture was centrifuged (13.000 rpm, 5 min, 4°C) in a microcentrifuge tube, supernatant was discarded. Pelleted bacterial cells were dissolved completely in 160 µl resuspension buffer. 300 µl Lysis Buffer were added, followed by thoroughly mixing by inverting the tube 4–6 times and incubation for 5 min at RT. After adding chilled 350 µl neutralization buffer, the lysate was mixed immediately and thoroughly by vigorously inverting the tube 4–6 times and centrifuged for 10 min at 13,000 rpm (~17,900 x g) in a table-top micro centrifuge. The supernatant was transferred to a fresh tube containing 600 µl room-temperature isopropanol, mixed and centrifuged immediately at ≥15,000 x *g* for 30 min at 4°C. Supernatant was decanted carefully. Next DNA pellet was washed with 70 % EtOH and centrifuged again. The supernatant was decanted and the pellet was air dried for 5-10 min and resuspended in 20 µl TE buffer (10 mM Tris, 1 mM EDTA, pH8.8)

2.1.1.4. Plasmid Midi, Maxi and Mega preparations

To obtain large amounts of plasmid DNA, bacteria cultures were grown in 2x LB-Amp medium and midi, maxi and mega preparations were performed using QIAfilter® Plasmid Kits

according to manufacturer's instructions. A preculture of 100 ml was used to inoculate 1 l 2x LB-Amp medium to produce ~ 0.5-1.0 mg plasmid DNA required for preparation of viral vectors.

2.1.2. Isolation of genomic DNA from mouse tail biopsies

TENS buffer for isolation of genomic DNA

TENS buffer: 100 mM Tris-HCl, 5 mM EDTA, 200 mM NaCl, 0.2% SDS, pH 8.5

Mouse tail biopsies of 0.2-0.5 cm were placed in 1.5 ml reaction tubes and incubated in 0.75 ml TENS buffer containing 0.5 mg/ml Proteinase K in a thermomixer at 650 rpm, o/n at 56°C. 250 µl of 4 M NaCl was added and samples were mixed and centrifuged (13.000 rpm, 10 min, RT). 0.75 ml of the supernatant was carefully transferred to a reaction tube containing 0.5 ml isopropanol. Samples were thoroughly mixed by inverting the tubes 4–6 times and centrifuged for 10 min at 13,000 rpm at RT. Supernatant was decanted carefully. The DNA pellet was washed with 800 µl of 70 % EtOH and centrifuged again. The supernatant was discarded completely; the pellet was dried for 15-20 min at 42°C and resuspended in 50 µl TE buffer (10 mM Tris, 1 mM EDTA, pH8.8).

2.1.3. DNA precipitation

If increased purity and/or the concentration of DNA in the final solution were required, a phenol/chloroform purification followed by a precipitation step was included after the DNA extraction procedures.

An equal volume PCI (phenol/chloroform/isoamyl alcohol, 25:24:1) was added to the DNA solution. Samples were vigorously mixed for 10 sec and centrifuged (13.000 rpm, 10 min, RT). The upper aqueous phase was carefully transferred to a new reaction tube without touching the interphase and mixed with 100% isopropanol or EtOH (70% or 200% respectively of the original volumes) and 3 M Na-acetate (10% of the original volumes). The samples were centrifuged for 20 min at 4 ºC, the supernatant was discarded. The DNA pellets were rinsed with 70% EtOH and centrifuged again. EtOH was carefully removed and the precipitates were air-dried at RT for 5-10 min. The DNA pellet was resuspended in desired volume of ddH_2O or TE buffer.

2.1.4. PCR

PCR (polymerase chain reaction) was used to test plasmids for cDNA insertion and to add restriction sites, necessary for cloning of DNA fragments into respective plasmids, as well as epitope sequences to the cDNA by using corresponding primers.

Prior to the amplification of the DNA sequences of interest, optimal PCR conditions were selected by varying the concentration of $MgCl_2$, the amount of template DNA, annealing temperatures (50-60°C) and the use of additives (DMSO or glycerol). A standard PCR reaction mix typically contained:

reagent (stock concentration)	volume (final concentration)
template (cDNA/plasmid or genomic DNA)	variable (100-200 ng)
10x PCR buffer	2.5 µl
$MgCl_2$ (50 mM)	0.75 µl (1.5 mM)
dNTP mix, 10 mM each	0.2 µl (80 µM total)
forward primer (10 µM)	2.0 µl (125 nM)
reverse primer (10 µM)	2.0 µl (125 nM)
Taq-polymerase (5 U/µl)	0.25 µl
ddH_2O	ad 25 µl

The amplification was performed in Mastercycler Gradient or DNA engine PTC-200 thermocyclers using the following cycling conditions:

step	temperature	duration	number of cycles
initial denaturation	95°C	5 min	1
denaturation	95°C	30 sec	
primer annealing	55°C	1 min	30
elongation	72°C	1 min	
final elongation	72°C	10 min	1

Amplification for genotyping of A30Pα-synuclein required an increased $MgCl_2$ concentration of 2.0 mM and Ub^{G76V} of 2.5 mM. Ub^{G76V}-PCR reactions were additionally supplemented with 1.25% DMSO.

The amplification products were analyzed on 1% agarose gel by DNA electrophoresis. Amplified fragment designed to be inserted into plasmids were purified from the gel using a QIAquick® gel extraction kit.

2.1.5. DNA restriction, electrophoresis, gel extraction

Buffers and solutions for agarose gelelectrophoresis

TAE buffer : 40 mM Tris/Acetat; 1 mM EDTA; pH 8.0
6x TAE loading dye: 30% (v/v) glycerol, 0.25% (w/v) Bromophenol blue, 0.25% (w/v) xylenol cyanol
Agarose gel: 0.5% - 2% Agarose in TAE, 0,001% Ethidiumbromide

To obtain linearized plasmid vectors or to release cDNA fragments from plasmids, preparative restriction digests of 5-10 µg of plasmid DNA were used. Analytic digests to test newly generated plasmid constructs were performed with 100-200 ng plasmid DNA. Appropriate endonucleases in corresponding buffers (Fermentas) were mixed with DNA and left o/n at the temperature specified for each enzyme in the instruction manual of Fermentas. Analysis of the DNA size and purification of DNA fragments were performed by agarose gel electrophoresis. DNA samples were mixed with 6x DNA loading buffer and ddH_2O to reach a final volume of 15-20 µl and separated on an agarose gel in 1 x TAE buffer at 100 V. A DNA ladder (Fermentas) of appropriate range was used a size standard. The DNA bands were visualized by UV-light using a BIO-VISION™ fluorescence documentation system. DNA extraction after gel electrophoresis was performed following QIAquick® gel extraction kit protocol. The concentration of DNA in the final solution was measured with a Nanodrop spectrophotometer at 260 nm.

2.1.6. Cycle sequencing of PCR-amplified DNA

Cycle sequencing was performed in cooperation wit the Department for Neurodegenerative Diseases at the Hertie Institute for Clinical Brain Research, Tübingen using the ABI BigDye® Terminator v3.1 Cycle Sequencing Kit. The BigDye® v3.1 Terminator Ready Reaction Mix contained the four dNTPs with different fluorescence labels (BigDyeTM Terminators), unlabeled dNTPs, AmpliTaq DNA Polymerase FS, $MgCl_2$, Tris-HCl buffer (pH 9.0). Sequencing primers are listed in section **Fehler! Verweisquelle konnte nicht gefunden werden.**. The PCR reaction mix contained:

reagent (stock concentration)	volume (final concentration)
template (cDNA/plasmid DNA)	variable (500-700 ng)
5x PCR buffer	2.0 µl
BigDye® v3.1	2.0 µl
primer (10 µM)	0.5 µl (125 nM)
Taq-polymerase (5 U/µl)	0.25 µl

ddH_2O *ad* 10 µl

The amplification was performed in a DNA engine PTC-200 thermocycler using the following cycling conditions:

step	temperature	duration	number of cycles
initial denaturation	94°C	1 min	1
denaturation	94°C	10 sec	
primer annealing	50°C	5 sec	30
elongation	60°C	4 min	

To obtain clean sequencing data the extension product was purified by EtOH/Na-acetate precipitation. The resulting DNA pellet was redissolved in 15 µl ddH_2O and handed over to a technician of the Department for Neurodegenerative Diseases, who performed the sample electrophoresis on the ABI PRISM® DNA Analyzer capillary sequencer. Sequence analysis and alignment with reference cDNA were performed using the VectorNTI software.

2.1.7. Quantitative real-time PCR (qPCR)

Since our LV contained the WPRE-enhancer element, which becomes part of the 3`UTR of each lentiviral transgene mRNA transcript, the number of transcripts in transduced HEK293 cells was measured to assess lentiviral gene expression. (qPCR) was performed using the intercalating fluorescent SYBR® Green dye to determine titers of lentiviral vector preparations. HEK293 cells were plated in 12-well and treated with 8 µg/ml polybrene the day before transduction. Two wells per LV preparation were infected with 4 µl of the purified LV suspension. At 4 days after infection, total RNA was isolated using the “RNeasy Mini Kit” (Qiagen) according to manufacturer’s instructions. RNA concentration was determined with a Nanodrop spectrophotometer (Nanotech). RNA was digested by RQ1 RNase Free DNase (Promega) and protected against RNases by adding 20 U of RNase Inhibitor RNasin (Promega). 2.5 ug of total RNA was used for reverse transcriptase PCR (M-MLV; Promega). cDNA was diluted 1:50.

qPCR was also employed to analyze 4 ng of phenol-/chloroform-purified genomic DNA to distinguish between homo- and heterozygous A30PαSyn tg mice.

HPLC grade water was used for all reactions including standard or template dilutions. qPCR reactions were prepared using “ABsolute™ QPCR SYBR® Green ROX Mix” (ABgene). Primers are listed in the material section.

reagent (stock concentration)	volume (final concentration)
template (cDNA derived from RNA/genomic DNA)	2.0 µl
SYBR® Green ROX Mix	12,5 µl
forward primer (5 µM)	0.35 µl (70 nM)
reverse primer (5 µM)	0.35 µl (70 nM)
HPLC-grade H_2O	9.8 µl

qPCR was performed in a Stratagene Mx3000P Realtime device (Stratagene) using the following cycling conditions:

step	temperature	duration	number of cycles
enzyme activation	95°C	15 min	1
denaturation	95°C	15 sec	
primer annealing	primer T_m	30 sec	40
extension	72°C	30 sec	
	95°C	30 sec	
melting curve	60°C	30 sec	1
	60-95°C	in 0.5 °C steps	

Fluorescence is detected and measured in real time, and its geometric increase corresponding to exponential increase of the product is used to determine the threshold cycle (CT) in each reaction. The C_T value is characterized as the cycle in which the increasing fluorescence is significantly higher then the background fluorescence for the first time.

Beta-actin mRNA was chosen as reference gene for LV titer determination. Quantifications to determine the ratio between the gene of interest and the reference gene and were calculated using a standard curve based on known amounts of the reference gene. Thus, LV titers correspond to number of WPRE copies/10^4 β-actin copies per µl virus suspension.

GAPDH mRNA served as reference gene for A30PαSyn genotyping. Values were normalized for GAPDH and compared to DNA samples from non-tg, heterozygous, homozygous animals were used as controls of known genotype.

2.1.8. Plasmid construction

2.1.8.1. Cloning into pLV-plasmid

To construct pLV-CMV-HAHsp70, an N-terminal HA-epitope tag was fused to the coding sequence of human Hsp70 (GenBank accession number NM-005345) during PCR amplification from the pTR5-DC/hsp70-GFP*tk/hygro (Mosser *et al.* 2000) template plasmid (kindly provided by Dr. Ulrike Naumann, Hertie-Institute for Clinical Brain Research, Tübingen). The PCR product was inserted into the lentiviral transfer vector pRRLsin.PPTs.hCMV.EGFP (provided by Prof. Luigi Naldini, San Raffaele Telethon Institute for Gene Therapy, Milan, Italy) - after *Age*I/*Bsr*GI release of EGFP cDNA - via homolog recombination with In-Fusion™ PCR Cloning Kit according to manufacturer's instructions. Briefly, PCR was performed using proofreading *PfuTurbo*™ DNA polymerase, to combine high-fidelity DNA synthesis with high PCR product yield and target length capability. Primers are listed in the materials section. The primer sequences shared 15 bases of homology at the 5` end with the *Age*I/*Bsr*GI linearization site of the vector and the forward primer contained the sequence for the HA-tag.
The PCR reaction mix contained:

reagent (stock concentration)	volume (final concentration)
template (pTR5-DC/hsp70-GFP*tk/hygro)	1.0 µl (= 100ng)
10x *PfuTurbo*™ DNA buffer (Stratagene)	5.0 µl
dNTP mix, 10 mM each	0.5 µl (100 µM each)
HA-Hsp70InFusion fw primer(10 µM)	2.0 µl (125 nM)
HA-Hsp70InFusion rv primer (10 µM)	2.0 µl (125 nM)
PfuTurbo™ DNA polymerase (2.5 U/µl)	1.0 µl (2.5 U)
ddH_2O	38.5 µl

The sequential amplification program was performed in a DNA engine PTC-200 thermocycler using the following cycling conditions:

step	temperature	duration	number of cycles
initial denaturation	95°C	5 min	1
denaturation	95°C	1 min	
primer annealing	62°C	1 min	5
elongation	72°C	2 min	
denaturation	95°C	1 min	
primer annealing	65°C	1 min	25
elongation	72°C	2 min	

final elongation	72°C	10 min	1

The PCR fragment and the vector were purified by Ethidiumbromide-free agarose gel electrophoresis followed by gelextraction to avoid Ethidiumbromide-induced mutations and were mixed together at a 2:1 molar ratio in 10 µl of ddH_2O:

vector (6.7 kb)	3 µl (= 100 ng)
insert (2.1 kb)	2 µl (= 60 ng)
ddH_2O	5 µl

This mixture was added to the BD In-Fusion™ Dry-Down Mix reaction tube containing all of the necessary reaction lyophilized components, incubated at room temperature for 30 min and then transferred to ice. The BD In-Fusion reaction mixture was diluted with 40 µl TE buffer. Chemicompetent BD Fusion-Blue™ Competent Cells with an efficiency of ≥$1.0x10^8$ cfu/µg were heat-shock transformed with 2.5 µl of diluted reaction mixture, spread on separate, LB-Amp agar plates and incubated at 37°C o/n. Colonies were picked and pre-screened by colony PCR with the primer set used for Hsp70 insert amplification. Plasmid DNA was isolated via minipreparation. The presence of insert was further confirmed by *Age*I/*Bsr*GI restriction digest. Insert integrity was controlled by complete sequencing.

2.1.8.2. Cloning into pAAV-plasmid

Construction of AAV vectors has been described previously (Kügler, S. *et al.*, 2003). The pAAV-6P-SEWB plasmid (kindly provided by Dr. Sebastian Kügler) expressing EGFP as a fluorescent reporter driven by the human synapsin 1 gene promoter, was used as backbone for cloning of HAHsp70 by substitution of the EGFP cDNA employing a sequential sticky/blunt cloning strategy. The donor plasmid pLV-HAHsp70 was subjected to *Bam*HI/*Sal*I restriction digest to release HA-tagged human Hsp70 cDNA. The EGFP cDNA fragment was removed from pAAV-6P-SEWB via *Bam*HI/*Hind*III restriction digest. The *Bam*HI restriction sites were first ligated at a 1:1 molar ratio:

reagent (stock concentration)	volume (final concentration)
vector (4.8 kb)	1.0 µl (= 200 ng)
insert (2.1 kb)	2.0 µl (= 140 ng)
10x ligase buffer (Fermentas)	2.0 µl
ligase	0.4 µl
ddH_2O	14.6 µl

The *Sal*I and *Hind*III recessed 3`-termini were filled-in and ligated as follows:

reagent (stock concentration)	volume (final concentration)
ligase reaction	1.0 µl
10x ligase buffer	1.0 µl
dNTP mix, 10 mM each	0.2 µl (200 µM each)
Pfu Turbo DNA polymerase (2.5 U/µl)	0.4 µl (1 U)
Ligase (5 U/µl)	0.4 µl (2 U)
ddH_2O	7.0 µl

After incubation for 1 h at RT and then o/n at 4°C, chemicompetent Subcloning Efficiency® DH5alpha™ with an efficiency of ≥1.0x 10^6 cfu/µg were heat-shock transformed with the reaction mix and spread on LB-Amp agar plates. Colonies were picked and pre-screened by colony PCR with the primer set used for HAHsp70 insert amplification (see above). Plasmid DNA was isolated via minipreparation. The presence of insert was further confirmed by *Sma*I restriction digest.

2.2. Cell culture

2.2.1. Culture conditions, transient transfection

Human neuroblastoma SH-SY5Y cells and human embryonic kidney 293 (HEK293 and 293FT) cells were cultured in 75 cm^2 cell culture flasks in DMEM containing 10% FCS and 1% penicillin/streptomycin at 37 °C in a humidified atmosphere of 95% air and 5% CO_2 in a cell culture incubator.

Cells were passaged at 90% confluence one to two times per week: Under sterile conditions, cell culture medium was removed and cells were washed with PBS, before 1 ml of trypsin/EDTA solution was added. Cells were incubated at 37°C until they could be easily detached by tapping the flasks. The cells were thoroughly resuspended in 9 ml cell culture medium to obtain a single cell suspension. 1 ml of the suspension was transferred to a new flask containing 9 ml of fresh medium. With this 1:10 dilution cells reached confluence after 4-6 days.

The cell number was determined via light microscopy in a counting chamber. To perform cell culture experiments and viral vector production, cells were plated at an appropriate density in 6-well, 12-well, 24-well or 96-well cell culture plates or 10 cm or 15 cm dishes. Transient transfection of HEK293 cells with 1 µg of the target vector was carried out in six-well plates using Metafectene transfection reagent according to manufacturer’s instructions.

2.2.2. Viral Infection

For LV infections cells were plated and medium was exchanged to fresh medium containing with 8 µg/ml polybrene to increase infection efficiency of LV one day before infection. The next day, when cells reached 90 % confluence 1-4 µl LV were added.

To infect cells with AdV, the plating medium was exchanged for medium containing 60 MOI of AdV preparations in a volume reduced to 25 % of normal volume. The multiplicity of infection (MOI) is defined as the ratio of number of infectious virus units (PFU) to the number of cells. The corresponding amount of the AdV preparation was calculated as follows:

(MOI/virus titer)* cell number per well = µl of AdV corresponding to MOI

$5*10^5$ cell per well*(60MOI/$9.3x10^6$ PFU/µl) = 3.2 µl AdV preparation per well

After 60 min, another 75% of normal medium volume was added.

2.3. Cell death assays

2.3.1. LDH release assay

LDH (lactate dehydrogenase) release was measured using the Cytotoxicity Detection Kit following the manufacturer's instructions. Briefly, cell culture supernatant was transferred to a microtiter plate and kept at 4°. Cells were then lysed by addition of 5% Triton X-100 and the lysate also transferred to the microtiter plate. Assay reagent was added and LDH measured after incubation at room temperature using a Cytofluor II reader. MPP^+ toxicity was calculated as follows: (LDH in supernatant – *low*)/(*high* – *low*) with *high* = total LDH after cell lysis and *low* = LDH released without addition of MPP^+.

2.3.2. Trypan blue exclusion assay

Cells were seeded in 6-wells. After 12 h, cells were infected with adenoviruses or treated with geldanamycin. After another 24 h, medium was exchanged for new medium containing 5 mM or 15 mM MPP^+. After incubation for 48 and 24 h respectively, the culture medium was transferred to 15 ml tubes on ice, cells were incubated with trypsin/EDTA solution and also added to the tube. Samples were centrifuged (12000 rpm, 4°, 10 min) and pellets resuspended in 100 µl PBS on ice. 100 µl Trypan blue solution was added immediately before counting unstained (= viable) and total cells in a Neubauer chamber. 4 squares of around 100 cells each were counted per sample. Viability was calculated as viable/total cells.

2.3.3. Caspase-3 activity (DEVD-cleavage assay)

Armstrong Buffers for DEVD-cleavage assay

Armstrong Buffer A: 10 mM HEPES, 42 mM KCl, 5 mM $MgCl_2$, 0.1 mM EDTA, 0.1 mM EGTA, 1 mM DTT, 0.5% NP-40, proteinase inhibitor mix *complete* (Roche), pH 7.4
Armstrong Buffer B: 25 mM HEPES, 1 mM EDTA, 0.1% NP-40, 10% sucrose, 3 mM DTT, pH 7.5

Caspase3 activation was measured by cleavage of DEVD-amc as described by Armstrong *et al.* (Armstrong *et al.* 1997). Briefly, cells were plated on 96-well plates at a density of $7x10^4$ cells/well. 24 h later, cells were infected with 60 MOI of AdV-HSP70 or AdV-dE1. At 48 h, cells were exposed to 3 mM, 5 mM or 15 mM MPP^+ for 24 h, with and without addition of 100 µM zVAD-fmk. At 72 h, medium was aspirated and cells were lysed in 50 µl/well of Armstrong Buffer A during an incubation step of 10` at 37°C. DEVD-amc was added to a final concentration of 10 µM in 150 µl/well of Armstrong Buffer B. Fluorescent amc production was measured at excitation 360 nm, emission 460 nm, using a Cytofluor II reader. The activity was expressed as a change in fluorescence units per hour per 100,000 cells. For experiments examining the ability of ZVAD-fmk to inhibit the production of DEVD-amc cleaving activity, cells were washed three times with 200 µl PBS to remove residual inhibitor before cell lysis.

2.4. Proteinbiochemie

2.4.1. Protein extraction

RIPA Buffer for protein extraction

RIPA buffer: 50 mM Tris, pH 8.0, 0.15 M NaCl, 0.1% SDS, 1.0% NP-40, 0.5 % Na-Deoxycholate, 2 mM EDTA, Complete™ Protease Inhibitors, pH 7.4

2.4.1.1. Preparation of cell culture lysates

Medium was aspired from culture dishes and cells were washed with ice cold PBS. Cells were scraped in PBS with Complete protease inhibitor cocktail. In order to decrease the volume, cells were centrifuged for 15 min at 13000 rpm on 4°C. Pellet was resuspended in an appropriate volume of Ripa lysis buffer containing *Complete* protease inhibitor cocktail and left on ice for 30 min for lysis to occur. After centrifugation for 20 min at 13000 rpm at 4°C, supernatant was taken and the insoluble cell debris containing pellet was discarded. For preservation of proteins over a longer period of time aliquots were frozen and kept at -20°C.

2.4.1.2. Preparation of striatal brain tissue lysates

After PBS-perfusion, striata were rapidly dissected and kept in 1.5 ml reaction tubes on dry ice until Ripa buffer was added. Cells were lysed using a Precellys 24 homogenisator.

2.4.1.3. Determination of protein concentration

Protein concentration was determined using the coomassie blue G-based Bio-Rad Protein Assay. A 1:5 dilution of the assay reagent stock solution was prepared in ddH_2O. A standard curve was prepared using bovine serum albumine (BSA) with concentrations ranging from 0-12 µg/µl in ddH_2O. Triplets of known protein concentrations were added into 96-well plates (50 µl) together with samples of unknown concentrations (49 µl of ddH_2O and 1 µl of protein lysate). The assay reagent was added to the final volume of 200 µl. After incubating for 5 min at RT, protein concentrations were assayed by measuring absorbance at 595 nm using a Mithras LB 940 plate reader, equipped with Mikro Win software 2000.

2.4.2. Western blot analysis

2.4.2.1. SDS-PAGE

Buffers for protein separation on SDS polyacrylamide gels

5x Laemmli buffer: 10% Glycerol, 20% SDS (10% (w/v)) 12.5% 0.5 M Tris-Cl, pH 6.8, 5% β-Mercaptoethanol, 5% Bromphenol blue (1% (w/v))
10x Running Buffer: 250 mM Tris/HCl; 1.92 M Glycine; 2% SDS, pH 8.3

For SDS-PAGE the “Protean III mini-gel system was used. Gel components were mixed at the required percentage of acryl amide according to the list below. Samples in 5 x Laemmli buffer containing 20-50 µg of protein were boiled for 5 min on 95°C and cooled down on ice immediately after incubation on 95°C preventing renaturation of proteins. After brief centrifugation samples were subjected to gel electrophoresis at 150 V constant voltage in running buffer. A prestained marker was used as a protein size standard.

Running gel (all volumes in ml)

	8%	10%	12%	15%
30% Acrylamide	1,3	1,7	2	2,5
1.5 M Tris/HCl pH 8.8	1,3	1,3	1,3	1,3
10% SDS	0,05	0,05	0,05	0,05
10% APS	0,05	0,05	0,05	0,05
TEMED	0,002	0,002	0,002	0,002
H_2O	2,3	2	1,7	1,2

Stacking gel (all volumes in ml)

	4%
30% Acrylamide	0,33
0,5 M Tris/HCl pH 6.8	0,5
10% SDS	0,02
10% APS	0,02
TEMED	0,002
H_2O	1,25

2.4.2.2. Immuno blot

Buffers and Solution for protein transfer

Transfer buffer: 25 mM Tris, 192 mM Glycine, 20% methanol, pH 8.3
Ponceau solution: 0.1% Ponceau-S in 5% Acetic acid
TBS: 10 mM Tris/HCl, 150 mM NaCl, pH 7.5
TBS-T: TBS with 0.1 % (v/v) Tween20
Blocking solution: 5% (w/v) skim milk in TBS
Stripping buffer: 0.2 M Glycine, 0.5 M NaCl, pH 2.8

Separated proteins on SDS-PAGE were transferred to a nitrocellulose membrane. Nitrocellulose membrane, Whatmann paper and foam pads were first soaked in 1x Transfer buffer. A sandwich was built up on the cathode containing 1 x foam pad, 1 x 3 mm paper, gel, nitrocellulose membrane, 1 x 3 mm paper, 1 x foam pad. The anode was fitted and the transfer performed for 1 h at constant voltage (100 V). The transfer was checked by dying a membrane with Ponceau-S solution.

The transfer membrane was placed for 1 h in blocking solution. Subsequently membrane was incubated with the primary antibody, appropriately diluted in blocking solution at 4°C o/n. The next day, the membrane was washed 3x10 min with TBS-T and incubated with an

adequate HRP-coupled secondary antibody, appropriately diluted in locking solution, for 1 h at RT. Membrane was washed again 3 x 10 min prior to incubation with the Chemiglow chemiluminescent substrate (Alpha Innotech) for 5 min. Bound proteins were visualized using the AlphaImager video imaging device equipped with Fluor Chem 8900 software (Alpha Innotech), which was also used for signal quantification.

Primary and secondary antibodies were stripped off from the membrane, when the same membrane was incubated with another antibody. The membrane was washed in TBS-T (3x10 min, RT) and incubated in stripping buffer for 5 min at RT. After washing in TBS (3x5 min, RT), the membrane was subjected to another immuno blot detection.

2.5. Viral vector preparation

2.5.1. Adenovirus production

Adenoviral vectors coding for human wildtype (WT) and R621C mutant (R621C) synphilin-1 were generated according to standard protocols (Luo *et al.* 2007) and have been described previously (Marx 2004). Briefly, 5`-FLAG-tagged cDNA of WT (GenBank accession number NP 005451) and R621C (amino acid exchange introduced by directed *in vitro* mutagenesis) synphilin-1 were cloned into pAdTrack-CMV. This shuttle vector is an E1/E3 region deleted replication-defective adenovirus serotype 5 derivative and contains an independent EGFP reporter driven by a CMV promoter. Recombinant adenoviral plasmids were generated in *E. coli* by homologous recombination between the shuttle and pAdEasy-1 backbone vectors.

Viral particles were produced by transfection of HEK293 suspension cells with such plasmids. Viruses were concentrated and purified by a cesium chloride (CsCl) density gradient banding procedure. The virus bands from each AdV were collected and pooled. The final virus pool was then transferred into Slide-A-Lyzer dialysis cassette with molecular weight cut-off of 10,000 and dialyzed extensively against 2.5 l dialysis/storage buffer (PBS with 10% glycerol). The virus titer (plaque forming units/µl) was determined by limited dilution plaque assay on HEK293 cells. The titers of wt (AdV-wtSph) and R621C syphilin-1 (AdV-R621CSph) adenoviruses were $1x10^8$ PFU/µl. Adenoviruses generated from pAdTrack-CMV expressing the EGFP reporter with a titer of $0.4x10^8$ PFU/µl served as vector control.

2.5.2. Lentivirus production

LV coding for HA-tagged Hsp70 or eGFP were produced in 293FT cells by calcium phosphate-mediated transient transfection of four plasmids: a transfer vector, the core packaging construct, the reverse transcriptase construct and the envelope construct. Viral particles were purified by ultracentrifugation according the protocol from the Tronolab

webpage. It is noteworthy that the pRRLsin transfer construct contains a woodchuck hepatitis post-transcriptional control element (WPRE) which stabilizes mRNA, resulting in a higher rate of protein expression

1.0-1.2x10^7 293FT cells were seeded in 17 ml DMEM per 15 cm dish 24 h prior to transfection. To prepare 2 ml calcium-phosphate precipitate for each 15 cm dish (8-16 dishes per virus preparation) a plasmid DNA mix was prepared as follows:

9.0 µg pMD2G (envelope)
16.25 µg pMDLg/p (core packaging)
6.25µg pRSV-Rev (reverse transciptase)
25 µg pRRLsin (transfer vector)

The plasmid solution was filled up to 1125µl with 0.1xTE/H_2O (2:1) and mixed with 125µl 2.5 M $CaCl_2$. Then 1250 µl 2x HBS buffer (280mM NaCl, 100mM Hepes, 1.5mM Na_2HPO4, 7.11≤pH≤7.13) was added drop wise while vortexing full speed. The precipitate was kept for 30` at room temperature and then added drop wise to the cells. After 14-16 h medium was replaced with 20 ml HEPES buffered fresh medium. Cell supernatant was collected at 48 h and 72 h post transfection, spinned (3000 rpm/5 min/RT), filtered through a 0.45 µm sterile filter and stored at 4°C until all supernatants was harvested.

Supernatants were transferred to 33 ml ultracentrifugation tubes to concentrate the lentiviral vectors by ultracentrifugation (26000 rpm/2 h/4°C) in a swing-out rotor. The resulting pellets were pooled and resuspended as completely as possible in 100-300 µl DPBS (Invitrogen). Aliquots were stored at -80°C.

2.5.3. Adeno-associated virus production

AAV-2 were produced by Sebastian Kügler according to standard protocols of the CMPB viral vector service platform (Shevtsova 2006). Briefly, vectors were propagated in AAV-293 cells (Stratagene) using pDP as helper plasmid. Viruses were concentrated and purified by an iodixanol (Opti PrepTM Fresenius Kabi, Norge, Axis-Shield) step gradient procedure. The virus was further purified and concentrated by collecting the “peak” elution phase on Äkta-FPLC system using HiTrapTM Heparin HP columns (Amersham). Further concentration and purification of rAAV-2 particles was done by dialysis using Slide-A-Lyzer, (molecular weight cut-off = 10,000). The final virus solution was subjected to real-time PCR (RT-PCR) quantification of the rAAV-vector genome particle titer. Purity of the vectors was determined by SDS-gel electrophoresis and infectious titer by transduction of cultured primary cortical neurons. The genome particles to transducing units (TU) ratio typically was 25:1 - 35:1 and

was calculated as 30:1. The AAV vectors were aliquoted and stored at -80°C until used. During all procedures with AAV vectors, 0.5% SDS solution in water was used for disinfection.
The genome titers of AAV used in this study were $10.0x10^9$/µl for AAV-HAHsp70 and $4.7x10^9$/µl for AAV-EGFP, resulting in a transducing titer $3.0x10^8$ TU/µl for AAV-HAHsp70 and $1.6x10^8$ TU/µl for AAV-EGFP.

2.6. Animal work

PBS (Phosphate buffered saline) of the following formulation was commonly used in many of the methods described below:

10x Stock Solution of PBS buffer

10x PBS: 1.37 M NaCl, 82 mM Na_2HPO_4, 15 mM KH_2PO_4, 27 mM KCl, pH 7.4

2.6.1. Housing, strains and genotyping

2.6.1.1. Animal housing and strains

Animal experiments were carried out on mice, in accordance with the German Animal Welfare Act (TierSchG) and approved by Regierungspräsidium Tuebingen and Hannover.
Male and female mice were obtained from Charles River or were breed in the animal facilities of the Universities of Tuebingen and Goettingen respectively. Mice were maintained in a temperature/humidity-controlled environment under a 12 h light/dark cycle with free access to food and water.
The following mouse strains were used:

C57Bl/6-J non-transgenic wildtype mice, designated as non-tg mice.

(Thy1)-h[A30P]αSynuclein transgenic mice, designated as A30PαSyn mice (see section 3.1).

UbG^{76V}-GFPxA30PαSyn double transgenic mice, designated as UbGFPxA30P mice.

2.6.1.2. Genotyping

Genotyping of transgenic mice was performed by PCR using genomic DNA extracted from tail biopsies as template with the primer sets previously described by the suppliers of the

transgenic mouse line (see section **Fehler! Verweisquelle konnte nicht gefunden werden.**).

2.6.2. Surgery

2.6.2.1. Stereotaxical injections

Mice were anesthetized with an intraperitoneal injection of ketamine/xylazine solution (100 respectively 5 mg/kg bodyweight) and placed with flat skull position in a stereotaxic frame. A mineral oil-sealed glass capillary was fitted into a Nanoliter2000 microinjector and filled with the required volume of virus preparation. After slitting the scalp with a scalpel, a hole of 1 mm diameter was milled into the skull to insert the tip of the capillary to the respective coordinates relative to bregma. Injections were made as one or two deposits along the needle tract at the coordinates listed below.

Structure (total inject. vol)	Needle tract	anterior	lateral (left)	ventral (from skull surface)
Striatum (6 µl)	rostal-medial	+1.0 mm	1.9 mm	3.0, 4.0 mm
	caudal-lateral	+/- 0 mm	2.5 mm	2.2, 3.5 mm
S. nigra (1.5 µl)	rostral	-2.7 mm	1.3 mm	4.2 mm
	caudal	-3.4 mm	1.3 mm	4.2 mm
Pons (2µl)		-5.5 mm	1.0 mm	4.5, 5.0 mm

After two minutes injection was started with a rate of 250 nl/min. The capillary was left in place for an additional 2 min before moving to the after coordinates in the same needle tract and 5 min before withdrawal.

As post-operative treatment, mice were kept warm with a heating pad and received two subcutaneous 0.5 ml deposits of glucose and NaCl solution and were provided with wet mashed food.

2.6.2.2. Continuous minipump infusion of MPTP

Mice were subcutaneously implanted with osmotic minipumps (Alzet) that released MPTP-HCl at 30 mg per kg bodyweight and day according to Fornai *et al.* Each pump was filled with 242 ml saline containing MPTP (nominal rate of delivery: 6.24 ml/day; MPTP concentrations was 96 mg/ml corresponding to 30 mg/kg and day of MPTP free base).

2.6.3. Tissue preparation and processing

2.6.3.1. Paraffin sections

Mice were sacrificed using CO_2 and transcardially perfused immediately with 35 ml of 0.1 M PBS (pH 7.4) followed by 35 ml of ice-cold 4% paraformaldehyde in PBS after pinching *aorta abdominalis*. Brains were removed, post fixed in the same fixative o/n and dissected either sagitally or coronally between striatum and substantia nigra using a matrix. Coronal sections were trimmed to 3 mm thickness. The tissue was further processed in an automatic tissue processing station (Leica Microsystems, Bensheim) using a standard protocol, supplied by the manufacturer before being cast in paraffin blocks using a paraffin tissue embedding station (Leica Microsystems, Bensheim). Rotary microtome sections (6 µm thick) were mounted on charged glass slides (SuperfrostPlus®) or on nitrocellulose membrane for PK-PET blot.

2.6.3.2. Cryosections

Mice were sacrificed using CO_2, the brains were rapidly removed, immersion fixed in 4% paraformaldehyde (PFA) in PBS o/n and cryoprotected in 20% sucrose until tissue was heavier than PBS on a rolling incubator, at 4°C, and then rapidly frozen by immersion in isopentane on dry ice. Complete sets of serial coronal sections were cut through striatum and Substantia nigra pars compacta (SNc) at 30 µm on a cryomicrotome and collected in 24 well plates in PBS with 0.1% NaN_3.

2.6.4. Behavior

The motor activity of the AAV-injected cohort was examined by monitoring their horizontal and vertical movements in an open field to determine, whether there was a difference between the EGFP control and the HAHsp70-treated group. Since these 18-month old syn-tg mice already showed a slightly unsteady gait, the motor activity of mice was increased amphetamine to elucidate differences which might be covered by the deteriorated motor function. Animals were surveyed in a 50 x 50 cm arena by using the “Videomot2” video tracking system (TSE Systems GmbH, Homburg) during the whole experiment. Rearing was detected by infrared beams. The tracking arena was divided into a “center” and a “border” zone using the Vidoemot 2 software. The time, distance, number of visits, latency, number of rearing and rear time in each area was tracked for trails of 5 min.

At 8 weeks after AAV-injection, mice were placed separately into the arena, which was virtually dived into a center and a border zone. After a tracking period of 30 min each mouse

was subjected to intraperitoneal amphetamine injection (3 mg/kg body weight) and tracked for another 90 min. At the end of the experiments, mice were returned to their housing cages.

2.6.5. Histology

Histological staining of 30 µm cryosections was done after placing the sections on glass slides. Immunohistochemistry was performed free-floating.
6 µm paraffin sections had to be deparaffinized with xylene (2x10 min) and rehydrated using a descending ethanol series (100%, 96%, 90%, and 70%, vol/vol EtOH, ddH_2O, 2x5 min each) before staining.

2.6.5.1. General histology

Nissl Staining

After deparaffinization und hydration to distilled water or following DAB immunohistochemical staining, paraffin sections were rinsed in ddH_2O, stained in a solution containing 0.1% thionin, pH 5.5 for 5-7 minutes, rinsed in ddH_2O, pre-dehydrated in 70% and 90% EtOH (2 min each) and differentiated in 96% EtOH for 5 minutes, dehydrated in 100% isopropanol (2x5 min), cleared in xylene (2x5 min) and mounted with resinous medium (DPX mount).

Thioflavine S

Slides were rinsed in distilled water, placed in 1% ThioflavineS solution for 5 min, differentiated in 70% EtOH for 5 minutes, rinsed in ddH_2O thoroughly (at least two changes) and mounted in mowiol-containing medium.

2.6.5.2. Immunohistochemistry and immunocytochemistry

Buffers for histology staining

PBS: 137mM NaCl, 8.2 mM Na_2HPO_4, 1.5 mM KH_2PO_4, 2.7 mM KCl, pH 7.4
PBS: PBS/0.02% TritonX100
TBS: 0.1 M Tris, 150 mM NaCl, pH 7.4
Citrate Buffer: 10 mM Citric Acid, pH 6.0, for heat induced antigen retrieval
(3x15 min microwave boiling, let cool down to RT)
Mowiol-mounting medium: 24% w/v Glycerol, 0.1 M Tris-base pH 8.5, 9.6% w/v Mowiol 4.88 and 2.5% w/v DABCO.

Antibodies are listed in section 2.10.7.

All immunohistochemical stains were performed according to the following general protocol: After washing 3x5 min with washing buffer, sections were pretreated for epitope retrieval, if necessary, washed again and incubated in blocking solution for 1h at room temperature. Incubation with the primary antibody was followed by 1h incubation with the secondary antibody, washing and mounting.

For fluorescent (multiple) labeling, fluorochrome-conjugated secondary antibodies were used. For light microscopy, the antibody reaction was visualized by 3,3V-diaminobenzidene (DAB) staining using the avidin–biotin complex (ABC) Vector kit. Detailed protocols depending on tissue type and detection method are listed below. Note that detection of the HA-tag was only possible, when blocking was omitted.

<table>
<tr><th></th><th colspan="2">Light microscopy</th><th colspan="2">Fluorescent microscopy</th><th>HA-tag</th></tr>
<tr><td>Section type</td><td>free floating cryo section</td><td>paraffin section mounted on glass slide</td><td>free floating cryo section</td><td>paraffin section mounted on glass slide</td><td>paraffin section mounted on glass slide</td></tr>
<tr><td>Wash</td><td colspan="2">3x5 min in TBS</td><td>PBS-T 3x5 min</td><td>3x5 min in PBS</td><td>3x5 min in TBS</td></tr>
<tr><td>Pre-treatment</td><td colspan="2">Quenching endogen peroxidase (5 min 3%H_2O_2/10%Methanol)</td><td></td><td>microwave (Citrate buffer) if necessary</td><td>40 min TBS/0.02% Triton</td></tr>
<tr><td>Wash</td><td colspan="5">see above</td></tr>
<tr><td>Block</td><td colspan="4">10% NGS</td><td>NO!</td></tr>
<tr><td rowspan="2">1st Ab</td><td colspan="2">diluted in TBS/2% NGS</td><td colspan="2">diluted in PBS/2% NGS</td><td rowspan="2">diluted in TBS, o/n 4°C and 1h 37°C</td></tr>
<tr><td colspan="4">o/n 4°C</td></tr>
<tr><td>(Wash)</td><td colspan="5">see above</td></tr>
<tr><td>2nd Ab</td><td colspan="2">biotin-conjugated, diluted in TBS 2% NGS</td><td colspan="2">fluorochrome-conjugated, diluted in PBS 2% NGS</td><td>diluted in TBS 1% BSA</td></tr>
<tr><td>Wash</td><td colspan="5">see above</td></tr>
<tr><td>Detection</td><td colspan="2">ABC-Kit/DAB</td><td colspan="2">fluorescence</td><td>(i) ABC-Kit/DAB or (ii) fluorescence</td></tr>
<tr><td>Mounting</td><td colspan="2">DPX mount</td><td colspan="2">mowiol</td><td>(i) DPX (ii) mowiol</td></tr>
</table>

2.6.5.3. PK-digested paraffin-embedded tissue blot

Buffers and solutions for PK-PET blot staining

TBS-T: 10mM Tris-HCl, pH 7.8, 100 mM NaCl, 0.05% Tween-20
PK-Digest Buffer: 10 mM Tris-HCl, pH 7.8; 100 mM NaCl; 0.1%Brij-35
Denaturation Buffer: 4 M guanidine isothiocyanate in 10 mM Tris-HCl, pH 7.8
Blocking solution: 0.2% casein (Applied Biosystems), in TBS-T
NTM Buffer: 100 mM Tris-HCl, pH 9.5; 100 mM NaCl; 50 mM $MgCl_2$

The PK-digested paraffin-embedded tissue (PK-PET) blot was performed as described by (Neumann *et al.* 2002) with minor modifications: 6-µm sections from paraffin-embedded tissue were cut on a rotary microtome, placed in a water bath (55°C), collected on a wet 0.45-µm nitrocellulose membrane, dried and weight down o/n at 55°C. The sections on the nitrocellulose membrane were deparaffinized with xylene and rehydrated using a descending isopropanol series, prewetted with TBS-T and digested o/n at 55°C with 50 µg/ml Proteinase K (PK) in PK-Digest-Buffer. After washing 3x5 min with TBS-T, the membranes were treated with denaturation buffer for 15 min for optimal epitope retrieval, followed by 3 washes and preincubation in blocking solution for 1 h. Immunostaining of α-synuclein was performed with monoclonal LB509 anti- α-synuclein antibody (epitope amino acids 115-122, 1:1000 in blocking solution for 1 h) and an alkaline phosphatase-coupled goat anti-mouse antibody as a secondary antibody (1:250 in blocking solution, for at least 1 h). Antibody incubation steps were followed by washing 5x10 min with TBS-T. After adjusting the membranes to alkaline pH by incubation 2x5 min in NTM buffer. Antibody reaction was visualized the by formazan reaction using a nitro blue tetrazolium chloride/5-bromo-4-chloro-3-indolyl phosphate, toluidine salt solution (NBT/BCIP, stock solution 1:50 in NTM buffer). To facilitate microscopy, blots were mounted on glass slides with Sylgard® silicone elastomer.

2.7. Microscopy

Confocal images were collected with a Leica DMIRE2 microscope (63x oil immersion objective) equipped with a TCS SP2 AOBS system and Leica DM SDK software (Leica Microsystems, Bensheim).

Cell culture was observed and documented using an inverted Nikon Eclipse TS100 fluorescence microscope (Nikon, Düsseldorf) equipped with a Nikon E5400 digital camera (Nikon, Düsseldorf).

All other images were acquired using an inverted fluorescence microscope (Leica DMI6000B) equipped with 2.5x, 10x, 20x, 40x, 63x dry and 63x water objectives , Leica

FX350 (black/white) and FX450 (color) digital cameras digital cameras and the Leica Advanced Flurorescence Software.

2.8. Quantifications

All quantifications were performed blinded for treatment.

2.8.1. Manual counting

Images acquired with a 20x objective were used to count EGFP-positive neurons among TH-positive neurons to determine the percentage of infected neurons. The percentage of infected neurons containing ThioS-positive inclusions was determined as follows: only EGFP-positive neurons were evaluated for ThioS staining. Many large cells showed a round, 'soft' ThioS-positive structure in the nucleus. This was not sufficient to consider a cell ThioS-positive. Three sets of images were evaluated per animal.

2.8.2. Particle analysis

PK-PET blots from sagital sections of both hemispheres were analyzed by automatic particle counting using the ImageJ software (NIH, USA). The left hemisphere was investigated for viral vector-mediated effects, while the right hemisphere served as internal negative control.
Mosaic images of the whole pons region composed of 50-60 single pictures were acquired with a 20x objective (DMI6000B) using the ScanModule of the Leica Advanced Flurorescence Software. The region of interest was defined on mosaic images from adjacent paraffin sections by outlining the virus expression area detected by using the EGFP fluorescence or anti-HA-tagged Hsp70 immunohistochemistry signals. The number of particles on PK-PET blots within this region of interest was then evaluated using the AnalyzeParticles feature of the ImageJ software. The number of particles was normalized with respect to the non-injected contralateral hemisphere.

2.8.3. Stereology

Stereological counts were carried out with the optical fractionator method (StereoInvestigator, MBF Bioscience, Magdeburg). The criterion for counting an individual signal (cell or aggregate) was its presence either within the counting frame, or touching the right or top frame lines (green), but not touching the left or bottom lines (red). The total number of was then determined by the StereoInvestigator program.
The number of PK-resistant α-syn aggregates was counted using an oil-immersion 63x objective (Axioskop 2, Zeiss), a counting frame of 100x100 µm and a grid size of 200x200 µm.

The number of SNc dopaminergic neurons was determined by counting Nissl-positive and TH-immunoreactive neurons in that same fashion using a counting frame of 50x50 µm and a grid size of 100x100 µm, while the region of interest was confined to the SNc.

2.8.4. Optical density

To quantify TH-IR terminals in the striatum, seven coronal sections throughout the striatum were stained for TH with ABC Plus kit as described above and the optical density of photographs evaluated with ImageJ software. The regions of interest (striatum or cortex) on the sections were outlined and the mean gray values for the regions were determined. Striatal values were normalized by subtracting the background staining, measured in the cortex of the same section. To determine the effect of viral over-expression of synphilin-1, the density of TH-IR terminals was normalized with respect to the uninjected contralateral side.

2.9. Statistics

Data are expressed as means + SEM. Statistical analysis was performed by One-way ANOVA with Bonferroni post test and unpaired t-tests using GraphPad Prism 4.0 (GraphPad Software). Significance levels were set at *P < 0.05, **P < 0.01 and ***P < 0.001.

2.10. Materials

All supplier companies listed below are located in Germany unless otherwise stated.

2.10.1. Equipment

Instruments

Autoclave	
Systec V-50	Systec GmbH, Wettenberg
Capillary Sequencer	
ABI PRISM® DNA Analyzer	Applied Biosystems, Foster City, USA
Cell-counting chamber	
Neubauer cell chamber	Glaswarenfabrik Hecht GmbH, Sondheim/Rhön
Centrifuges and Rotors	
Biofuge Fresco with rotor 3325	Thermo Fisher Scientific, Dreieich
Biofuge Pico with rotor 3324	
Megafuge 1.0R with rotor 2252	
Sorvall® RC 5C plus	

with rotors SLA-3000 and SLA-600 TC	
Developing machine	
FMP 800 A	Fujifilm Europe, Düsseldorf
ECL-camera system	
AlphaImager EC	Alpha Innotec Corporation, San Leandro, USA
Electrophoresis chambers for agarose gels	
Mini Sub Cell GT	Bio-Rad Laboratories GmbH, München
Fluorescence multiwell plate reader	
Cytofluor II	Applied Biosystems, Foster City, USA
Gel documentation	
BioVision Video documentation system	Peqlab Biotechnologie, Erlangen
Heat blocks	
Thermofixer comfort	Eppendorf Deutschland, Hamburg
Incubators	
Sanyo CO_2-Inkubator MCO 18AIC	MS Laborgeräte, Wiesloch
Luminometer	
Mithras LB 940 plate reader	Berthold Technologies, Bad Wildbad
Micromanipulator	
Nanoliter2000 microinjector	WPI (World Precision Instruments), Berlin
Microtomes	
Rotary Microtome RM2245	Leica Microsystems, Bensheim
Cryostat	
Microscopes	
Axioskop 2	Zeiss, Göttingen
Leica DMI6000B	Leica Microsystems, Bensheim
Leica DMIRE2 microscope (confocal)	
Wilowert A	Helmut Hund GmbH, Wetzlar
pH meter	
CG843/14pH	Schott Instruments GmbH,
Pipets	
Biohit mLine (10, 20, 200, 1000 µl)	Biohit Deutschland GmbH, Rosbach v. d. Höhe
Gilson Pipetman (10, 20, 200, 1000 µl)	Gilson International B.V., Limburg-Offheim
Eppendorf Reference (10, 20, 200, 1000 µl)	Eppendorf Deutschland, Hamburg
Photometers	
NanoDrop 1000 Spectrophotometer	Thermo Fisher Scientific, Dreieich
Spectrafluor Fluorescence Spectrophotometer	Tecan Deutschland GmbH, Crailsheim
Power supplies	
Power-Pac 300	Bio-Rad Laboratories GmbH, München
Power-Pac 3000	
SDS-PAGE- and Blotting-Apparatus	
Mini-PROTEAN® II-Electrophoresis-System	Bio-Rad Laboratories GmbH, München

PROTEAN® II xi-Electrophoresis-System	
Shakers	
Incubation shaker Unitron	Infors HT, Einsbach
Roller Shaker "Assistent" RM5	Glaswarenfabrik Hecht GmbH, Sondheim/Rhön
Orbital platform shaker Rotamax 120	Heidolph Instruments GmbH & Co.KG, Schwabach
Vortex-Genie 2	neoLab Migge Laborbedarf GmbH, Heidelberg
Sterile bench	
HeraSafe HSP	Thermo Fisher Scientific, Dreieich
stereotaxic frame	WPI (World Precision Instruments), Berlin
Scales	
MC1 Laboratory LC420	Sartorius AG, Göttingen
Micro, Type M5P	
Thermocycler	
Mastercycler Gradient	Eppendorf Deutschland, Hamburg
MJ research DNA Enginge PTC-200	Bio-Rad Laboratories GmbH, München
MX3000P™ Real time PCR system	Stratagene, La Jolla, USA

Consumables

Gel blotting paper	
Type GB3000	Whatman GmbH, Dassel
Nitrocellulose membranes	
PROTRAN® Nitrocellulose transfer membrane	Whatman GmbH, Dassel
0.45 µm nitrocellulose membrane	Bio-Rad Laboratories GmbH, München
Cell culture plastic	
BD Falcon 6-/24-/48-/96-*well* cell culture plates	BD Biosciences, Heidelberg
Costar® cell culture bottles, 75 cm^2	Corning GmbH, Life Sciences, Wiesbaden
Cell scraper	Corning GmbH, Life Sciences, Wiesbaden
Histology/PK-PET blot	
SuperfrostPlus® glass slides	Menzel-Gläser, Braunschweig
Surgery:	
sterile scalpel blades, syringes, canules	B. Braun Melsungen AG, Melsungen

2.10.2. Chemicals and Biochemicals

All chemicals not listed below were purchased from the following companies: Amersham Pharmacia Biotech (Freiburg), Merck KGaA (Darmstadt), Carl Roth GmbH (Karlsruhe), or Sigma-Aldrich Chemie GmbH, Taufkirchen.

Chemicals and Biochmicals

Ac-DEVD-AMC	Bachem Distribution services Weil am Rhein
Acrylamide 2K-Solution (30%, Mix Acrylamide:Bisacrylamide; 37,5:1)	AppliChem, Darmstadt
Ammoniumpersulfate (APS)	Sigma-Aldrich Chemie GmbH, Taufkirchen
Ampicillin	Sigma-Aldrich Chemie GmbH, Taufkirchen
BenchMark® Prestained Protein Ladder	Invitrogen, Karlsruhe
Bovine serum albumin (BSA)	Sigma-Aldrich Chemie GmbH, Taufkirchen
Brij-35	Sigma-Aldrich Chemie GmbH, Taufkirchen
Bromphenolblue	Merck, Darmstadt
Casein-I-Block	Applied Biosystems, Foster City, USA
CHAPS	Sigma-Aldrich Chemie GmbH, Taufkirchen
Chemiglow chemiluminescent substrate	Alpha Innotec, San Leandro, USA
Chloroform	Sigma-Aldrich Chemie GmbH, Taufkirchen
Complete® Proteases-Inhibitor-Cocktail	Roche Diagnostics GmbH, Mannheim
DAB	Sigma-Aldrich Chemie GmbH, Taufkirchen
DABCO	Sigma-Aldrich Chemie GmbH, Taufkirchen
Desoxynucleosid-5'-triphosphate (dNTPs)	Invitrogen GmbH, Karlsruhe
Dimethylsulfoxide (DMSO)	Sigma-Aldrich Chemie GmbH, Taufkirchen
DPX mounting medium	Fluka, Neu-Ulm
EDTA-solution (0.5 M)	BioWhittaker, USA
Ethanol, absolute extra pure	Merck, Darmstadt
Ethidiumbromide	Sigma-Aldrich Chemie GmbH, Taufkirchen
GeneRuler® 1 kb-DNA-Ladder	Fermentas Life Sciences, St. Leon-Rot
GeneRuler® 100 bp-DNA-Ladder	Fermentas Life Sciences, St. Leon-Rot
Glycine	AppliChem, Darmstadt
Guanidine isothiocyanate	Mobitec Molecular Biotechnology, Göttingen
HEPES	Fluka, Neu-Ulm
Hoechst 33258	Molecular Probes, USA
Hydrogen peroxide (30%)	Merck KGaA, Darmstadt
Isopropanol (molecular grade)	Sigma-Aldrich Chemie GmbH, Taufkirchen
Metafectene transfection reagent	Biontex Laboratories, Martinsried
Mowiol 4.88	Calbiochem, Darmstadt
N,N,N',N'-Tetramethylethylendiamin (TEMED)	Carl Roth GmbH, Karlsruhe
NaCl solution (0.9%, steril, for injection)	B. Braun Melsungen AG, Melsungen
Naturaflor® Milk powder	Töpfer GmbH, Dietmannsried
NBT/BCIP stock solution	Roche Diagnostics GmbH, Mannheim
NP-40	Sigma-Aldrich Chemie GmbH, Taufkirchen
Paraformaldehyde (PFA)	Riedel-deHaën, Seelze
Polybrene	Sigma-Aldrich Chemie GmbH, Taufkirchen

Ponceau S	Sigma-Aldrich Chemie GmbH, Taufkirchen
Potassium chloride	Roth,Karlruhe
Potassium dihydrogen phosphate	Fluka, Neu-Ulm
Prestained SDS-PAGE Standard (Broad Range)	Bio-Rad, München
Sodiumdodecylsulphate (SDS)	AppliChem GmbH, Darmstadt
ß-Mercaptoethanol	Fluka (Sigma-Aldrich)
Sulfosalicylic acid	Sigma-Aldrich Chemie GmbH, Taufkirchen
Thioflavine S	Sigma-Aldrich Chemie GmbH, Taufkirchen
Trichloracetic acid	Merck KGaA, Darmstadt
Triton X-100	Sigma-Aldrich Chemie GmbH, Taufkirchen
Trypan Blue solution (0.4%)	Sigma-Aldrich Chemie GmbH, Taufkirchen
Tween® 20	Roth, Karlsruhe
Xylencyanol	Fluka (Sigma-Aldrich)
z-VAD-FMK	Bachem Distribution services Weil am Rhein

2.10.3. Media, supplements and buffers for cell culture

Dulbecco's Modified Eagle Medium (DMEM)	PAN-Biotech, Aidenbach
Dulbecco's Phosphate Buffered Saline (DPBS),	Invitrogen GmbH, Karlsruhe
Fetale Calf Serum (FCS)	Invitrogen GmbH, Karlsruhe
Penicillin/Streptomycin	PAN Biotech, Aidenbach

2.10.4. Enzymes

ABsolute™ QPCR SYBR® Green Rox Mix	Abgene, Epsom, UK
Complete™ protease inhibitors	Roche Diagnostics GmbH, Mannheim
PfuTurbo™ DNA polymerase	Stratagene, La Jolla, USA
Proteinase K	Roche Diagnostics GmbH, Mannheim
Restriction endonucleases	Fermentas Life Sciences, St. Leon-Rot
T4 ligase	Fermentas Life Sciences, St. Leon-Rot
Taq Polymerase	Fermentas Life Sciences, St. Leon-Rot
Trypsin/EDTA	Invitrogen GmbH, Karlsruhe

2.10.5. Pharmaca and Narcotics

Bepanthen eye and nose ointment	Bayer, Leverkusen
D-Amphetaminesulfate	Sigma-Aldrich Chemie GmbH, Taufkirchen
Ketamine solution Ketanest-S	Pfizer Pharma GmbH, Berlin
MPTP	Sigma-Aldrich Chemie GmbH, Taufkirchen
Xylazine	

2.10.6. Kits

Vectastain® ABC Kit	Vector Laboratories Inc., Burlingham, USA
ABI BigDye® Terminator v3.1Sequencing Kit	Applied Biosystems Inc, Foster City, USA
Biorad Protein Assay	Bio-Rad Laboratories GmbH, München
Cytotoxicity Detection Kit (LDH)	Roche Diagnostics GmbH, Mannheim
In-Fusion™ Dry-Down PCR Kit	BD Biosciences, Heidelberg
QIAfilter® Plasmid purification Kits	Qiagen GmbH, Hilden
QIAquick® Gel extraction Kit	Qiagen GmbH, Hilden
QIAquick® PCR purification Kit	Qiagen GmbH, Hilden
Sylgard® silicone elastomer Kit	WPI (World Precision Instruments), Berlin

2.10.7. Antibodies

Primary antibodies	
EGFP, polyclonal rabbit, # SC-8334 (WB: 1:3000; IHC: 1:500)	Santa Cruz Inc. Santa Cruz, USA
FLAG, mooclonal mouse, # 200471, 1:2000	Stratagene, La Jolla, USA
GFAP, polyclonal rabbit, # Z0334, 1:500	Dako Deutschland GmbH, Hamburg
HA, monoclonal mouse, # MMS-101R (WB: 1:1000; IHC: 1:500)	Covance Inc., USA,
NeuN, monoclonal mouse # MAB377, 1:500	Chemicon Temecula, USA
synphilin-1, polyclonal rabbit, # S5946, 1:200	Sigma-Aldrich Chemie GmbH, Taufkirchen
synphilin-1, polyclonal rabbit, # 1007, 1:1000	provided by C. O'Farrell, Jacksonville, USA
TH, monoclonal mouse, # MAB5280, 1:1000	Chemicon Temecula, USA
TH, polyclonal rabbit, # AB152, 1:1000	Chemicon Temecula, USA
α-synuclein, monoclonal mouse, # LB509, 1:1000 (epitope aminoacids 115–122)	Zymed, Berlin
β-Actin, monoclonal mouse, # A-5441, 1:10000	Sigma-Aldrich Chemie GmbH, Taufkirchen

secondary antibodies	
HRP-sheep anti-mouse Ig, #NXA931, 1:5000	Amersham Pharmacia Biotech, USA
HRP-donkey anti-rabbit IgG, #NA934V, 1:5000	Amersham Pharmacia Biotech, USA
Alexa555 goat anti-rabbit IgG, (red), 1:1000	Invitrogen GmbH, Karlsruhe
Alexa555 goat anti-mouse IgG, (red), 1:1000	Invitrogen GmbH, Karlsruhe
Alexa488 goat anti-mouse IgG, (red), 1:1000	Invitrogen GmbH, Karlsruhe
Alexa488 goat anti-rabbit IgG, (red), 1:1000	Invitrogen GmbH, Karlsruhe
Biotin goat anti-rabbit IgG, 1:200	Jackson ImmunoResearch Laboratories, Inc.USA

2.10.8. Cell lines

293FT (HEK293 cells expressing SV40 T-antigen)	Invitrogen GmbH, Karlsruhe
HEK293 (human embryonic kidney)	Microbix Biosystems, Canada
SH -SY5Y (human neuroblastoma)	DSMZ, Detusche Sammlung von Mikroorganismen und Zellkulturen, GmbH, Braunschweig

3. Results

3.1. The (Thy1)-h[A30P]αSyn transgenic mouse model

(Thy1)-h[A30P]αSyn-transgenic mice (A30PαSyn) were generated and characterized by Prof. P.J. Kahle (Neumann *et al.* 2002) to study the *in vivo* consequences of expression of human [A30P] α-synuclein, driven by the brain neuron-specific promoter Thy-1. Mice of the line 31 used in the present study express high levels of transgenic protein (~ two times more relative to the endogenous α-synuclein level) in whole brain (Kahle *et al.* 2000). In most cases the animals showed no movement disability, up to 16 month of age. With increasing age a progressive deterioration of locomotor function was observed in all animals, accompanied by aggregation of the transgenic A30P α-synuclein into PK-resistant inclusions (Fig. 3. 1).

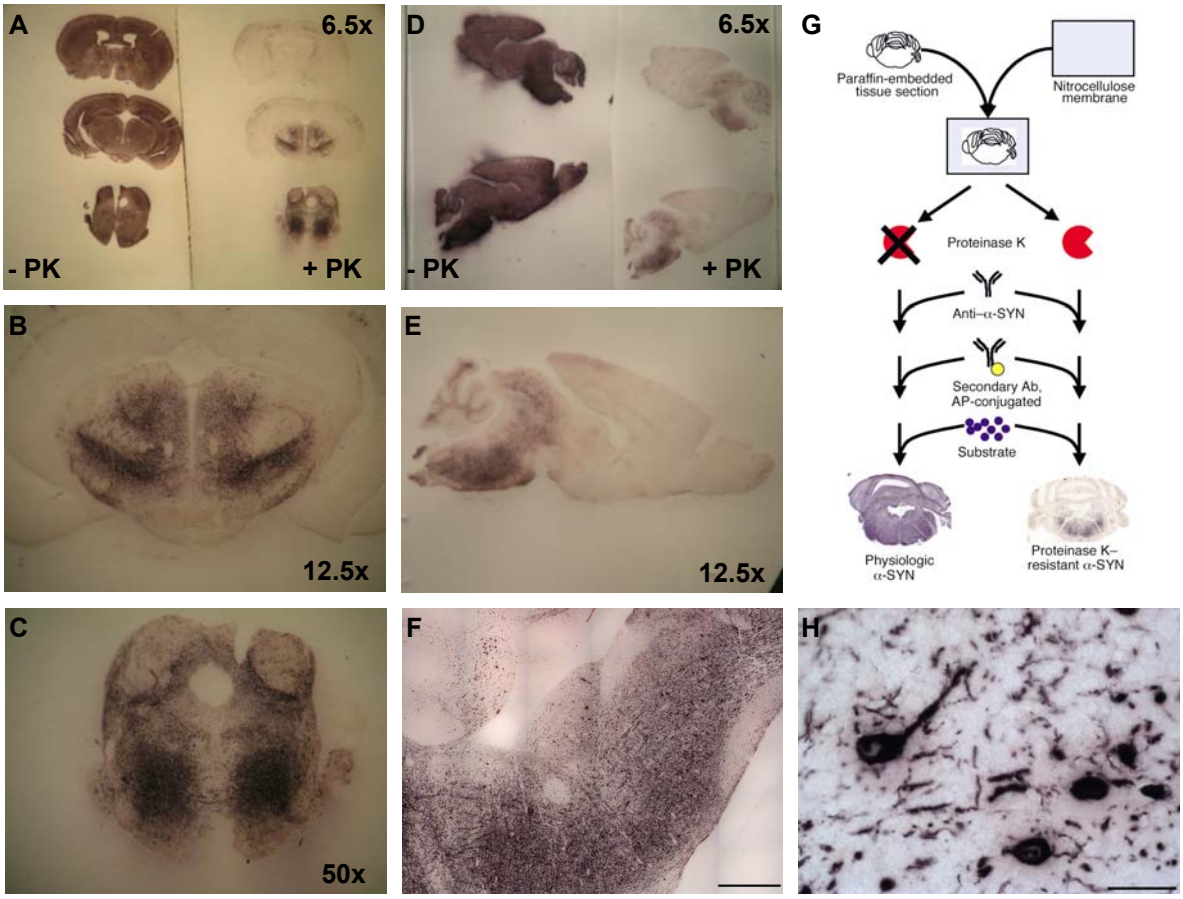

Fig. 3. 1 Detection of PK-resistant α-synuclein in aged A30PαSyn mice using the PK-Pet blot technique. (A-C) Coronal sections and **(D-F, H)** sagital sections of aged, 18-month-old (Thy1)-h[A30P]αSyn-tg mice showing Proteinase K (PK)-resistant α-synuclein predominantly in the pons/midbrain region. Control sections in left panels of (A) and (D) were not treated with PK (-PK), which leads to an equal staining for transgenically overexpressed A30P-α-synuclein. **(B, C)** Higher magnifications of (A), **(E)** higher magnification of (D) **(A-D)** were acquired from dry PK-PET blots using a stereoscope and a digital camera. X-times numbers indicate overall magnification. **(F)** Mosaic image of the whole pons region composed of 36 single pictures, acquired with a 20x objective from a Sylgard-embedded PK-PET blot. Scale bar is 1 mm. **(G)** General principle of the PK-PET blot

technique (Dickson 2002). Paraffin-embedded paraffin sections are blotted onto nitrocellulose membrane and dried. After deparaffinization and rehydration, the diagnostic blots are reacted harshly with the proteolytic enzyme PK (right), while control blots are incubated without PK (left). The enzymatic reaction followed by immunodetection of α-synuclein using an appropriate primary antibody. Immunoreactive profiles are visualized by binding of a matched secondary antibody coupled to alkaline phosphatase (AP) which reacts with a colorigenic formazan dye. While undigested PET blots display the abundantly expressed "normal" α-synuclein (lower left), the PK PET blots reveal the pathological protease-resistant α-synuclein (lower right). This procedure provides the basis of a novel diagnostic method to detect and characterize protein deposits in neurodegenerative diseases. **(H)** Higher magnification of (F) showing the fine structure of the PK-resistant α-synuclein inclusions. Scale bar is 50 µm.

The onset of symptoms correlated with the timepoint when these aggregates became detectable with the PK PET blot technique and Thioflavine S (Fig. 3. 2), which is an established stain of beta-sheet structure, but varied within a time window of up to 2 months. Consequently, the extent of the aggregate burden to a certain timepoint was hard to predict. Therefore, the animals were classified as “symptomatic” as soon as they showed an unsteady gait. This criterion in our hands assured that the aggregate load was above the detection limit of PK PET blot and ThioS staining. This was mainly the case at an age of 18 month. As described by Kahle and Neumann, counterstaining with an anti-TH antibody revealed no ThioS aggregates in TH-positive neurons in the SNc, but abundant aggregates in the pons.

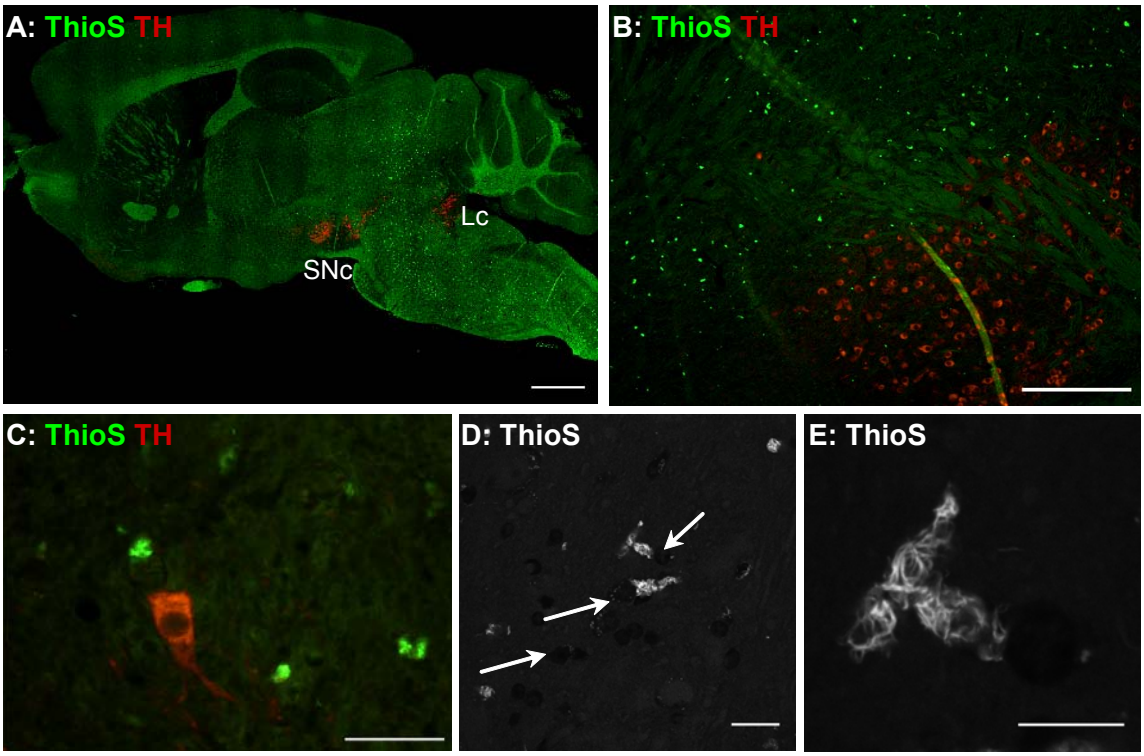

Fig. 3. 2 Thioflavine S aggregates in aged A30PαSyn mice. (A-C) Sagital paraffin section of an aged, symptomatic 18-month-old A30PαSyn mouse showing numerous ThioS stained inclusions (green) in the pons/midbrain region, but not in dopaminergic neurons of the *Substantia nigra pars compacta* (SNc) and the *locus coeruleus* (Lc). Dopaminergic neurons were counterstained by an antibody against tyrosine hydroxylase (red). **(A)** Mosaic image composed of 128 single pictures using a 10x objective. Scale bar is 1 mm. **(B, C)** are higher magnifications of the SNc region in (A), scale

bars are 200 µm (B) and in 50 µm in (C). **(D, E)** Confocal images of ThioS stained inclusions showing the fibrillary fine structure of the ThioS-positive inclusions. Haematoxilin staining was used to quench unspecific ThioS background staining and to counterstain cell nuclei (arrows). Scale bar in (D) represents 20 µm. (E) higher magnification of (D), scale bar is 10 µm.

3.2. Aggregate formation and toxicity by wild-type and R621C synphilin-1 via adenoviral gene transfer

The aim of this project was to determine the influence of synphilin-1 on aggregate formation and neuronal viability in an animal model. Since our laboratory successfully used adenoviral gene transfer to the nigrostriatal system (Eberhardt *et al.* 2000), we used human wildtype as well as R621C mutant synphilin-1 expressing AdV (AdV- AdV-sphWT, AdV-sphR621C) to in addition investigate the role of the R621C mutation. The AdV contained an additional independent EGFP reporter gene cassette; infected cells thus expressed not only synphilin-1 but also EGFP. To control for unspecific effects of virus infection, an AdV encoding for EGFP only (AdV-EGFP) was used. The plasmid constructs used for the production AdV-EGFP, AdV-wtSph and AdV-R621CSph were previously cloned and tested for transgene expression in cell culture in our laboratory (Marx 2004).

We first determined whether synphilin-1 could induce aggregates in the aggregation-prone pons region of young, presymptomatic A30PαSyn mice. This experiment served as a qualitative preliminary test and was carried out without a control group. We therefore did not perform a quantitative analysis. Indeed, injection of WT synphilin-1 (AdV-sphWT) and R621C synphilin-1 (AdV-sphR621C) expressing adenoviral vectors induced the formation of PK-resistant α-synuclein aggregates in young adult 3-month-old non-symptomatic A30PαSyn mice assayed by the PET blot technique (Fig. 3. 3.)

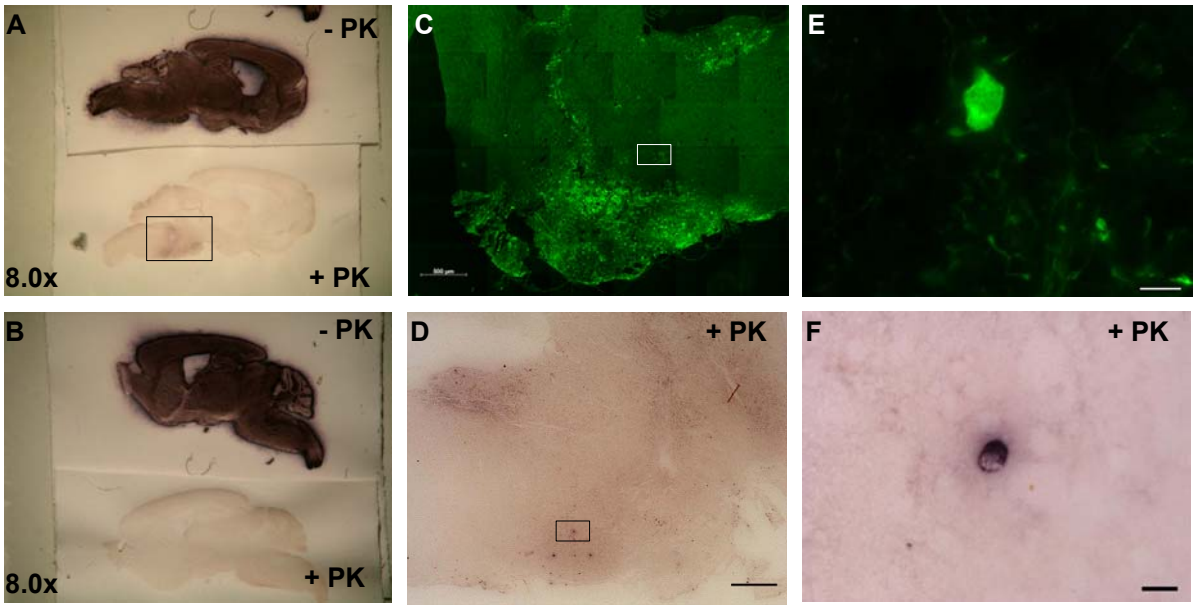

Fig. 3. 3 PK-resistant α-synuclein inclusions induced by synphilin-1 expression in the pons of young, pre-symptomatic A30PαSyn mice. (A-F) Sagital paraffin sections of a young, adult pre-symptomatic 3-month-old A30PαSyn mouse two weeks after injection of 1.5 µl AdV-sphWT. **(A, B, D, F)** PK PET blots for detection of PK-resistant α-synuclein in the **(A)** left (injected) hemisphere (arrow) and **(B)** right hemisphere (non-injected control). Control sections in upper panels of (A) and (B) were not treated with PK (-PK), which leads to an equal staining for transgenically overexpressed A30P-α-synuclein. **(A,B)** were acquired from dry PK-PET blots using a stereoscope and a digital camera. X-times numbers indicate overall magnification. **(C)** Mosaic image of the pons region composed of 36 single pictures. Scale bar is 500 µm. **(E)** Higher magnification of (C) showing a single EGFP, meaning AdV-infected cell in the region boxed in (C). Scale is 10 µm. **(D)** Pons region of a Sylgard-embedded PK PET blot, showing the region boxed in (A). Scale bar is 1 mm. **(F)** Higher magnification of (D) showing the fine structure of synphilin-1 induced inclusion in the region boxed in (D). Scale is 10 µm.

3.2.1. Targeted transduction of the nigrostriatal system by stereotaxic AdV injection

To express synphilin-1 in dopaminergic neurons *in situ*, we took advantage of the fact that the delivery of adenoviral vectors (AdV) to the striatum allows transgene expression in the substantia nigra pars compacta (SNc) by retrograde axonal virus transport, which entails fewer side-effects than a direct injection of virus into the SNc.

AdV for an EGFP reporter cassette in combination with wildtype (WT) (AdV-sphWT) or mutant R621C synphilin-1 (AdV-sphR621C) were stereotaxically injected into the left striatum of mice. Unspecific effects of virus infection were controlled with an AdV expressing EGFP only (AdV-EGFP). To obtain an effective distribution of the AdVs throughout the striatum, AdVs were unilaterally injected in four sites as two deposits along two needle tracts. This resulted in a broad transgene expression throughout the striatum (Fig. 3.5A). As a result of virus uptake by dopaminergic axon terminals in the striatum and retrograde transport to the SNc, dopaminergic neurons in the SNc were similarly infected. Stereologically countings of TH-positive neurons were used to determine the viability of dopaminergic neurons in the SNc. Since transgene expression was restricted to the injected side in all animals, we used the uninfected contralateral hemisphere as an internal control.

In aged A30PαSyn mice injection of $3.0x10^8$ PFU of the AdVs in a total volume of 8 µl and an expression period of 14 days had severe side effects characterized by inflammatory infiltrates (Fig. 3.4C) and pearl chain-like appearance of dendrites in the SNc (Fig. 3.4D), which were due to inflammatory tissue reactions.

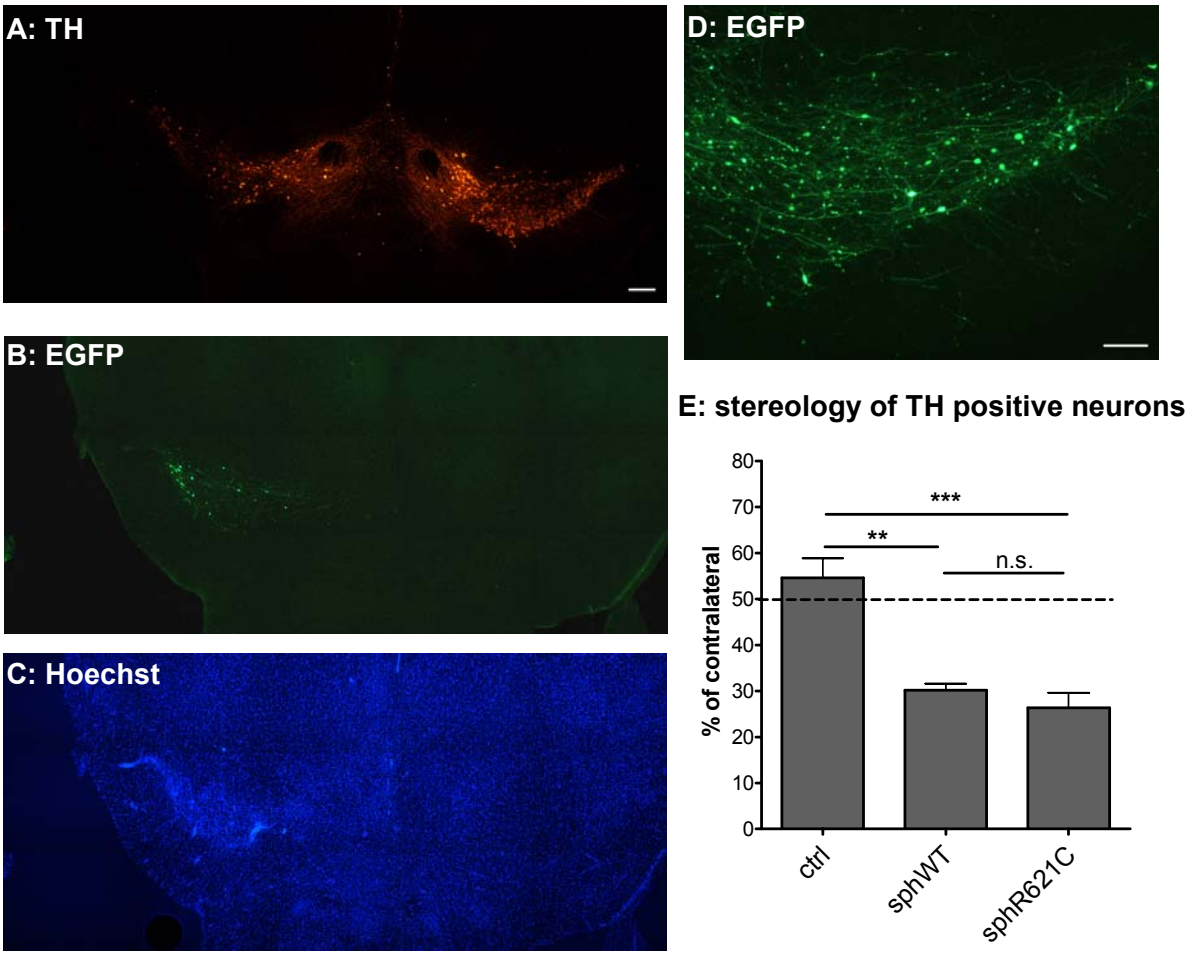

Fig. 3.4 Transgene expression in substantia nigra after adenovirus mediated gene transfer into the striatum of aged A30PαSyn mice. (A-D) Coronal midbrain sections 14 days after infection of control adenovirus expressing the EGFP reporter (AdV-EGFP, $3.0x10^8$ PFU) into the ipsilateral striatum of a A30PαSyn mouse showing **(A)** SNc dopaminergic neurons stained for TH (scale bar in (A) is 200 µm), **(B)** EGFP fluorescence and **(C)** nuclear staining with Hoechst indicating infiltration of immune cells. **(D)** Close-up of the SNc showing infection and expression of EGFP. **(E)** The number of dopaminergic neurons in the SNc was counted by stereology of TH-positive neurons. Adenoviral vectors were injected into the striatum of aged, 1-year-old A30PαSyn animals. Bars represent the number of dopaminergic neurons relative to the uninjected side as mean ± SEM; n = 3 animals for ctrl and n = 4 for sphWT and sphR621C. Comparisons were made by one-way ANOVA and Bonferroni posttest. **P < 0.01, *P < 0.0005.

After injection of the AdV-EGFP control vector, we observed AdV-induced toxicity, which reduced viability of dopaminergic neurons to 50%. Both synphilin-1 vectors induced a similar loss of dopaminergic neurons of about 70% (Fig. 3.4E).

Thus, the experimental conditions were varied to establish a set of parameters, which showed low toxic side effects together with acceptable infection efficiency. $2.4x10^8$ PFU of the AdVs in a total volume of 6 µl were used with an expression period of seven days. Besides that, we decided to perform the experiment in young animals and to include non-transgenic C57Bl/6 mice (non-tg).

Injection of AdV-EGFP, AdV-sphWT, AdV-sphR621C into the left striatum of 6-month-old non-tg and mice gave widespread transgene expression in striatum (Fig. 3.5A) and SNc (Fig. 3.5B,C). Expression of synphilin-1 in dopaminergic neurons was verified by immunohistochemistry against synphilin-1 (Fig. 3.5D-F).

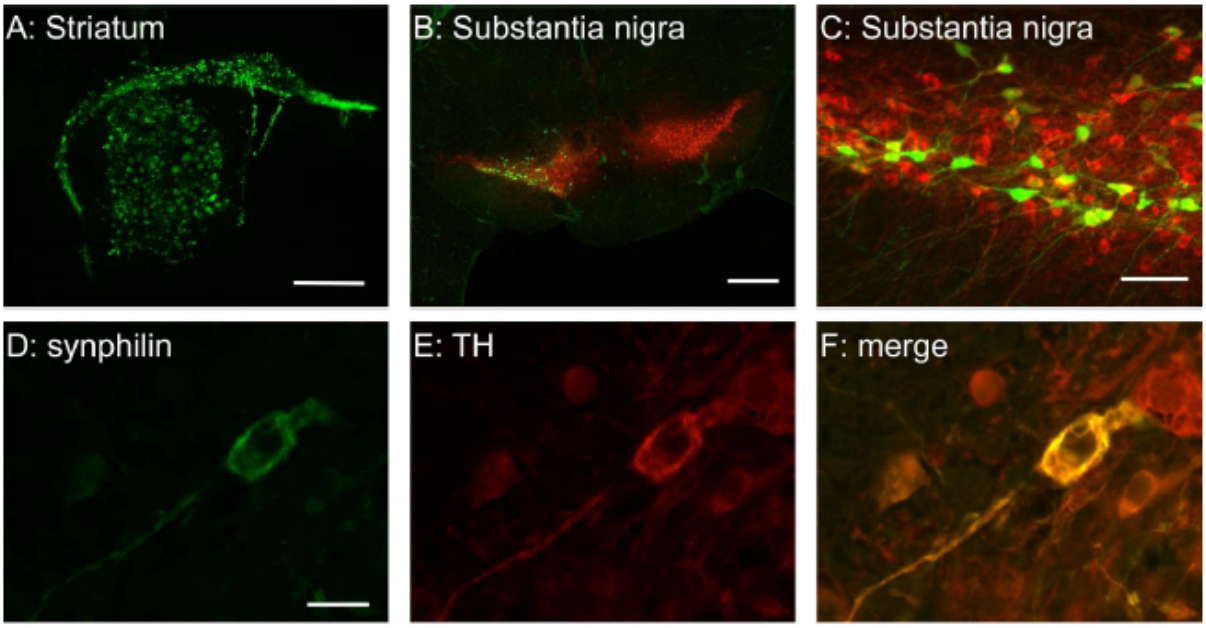

Fig. 3.5 Transgene expression in striatum and substantia nigra after adenovirus mediated gene transfer into the striatum. (A) Overview of a coronal section showing expression of EGFP in the *corpus callosum* and throughout most of the striatum after infection with an adenovirus expressing WT synphilin-1 (AdV-sphWT, $2.4x10^8$ PFU). Scale bar is 1 mm. **(B)** Overview of the midbrain showing EGFP fluorescence (green) in the substantia nigra pars compacta (SNc) after injection of AdV-sphWT into the ipsilateral striatum. Dopaminergic neurons were counterstained by an antibody against tyrosine hydroxylase (TH, red). Scale bar is 1 mm. **(C)** Close-up of the SNc showing infection and EGFP expression (green) in a subset of SNc dopaminergic neurons stained for TH (red). Scale bar is 50 µm. **(D-F)** Staining with an antibody against synphilin-1 (green) in a neuron also stained for TH (red) in the SNc after injection of AdV-sphWT into the ipsilateral striatum. Scale bar is 25 µm.

We achieved a nigral infection rate of about 35-40% assayed by EGFP reporter fluorescence without differences in infection efficiencies between the three adenoviral vectors used (Fig. 3.6A). Levels of FLAG-tagged synphilin-1 protein expressed by AdV-sphWT and AdV sphR621C, assayed by western blots with detection of synphilin-1 or FLAG were similar in the striatum (Fig. 3.6B-G). Stereologically counting of dopaminergic neurons in the SNc after injection of the AdV-EGFP control vector revealed no significant reduction of neuronal viability in the SNc (Fig. 3. 8, ctrl), indicating that gene transfer to striatum and by intrastriatal stereotaxical injection of the AdV using the adjusted experimental paradigm entailed few toxic side-effects.

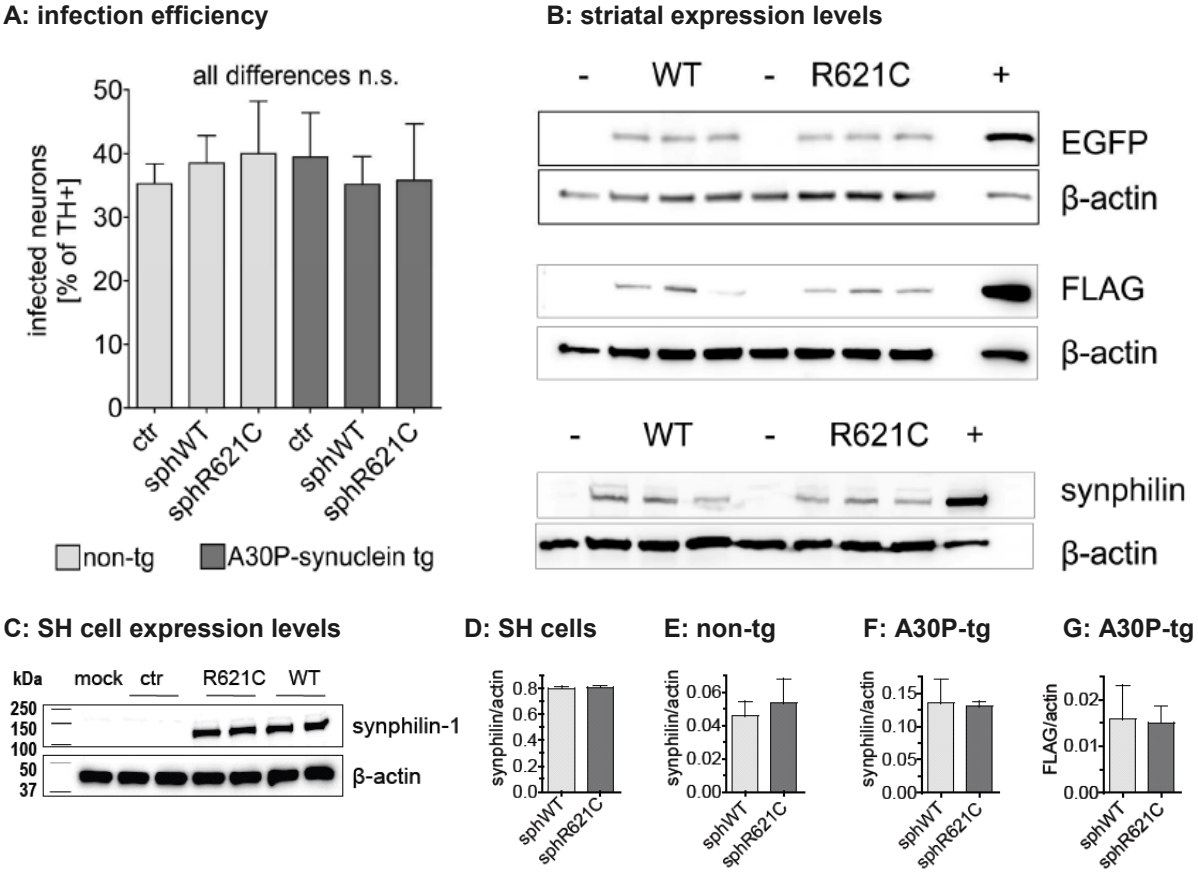

Fig. 3.6 Infection efficiency of adenoviral vectors. (A) Infection efficiency was quantified by determining the percentages of TH-positive cells that were also GFP-positive, meaning infected, by counting 4-6 sections of one animal per group after injection of AdV vectors into the striatum of non-transgenic (non-tg, light bars) and A30P α-synuclein transgenic animals (A30P-syn-tg, dark bars). Vectors were AdV-EGFP (ctrl), AdV-sphWT (sphWT) and AdV-sphR621C (sphR621C). Bars represent mean ± SEM. ANOVA revealed no significant differences between the adenoviral vectors. **(B)** Expression levels in brain lysates from striatum after injection of no virus (-), AdV-sphWT (WT) or AdV-sphR621C(R621C) in A30P α-synuclein transgenic animals. Positive control (+) was from an infection of SH-SY5Y cells with AdV-sphWT. Expression of EGFP and (FLAG-tagged) synphilin-1 was confirmed with antibodies against EGFP, FLAG and synphilin-1. **(C)** SH-SY5Y cells were infected with AdV-EGFP (ctr), AdV-sphWT (WT) and AdV-sphR621C (R621C). Cell lysates were subjected to electrophoresis and blotting, membranes were developed with antibodies against synphilin-1 and beta-actin. **(D)** Quantification of the western blot in (C), synphilin-1 expression normalized for beta-actin levels. **(E-G)** Non-tg mice **(E)** and A30P-alpha-synclein transgenic mice **(F, G)** were injected with AdV-sphWT (sphWT) and AdV-sphR621C (sphR621C), striatal lysates were subjected to electrophoresis and blotting, membranes were developed with antibodies against synphilin-1 (E, F) and FLAG (G). Intensities were normalized with respect to beta-actin. All differences were not statistically significant (t-test).

3.2.2. Synphilin-1 induced aggregate formation

We expressed synphilin-1 in the nigrostriatal system, to elucidate, whether WT and/or mutant R621C synphilin-1 overexpression would trigger aggregate formation and death of dopaminergic neurons in the SNc, the two main features of PD which are lacking in the syn-tg mouse model.

To distinguish effects only mediated by synphilin-1 from effects of synphilin-1 interacting with transgenic A30P α-synuclein, we investigated the influence of WT and R621C synphilin-1

overexpression in aggregation and cell viability in both non-transgenic C57Bl/6 (non-tg) and A30PαSyn mice.

We first were interested in whether expression of synphilin-1 would lead to the formation of aggregates in infected neurons. We used Thioflavine S (ThioS), an established stain of beta-sheet structure, which also stained the aggregates found in pons and midbrain of aged, symptomatic A30PαSyn mice (see section 3.1). Next to a nonspecific, “soft” staining in the nucleus (Fig. 3.7C, arrowheads), many neurons showed several small ThioS-positive inclusions (Fig. 3.7C, arrows) or confluent inclusions covering much of the cytosol (Fig. 3.7E). These ThioS-positive inclusions were observed in infected neurons (EGFP-positive, Fig. 3.7A) and stained with an antibody against synphlilin-1 (Fig. 3.7D). As expected, neurons infected with AdV-sphWT showed significantly more aggregates than with AdV-EGFP (Fig. 3.7G and Fig. 3.7J, light bars). Aggregates were observed both in the SNc and in the striatum. The frequency of ThioS-positive inclusions induced by R621C synphilin-1 was similar to WT synphilin-1 in non-tg animals.

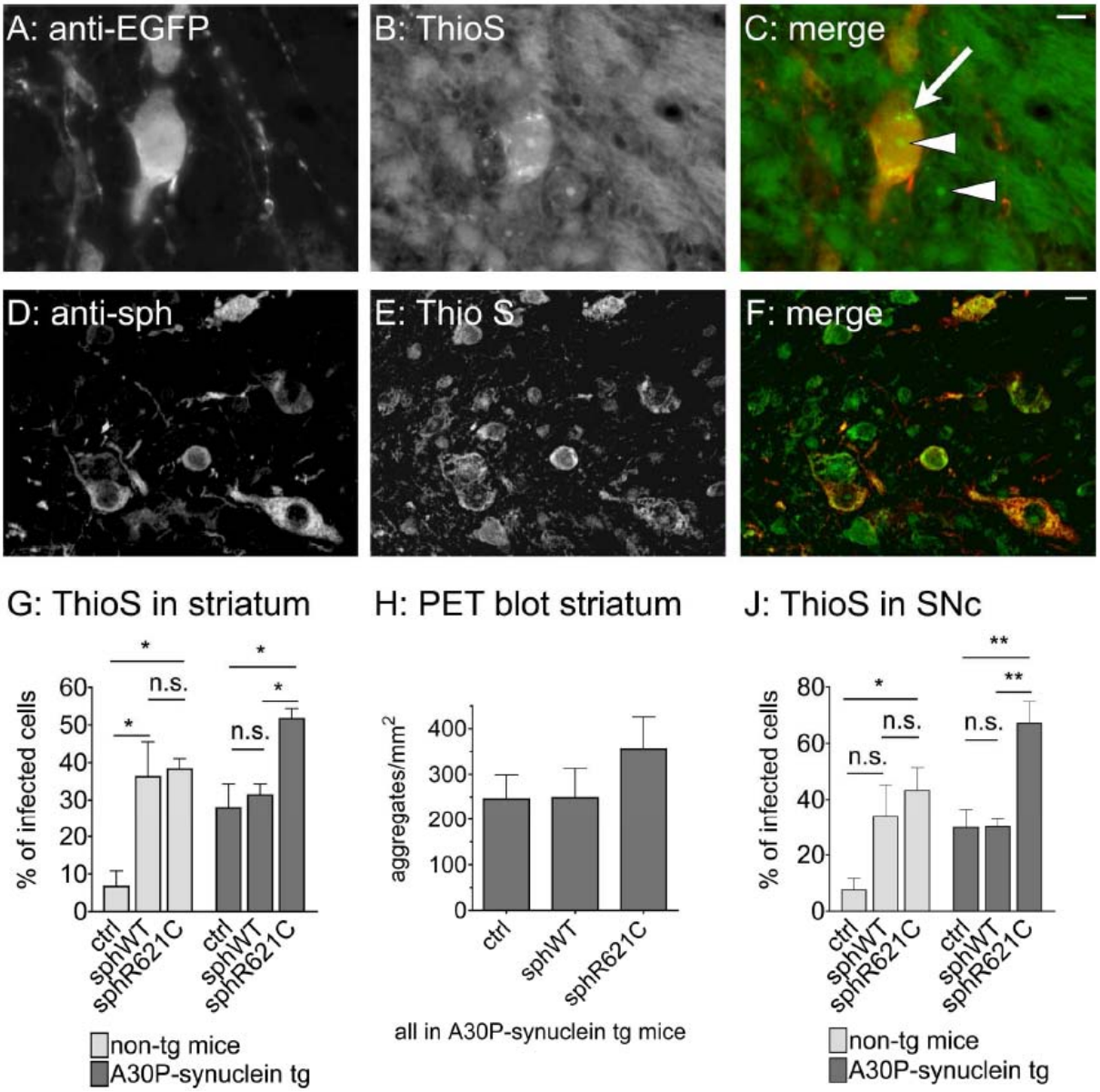

Fig. 3.7 Thioflavine S-positive inclusions induced by synphilin-1 expression. (A-F) To detect and quantify aggregates, endogenous EGFP fluorescence was eliminated by microwave boiling. Infected cells were then stained by immunohistochemistry against EGFP (anti-EGFP, red). Aggregates were stained with Thioflavine S (ThioS, green). Many cells contained "soft" ThioS-positive structures in the nucleus (C, arrowheads). ThioS-positive cells in addition contained several "hard" structures (C, arrow). ThioS-positive inclusions stained with an antibody against synphilin-1 **(D)**. A-C are from non-tg animals infected with AdV-sphWT, D-F are confocal images from an AdV-sphR621C infected non-tg animal. Scale bars represent 10 µm. **(G, J)** Percentages of infected cells that also showed ThioS positive inclusions after injection of AdV vectors into the striatum of non-transgenic (non-tg, light bars) and A30P α-synuclein transgenic animals (A30P-synuclein tg, dark bars). Vectors were AdV-EGFP (ctrl), AdV sphWT (sphWT) and AdV-sphR621C (sphR621C). Cells were counted both in the SNc **(J)** and in the striatum **(G)**. Bars represent mean ± SEM; n = 3 animals for each group in non-tg mice; n = 5 animals for each group in syn-tg mice. Comparisons were made by one-way ANOVA and Bonferroni posttest. **P* < 0.05, ***P* < 0.01. **(H)** Aggregates of proteinase K resistant α-synuclein were counted by stereology in striatal PET blots of A30PαSyn mice. Bars represent mean ± SEM; n = 5 animals for ctrl and sphWT and n = 6 for sphR621C. ANOVA showed no significant differences between adenoviral vectors.

To investigate the interaction of synphilin-1 with α-synuclein in an animal model, we used the same set of AdV in A30P-α-synuclein transgenic mice (A30PαSyn). The frequency of ThioS positive inclusions in TH-positive neurons of the uninfected side was around 5% with no significant difference between non-tg and syn-tg mice or between animals treated in the other hemisphere with the three different viruses.

	AdV-EGFP	AdV-sphWT	AdV-sphR621C
non-tg	5.5 ± 1.5	4.3 ± 1.3	7.0 ± 1.9
A30PαSyn	4.7 ± 1.4	6.8 ± 1.3	4.1 ± 1.7

Tab. 3.1 Frequency of TH-positive neurons that contained ThioS-positive inclusions. Numbers represent mean percentages ± SEM; n=3 animals per group of non-tg animals and n=5 animals per group of A30PαSyn animals.

In contrast to non-tg mice, A30PαSyn mice showed ThioS-positive inclusions in a substantial percentage of neurons infected with the control vector AdV EGFP, both in the striatum and in the SNc (Fig. 3.7G and Fig. 3.7J, dark bars). The frequency of aggregates was further increased by expression of R621C synphilin-1 but not by WT synphilin-1.

To validate these results obtained with Thioflavine S, we also assayed aggregation by stereologically counting proteinase K resistant aggregates of α-synuclein using the PET blot technique. The results for the striatum of A30P syn-tg animals were similar as with Thioflavine S, but differences did not reach statistical significance (Fig. 3.7H). This technique could not be used to quantify aggregates in the SNc because the SNc cannot be defined adequately in PET blot sections. Neither could it be used with non-tg mice since they do not express sufficient amounts of α-synuclein to be detected by PET blot.

3.2.3. Synphilin-1 induced toxicity

By stereologically counting dopaminergic neurons in the SNc, we then assayed the toxicity induced by synphilin-1 expression. Even though not all dopaminergic neurons were infected by our procedure, infection with AdV-sphWT resulted in a significant reduction of dopaminergic neurons in the SNc of non-tg mice, whereas AdV-EGFP did not (Fig. 3. 8A and Fig. 3. 8B, light bars). Again, R621C synphilin-1 had similar effects as WT synphilin-1. Counting Nissl-positive cells produced the same results as counting TH positive cells in the SNc (not shown), which confirms the loss of dopaminergic neurons and not only the downregulation of TH. The toxicity of WT synphilin-1 and R621C synphilin-1 was also studied in A30PαSyn animals. Interestingly, both synphilin-1 vectors induced a similar loss of dopaminergic neurons to a similar degree and not significantly different from non-tg animals

(Fig. 3. 8A and Fig. 3. 8B, dark bars, 2-way ANOVA). This finding indicates that effects on aggregation and toxicity can be dissociated.

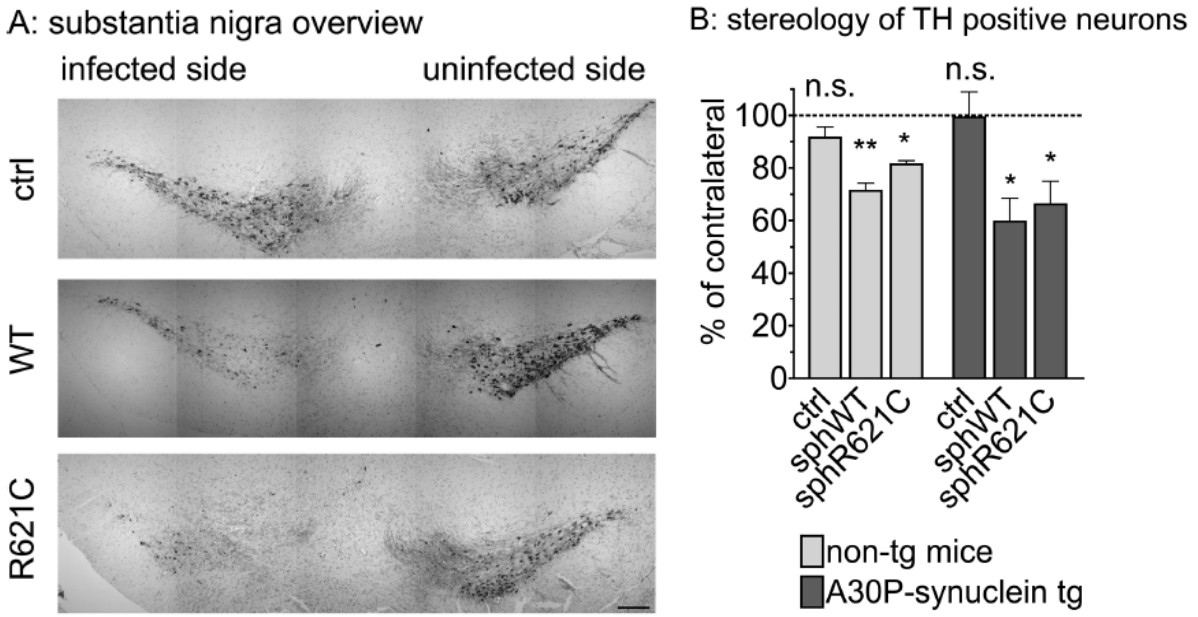

Fig. 3. 8 Toxicity of synphilin-1 in the substantia nigra pars compacta. (A) Midbrain dopaminergic neurons were visualized with immunohistochemistry for tyrosine hydroxylase (TH) following injection of AdV-EGFP (ctrl), AdV-sphWT (WT) and AdV-sphR621C (R621C) into the striatum of A30P-α-synuclein transgenic animals. Scale bar represents 200 µm. **(B)** The number of dopaminergic neurons in the substantia nigra pars compacta was counted by stereology of TH-positive neurons. Adenoviral vectors were injected into the striatum of non-tg (light bars) and A30PαSyn (dark bars) animals. Bars represent the number of dopaminergic neurons relative to the uninjected side as mean ± SEM; n = 3 animals for each group in non-tg mice; n = 5 for ctrl and sphWT, n = 4 for sphR621C in syn-tg mice. P values are depicted with respect to 100%. **P* < 0.05, ***P* < 0.01.

3.3. No impairment of the ubiquitin proteasom system in A30PαSyn mice

Several lines of evidence suggest that protein mishandling and an impairment of the ubiquitin proteasom system might play a role in the pathogenesis of PD. Chaperones and components of the UPS, including UCH-L1, proteasomal subunits and ubiquitin are present in LBs in post mortem tissue of PD patients (see section 1.2.2). Moreover, a subset of the LB-like inclusions and dystrophic neurites in the aggregation affected brain regions characterized by Neumann *et al.* was immunoreactive for ubiquitin (Neumann *et al.* 2002).

Thus, we intended to employ a transgenic *in vivo* reporter mouse line to assess proteasomal activity in the (Thy1)-h[A30P]αSyn transgenic mouse model (A30PαSyn). UbG^{76V}-GFP mice are transgenic for GFP carrying a constitutively active degradation signal, which only results in accumulation of GFP in the presence of an inhibited or impaired UPS.

A30PαSyn mice were crossed with UbG^{76V}-GFP transgenic mice to monitor if and when proteasomal impairment occurs during formation of PK-resistant α-synuclein aggregates.

To assure that the double transgenic mice developed PK-resistant A30P-α-synuclein aggregates during 18 month of age, double transgenic mice, homozygous for A30P-α-synuclein and heterozygous for Ub^{G76V}-GFP were bred.

Genotyping for UbG^{76V}-GFP was performed by PCR. Real-time PCR was used to test for homozygosity of the A30PsαSyn transgene. In the following generations A30PαSyn homozygosity was preserved by crossbreeding animals of the required genotype (A30P-tg+/+;UbGFP+/-) with homozygous A30PαSyn mice.

Young adult (6 month old), aged pre-symptomatic (12-month-old) and aged symptomatic (18-month-old) A30PαSyn +/+;UbGFP+/- mice were investigated. Aged matched heterozygous UbG^{76V}-GFP animals served as controls.

Fluorescence microscopy on sagital 6 µm paraffin-embedded brain sections to observe the native GFP fluorescence was used to assess changes in Ub^{G76V}-GFP levels. Furthermore, the UbG^{76V}-GFP protein was detected using bright field microscopy on sections stained for GFP with an anti-GFP antibody, followed by treatment for signal enhancement with the Avidin-Biotin-complex (ABC) technique and DAB visualization.

Analysis of the UPS reporter levels in animals of all examined ages revealed no difference between the distribution pattern of GFP-positive cells in the aggregate-affected brain regions from A30PαSyn+/+;UbGFP+/- and A30PαSyn negative controls (data not shown).

3.4. Therapeutic approaches using the molecular chaperone HSP70

3.4.1. Hsp70 in cellular models of PD

3.4.1.1. Hsp70 inhibits MPP^+-induced toxicity in neuroblastoma cells

Adenoviral gene transfer of Hsp70 to SHSY-5Y neuroblastoma cells

To study the effect of Hsp70 on cell death caused by the mitochondrial complex I inhibitor MPP^+ we performed toxicity assays in SH-SY5Y neuroblastoma cells expressing human Hsp70 induced by adenoviral gene transfer (AdV-Hsp70). These AdV were generated and positively tested for transgene expression before (Beaucamp *et al.* 1998). The same laboratory successfully used AdV-Hsp70 to investigate anti-apoptotic effects of Hsp70 in primary neurons following nerve growth factor withdrawal, which confirmed functionality of AdV-Hsp70.

A viral vector preparation of AdV-Hsp70 expressing human Hsp70 driven by the human CMV promoter was a generous gift of Dr. Ulrike Naumann (Hertie Institute for Clinical Brain Research, General Neurology, Tübingen), who also tested the viral vector preparation for transgene expression and determined the titer according to standard protocols established this laboratory.

Increased viability in cell death assays

To study the effect of the molecular chaperone Hsp70 on cell death elicited by MPP^+, we performed toxicity assays in SH-SY5Y neuroblastoma cells. Hsp70 was expressed by adenoviral gene transfer (AdV-Hsp70) 24h before exposition to MPP^+. Hsp70 expression was also induced by geldanamycin (GA), which initiates a stress response by binding to Hsp90, a negative regulator of the transcription factor HSF1 that leads to transcription of the Hsp70 gene.

We used the trypan blue exclusion assay as a morphological marker for cell viability. This assay uses the fact that viable cells can exclude the dye trypan blue whereas dead cells are stained. The number of viable among the total number of cells was counted.

The possibility the AdVs might have caused acute toxicity to the SH-SY5Y cells in the absence of MPP^+ could be excluded, because the remaining numbers of AdV-infected cells did not differ significantly from untreated controls (Fig. 3.9A). To find a useful MPP^+ concentration, different paradigms ranging from 1 mM to 15 mM (Fig. 3.9B-F) were tested.

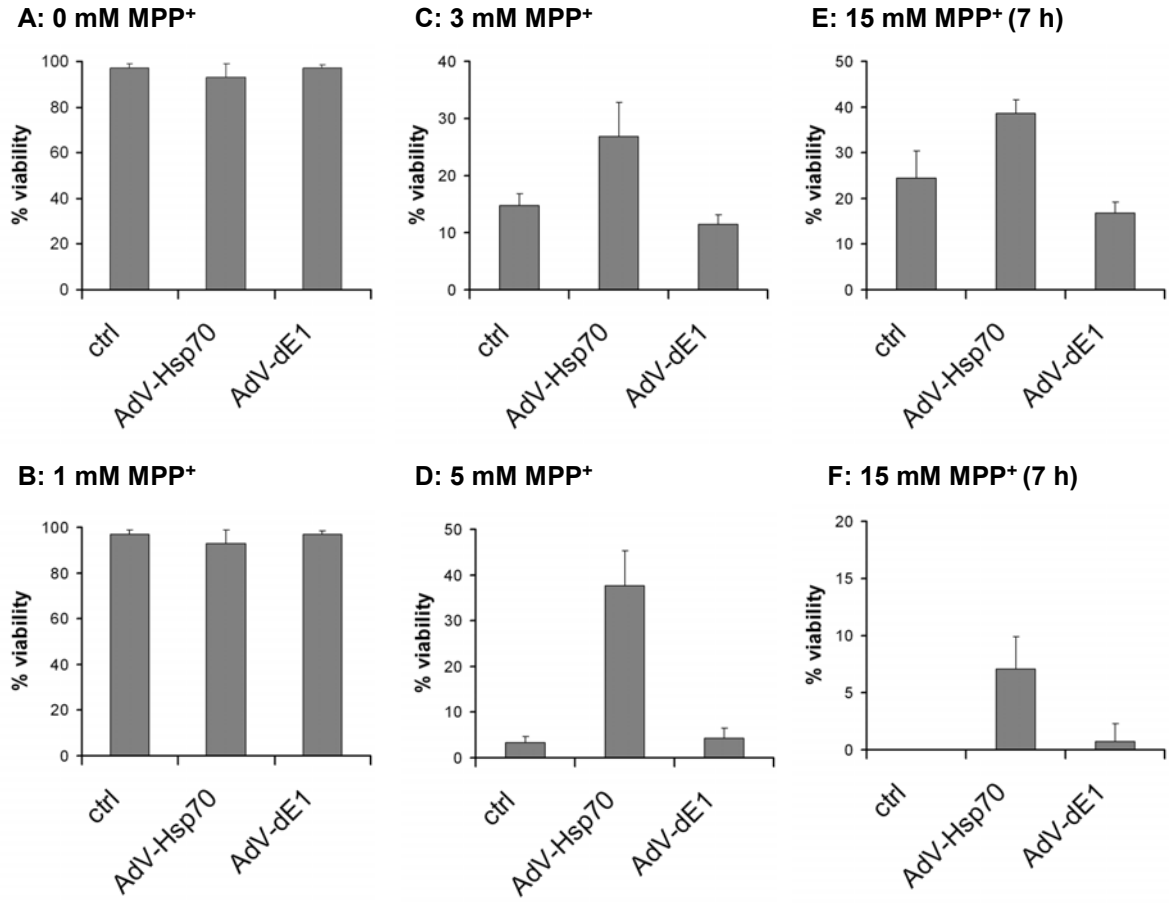

Fig. 3.9 Hsp70 protects against MPP^+ toxicity (trypan blue exclusion assay). SH-SY5Y neuroblastoma cells were infected with either a recombinant adenovirus expressing Hsp70 (AdV-Hsp70) or an E1-deleted control virus (AdV-dE1), 24 h before exposition MPP^+. Viability was determined by the trypan blue exclusion assay 48 h after addition of 0 (A) 1 (B), 3 (C, p=0.0034), 5 (D, p=0.00006) and 15 (E) mM MPP^+ for, 24 h or 7 h (F) after addition of 15 mM MPP^+. The result for 5 mM MPP was reproduced n=6 times. Bars represent cellular viability as percentage of the overall-cell number by mean ± SEM.

The mean cellular survival after exposition to MPP^+ was higher in cells infected with AdV-Hsp70 than in uninfected cells or in cells infected with the empty control virus (AdV-dE1) (Fig. 3.9B-F). 5 mM MPP^+ for 48 h was chosen as the most reliable paradigm. For this concentration, AdV- cellular survival was increased by adenoviral-mediated Hsp70-induction to a proper extent. The rescue effect was statistically significant with p=0.00006 (Fig. 3.9D). Comparisons using the t-test were one-tailed.

We used the release of LDH (lactate dehydrogenase) from dying cells to calculate MPP^+ toxicity with or without expression of Hsp70, to confirm the findings from the trypan blue exclusion assay with a different method. For these experiments, SH-SY5Y cells were exposed to an intense regimen of 15 mM MPP^+ for 24 h.

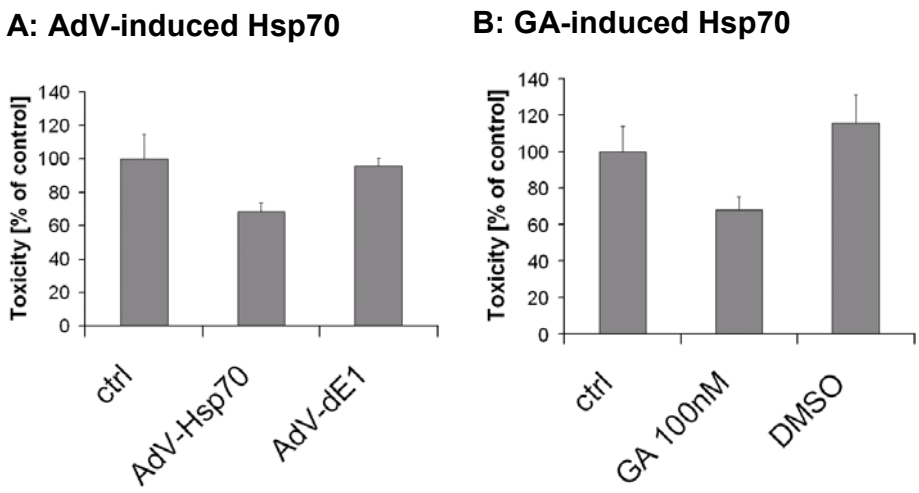

Fig. 3.10 Hsp70 protects against MPP^+ toxicity (LDH assay). MPP^+ toxicity was determined by measuring released LDH and normalized to MPP^+ treatment alone (ctrl). **(A)** Cells were infected with recombinant adenovirus and exposed to 15 mM MPP^+ for 24h. A summary of 4 independent experiments is shown, p=0.002. Infection with AdV-Hsp70 resulted in a significant reduction of MPP^+ toxicity when compared to infection with AdV-dE1. **(B)** Hsp70 was induced by pretreatment with 100 nM geldanamycin (GA). A summary of 3 independent experiments is shown. In contrast to vehicle treatment (DMSO alone), geldanamycin significantly reduced the toxicity of 15 mM MPP^+ (p=0.01). Bars represent LDH-release relative to MPP^+ treatment alone (ctrl) as mean ± SEM.

In contrast to infection with the control virus, AdV-Hsp70 resulted in a significant reduction of MPP^+ toxicity (Fig. 3.10A, p=0.002). 100 nM geldanamycin significantly reduced MPP^+ toxicity with respect to DMSO alone (Fig. 3.10B). Comparisons using the t-test were one-tailed.

The effect of HSP70 is not purely anti-apoptotic

Following exposition to MPP^+, cell death may occur in a caspase-dependent or caspase-independent way, depending on the paradigm used. In our hands, 5 mM MPP^+, but not 3 or 15 mM MPP^+ elicited caspase-3 activation as measured by DEVD-amc cleavage assay. Infection with AdV-Hsp70 significantly decreased caspase activation by 5 mM MPP^+, as did the caspase inhibitor zVAD-fmk (Fig. 3.11A).

We also tested AdV-Hsp70 in conditions where caspase-3 activation is not responsible for cell death. First, 5 mM MPP^+ was administered in the presence of the caspase inhibitor zVAD-fmk (100 nM). In this experiment, infection with AdV-Hsp70 but not control virus significantly increased survival (Fig. 3.11B). Second, viability following 15 mM MPP^+, with and without zVAD-fmk, was measured by the trypan blue exclusion and LDH assay Fig. 3.10. As expected, zVAD-fmk had little effect (Fig. 3.11C), but AdV-Hsp70 was protective in the in the trypan blue exclusion assay (Fig. 3.9E, F) and in the LDH assay (Fig. 3.10A) as was geldanamycin (Fig. 3.10B).

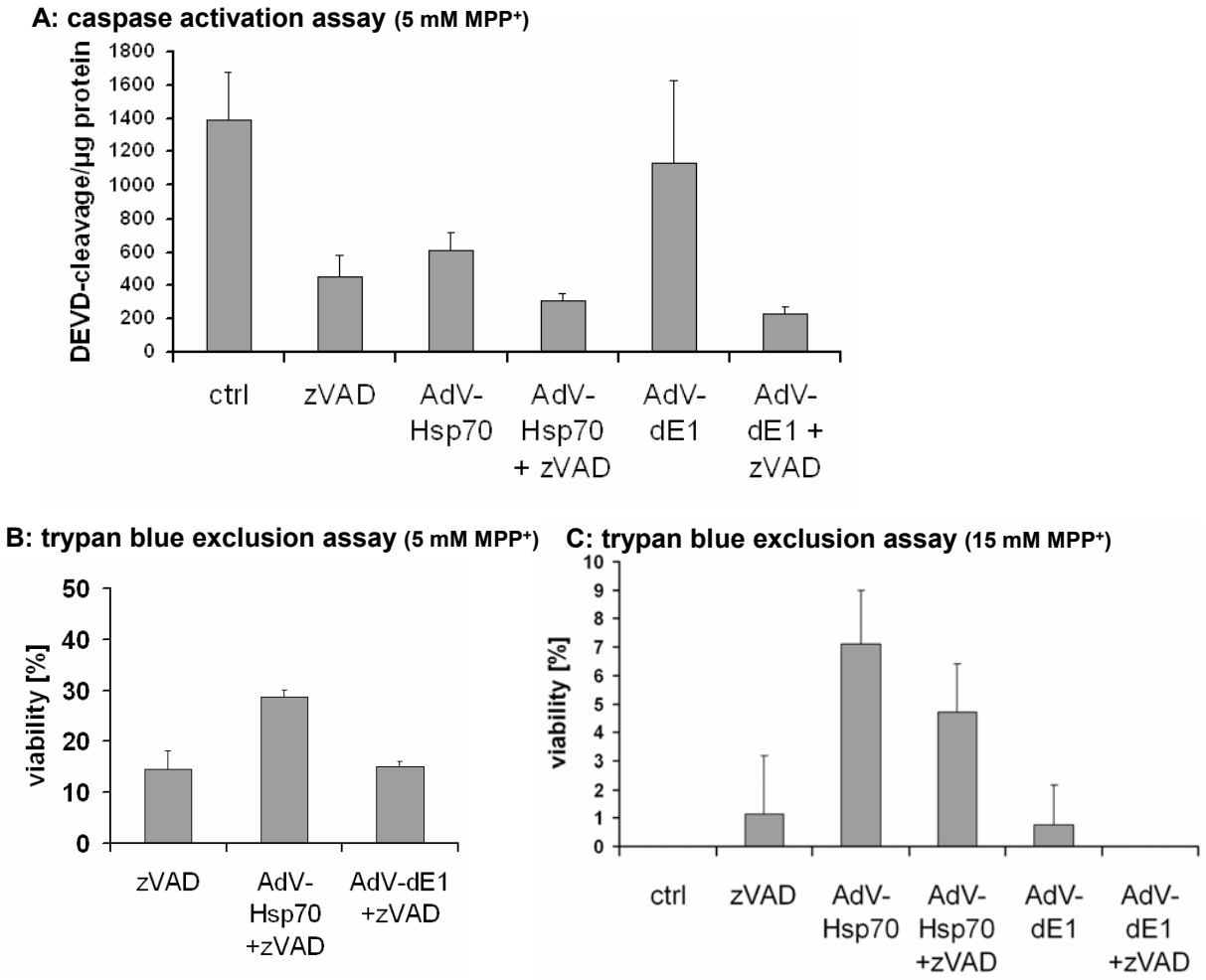

Fig. 3.11 Hsp70 does not act by directly inhibiting caspase activation. (A) Caspase activation was measured by DEVD-amc cleavage. Infection with AdV-Hsp70 and the caspase inhibitor zVAD-fmk (zVAD) (100 nM) decreased the caspase activation induced by 5 mM MPP^+. **(B)** Cell viability was measured by the trypan blue exclusion assay, 48 h after exposition to 5 mM MPP. In the presence of the caspase inhibitor zVAD-fmk (100 nM), infection with AdV-Hsp70 significantly increased survival compared to zVAD-fmk alone (p=0.0004). **(C)** Cell viability was measured by the trypan blue exclusion assay, 24h after exposition to 15 mM MPP^+. In this condition, zVAD-fmk (100 nM) had no significant effect, but infection with AdV-Hsp70, alone (p=0.0013) or in combination with zVAD-fmk (p=0.0014), significantly increased cell survival.

In this part of the cell culture study, AdV-Hsp70 infected cells were exposed to 5 mM MPP^+ and viability was measured by the trypan blue exclusion assay. Infection with AdV-Hsp70, but not with the empty control virus reliably increased survival after exposition. To confirm these findings with a different method, the release of LDH from dying cells was used to measure MPP^+ toxicity with or without expression of Hsp70 in the more intense paradigm of 15 mM MPP^+. In contrast to infection with the control virus, AdV-Hsp70 resulted in a significant reduction of MPP^+ toxicity.

Taken together, Hsp70 induction by adenoviral gene transfer or by administration of geldanamycin, prior to exposure to MPP^+, reduced MPP^+ toxicity and increased cell viability when compared to vehicle treatment. This effect occurred in paradigms with and without

caspase activation, suggesting that neuroprotection by Hsp70 most likely results from its effect on oxidized and/or misfolded proteins rather than from caspase inhibition.
After we investigated the effect of Hsp70 on cell death caused by the mitochondrial complex I inhibitor MPP^+, we intend to explore the influence of Hsp70 on α-synuclein aggregation and toxicity in a cellular model system.

3.4.1.2. Hsp70 reduces α-synuclein–induced toxicity and aggregate load

A new cellular model system developed in our laboratory was used to examine effects of Hsp70 on α-synuclein aggregation. To characterize the formation of α-synuclein aggregates in living cells, α-synuclein was visualized by fluorescence microscopy: α-synuclein was tagged with a C-terminal 6 amino acid PDZ binding motif and coexpressed with the corresponding PDZ domain fused to EGFP. It allowed us to compare α-synuclein variants. A C-terminally truncated α-synuclein variant (ΔC) showed the highest prevalence of aggregates and toxicity. The characterization of Hsp70-mediated effects was part of this project and was performed in cooperation with Dr. Björn Falkenburger and Felipe Opazo (PhD) (Opazo *et al.* 2008). To determine the effects of Hsp70 on aggregation and toxicity of α-synuclein, ΔC-α-synuclein as the variant with most abundant aggregate formation and highest toxicity was chosen. HEK293 cells were co-transfected with pLV-HAHsp70 together with either PDZ-EGFP alone or with the plasmid expressing ΔC-α-synuclein and PDZ-EGFP (Fig.3.12).

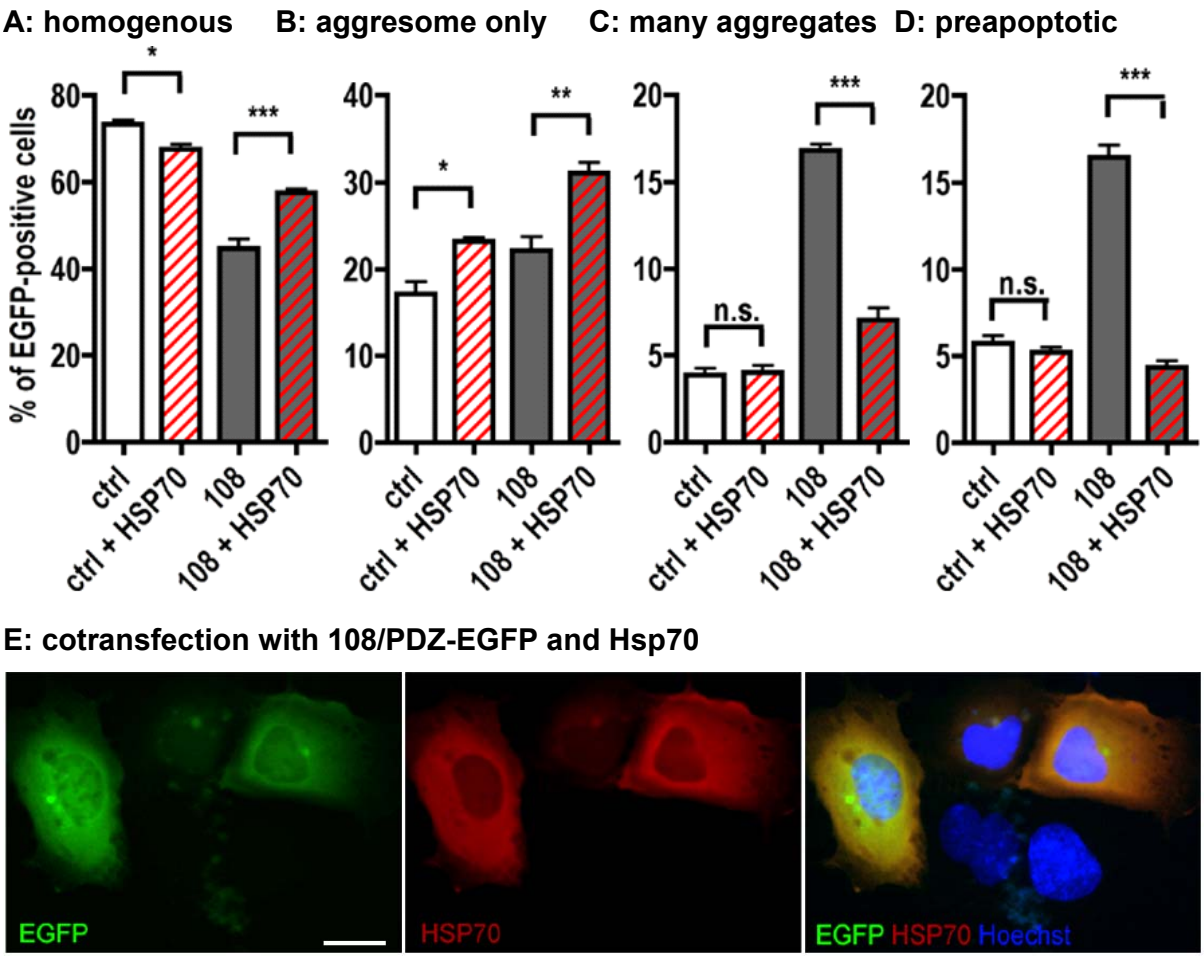

Fig.3.12 Effect of the molecular chaperone Hsp70. (A-D) EGFP distribution patterns in cells expressing PDZ-EGFP alone (ctrl) or tagged, C-terminally truncated -synuclein and PDZ-EGFP (ΔC), both with and without Hsp70. Comparisons were made by oneway ANOVA and Bonferroni post hoc tests. Independent experiments (n): Ctrl (3), ctrl + HSP70 (3), ΔC, ΔC + Hsp70 (8). **(E)** Representative image after co-transfection with DC/PDZ-EGFP and Hsp70 showing expression of both EGFP (left) and Hsp70 (middle) in nearly every cell. Right: overlay of EGFP (green), Hsp70 (red) and Hoechst (blue). Scale bar represents 20 µm.

EGFP distribution patterns were counted 24h after transfection. Coexpression of Hsp70 with ΔC-α-synuclein and PDZ-EGFP led to a 58% reduction in the prevalence of aggregates (Fig.3.12C) and to an even more pronounced 74% reduction in the prevalence of preapoptotic cells (Fig.3.12D). In fact, Hsp70 reduced aggregation and toxicity of ΔC-α-synuclein virtually to the baseline levels observed with PDZ-EGFP alone. This effect on aggregation and toxicity was specific to aggregates induced by α-synuclein, since aggregation and toxicity observed with expression of PDZ-EGFP alone was unaltered by Hsp70. Interestingly, the prevalence of aggresomes was increased with Hsp70 (Fig.3.12B). This increase was observed both with PDZ-EGFP alone and with ΔC-α-synuclein and PDZ-EGFP.

We then characterized the effects of Hsp70 on aggregate formation in more detail using time-lapse imaging (Fig. 3.13). Unexpectedly, Hsp70 did not increase the formation of an

aggresome in homogeneous cells (Fig. 3.13A). Instead, it decreased the formation of small peripheral aggregates in homogeneous cells (Fig. 3.13F) and the likelihood of aggregate progression both from a single aggresome and from small peripheral aggregates to a state of many or large aggregates (Fig. 3.13C and H, respectively). Moreover, Hsp70 increased the likelihood of cells with many or large aggregates to reduce their aggregate load towards a single aggresome (Fig. 3.13D) and increased the clearance of both the single aggresome and small peripheral aggregates from the cytosol (Fig. 3.13B and G, respectively).

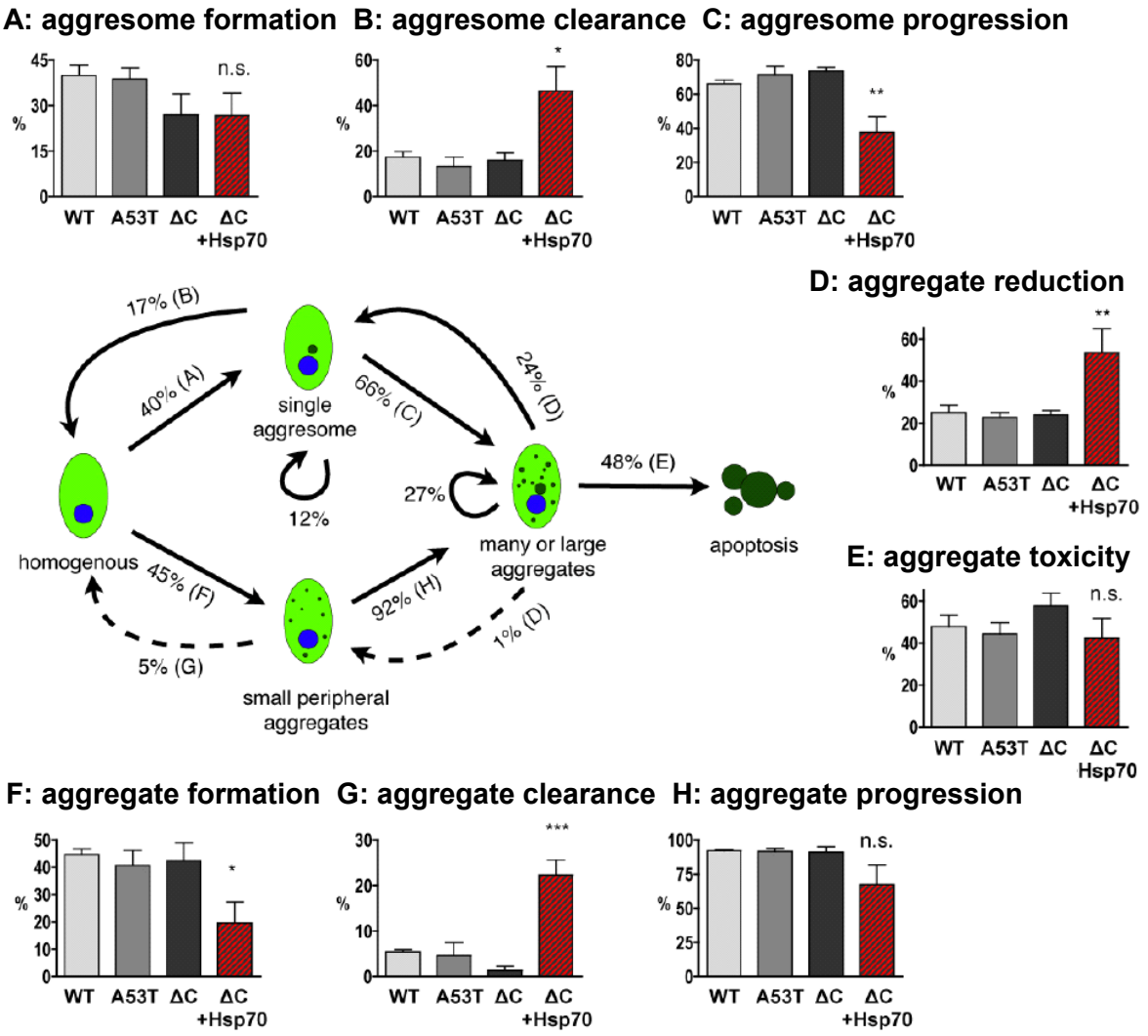

Fig. 3.13 Summary of transitions between EGFP distribution patterns observed by time-lapse imaging. Homogeneously labeled cells either first acquire a single aggresome **(A)** or small peripheral aggregates **(B)**, which then progress into cells with many or large aggregates (C and H respectively). These cells undergo apoptosis **(E)** or reduce their aggregate load, primarily to a single aggresome **(D)**, which can also be cleared from the cytosol **(B)**, as occasionally also seen for small peripheral aggregates **(G)**. Numbers at the arrows signify percentage relative to all transitions starting from the same appearance for WT-α-synuclein. No change in appearance was observed relatively frequently for cells with a single aggresome. Even though many cells with many or large aggregates accumulated even more or even larger aggregates, no change of category was counted in 27% of these cells. Some rare transitions are not depicted in the graph for clarity, for example apoptosis from other categories than many or large aggregates. Letters at the arrows refer to the corresponding bar graphs: The upper line of bar graphs relates to the pathway starting with a single aggresome **(A-C)**,

the lower line to the pathway starting with small peripheral aggregates **(F-H)** and the right column to the fate of cells with many or large aggregates **(D and E)**. Significances depicted in the bar graphs refer to the comparison of ΔC-α-synuclein with and without Hsp70. All comparisons between α-synuclein variants were n.s. (ANOVA and Bonferroni post-hoc tests). The number of cells analyzed for each genotype was WT: 674, A53T: 599, ΔC: 569, ΔC+Hsp70: 372.

The increased prevalence of aggresomes observed at the single timepoint (Fig.3.12B) thus did not result from an increased formation of aggresomes in homogeneous cells but from increased aggregates reduction to a single aggresome. The likelihood of cells with large and many aggregates to undergo apoptosis was not reduced by Hsp70, indicating that Hsp70 did not inhibit the toxic effects of large aggregates directly. The decreased toxicity observed with Hsp70 was therefore likely to result mainly from the decreased prevalence of cells with many or large aggregates.

As these experiments used the CMV-HAHsp70 expression cassette of the pLV-HAHsp70 plasmid, we were confident about its biological effects prior to the LV production procedure (see below section 3.4.2.1).

3.4.2. Hsp70 in mouse models for PD

To test the therapeutic potential of Hsp70 in mouse models of PD, different vector systems were evaluated for their applicability to express my protein of interest (Hsp70) in the region of interest in mouse brain.

Constructs for lentiviral (LV) or Adeno-associated-viral (AAV) vector preparations and the corresponding EGFP expressing vector control constructs were tested for transgene expression before they were used for viral vector production.

AAV and LV vector preparations were tested for their infection efficacy *in vivo* in the brain region of interest. Viruses were injected stereotaxically into the left hemisphere, the right hemisphere served as internal negative control. In all animals, the transgene expression was restricted to the injected side.

3.4.2.1. Lentiviral vector-mediated genetransfer to mouse models of PD

Determination of LV titer based on WPRE copy number

To compare the Hsp70-expressing virus with the control virus, accurate titer determination was important. In AdV, this is done by the plaque test, in LV there have been different possibilities, including assessment of the p24 antigen or vector RNA sequences in supernatants, of DNA or mRNA sequences in transduced cells, and vector expression in transduced cells. We chose WPRE rtPCR because our LV contained the WPRE-enhancer element, which becomes part of the 3`UTR of each lentiviral transgene mRNA transcript.

Thus the number of transcripts in transduced HEK293 cells was measured to assess lentiviral gene expression.

Total RNA was purified from HEK293 cells transduced with LV-EGFP or LV-HaHsp70. Reverse transcription into cDNA followed by quantitative real-time PCR (qRT-PCR) with WPRE-specific primers was used to determine the WPRE copy number. mRNA copy number of the house keeping gene GAPDH was measured simultaneously as a control to normalize for RNA preparation efficiency. The titers of the LV used in this study were 3062 for LV-HAHsp70 and 4438 for LV-EGFP. Titers correspond to the number of WPRE copies/10^4 beta-actin copies per µl virus suspension.

Analysis of plasmids and viral vector preparations in cell culture and mouse brain

Protein lysates from HEK293 cells transiently transfected with the lentiviral vector construct pLV-HAHSp70 or the corresponding EGFP expressing vector control construct pLV-EGFP for 48 h were analyzed on Western blots using anti-HA and anti-EGFP antibodies. Lysates from untreated cells were used as negative controls, detection of β-actin (30 kDa) was used to control for equal loading. Detection of HA-tagged Hsp70 and EGFP revealed protein bands with the expected size of ~ 70 kDa and 27 kDa respectively. These protein lysates served as positive control for the analysis of the viral vector preparation (Fig. 3.14G,H).

Moreover, the CMV-Hsp70 expression cassette of the pLV-HAHsp70 plasmid was tested for Hsp70 expression and chaperone function prior to the LV production procedure in the cellular model system described above (see section 3.4.1.2).

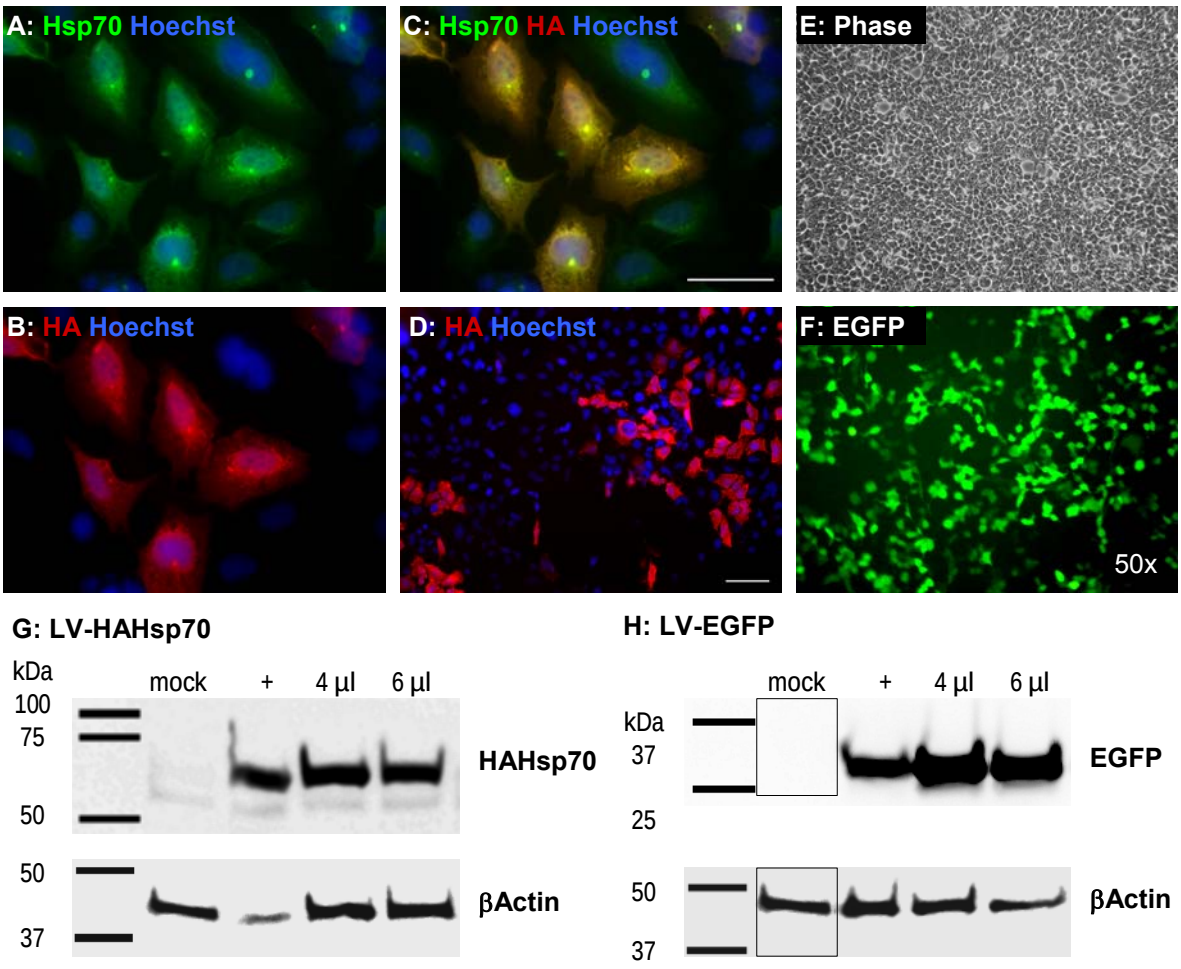

Fig. 3.14 Expression analysis of lentiviral vector preparations *in vitro*. LV vectors expressing HA-tagged Hsp70 (A-D,G) or EGFP (E,F,H) were used to transduce HEK293 cells pretreated with 8 µg/ml polybrene. **(A-D)** HEK293 cells plated in 24-well-plates were infected with 1 µl LV-HAHsp70 suspension (corresponding to 3062 WPRE copies/10^4 beta-actin copies), fixed at 4 days after infection and stained with anti-hemagglutinin ((A-D), HA, red) and anti-Hsp70 ((A-C)Hsp70, green) antibodies. Nuclei were counterstained with Hoechst. The anti-Hsp70 antibody stained both HA-tagged transgenic and endogenous Hsp70. Scalebar in (C) is 50 µm **(D)** Overview of (B), showing infection efficiency of the LV-HAHsp70 preparation. Scale bar represents 100 µm. **(E,F)** Phase contrast (E) EGFP fluorescence (F) of living HEK293 cells plated in a 24-well-plate, recorded at an inverse fluorescent microscope equipped with a digital camera at day 4 after transduction with 1 µl LV-EGFP suspension (corresponding to 4438 WPRE copies/10^4 beta-actin copies), showing the infection efficiency of the LV-EGFP preparation. 50x- indicates the overall magnification. **(G,H)** Western blot LV-expression analysis in cell lysates after infection of HEK293 plated in 6-well-plates with no virus (mock) or 4 or 6 µl of LV-HAHsp70 (G) or LV-EGFP (H) in HEK293. Positive control (+) was from a transfection of HEK293 cells with pLV-HAHsp70 (G) or pLV-EGFP. Cell lysates were subjected to electrophoresis and blotting, membranes were developed with antibodies against β-actin (as loading control) and HA (hemagglutinin) (G) or EGFP (H). Note that mock control in (H) shows the lane as (G), since all samples in (G) and (H) were separated in the same gel and detected on the same membrane.

LV preparations were tested for transgene expression by infecting HEK293. Lentiviral expression was verified in HEK293 cells at 4 dpi by fluorescence microscopy of EGFP and HA-tagged Hsp70 after ICC staining for HA (Fig. 3.14A-F). ICC staining for Hsp70 detected transgenic as well as endogenous Hsp70 in HEK293 cells. In addition, cells were harvested for Western blots and analyzed as described above for the plasmid constructs at 4 days post infection (dpi) (Fig. 3.14G,H).

Furthermore, Lentiviral vector preparations were also positively tested for transgene expression in mouse brain. 2 µl of the LV-HaHsp70 or LV-EGFP were stereotaxically injected into the striatum of young adult non-tg mice. Transgene expression was assayed by Western Blot (Fig. 3.15,E,F). As the pons is the region mainly affected by α-synucleinopathy in aged, symptomatic A30P-tg transgenic mice, we tested whether LV delivery to pons was suitable to achieve longterm overexpression human Hsp70 in this brain region.

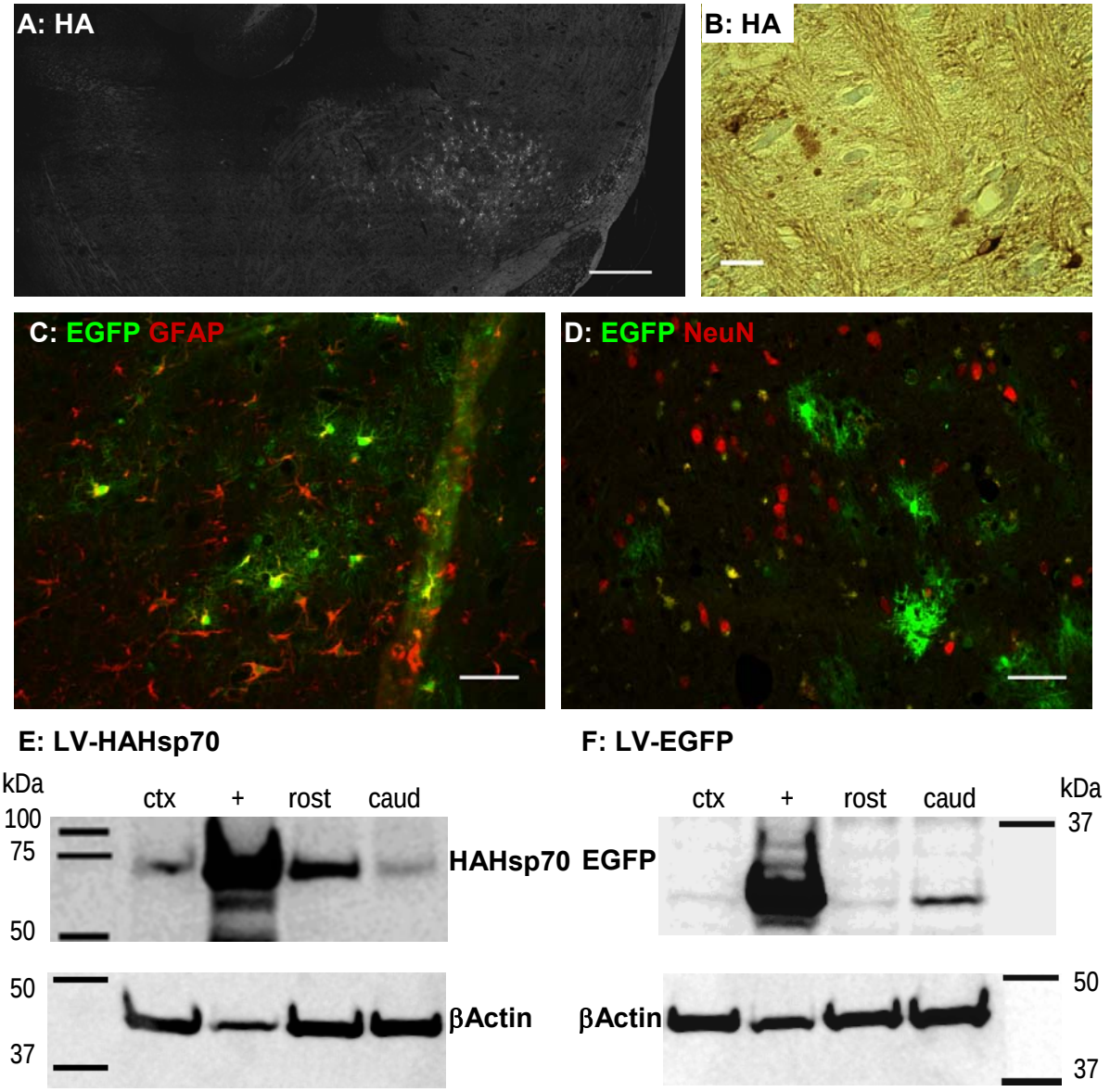

Fig. 3.15 Expression analysis of lentiviral vector preparations *in vivo*. (A-D) Sagital sections of the pons region at day 14 after injection of 1.5 µl LV-HAHsp70 (corresponding to 4593 WPRE copies/10^4 beta-actin copies) (A,B) or LV-EGFP (corresponding to 6657 WPRE copies/10^4 beta-actin copies) (C,D). **(A)** Mosaic image composed of 128 single pictures showing an overview of the pons region stained for HA detecting expression of HA-tagged Hsp70. Scale bar is 500 µm. **(B)** Close-up of the pons stained for HA (brown) showing expression of HA-tagged Hsp70 in cells neuronal morphology. **(C,D)** Close-up of the pons showing infection and EGFP expression (green) in a subset of glia stained for the glia-specific marker GFAP (glial fibrillary acidic protein (red) (C) or neurons stained for the neuron-specific marker NeuN (neural nuclei protein (red) in the yellow merge (D). Scale bars in (B-D) represent 50 µm. **(E,F)** LV expression in brain lysates from striatum after injection of LV-HAHsp70 (E) or LV-EGFP (F) in young, adult non-tg mice. Positive control (+) was from a transfection of HEK293 cells with pLV-HAHsp70 (E) or pLV-EGFP (F). Negative control was a lysate from the non-

infected cortex (ctx). Striatal lysates were subjected to electrophoresis and blotting, membranes were developed with antibodies against with antibodies against β-actin (as loading control) and HA (hemagglutinin) (E) or EGFP (F) to confirm transgene expression.

LV-HAHsp70 and LV-EGFP were injected into the pons of aged, 16-month-old A30P-tg mice. Injection of a total volume of 1.5 µl of the LV in two sites as two deposits along one needle tract caused a substantial distribution of the virus suspension throughout the pons (Fig. 3.15,A) for up to 12 weeks. When morphological criteria and ICC staining for cell type specific markers were taken into account, LV infected neuronal (Fig. 3.15,B,D) as well as glial cells (Fig. 3.15,C). Unfortunately, the infection of neurons appeared to be less efficient than of glial cells. Nevertheless, the number of neurons showing transgene expression was considered to be sufficient to induce transgene-specific effects.

Lentiviral gene transfer to SNc

Although AdV has been successfully used in the present study and other projects of our laboratory, these vectors, however, have their limitations. AdV induce strong immune response, which can lead to short term expression of the transgene. Thus, we analyzed the efficacy of LV to mediate transgene expression to dopaminergic neurons of the SNc.

LV expressing EGFP under control of different promoters, several LV preparations varying in the purification protocol and different combinations of stereotaxical injection parameters were injected into the substantia nigra pars compacta (SNc). Viral expression was examined at 14 dpi.

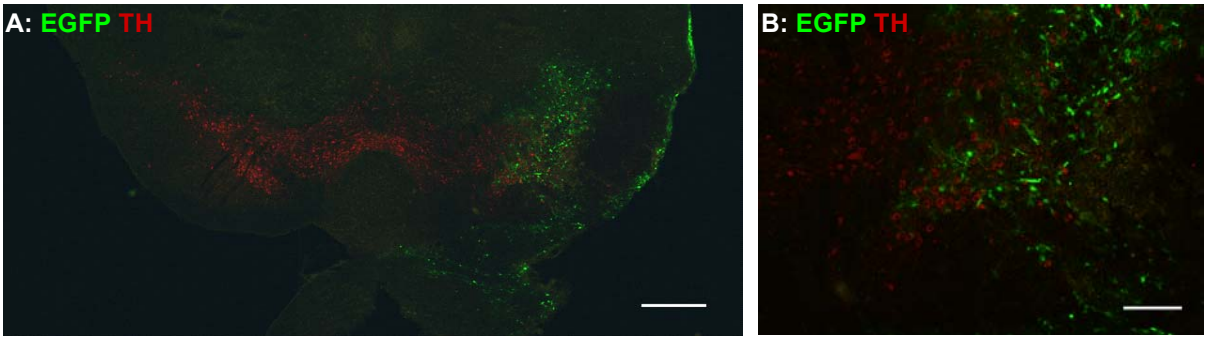

Fig. 3.16 Expression analysis of a lentiviral vector preparation in the substantia nigra. (A) Mosaic image composed of 20 single pictures showing overview of the midbrain on a coronal section for detection of EGFP fluorescence (green) in the substantia nigra pars compacta (SNc) after injection of a lentiviral vector expressing EGFP driven by the neuron-specific human synapsin-promoter (corresponding to 18256 WPRE copies/10^4 beta-actin copies). Dopaminergic neurons were counterstained by an antibody against tyrosine hydroxylase (TH, red). Scale bar is 500 µm. **(B)** Close-up of the SNc showing no infection and EGFP expression (green) in SNc dopaminergic neurons stained for TH (red). Scale bar represents 150 µm.

Even though EGFP was expressed in neurons surrounding the SNc, we did not detect substantial and reliable transgene expression in nigral dopaminergic neurons with lentiviral infection (Fig. 3.16).

3.4.2.2. Lentiviral Hsp70 expression in the chronic MPTP mouse model

It has been shown by Fornai *et al.* that, in contrast to other application paradigms, continuous administration of MPTP induced aggregate formation in lesioned SNc (Fornai *et al.* 2005). We tried to replicate this chronic regimen of MPTP application.

A preliminary experiment for continuous MPTP application was carried out in a small cohort of in young adult 9-week-old C57Bl/6 mice. Some of these animals had received a unilateral intranigral injection of LV-HAHsp70 or LV-EGFP, corresponding to 6100 or 8800 WPRE copies, respectively. The virus suspension was applied as two deposits along the needle tract in a total volume of 2 µl.

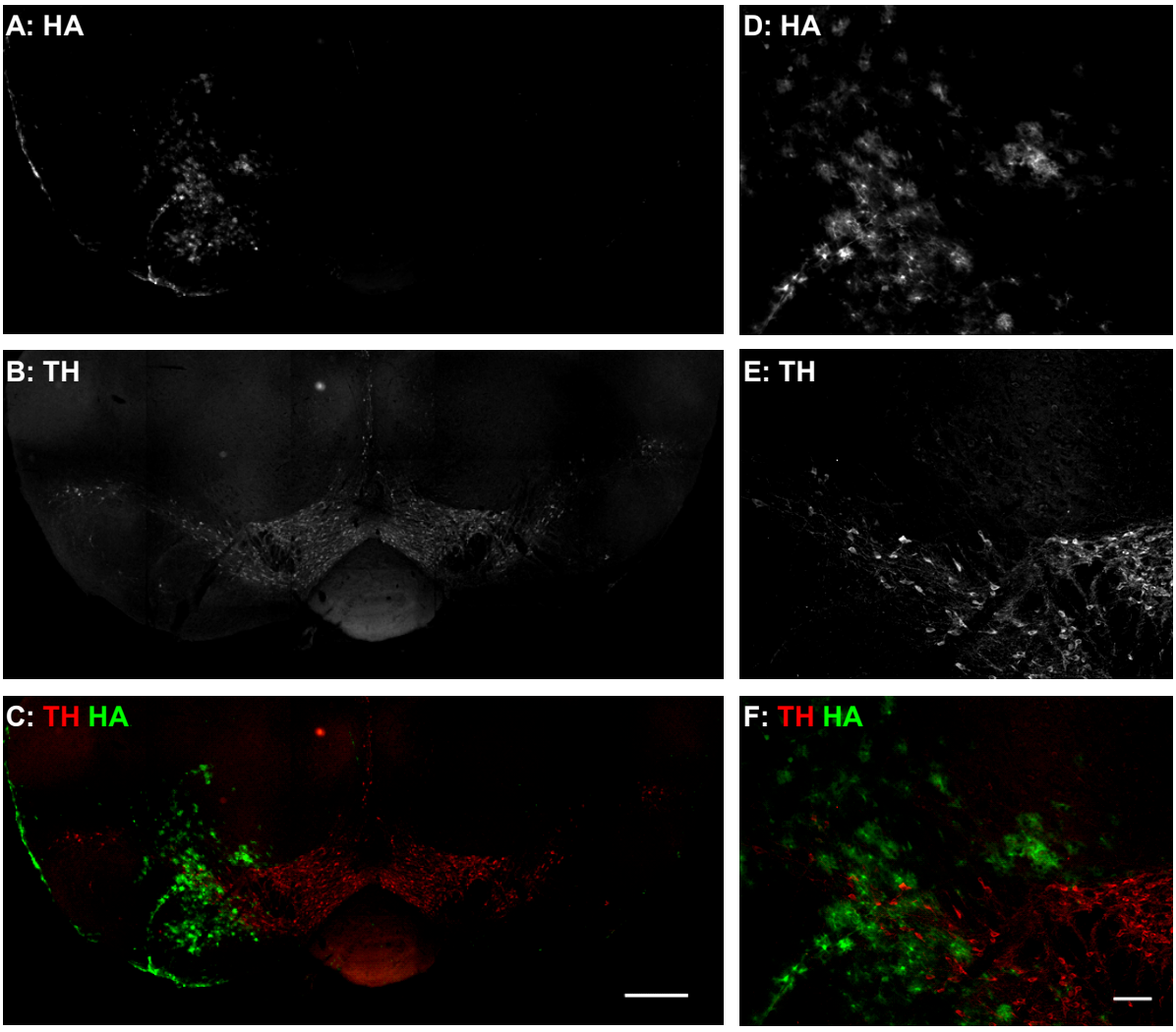

Fig.3.17 Transgene expression in the substantia nigra (SNc) after lentivirus mediated gene transfer to the SNc. (A-C) Mosaic images composed of 15 single pictures showing overview of a coronal midbrain section representing expression of HA-tagged Hsp70 stained with an antibody

against HA (A), dopaminergic neurons stained for TH (B) after infection with LV-HAHsp70 (6100 WPRE copies) and merge (C) of (A,B); scale bar is 500 µm. **(D-F)** Close-up pictures of (A-C). Scale bar in (F) is 100 µm. Note the merge images (C,F) reveal no HA-staining in TH-positive neurons.

By combining both approaches we addressed the question for infection efficacy of the LV preparations, whether the MPTP paradigm was feasible in our hands and if so, whether LV induced Hsp70 expression was sufficient to protect against MPTP toxicity. At 5 dpi osmotic minipumps filled with either MPTP (30 mg/kg) were subcutaneously implanted in these mice. Control mice were either completely untreated or received lentiviral injection only. Minipump-implanted as well as control mice were sacrificed after 4 weeks, 30 µm cryosections of the SNc were examined for lentiviral transgene expression (Fig.3.17) and viability of dopaminergic neurons (Fig. 3.18).

Stereological counting of TH-positive neurons in the uninjected SNc revealed that the number of dopaminergic neurons was significantly reduced to 60% in all MPTP-treated animals, but not in untreated or saline-treated controls (Fig. 3.18A). To investigate if neuronal cell death in SNc led to a decrease in striatal dopaminergic innervations, we examined the density of dopaminergic terminals in the striatum of the non-injected hemisphere by measuring TH-positive innervations via optical density analysis. As expected we also found the dopaminergic terminal density in the striatum significantly reduced (to about 30%, Fig. 3.18B).

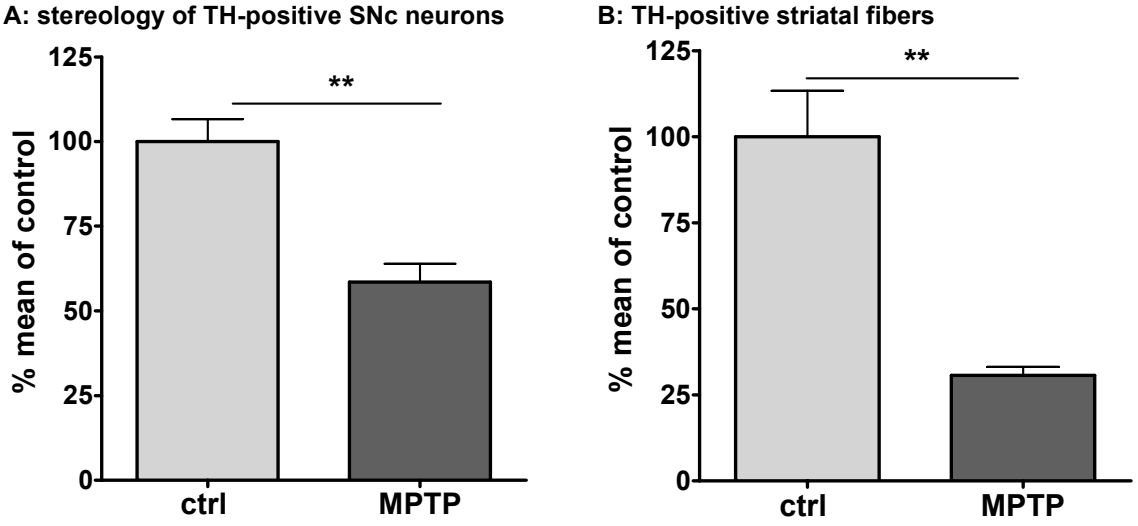

Fig. 3.18 MPTP-induced loss of TH-positive neurons in the SNc and TH-positive striatal fibers. The control group represents untreated and saline treated animals; n= 3 for ctrl and n = 4 for MPTP. Comparisons were made by one-tailed t-test. P values are depicted with respect to the control group; $^{**}P < 0.01$. **(A)** The number of dopaminergic neurons in the SNc of uninjected hemispheres was counted by stereology of TH-positive neurons. Bars represent the percentage of dopaminergic neurons relative to the mean value of the control group (ctrl) as mean +SEM. **(B)** The TH-signal in the striatum of uninjected hemispheres was densitometrically measured. Bars represent the percentage of the optical density relative to the mean value of the control group (ctrl) as mean +SEM.

Counting Nissl-positive cells produced the same results as counting TH positive cells in the SNc (data not shown), which confirms the loss of dopaminergic neurons and not only the downregulation of TH.
When we compared data from the LV-injected hemispheres, we found neither a difference between the numbers of surviving neurons in the SNc nor in the striatal TH fiber density after LV-Hsp70 or LV-EGFP infection or no infection (data not shown). Thus, Hsp70 expression was not protective in the MPTP paradigm used here, which was most likely due to the poor LV-infection efficiency in the SNc (Fig.3.17 and section 3.4.2.1).
Since the 30 µm cryostat sections used for the histological analysis, detection of aggregates by Thioflavine S staining or the PK-PET blot did not work well in this experiment. Therefore, we did not find out, whether the continuous MPTP application induced the formation of aggregates in the SNc. Nevertheless, the continuous MPTP regimen resulting in significant loss of dopaminergic neurons and reduction of striatal fiber density was successfully established and could be used for further experiments concerning MPTP induced aggregate formation.

3.4.2.3. Lentiviral Hsp70 expression in the A30PαSyn transgenic mouse model

Since the pons/midbrain was mainly affected by inclusion formation, it was the region of interest for lentiviral vector-mediated expression of Hsp70 to test the potency of a chaperone therapy in a transgenic model of α-synucleinopathy.
Aged, 16-month-old A30PαSyn transgenic mice in an early symptomatic stage (classified as described in section 3.1) received a unilateral intrapontine injection of 1.5 µl LV suspension in two sites as two deposits along one needle tract containing either LV-EGFP or LV-HAHssp70. Dependent on progression of the symptoms, the animals were sacrificed between eight and 12 weeks after infection. In cases where an animal was in the end stadium of the disease (as defined in section 3.1) it was sacrificed earlier (e.g. after two or seven weeks) for ethical reasons.
Brain tissue was processed for histological analysis to investigate whether the aggregate load was reduced by Hsp70 expression. Brains were dissected along the midline and both hemispheres were embedded in the same paraffin block in an orientation, which allowed bilateral histological examination of the same brain region.
Transgene expression was examined by IHC for EGFP using an anti-GFP antibody or for Hsp70 an anti-HA antibody on a set of three section per animal. Visualization of Hsp70 via its epitope tag guaranteed a specific detection of the Hsp70 expression levels induced by lentiviral vector mediated gene transfer. IHC was followed by ThioS staining, which gives a green fluorescence signal. Therefore, the sections were pretreated by microwave boiling in

citric acid buffer, which allowed elimination of the EGFP fluorescence and antigen unmasking for optimal epitope retrieval in one step.

The aggregate burden was determined by manual counting of ThioS-positive aggregates on microphotographs of the whole pons/midbrain within a region of interest defined by transgene expression (EGFP or HAHsp70) using the ImageJ software. Multisite photomicrographs were acquired at 200x magnification to achieve sufficient resolution. A30PαSyn mice of same age are highly variable in their aggregate load. A region of interest of the same dimension and orientation corresponding to the transgene expression area was therefore used on the contralateral side to quantify the basic aggregate level of individual animals for base-line normalization to the uninjected control side. Lentiviral overexpression of HAHsp70 showed a slight non-significant tendency to increase the ThioS aggregate load (Fig. 3.19A).

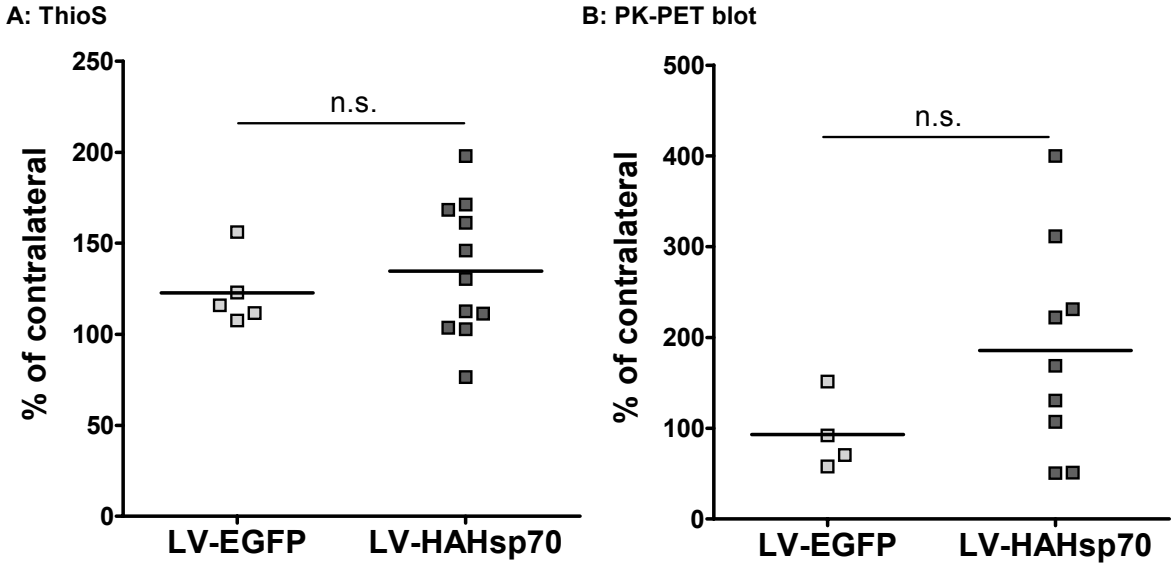

Fig. 3.19 Influence of LV-mediated Hsp70 expression on inclusion load in aged A30PαSyn mice. **(A,B)** Quantification of the inclusion load in the pons region of 18-month-old, symptomatic A30PαSyn mice after injection of 1.5 µl LV-HAHsp70 (dark squares; corresponding to 4593 WPRE copies/10^4 beta-actin copies) or LV-EGFP (light squares; corresponding to 6657 WPRE copies/10^4 beta-actin copies). Inclusions were determined both in a region of interest defined by transgene expression (EGFP or HAHsp70) and in a region of interest of the same dimension and orientation on the corresponding contralateral internal control side. In the case of LV-EGFP, an antigen retrieval procedure of microwave boiling in citric acid buffer generally used for IHC staining on paraffin sections was employed to eliminate EGFP. Infected cells were then stained by immunohistochemistry against EGFP or HA-tagged Hsp70, respectively. Means of n=3 sections of individual animals are represented as single squares. T-test revealed no significant difference between LV-HaHsp70 and LV-EGFP-treated groups. **(A)** The graph shows the number of ThioS-positive inclusions relative to the uninjected side as mean (line) and single values representing individual animals (squares). **(B)** Aggregates of proteinase K (PK) resistant α-synuclein on PK-PET blots were analyzed using the particle analysis tool of the ImageJ software. Adjacent sections stained for transgene expression (EGFP or HAHsp70 were used to define the region of interest, see above). The graph shows the number of PK-resistant α-synuclein particles relative to the uninjected side as mean (line) and single values representing individual animals (squares).

Since staining for beta-sheet structures with ThioS is a quite unspecific approach, the PK-PET blot technique was applied to visualize PK-resistant α-synuclein aggregates on a set of three sections adjacent to the sections stained with ThioS using an anti-α-synuclein antibody, which showed no crossreaction with endogenous mouse α-synuclein. Multisite photomicrographs of the PK-PET blots were acquired with a 20x objective to achieve a sufficient resolution and he PK-PET blots were analyzed by automatic particle counting using the ImageJ software. The aggregate load depicted in (Fig. 3.19B) is expressed as the fraction of the area of interest containing particles. This region of interest again was determined by anti-HA or respectively anti-EGFP IHC staining on adjacent sections. The same ROI was used to normalize the values of the injected side to the contralateral non-injected hemisphere. Again the variance between individual animals in the untreated as well as after HAHsp70 or EGFP overexpression was relatively high, consistent with the high variance in the onset of both motor phenotype and histological aggregates (Fig. 3.19B).

Both aggregate detection methods revealed a non-significant trend towards an Hsp70-mediated increase in the aggregate load. Since these indistinct results might be due to the low transgene expression levels achieved with lentiviral vectors, the viral expression system was changed to Adeno-associated viral (AAV) vectors.

3.4.2.4. Evaluation of AAV-mediated gene transfer to improve overexpression of Hsp70 in A30PαSyn transgenic mice

Since LV showed a limited transgene expression in neurons, we tested whether AAV were more suitable to fulfill the requirements for efficient intraneuronal expression of Hsp70 in the pons/midbrain region.

The AAV generated for this project contained cDNA encoding HA-tagged Hsp70 (or EGFP for control vectors) under control of the neuron-specific synapsin promoter. This, in addition to the neuronal tropism of serotype 2-AAV used here, was supposed to restrict transgene expression to neuronal cells.

The AAV preparation AAV2-HAHsp70, expressing HA-tagged Hsp70 under control of the synapsin promoter was produced and the titer was determined by the viral vector platform of the DFG center for molecular physiology of the brain (CMPB) in cooperation with Dr. Sebastian Kügler according to standard protocols (Shevtsova 2006). The AAV-HAHsp70 preparation was positively tested for transgene expression by infecting primary cortical neurons (generously provided by Dr. Sebastian Kügler) with $2x10^8$ and $4x10^8$ transducing units (TU). At 5 dpi cells were harvested and protein lysates were analyzed for Hsp70 expression by Western blot with an antibody for HA. A lysate of HEK293 cells, which surprisingly express transgenes driven by the neuron specific synapsin-promoter, transfected with the pAAV-HAHsp70 to test the AAV plasmid construct for HA-Hsp70 expression, served as positive control (Fig. 3.20H). An EGFP expressing control vector (AAV2-GFP) tested and described by Dr. Zinayida Shevtsova (Shevtsova 2006) was kindly provided by Dr. S. Kügler.

When 3.5 TU of AAV2-HAHsp70 or of the control vector AAV2-EGFP were injected into pons under the same conditions as described above for LV-HAHsp70 (see section 3.4.2.1), high transgene expression levels in a large number of NeuN-positive (Fig. 3.20D) neurons accompanied by a wide distribution throughout the pons (Fig. 3.20A-C) was achieved, while counterstaining for the glial marker GFAP was negative (Fig. 3.20E).

As mentioned above (see section 3.4.2.1), we also intended to find a viral vector system for transgene expression in the substantia nigra as an alternative to the AdV we used for short term transgene expression (see section 3.2.1). Therefore, AAV had been tested for their efficacy to mediate transgene expression to dopaminergic neurons of the SNc. In fact, we found transgene expression in a substantial proportion of SNc dopaminergic neurons stained for TH (Fig. 3.20F,G). Compared to LV (see section 3.4.2.2), the use of AAV enormously improved transduction of the SNc. This suggests AAV as an alternative to LV for projects, which require long-term transgene expression in SNc.

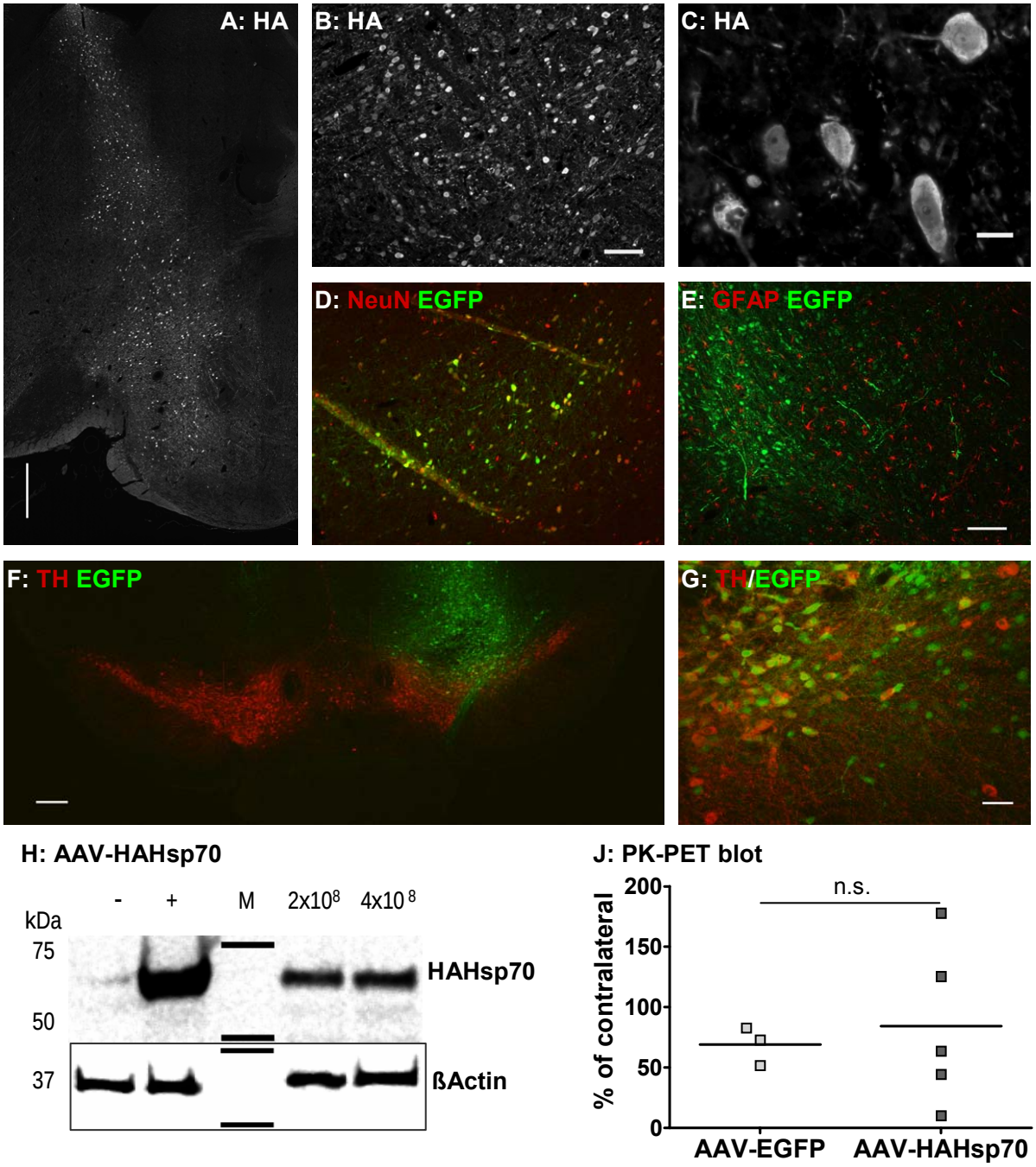

Fig. 3.20 Effects of AAV mediated transgene expression in A30PαSyn. (A-E) Sagital sections of the pons region at eight weeks after injection of 1.0 µl (corresponding to 3.5 TU) AAV-HAHsp70 or AAV-EGFP). **(A)** Mosaic image composed of 96 single pictures showing an overview of the pons region stained for HA detecting expression of HA-tagged Hsp70 in cells with neuronal morphology. Scale bar is 500 µm. **(B,C)** Close-up of the pons stained for HA showing expression of HA-tagged Hsp70 in a large number of cells with neuronal morphology. Scale bars represent 50 µm (B) and 20 µm (C). **(D,E)** Close-up of the pons showing infection and EGFP expression (green) in a subset of glia stained for the glia-specific marker GFAP (glial fibrillary acidic protein (red) (D) or neurons stained for the neuron-specific marker NeuN (neural nuclei protein (red) in the yellow merge (E). Scale bar in (E) represent 100 µm. **(F)** Mosaic image composed of ten single pictures showing an overview of the midbrain showing EGFP fluorescence (green) in the SNc after injection of AAV-EGFP. Dopaminergic neurons were counterstained by an antibody against tyrosine hydroxylase (TH, red). Scale bar is 200 µm. (C) Close-up of the SNc showing infection and EGFP expression (green) in a subset of SNc dopaminergic neurons stained for TH (red). Scale bar is 50 µm. **(H)** AAV expression in lysates from primary cortical neurons (PCNs) after infection with $2x10^8$ and $4x10^8$ TU. Positive control (+) was from

a transfection of HEK293 cells with pAAV-HAHsp70. Negative control (-) was a lysate from non-infected PCNs. Lysates were subjected to electrophoresis and blotting, membranes were developed with antibodies against with antibodies against β-actin (as loading control) and HA (hemagglutinin) to confirm transgene expression. **(J)** Quantification of the inclusion load in the pons region of 18-month-old, symptomatic A30PαSyn mice at eight weeks after. Aggregates of proteinase K (PK) resistant α-synuclein on PK-PET blots were analyzed using the particle analysis tool of the ImageJ software. The inclusion load were determined both in a region of interest defined by transgene expression (EGFP or HAHsp70) and in a region of interest of the same dimension and orientation on the corresponding contralateral internal control side. Adjacent sections stained for transgene expression (EGFP or HAHsp70) were used to define the region of interest). The graph shows the number of PK-resistant α-synuclein particles relative to the uninjected side as mean (line) and single values representing individual animals (squares). Means of n=3 sections per individual animal are represented as single squares. T-test revealed no significant difference between LV-HaHsp70 and LV-EGFP-treated group.

When we analyzed AAV-treated mice for changes in their inclusion load, ThioS staining unfortunately turned out to be not useful in AAV-infected tissue, because microscope imaging using higher magnification revealed staining artifacts within the injection area, which caused false-positive signals in the quantification routine in some cases, making it impossible to obtain reliable results. Thus, we obtained data with the PK-PET blot method only. Detection of PK resistant α-synuclein aggregates by PK-PET blot staining and data analysis was performed as described above.

AAV-mediated Hsp70 expression had a non-significant trend to increase in the aggregate load (Fig. 3.20J), confirming the findings derived from lentiviral expression of Hsp70 (see section 3.4.2.3). This effect is in line with results from our α-synuclein-based cellular PD model, where Hsp70 on the one hand prevented formation of aggregates and increased their reduction and clearance. But on the other hand, the prevalence of aggresomes was increased with Hsp70 in this *in vitro* model independent from α-synuclein (see section 3.4.1.2). Thus, the inclusions we determined both with ThioS and PK PET blot staining in A30PαSyn transgenic mice might in fact be aggresomes. Since LBs share many properties with aggresomes (McNaught et al. 2002), our assumption is accordance with the characterization of the A30PαSyn transgenic mouse line, where the ThioS-positive and PK-resistant α-synuclein inclusion have been described as “LB-like”.

4. Discussion

4.1. Synphilin-1 induced aggregate formation and toxicity

We created a new mouse model based on adenoviral gene transfer to investigate effects synphilin-1 *in vivo* to elucidate whether WT compared to R621C mutated synphilin-1 can induce aggregate formation and cell death in the dopaminergic system. Furthermore, we used viral vector targeted overexpression of synphilin-1 in A30PαSyn mice to determine whether the additional overexpression of transgenic α-synuclein would exert influence on the results. We have shown that AdV-mediated expression of synphilin-1 *in vivo* leads to formation of aggregates and to the death of dopaminergic neurons. Interestingly, the induction of aggregates in α-synuclein transgenic animals was increased only by R621C but not by WT synphilin-1 whereas both variants decreased the number of dopaminergic neurons to a similar extent.

4.1.1. Effects of AdV-EGFP control vector

The adenoviral vectors used here did not induce significant toxicity at the timepoint investigated (seven days after infection) in either non-tg or A30PαSyn animals, demonstrated by no loss of dopaminergic neurons upon expression of AdV-EGFP. However – as commonly the case when using adenoviral vectors – inflammatory infiltrates and pearl chain-like appearance of dendrites were observed at later timepoints (2 weeks after infection).

In about 5% of TH-positive neurons we found ThioS-positive inclusions under control conditions. These conditions included AdV-mediated EGFP expression in non-tg and A30PαSyn mice, and the contralateral, non-infected SNc in non-tg and A30PαSyn mice. This is in line with earlier reports of non-specific staining with ThioS staining (Vallet *et al.* 1992). These signals were considered as the basal level of the ThioS-assay representing a false-positive threshold proportion. A30PαSyn mice infected with AdV-EGFP showed ThioS-positive inclusions in a substantial proportion of infected cells of both the SNc and the striatum, whereas we saw no difference between the uninfected hemispheres of A30PαSyn and non-tg animals. This is consistent with earlier studies that did not find inclusions in dopaminergic neurons of this mouse line (Neumann *et al.* 2002). Moreover, we (see section 3.1) and others (Neumann *et al.* 2002) did not observe inclusion formation in any brain region in young, pre-symptomatic A30PαSyn transgenic mice Inclusions have been described in other lines (Masliah *et al.* 2000; Tofaris *et al.* 2006) and in studies using viral overexpression of α-synuclein in mice (Lauwers *et al.* 2003), rats (Kirik *et al.* 2002; Lo Bianco *et al.* 2002) and primates (Kirik *et al.* 2003). In cell culture, aggregates have not been observed upon expression of α-synuclein alone (McLean *et al.* 2001), but were observed when expression of α-synuclein was paired with an additional stressor to the cell, such as iron (Hasegawa *et al.*

2004; Roberti *et al.* 2007), proteasome inhibition (McLean *et al.* 2001), MPP^+ (Fan *et al.* 2006) or H_2O_2 (Jiang *et al.* 2007). It is therefore possible that the stress entailed by infection with an adenoviral vector similarly triggered α-synuclein aggregation in our A30PαSyn animals.

4.1.2. WT synphilin-1 induces inclusion formation and toxicity

We have shown that overexpression of synphilin-1 stimulates the formation of aggregates in non-tg mice. Aggregates also have been described with synphilin-1-EGFP fusion constructs in SH-SY5Y (Marx *et al.* 2003) and in HEK293 cells (O'Farrell *et al.* 2001).

In untreated SH-SY5Y cells aggregation was much lower (0.2 %) (Engelender *et al.* 1999; McLean *et al.* 2001; Lee *et al.* 2002a; Tanaka *et al.* 2004) than with adenoviral overexpression in striatum or SNc (30-40 %) in the present study. In these models, treatment with proteasomal inhibitors was necessary to induce inclusions in about 30% of the transfected cells. Apparently, the *in vivo* context facilitates or is even required for aggregate formation by synphilin-1 in a neuronal cell. There was no difference in the frequency of aggregates between the SNc and the striatum, indicating that a dopaminergic phenotype was not required for aggregate formation by synphilin-1.

In A30PαSyn transgenic animals, WT synphilin-1 did not induce aggregates beyond the control vector. Although an *in vitro* study reported that A30PαSyn did not co-localize with WT synphilin-1 in cytoplasmatic inclusions in primary neurons and H4 cells (McLean et al. 2001), our data imply that a WT synphilin-1/A30PαSyn interaction exists, because otherwise the aggregate forming processes induced by transgenic A30PαSyn and adenovirally expressed WT synphilin-1 would have taken place independent from each other in our model. Consequently, there should be an additive effect fact leading to an increased aggregate load, which is not the fact. Consistently, synphilin-1 and α-synuclein have been shown to interact at synaptic vesicles (Ribeiro *et al.* 2002).

Viral overexpression of WT synphilin-1 but not of control vector AdV-EGFP led to the degeneration of dopaminergic neurons. Other investigators report that synphilin-1 strongly increases α-synuclein toxicity in cultured cells. In these studies, cells that exhibited synphilin-1/α-synuclein inclusion bodies were relatively spared, implying a cytoprotective role for intracellular inclusions (Tanaka *et al.* 2004). No *in vitro* study, which analyzed cells for inclusion formation at 48 h after transfection, reports that WT synphilin-1 overexpression alone leads to cell death. Nonetheless, synphilin-1 has been shown to increase cell's vulnerability to toxic agents such as proteasomal inhibitors (O'Farrell *et al.* 2001; Lee *et al.* 2002a) or an apoptotic stimulus (Marx *et al.* 2003). This suggests that the *in vivo* condition and/or the prolonged incubation time of 7 days facilitate synphilin-1-induced cell death.

In our model synphilin-1 affected the neuronal viability to a slightly larger extent in A30PαSyn mice than in non-tg mice. While this difference is consistent with the *in vitro* data, its small size indicates that *in vivo*, A30P-α-synuclein is not very important for synphilin-1-induced cell death.

While this study was in progress, Jin and colleagues described a transgenic mouse expressing human synphilin-1 (Jin *et al.* 2008). Although the synphilin-1 transgenic mice did not show a loss of TH-positive neurons at 24 to 34 weeks of age, they presented with gait abnormalities and reduced Rotarod performance at week 40 to 41. The discrepancy between loss of TH-positive cells in virus-induced expression of synphilin-1 and no reduction of TH-positive cells in transgenic mice is reminiscent of those between viral expression of α-synuclein and transgenic mouse lines (Kirik *et al.* 2002; Lo Bianco *et al.* 2002; St Martin *et al.* 2007).

In the present study, the effects of viral synphilin-1 overexpression have been described in an animal model for the first time. The discrepancies between to results in cell culture demonstrate the relevance of animal models to link proteins and mutations to human disease.

4.1.3. Effect of R621C mutant synphilin-1 on inclusion formation and toxicity

Overexpression of R621C synphilin-1 stimulated the formation of aggregates in non-tg mice to a similar extent like WT synphilin-1, consistent with the *in vitro* findings in SHSY-5Y cells not challenged with proteasome inhibitors described by Marx et al. When we treated A30PαSyn mice with the AdV constructs, only R621C but not WT synphilin-1 further extended the aggregate load compared to the basic aggregate load of vector control treated non-tg mice. Conversely, aggregation of WT synphilin-1 increased upon proteasome inhibition, whereas aggregation of R621C synphilin-1 did not (Marx *et al.* 2003). Further studies will be required to resolve this discrepancy. Possibly, aggregates observed with EGFP-fusion proteins are not identical with ThioS-positive inclusions. As discussed for the Hsp70 project above (see section 4.3.6), the inclusions we determined both with ThioS and PK PET blot staining in A30PαSyn transgenic mice might be rather aggresomes than aggregates. Consistently, overexpression of synphilin-1 in HEK293 cells induced the formation of multiple small highly mobile aggregates in a recent study, while proteasome or Hsp90 inhibition rapidly triggered their translocation into the aggresome, indicating that aggresome formation, but not aggregation of synphilin-1, is a cellular response to a dysfunction of the proteasome/chaperone machinery (Zaarur *et al.* 2008). Moreover, consequences of proteasome inhibition are expected to differ from expression of A30PαSyn.

In contrast to the results for inclusions, there was no difference in toxicity between

WT synphilin-1 and the R621C mutation. It is possible that the difference in aggregation did not have time to translate into a difference in toxicity at the timepoint investigated here (7 days post-infection). This would be consistent with the identification of R621C as a susceptibility factor for PD (Marx *et al.* 2003), which is a slowly progressive neurodegenerative disorder. It can also be interpreted in the sense that aggregation and toxicity may be dissociated, as suggested by the hypothesis that toxicity is generated not by visible aggregate species but by oligomere precursors (Goldberg and Lansbury 2000).

Recently, an isoform of synphilin-1, called synphilin-1A, was identified, that induces aggregate formation in cell culture and is present in aggregates from α-synucleinopathy patients. Overexpression of synphilin-1A, but not of synphilin-1 was found to promote apoptotic death in transfected primary neurons (Eyal *et al.* 2006). This indicates that other entities of synphilin-1 different from the WT form like the synphilin-1A isoform or the R621C variation are involved in LB-formation in PD and are suitable to model PD cellular or animal models.

The importance of the R621C variation for PD pathogenesis still needs to be established further, since recent findings are somewhat inconstant: A microarray based gene expression analysis of dopaminergic SH-SY5Y cells overexpressing WT or R621C synphilin-1 were investigated for differentially regulated genes. It revealed specific effects of the R621C mutation on gene expression, which further supported its role as a susceptibility factor in PD (Bonin *et al.* 2008). On the other hand rare synphilin-1 single nucleotide polymorphisms (SNPs) of a Norwegian cohort were assessed to identify amino acid substitutions that might confer risk of PD. None of the investigated rare variations including the R621C substitution were associated with disease. The frequency of the R621C substitution was not significantly different between PD and control subjects. The authors suggest the R621C only to be a polymorphism (Myhre *et al.* 2008). A reason for this discrepancy might be that the different genetic background of the different cohorts analyzed in the two genetic studies might have an impact on SNP-induced effects.

4.1.4. Differential interaction of synphilin-1 variants with α-synuclein in non-tg and A30PαSyn mice – a hypothesis

Synphilin-1 and α-synuclein have been shown to interact at synaptic vesicles, and it has been suggested that synphilin-1 is involved in α-synuclein function (Ribeiro *et al.* 2002). A30P mice overexpress A30P-α-synuclein, so there might be an excess of α-synuclein without binding partner that then aggregates. Hypothetically, overexpression of human WT synphilin-1 might then have actually increased the amount of functional synaptic A30Pα-synuclein by mediating synaptic vesicle binding of A30Pα-synuclein. This effect might have

compensated an increase in pathological somal A30Pα-synuclein accumulation, mediated by WT synphilin-1, too. It is conceivable that this functional interaction reduces the propensity of synphilin-1 and/or alpha-synuclein to aggregate. This hypothesis might thus help explain why there are not more aggregates with WT synphilin-1 in A30PαSyn mice. As cell lines do not show a compartment with synaptic vesicles, they tend to show only the effect at the soma.

This hypothesis demonstrates the ambivalent character of the synphilin-1/α-synuclein-interaction. On the one hand the functional interaction of α-synuclein with synaptic vesicles is believed to be reversible (Kahle *et al.* 2000; Fortin *et al.* 2004) and mediated by synphilin-1 (Ribeiro *et al.* 2002). On the other hand, it was suggested by Ribeiro *et al.* that synphilin-1 becomes available as a core for aggregate formation, if abnormal intracellular distribution leads to its persistence in the neuronal soma (Ribeiro *et al.* 2002). This is supported by investigations of developmental stages of cortical LB in brains of patients with dementia with LB, proposing that chronic axonal transport blockage is implicated in the development of LB (Katsuse *et al.* 2003). In A30PαSyn mice the abnormal accumulation of transgenic α-synuclein might have caused such a blockage (Kahle *et al.* 2000). Our time-lapse imaging experiments with fluorescently labeled α-synuclein (see section 4.3.2) demonstrated that the formation of aggregates is not slow or irreversible, but rather a highly dynamic process with simultaneous generation, accumulation, reduction, and clearance of aggregates (Opazo *et al.* 2008).

All these data imply the existence of a dynamic equilibrium between synaptic function, proteasome-mediated protein degradation and somal accumulation. If this balance is disturbed by overexpression or mutation of one of the interaction partners or proteasomal dysfunction, it might shift to a pathological state, were synphilin-1/α-synuclein aggregates act as an “inoculum” for the assembly of insoluble multi-protein complexes as proposed for cellular models by Eyal and Engelender (Eyal and Engelender 2006).

In vitro assays revealed a less efficient association of mutant A30Pα-synuclein with cellular vesicles (Jensen *et al.* 1998), lipid membranes (Jo *et al.* 2002) and lipid rafts (Fortin *et al.* 2004), suggesting a deficiency of axonal transport for A30PαSyn transgenic mice. Surprisingly, the transport of synaptic vesicle proteins was not generally abolished in transgenic mice expressing human WT or A30PαSyn, rather a pathological accumulation of the transgenic human α-synuclein in neuronal cell bodies and neuritis was observed, whereas endogenous mouse α-synuclein was not retained (Kahle *et al.* 2000). In our model WT synphilin-1 overexpression was not sufficient to induce more aggregates than the control virus. An increase in pathological somal A30Pα-synuclein accumulation mediated by overexpression of human WT synphilin-1 might be compensated by an increase in synaptic localization of A30Pα-synuclein, mediated by overexpression of human WT synphilin-1, too.

However, this effect apparently requires a mature differentiated presynapse since synphilin-1 increased the aggregation of alpha-synuclein in cell lines (McLean *et al.* 2001).

The R621C mutation seemed to disable synphilin-1 to mediate synaptic localization of α-synuclein and thereby increased the aggregate formation in our model. A recent study revealed the amino acid sequence 610–640 to represent the primary determinant site for phospholipid binding of synphilin-1, which was abolished by the R621C mutation, residing within the same sequence (Takahashi *et al.* 2006). According to interaction between WT synphilin-1 and A30PαSyn hypothesized above, if there would be no interaction between synphilin-1 and α-synuclein, one would expect the frequency of aggregates to be the sum of aggregates induced by the two proteins alone, which is the case for R621C mutated synphilin-1. This may explain why the R621C mutation led to added aggregation in A30PαSyn animals, which is consistent with the fact that the mutation destroys the phospholipids binding of synphilin-1 *in vitro* (Takahashi *et al.* 2006). This implies that the R621C mutation exerts its effect not by a direct toxic gain of function, but rather impairs the physiological function of synphilin-1, leading to free and thus aggregating synphilin-1.

Hypothetically, changes in the equilibrium between functional synaptic localization, protein degradation and somal accumulation mentioned above (see page 113) may lead to aggregate formation in a first step. This mechanism probably reflects the ability of the cell to cope with non-physiological protein entities, like over-expressed or mutated α-synuclein or synphilin-1 by sequestering them in insoluble inclusion. If the cell loses this capability cell death could be the second step and the final consequence of an overload of the cellular machinery.

Taken together, it could be shown that expression of synphilin-1 in mouse brain by adenoviral gene transfer induced formation of aggregates and the death of dopaminergic neurons. These two core characteristics of PD have been difficult to observe in combination in previous mouse models for PD based on overexpression of α-synuclein. Overexpression of synphilin-1 may therefore provide a new mouse model for PD that better imitates the core histological characteristics found in PD patients.

4.2. A30PαSyn/UbGFP reporter mice reveal no UPS impairment

There is growing evidence, that protein misfolding and impairment of proteasome function is involved in the pathogenesis of familial and sporadic PD (Giasson and Lee 2003; Moore *et al.* 2003). In contrast to WT, A53T and A30P mutant forms of α-synuclein were reported to inhibit proteasome function (Stefanis *et al.* 2001; Jiang *et al.* 2007). Proteasome function was reported to be impaired in nigral dopaminergic neurons of sporadic PD patients (McNaught *et*

al. 2002; McNaught *et al.* 2003) and pharmacological inhibition of the UPS mimicked key characteristics of PD in rats (McNaught *et al.* 2004).

Therefore, we addressed the question if and when proteasomal impairment occurs during formation of PK-resistant α-synuclein aggregates in A30PαSyn mice. A30PαSyn were crossbred with a transgenic reporter mouse line which was generated to monitor proteasome impairment *in vivo*. Analysis of the UPS reporter levels in animals of all examined ages revealed no difference between the distribution pattern of GFP-positive cells in the aggregate-affected brain regions from A30PαSyn+/+;UbGFP^{G76V}+/- and controls. Our findings are in line with a study using the same Ub^{G76V}-GFP reporter mouse line to assess UPS function in transgenic knock-in mouse model for human spinocerebellar ataxia 7 (SCA7), showing functional impairments and accumulation of insoluble ataxin-7 aggregates. No increase in the reporter protein levels was found in early stages of the disease, while the increase observed during disease progression was due to increased mRNA levels of Ub^{G76V}-GFP. The authors suggest that inclusion formation and neuronal dysfunction occurred in the presence of a functional with UPS impairment or reduced proteasome activity, which was confirmed by an *in vitro* assay for proteolytic activity of the proteasome, ruling out UPS impairment as a necessary event for polyglutamine neuropathology in this model (Bowman *et al.* 2005). In combination with our findings these data make a causative role for proteasome dysfunction in aggregate formation and neurodegeneration unlikely.

This assumption is supported by a putative model for the molecular pathogenesis of PD, which was proposed by Moore and colleagues: Mitochondrial complex-I inhibition, followed by deficits in the ATP synthesis, increased oxidative stress and α-synuclein aggregation, induced by environmental or genetic factors, might cause impairment in UPS function, suggesting it to be a common endpoint during the molecular pathogenesis of PD, which culminates in the degeneration of dopaminergic neurons (Moore *et al.* 2005). Another possibility is that dysfunction of other protein clearance pathways are involved in LB formation in PD.

It has been reported that proteasomal, lysosomal and autophagic pathways appear to be involved in PD: Dopaminergic neurons in the SNc of PD patients show impaired proteasom activity (McNaught and Jenner 2001) and the incidence of PD is increased in the lysosomal storage disorder Gaucher disease (Aharon-Peretz *et al.* 2004). Also, expression of mutant A53T α-synuclein has been demonstrated to cause loss of dopamine release, alterations in the ubiquitin-dependent and autophagic cell death (Stefanis *et al.* 2001). However, whether α-synuclein is degraded via the proteasom (Bennett *et al.* 1999; Webb *et al.* 2003), chaperone-mediated autophagy (Cuervo *et al.* 2004) or macro-autophagy (Paxinou *et al.* 2001) is under debate. In a recent study all three pathways were found to contribute to α-synuclein degradation albeit autophagy was suggested to play the major role: autophagy

inhibition resulted in the accumulation of monoubiquitinated α-synuclein forms and subsequent aggregation (Rott *et al.* 2008). This is supported by the finding that α-synuclein was detected autophagic vesicles and pharmacologically activation of autophagy by rapamycin induced its clearance (Webb *et al.* 2003). In contrast to that, there is evidence that proteasom dysfunction plays the most important role in PD pathogenesis. Functional as well as structural deficits in the proteasom were identified in the SNc of PD patients (McNaught *et al.* 2002; McNaught *et al.* 2003). In the our PDZ life-imaging study mentioned above blocking of all three proteolytic pathways revealed the removal of α-synuclein aggregates to be mainly dependent on proteasom activity. Moreover, expression of the most aggregation-prone ΔCα-synuclein variant enhanced the prevalence cells with many aggregates presumably by decreasing the occurrence cells bearing a sole aggresome when proteasome function was pharmacologically inhibited. We assumed that under these conditions cells had lost their ability to decrease their aggregate burden via aggresome formation, which implicates the UPS to play an important role in this repair mechanism (Opazo *et al.* 2008), which is consistent with the lack of proteasome impairment in A30PαSyn/UbGFP reporter mice.
Taken together these data imply that proteasomal impairment might be rather a consequence of than a reason for aggregate formation in neurodegenerative diseases, at least in the investigated *in vivo* paradigm.

4.3. The therapeutic potential of Hsp70 in several model systems of PD

Chaperones are currently being considered for the potential treatment of diseases involving protein aggregation and misfolding ranging from neurodegenerative diseases (Bonini 2002) to cancer (Didelot *et al.* 2007). Several studies demonstrated a protection of different cell lines against excitotoxicity, oxidative, and thermal stress by increased expression of Hsp70 to (Amin *et al.* 1995; Wong *et al.* 1996; Kelly *et al.* 2001; Quigney *et al.* 2003; Lai *et al.* 2005).

The aim of the present study was to demonstrate the therapeutic potential of viral vector-mediated expression of the molecular chaperone Hsp70 in several PD model systems.

4.3.1. Hsp70 inhibits MPP^+-induced toxicity in cell culture

We could show that Hsp70 induction by adenoviral gene transfer or by administration of geldanamycin, prior to exposure to the mitochondrial complex I inhibitor MPP^+, reduced MPP^+ toxicity and increased cell viability when compared to vehicle treatment. Infection with AdV-Hsp70 significantly decreased caspase activation by MPP^+, as did the caspase inhibitor zVAD-fmk. Hsp70 has been shown by other investigators to inhibit cytochrome c release from mitochondria (Beere *et al.* 2000) by preventing the activation of c-Jun (Bienemann *et al.*

2008) and formation of the apoptosome out of cytochrome c, Apaf-1 and caspase 9 by binding to the caspase recruitment domain of Apaf-1 (Beere *et al.* 2000; Li *et al.* 2000; Saleh *et al.* 2000). This suggests that the effects of Hsp70 may result from direct inhibition of the apoptotic cascade. However, when we tested AdV-Hsp70 in conditions where caspase activation is not responsible for cell death, zVAD-fmk-induced caspase inhibition had little effect, but AdV-Hsp70 was protective in the LDH assay and in the trypan blue exclusion assay as was geldanamycin.

Our findings are in line with the results of a heat shock pre-treatment of rat neuroblastoma cells prior to the addition of MPP^+, which led to an increase in the synthesis of Hsp27 and Hsp70 proteins and significantly reduced cell death (Donaire *et al.* 2005). Hsp70 was also found to antagonize apoptosis inducing factor (AIF) in a caspase-independent way (Susin *et al.* 1999; Ravagnan *et al.* 2001). Furthermore, heat shock has been shown to induce Hsp70 and protect cells from MPP^+-induced necrotic cell death, which occurs independent of the caspase cascade (Quigney *et al.* 2003); even though Quigney and colleagues have not directly shown that Hsp70 mediates the protective effect of heat shock. As mentioned above, cell death following MPP^+ treatment most likely not only results from direct activation of caspases (Dodel *et al.* 1998; von Coelln *et al.* 2001) but also from generation of reactive oxygen species and subsequent damage to proteins, lipids and DNA (Schulz *et al.* 2000).

The pharmacological induction of Hsp70 with geldanamycin (GA) was reported to be neuroprotective against focal brain ischemia (Lu *et al.* 2002). It is believed to act via inhibition of Hsp90 (Whitesell *et al.* 1994), which is a negative regulator of the key mediator of the heat shock response cascade HSF (the heat shock transcription factor) (Morimoto 1998; Zou *et al.* 1998). In our cell culture model pretreatment with geldanamycin led to a significant reduction of MPP^+ toxicity with respect to the DMSO vehicle control. Consistently with our data, GA also prevented dopaminergic neuron death caused by overexpression of α-synuclein in *Drosophila* (Auluck *et al.* 2005) and attenuated α-synuclein-mediated neurotoxicity in human H4 neuroglioa cells (McLean *et al.* 2004).

Oxidation can increase the tendency of proteiens to aggregate (Giasson *et al.* 2000; Kowall *et al.* 2000; Lee *et al.* 2002b; Meredith *et al.* 2002) and Hsp70 has been shown to decrease toxicity resulting from aggregating proteins, including huntingtin, ataxin-1, SOD1 and α-synuclein (Warrick *et al.* 1999; Carmichael *et al.* 2000; Muchowski *et al.* 2000b; Cummings *et al.* 2001; Auluck *et al.* 2002; Takeuchi *et al.* 2002; Klucken *et al.* 2004b; Wyttenbach 2004). The caspase-independent effect of Hsp70 on MPP^+-induced toxicity therefore most likely resulted from its effect on oxidized and/or misfolded proteins (Giffard *et al.* 2004). We next intended to explore the influence of Hsp70 on α-synuclein aggregation and toxicity in a cellular model system.

4.3.2. Hsp70 reduces α-synuclein aggregation and toxicity in cell culture

A new strategy to fluorescently label α-synuclein and to characterize aggregate formation and toxicity in living cells, which was developed in our laboratory, was employed to examine effects of Hsp70 α-synuclein aggregation and toxicity (Opazo *et al.* 2008).

The prevalence of preapoptotic cells served as a marker for cellular toxicity in this system. Hsp70 expression significantly reduced the ΔCα-Syn-induced toxicity, which strikingly demonstrated the protective potential of Hsp70 in cell culture in a dynamic detection system. It corroborated previous studies, which found Hsp70 to be protective against α-synuclein-induced toxicity in a Drosophila model for PD (Auluck *et al.* 2002) and in neuroglioma cells (Klucken *et al.* 2004a).

The ratio of aggregate progression, reduction and clearance in time-lapse imaging was significantly altered by addition of the molecular chaperone Hsp70. Consistently, the prevalence of aggregates was also reduced in previous studies (Auluck *et al.* 2002; Klucken *et al.* 2004a; Klucken *et al.* 2004c). However, these previous studies could not differentiate between the prevention of aggregate production and a potential removal of aggregates. This difference is clinically relevant, because PD patients have already accumulated a significant aggregate load and loss of neurons at the time of diagnosis, which limits the therapeutic potential of purely preventive strategies. Our time-lapse experiments demonstrated for the first time that Hsp70 increased the clearance of protein aggregates, which occurred primarily through the aggresome. This underlines the therapeutic potential of Hsp70 or small molecules with similar effects. Hsp70 also increased the removal of small aggregates and aggresomes from the cytosol. Finally, Hsp70 decreased the formation of small peripheral aggregates in homogeneous cells and reduced the progression from single aggresomes to more and larger aggregates, which might be explained by the inhibition of aggregate formation observed *in vitro* (Dedmon *et al.* 2005). Consistent with neuroprotective consequences of Hsp70-aggregate removal via the aggresome, the microtubule depolymerizing agent nocodazole inhibited the heat-shock-provoked protection of dopaminergic neurons from lactacystin-induced cell death (Ahn and Jeon 2006).

4.3.3. The “chronic” MPTP mouse model for PD

We further attempted to adopt a chronic of MPTP application regimen in our laboratory and to test lentiviral expressed Hsp70 for functionality *in vivo* simultaneously.

Systemic administration of the toxin MPTP resulting in specific degeneration of dopaminergic neurons as one of the most commonly used pharmacological animal models for PD. It mimics clinical, biochemical, and neuropathological alterations occurring in PD. Nevertheless, acute as well as subchronic MPTP model systems, which are used in most studies, do not induce aggregates and thereby lack the second histopathological core

characteristic of PD, LBs or at least LB-like inclusion. However, it is desirable to mimic both, dopaminergic cell loss and aggregate formation in the SNc in a useful animal model for PD.
In contrast to subchronic or acute application regimens, where the toxin is completely metabolized, when the animals are sacrificed, the mouse body including brain tissue was still contaminated with MPTP in continuous MPTP infusion regimen at the timepoint of scarification. This presents an apparent disadvantage, because it complicates tissue processing. For safety reasons we decided to perform cryo instead of paraffin sectioning. In these sections, we were not able to detect α-synuclein aggregates. Fornai and colleagues had reported that, in contrast to other application paradigms, continuous administration of MPTP via subcutaneously implanted osmotic minipumps has been shown to induce aggregate formation in the lesioned SNc (Fornai *et al.* 2005), whereas this finding could not reproduced by other laboratories (Shimoji *et al.* 2005; Alvarez-Fischer *et al.* 2008).
The objective to establish degeneration of nigral dopaminergic neurons including their striatal terminals to an adequate extent by continuous MPTP infusion was accomplished in our preliminary trial. Consistent with the findings of Fornai and colleagues, continuous MPTP infusion induced loss of dopaminergic neurons in the SNc, accompanied by a reduced density of TH-positive fibers in our hands, albeit to a smaller extent. The observed decline of ~ 50% of TH-positive neurons is rather in the range routinely observed after repeated injections in the subchronic MPTP regimen of 5x30 mg MPTP in our laboratory (Eberhardt *et al.* 2000; Rathke-Hartlieb *et al.* 2001; Kowsky *et al.* 2007) and by other investigators (Dong *et al.* 2005; Schober *et al.* 2007). Thus, in our hands the continuous infusion regimen was not worthwhile the additional technical difficulties.

4.3.4. Hsp70 expression in the “chronic” MPTP mouse model for PD

As mentioned above, we and others have demonstrated that Hsp70 induction by heat-shock, plasmid-mediated overexpression or geldanamycin treatment was protective in the MPP^+ cell culture model (see section 4.3.1). Next, we addressed the question whether LV-induced Hsp70 expression was sufficient to be neuroprotective in the MPTP mouse model. We did not observe Hsp70 to be protective against MPTP toxicity in this paradigm. This finding was consistent with the lacking effect of AdV-mediated Hsp70 expression in the subchronic MPTP model of PD (Falkenburger and Eberhardt, unpublished).
In contrast to our result, other investigators reported that the toxic insult of MPTP to the nigrostriatal system was reduced by Hsp70, when the protein was systemically applied in fusion with the HIV-derived cell penetrating peptide Tat (trans-activator of transduction) (Nagel *et al.* 2008) or when Hsp70 was expressed via targeted AAV-mediated gene transfer (Dong *et al.* 2005). An intracerebral ventricular injection of geldanamycin 24 h prior MPTP

treatment preserved TH immunoreactivity and dopamine content in the striatum (Shen *et al.* 2005). Since Shen and colleagues did not examine the SNc in this study, it remained unclear, whether the observed effect would exert neuroprotection against MPTP in the SNc, too. We assume that the lacking effect of Hsp70 might be due to the poor infection efficacy of LV in dopaminergic neurons in the SNc (see section 4.4). Since the same CMV-Hsp70 expression cassette was used in the α-synuclein cell culture model (see section 4.3.2), we could exclude problems with integrity or functionality of the plasmid construct.

4.3.5. Hsp70 expression in the A30PαSyn transgenic mouse model for PD

Major efforts are expended to elucidate the mechanisms of α-synuclein aggregation and toxicity *in vitro*, in cell culture and in a variety of animal models. These model systems are used to develop therapeutic strategies, too. It has been demonstrated before that Hsp70 can reduce α-synuclein aggregation in cell culture. Hsp70 was reported to reduce to the neurotoxic aggregation of several proteins which are known to be involved in neurodegeneration mediated by the formation of protein inclusions including α-synuclein, ataxin, SOD1, huntingtin (Warrick *et al.* 1999; Carmichael *et al.* 2000; Muchowski *et al.* 2000a; Cummings *et al.* 2001; Auluck *et al.* 2002; Takeuchi *et al.* 2002; Klucken *et al.* 2004b; Wyttenbach 2004). In A30PαSyn mice pan-neuronal expression of human mutant A30Pα-synuclein leads to abnormal somatodendritic α-synuclein accumulation in various brain regions in early age, which results in the formation of PK-resistant, Thioflavine S positive, hyperphosphorylated α-synuclein aggregates, accompanied by progressive motor dysfunction in later age. Therefore, we attempted use of Hsp70`s anti-aggregation capacity to decrease the aggregate load in aged, symptomatic A30PαSyn mice.

LV-mediated Hsp70 expression induced a slight, non-significant increase in the aggregate load. Next, we aimed to confirm this result and to exclude the possibility that the Hsp70 expression level was too low to induce aggregate reduction. If expression levels would be low, this would be a result of the incomplete neuronal infectivity of LV, because the anti-apoptotic effect observed in the α-synuclein cell culture model (see section 4.3.2) had validated integrity and functionality of the Hsp70 plasmid construct used for LV production. Therefore, the viral vector platform as well as the promoter was changed to attain an adequate neuronal transgene expression. The use of AAV and neuron specific synapsin promoter remarkably improved the neuronal transgene expression efficacy. However, AAV-mediated Hsp70 expression again had a non-significant trend to increase in the aggregate load, which confirmed the findings derived from lentiviral expression of Hsp70.

To investigate the influence on Hsp70 misfolded α-synuclein-species, Klucken and colleagues generated an animal model by crossbreeding an Hsp70 overexpressing mouse line with α-synuclein transgenic mice (Klucken *et al.* 2004c). This α-synuclein mouse line was

reported to develop LB-like α-synuclein inclusions (Masliah *et al.* 2000). This study demonstrated that enhanced chaperone protein function mediated by transgenic overexpression of Hsp70 can alter α-synuclein misfolding in an animal model. It had proved the principle, but not yet the feasibility of a therapeutic approach. We employed a gene transfer technique to validate the therapeutic potential of Hsp70 overexpression. Whereas Klucken and colleagues had performed biochemical assays, we used histological analysis for aggregate detection. This makes it complicated to compare the results. However, the comparison of these two studies appears to suggest that Hsp70 *in vivo* requires a long time to have an effect, or needs to be present at an early stage of α-synuclein aggregation.

In contrast to the time-lapse imaging experiments in cell culture, we and others were not able to resolve the dynamics of aggregation process influenced by Hsp70 or other therapeutics in the animal model. It appears to be useful to investigate in the future the influence of viral-mediated Hsp70 overexpression on α-synuclein aggregation at different timepoints.

The histological evaluation of aggregates to a late stage of the α-synucleinopathy in the A30PαSyn model allowed us to investigate the *status quo* in the final state of the aggregation process influenced by Hsp70. It reflects the "clinical situation", because in human α-synucleinopathy patients the actual aggregate burden can only be determined *post-mortem*, too. Since PD patients have already a significant aggregate load and loss of neurons at the time of diagnosis, the therapeutic potential of purely preventive strategies are limited. Our results suggest that expression of Hsp70 at this late stage is not very effective at removing the aggregates detected by PET blot and ThioS staining.

Further experiments could employ biochemical assays, which were commonly used for the detection of misfolded, aggregated, hyperphosphorylated, detergent- or PK-insoluble or high molecular weight forms of α-synuclein (Neumann *et al.* 2002; Klucken *et al.* 2004c), too. The combination of histological and biochemical analysis after Hsp70 induction during aging could be helpful to elucidate the impact of a therapeutic Hsp70 treatment on the transition between and distribution pattern of different aggregation intermediates.

4.3.6. Evaluation of Hsp70 as a therapeutic strategy

To evaluate Hsp70 as a therapeutic strategy for PD we investigated effects of Hsp70-expression on cellular survival and on the aggregate burden in MPTP-based toxin models (see sections 4.3.1 and 4.3.3) and in α-synuclein-based genetic models (see sections 4.3.2 and 4.3.5) *in vitro* and *in vivo*. We found Hsp70 to be protective against MPP^+-toxicity in caspase-dependent as well as caspase-independent cell death and against toxicity of the ΔC-α-synuclein variant in cell culture (see sections 4.3.1 and 4.3.2.). This demonstrates the capability of Hsp70 to protect against cell death mechanism related to mitochondrial

dysfunction and oxidative stress and is consistent with previous results showing that Hsp70 is involved in the cellular defense against excitotoxicity, and oxidative and thermal stress (Amin *et al.* 1995; Wong *et al.* 1996; Quigney *et al.* 2003; Lai *et al.* 2005).

Our time-lapse experiments suggested that Hsp70 increased the clearance of protein aggregates, which occurred primarily through the aggresome. This underlines the therapeutic potential of Hsp70 or small molecules with similar effects. Hsp70 also increased the removal of small aggregates and aggresomes from the cytosol. In line with these findings, cells were capable to clear cytoplasmic as well as nuclear inclusions in animal models for HD (Yamamoto *et al.* 2000; Regulier *et al.* 2003; Harper *et al.* 2005; Yamamoto *et al.* 2006) and for SCA (Xia *et al.* 2004; Zu *et al.* 2004), too. It has to be mentioned that in these conditional transgenic models the aggregate removal occurred, when the continuous production of the mutant transgene was halted. If this would have been the case in our A30Pαsyn animal model, we might have observed an Hsp70-induced reduction of inclusions.

On the other hand, the inclusions we determined both with ThioS and PK PET blot staining in A30PαSyn transgenic mice might be rather aggresomes than aggregates. LB share many properties with aggresomes (McNaught et al. 2002) and the characterization of the A30PαSyn transgenic mouse line described ThioS-positive and PK-resistant α-synuclein inclusions as “LB-like” (Neumann *et al.* 2002). We and others demonstrated that aggresomes represent the predominant path of aggregate reduction and thereby are most likely a protective response of the cell and not a cause of cell death and that Hsp70 plays a role in this mechanism (Johnston *et al.* 1998; Garcia-Mata *et al.* 1999; Tanaka *et al.* 2004; Opazo *et al.* 2008; Zaarur *et al.* 2008). This is consistent with the lack of neuronal cell death in A30Pαsyn mice (Neumann *et al.* 2002). Under this assumption, our results from A30PαSyn mice are in line with our findings from the α-synuclein cell culture model of PD (see section 4.3.2), where Hsp70 not only decreased aggregate formation but also increased removal of aggregates via aggresome formation.

As mentioned above (see section 1.2), there is growing evidence that the combination of oxidative and nitrosative stress, the accumulation of aberrant or misfolded proteins, ubiquitin-proteasome system dysfunction and deficits in mitochondrial function are the most important pathways leading towards PD pathology (Moore *et al.* 2005). In line with previous findings from other investigators (see section 1.5.2), our findings suggest that a molecular chaperone like Hsp70 can contributes to the cellular protection against these pathological pathways at several levels (Auluck *et al.* 2002; McLean *et al.* 2002; Klucken *et al.* 2004c; McLean *et al.* 2004; Auluck *et al.* 2005; Muchowski and Wacker 2005; Nagel *et al.* 2008). Further implications for molecular chaperones as a treatment for PD and other aggregopathies emerges from a number studies were the pharmacological, transgenic or viral vector-induced expression of molecular chaperones have been shown to reduce neurodegeneration caused

by overexpression of a variety of aggregating proteins (see section 1.5.2.1), including huntingtin, atixin-1 and SOD1 (Warrick *et al.* 1999; Carmichael *et al.* 2000; Muchowski *et al.* 2000a; Cummings *et al.* 2001; Auluck *et al.* 2002; Takeuchi *et al.* 2002; Klucken *et al.* 2004c; Wyttenbach 2004).

We assume that the following line of evidence strongly emphasizes the therapeutic potential of molecular chaperones in PD and other neurodegenerative disorders: (i) Protein aggregates or inclusion bodies found in a variety of neurodegenerative disorders including AD, PD, FALS (familial amyotrophic lateral sclerosis) HD, and related poly-glutamine expansion diseases are associated with molecular chaperones and components of the UPS, suggesting to be a sign of irreversible protein retention, following a cellular incapability for chaperone-mediated refolding or degradation of aggregated proteins (Muchowski and Wacker 2005). (ii) Molecular chaperones are involved in removal of aggregates through the aggresome, representing another chaperone-based mechanism decrease the number of small and even larger aggregates (Johnston *et al.* 1998; Garcia-Mata *et al.* 1999; Tanaka *et al.* 2004; Opazo *et al.* 2008). (iii) Pharmacological, transgenic or viral vector-induced expression of molecular chaperones have been shown to reduce neurodegeneration caused by overexpression of a variety of aggregating proteins (see section 1.5.2.1), including huntingtin, atixin-1 and SOD1 (Warrick *et al.* 1999; Carmichael *et al.* 2000; Muchowski *et al.* 2000a; Cummings *et al.* 2001; Auluck *et al.* 2002; Takeuchi *et al.* 2002; Klucken *et al.* 2004c; Wyttenbach 2004). This demonstrates that induction of molecular chaperones beyond endogenous levels can enhance protection mechanisms, in cases where the endogenous capacity of the cell to sequester the protein overload in aggresomes is not sufficient. (iv) Molecular chaperones can protectively interfere with many components of the pathological processes of PD.

In conclusion, these data offer the therapeutic perspective to not only prevent but also reverse disease progression in PD and other disorders associated with protein aggregation.

4.3.7. Comparison of cellular models with animal models

Adequate models of PD are needed expand our understanding of the pathogenesis of the disease and to test novel therapeutic strategies. Both, cellular and animal model systems were employed to investigate the influence of Hsp70 on different aspects of cell death and/or inclusion formation.

Cultured cells are repeatedly accessible in high numbers. Pharmacological treatment with geldanamycin and MPP^+ and Hsp70 expression via transfection or viral vector-mediated gene transfer was easier to perform then in animal models. This allowed us to compare many different conditions e.g. different toxin concentrations in the same experiment.

Moreover, continuously proliferating cells give access to a more or less homogenous cell population, which is a prerequisite for reliable biochemical assays to investigate cellular processes including viability, cell death mechanisms and inclusion formation during the whole time course of the pathological process.

Our cell culture time-lapse imaging experiments revealed that the formation of aggregates is not slow or irreversible, but a rather highly dynamic process, which is characterized by simultaneous generation, accumulation, reduction and clearance of aggregates. We found that expression of the most aggregation-prone ΔCα-synuclein variant enhanced the prevalence cells with many aggregates presumably by decreasing the occurrence cells bearing a sole aggresome when proteasom function was pharmacologically inhibited in this model. We assumed that under these conditions cells had lost their ability to decrease their aggregate burden via aggresome formation, which implicates the UPS to play an important role in this repair mechanism. Blocking of all three proteolytic pathways revealed the removal of α-synuclein aggregates to be mainly dependent on proteasome activity. By contrast, our double transgenic A30PαSyn/UbGFP reporter mouse model revealed no UPS impairment (see section 4.2). As discussed above (see sections 4.3.1, 4.3.2), Hsp70 was protective against MPP^+ - and α-synuclein-induced toxicity in both cellular PD models. And the findings from A30Pαsyn mouse model concerning α-synuclein aggregation (see section 4.3.5 and 4.3.6) direct towards the same line like from the α-synuclein cell culture model of PD (see section 4.3.2): In both cases Hsp70 induced an increase the cellular load with α-synuclein inclusions. These examples of a comparison of results from cellular with animal models for PD are in one case consistent with and contradictory to each other. Cellular models gave more insights in mechanisms of PD pathology. Another advantage of the α-synuclein cell culture model was that, in contrast to animal models available today, it induced both cell death and inclusion formation. On the other hand, a general shortcoming of cell cultures includes the lack of natural neuronal networks and thereby deprivation of physiological afferent and efferent connections. Moreover, it has to be mentioned that the α-synuclein-based experiments were performed in HEK293 cells, which lack dopaminergic characteristics.

The animal models on the other hand allowed us to estimate whether the pharmacological or genetical manipulations would have an impact on the final outcome of PD pathology (see sections 4.3.3 and 4.3.5). If the ultimate goal of PD research is to cure the disease, or at least to slow its progression, by elucidating pathological mechanisms and by developing new therapies, both model systems are complementary and appear to be worthwhile to be used in combination.

4.3.8. Comparison of MPP^+-based models with synuclein-based models

Mitochondrial dysfunction and oxidative stress on the one hand and protein misfolding and aggregation along with UPS dysfunction on the other hand are the two major pathways implicated in PD pathogenesis, to date. Exposition to MPTP or its active metabolite MPP^+ leads to inhibition of the mitochondrial complex I and increased production of reactive oxygen species, followed by oxidative stress. Thus, the MPTP-model rather represents the mitochondrial pathway (see section 1.2.1). We used α-synuclein-based cell culture and animal models to further explore the impact of Hsp70 on protein aggregation (see section 4.3.2 and 0). These models were supposed to reflect the protein aggregation and degradation aspect of PD pathogenesis (see section 1.2.2).

An optimal animal model of PD would combine the Lewy pathology recapitulated in some transgenic mouse models with the selective loss of nigrostriatal DA neurons. Neither MPTP-exposition, which does not induce LB-like inclusions, nor transgenic A30P-α-synuclein overexpression, which does not induce neuronal death represent all aspects that pertain to PD in a mouse model. The selection of model system over the other should be done based by the question and the type of investigations to be undertaken Therefore, we employed both model systems to investigate effects of Hsp70-expression on both pathways to evaluate Hsp70 as a therapeutic strategy (see below, section 4.3.6). It might be also useful to combine transgenic α-synuclein-expression with other genetic risk factors like synphilin-1 (see section 4.1) or with neurotoxins. Indeed, there are studies combining genetic models are with PD-specific toxins to investigate the effect of the genetic modification on toxin susceptibility or vice versa the influence of toxins on the genetically-induced pathology (Rathke-Hartlieb *et al.* 2001; Dong *et al.* 2002; Nieto *et al.* 2006; Yu *et al.* 2008). Such complex animal model might reflect the pathological circumstances in PD patients, because the etiology of sporadic PD is believed to be a combination of environmental and genetic factors (see section 1.2).

4.4. Evaluation of different viral vectors to model or to treat PD

Since all projects described here were highly dependent on efficient gene transfer, one of our objectives was to compare viral vectors in their capacity to achieve efficient gene transfer to different target regions in the mouse brain dependent on the experimental requirements.

Consistent with their long history in experimental gene transfer *in vivo* including our laboratory (Eberhardt *et al.* 2000) (see also section1.5.3.1), AdV were successfully employed for gene transfer to the nigrostriatal system of mice. The possibility to transduce the SNc by delivery of AdV to the striatum followed by retrograde axonal virus transport was of great interest for us, because it entailed fewer side-effects than a direct injection of virus into the

SNc. Choosing this expression system in addition gave us the opportunity to investigate these effects in the striatum. However, the use of adenoviral-mediated gene transfer is limited. (i) Since adenoviral DNA does not integrate into the host genome, AdV allow only transient transgene expression. It was documented that transgene expression reaches its maximum during this first week post infection, while a progressive decline was observed during the following 1-3 weeks (Hermens *et al.* 1997; Kitao *et al.* 2007) (ii) AdV are know to induce unwanted toxic side effects due to inflammatory tissue reactions, which may lead to further inhibition of transgene expression (Lowenstein and Castro 2003) (see sections 3.2.1 and 4.1.1). This restricts the applicability of AdV to a short time window of one week and impeded their use in long-term studies. We also used AdV for transgene expression SH-SY5Y neuroblastoma cells *in vitro*, which are difficult to transfect by lipofection (Marx 2004) (see section 3.4.1.1). Consistent with AdV-characteristics described in literature (Le Gal La Salle *et al.* 1993; Mandel *et al.* 2008), our findings suggest AdV as the viral vector platform of choice for short-term *in vivo* studies especially for transduction of the whole nigrostriatal system. Since cultured cell cannot be afflicted by immune response, AdV are also useful for efficient and high level transgene expression in hard-to-transfect cell lines and primary (neuronal) cultures, which are usually hard to access with other transfection techniques. This is also reflected by the growing number of commercially available AdV expressing frequently used transgenes like Cre-recombinase and luciferase reporter.

In cases where long-term transgene expression in animal models is needed, or for suitability for clinical applications, alternative vectors are required. Therefore, we tested, whether lentiviral-mediated gene transfer in the SNc was capable to achieve efficient and long-lasting transgene expression in DA cells. Since the pons is mainly affected by A30P-α-synuclein-aggregation in the A30Pαsyn transgenic mouse model, we also aimed for efficient and long-lasting gene transfer to neurons in this region to investigate Hsp70`s influence on the aggregate load. Unfortunately, LV showed poor neuronal transduction efficiency in our hand in both regions. Other laboratories succeeded in using LV for SNc neuronal transduction *in vivo* (Bensadoun *et al.* 2000; Ridet *et al.* 2006). One possible explanation for this discrepancy might be related to the procedure of virus purification. Subsequent to the experiments described here, the purification protocol for lentiviral vectors in our laboratory was changed to a polyethylenglycol precipitation instead of ultracentrifugation (see section 2.5.2). This seemed to improve the neuronal transduction efficiency of LV: LV showed efficient transgene expression in NeuN-positive cells in the striatum and in primary cortical neurons (personal communication with Dr. Ellen Gerhardt and Christopher Spering). Even though the new virus preparations have not been tested in the SNc or the pons it is possible that the poor neuronal transduction was due to damaging or inhibitory side effects of the purification protocol used in the present study.

To improve transgene expression in SNc and pons, AAV-2 was employed as another gene transfer tool, since it preferentially transduces neurons in the CNS and has especially high affinity to DA neurons of SNc (Paterna *et al.* 2004; Shevtsova 2006). And indeed, AAV-2-mediated transgene expression driven by the neuron-specific synapsin promoter enormously increased the gene transfer efficiency to neurons in pons and SNc (see section 3.4.2.4) for up to eight weeks. These results made AAV the viral vector system most suitable to accomplish viral vector-mediated gene transfer to the mouse brain to modify or to treat models of PD in our hands. Our observations are in line with studies, using AAV or LV to develop overexpression models for PD in rats. Both vectors provided long-term expression in the transduced neurons, but AAV vectors were superior to LV vectors because they showed better targeting to a larger fraction of the nigral DA neurons, reaching up to 95% efficiency (Ulusoy *et al.* 2008). In combination with their lack of pathogenicity these encouraging results also imply AAV to be an excellent candidate for a human gene therapy. In fact phase I safety trials are already on the way (Kaplitt *et al.* 2007; Eberling *et al.* 2008) (see section 1.5.3.2).

5. Abstract

The core characteristics of Parkinson's disease (PD) are the loss of dopaminergic (DA) neurons in the *substantia nigra* (SN) leading to depletion of striatal dopamine levels, and the presence of intraneuronal proteinaceous cytoplasmatic inclusions, designated "Lewy bodies" (LB). We first tried to provide new mechanistic insights in the pathogenesis of PD. Next, we went on testing a therapeutic approach based on viral vector mediated gene transfer of Hsp70 in several models of PD.

Synphilin-1 is commonly found in LB and was described as a protein interacting with α-synuclein the main constituent of LBs. Our group has previously described and characterized *in vitro* a mutation in the synphilin-1 gene (R621C) in PD patients. To provide the first characterization of synphilin-1 expression in an animal model, we here used adenoviral gene transfer to study the effects of wild-type (WT) and R621C synphilin-1 in DA neurons in mouse brain. Since synphilin-1 is commonly used to trigger aggregation of α-synuclein in cell culture, we investigated not only non-transgenic C57Bl/6 mice but also (Thy1)-h[A30P]αsynuclein transgenic (A30PαSyn) animals. Both WT synphilin-1 and R621C synphilin-1 led to the formation of Thioflavine-S positive inclusions in C57Bl/6 mice and to the degeneration of DA neurons in the SN. R621C synphilin-1 induced more aggregates than WT synphilin-1 in A30P-α-synuclein transgenic mice, consistent with the role of the R621C mutation as a susceptibility factor for PD. Synphilin-1 expression may be used to improve current mouse models of PD, since it induced both the formation of aggregates and degeneration of dopaminergic neurons, two core characteristics of Parkinson's disease that have not been well reproduced with expression of α-synuclein.

Proteasomal inhibition is thought to be involved in aggregate formation in neurodegenerative diseases like PD. Ub^{G76V}-GFP mice transgenic for a GFP reporter carrying a constitutively active degradation signal were crossbred with A30PαSyn mice to monitor the status of the ubiquitin/proteasom system in A30PαSyn mice. The distribution pattern of GFP-positive cells in the aggregate-affected brain regions did not differ from controls (heterozygous or negative for A30Pα-synuclein) at any of the investigated time points. This suggests that proteasomal impairment unlikely occurs early in disease progression, at least in the investigated paradigm.

Even though the initial insult that provokes neurodegeneration in PD remains unclear, oxidative stress and accumulation of misfolded proteins have been identified as critical events. To model PD, oxidative stress can be pharmacologically initiated by the mitochondrial complex I inhibitor MPP^+. Protein aggregation is commonly investigated in the context of α-synuclein aggregation.

To determine the effects of Hsp70 on aggregation and toxicity of α-synuclein, HSp70 was coexpressed with ΔC-α-synuclein a variant with abundant aggregate formation and highest toxicity. Hsp70 not only prevented the formation of aggregates, but also increased their reduction and clearance, underlining its therapeutic potential. Interestingly, the prevalence of aggresomes was increased with Hsp70.

These findings prompted us to determine, whether Hsp70 can also preserve cellular viability in a toxin-based cell culture model. Hsp70 was induced in SH-SY5Y neuroblastoma cells by adenoviral gene transfer or by administration of geldanamycin, prior to exposure to MPP^+. Cell viability was measured by the trypan blue exclusion assay, MPP^+ toxicity was assessed by measuring released LDH. Both geldanamycin and adenoviral gene transfer reduced MPP^+ toxicity and increased cell viability when compared to vehicle treatment. This effect occurs in paradigms with and without caspase activation, suggesting that neuroprotection by Hsp70 most likely results from its effect on oxidized and/or misfolded proteins rather than from caspase inhibition.

Thus, we aimed to establish viral vector mediated expression of Hsp70 in the A30PαSyn transgenic mice to demonstrate the potency of a chaperone therapy in this mouse model for PD. Because adenoviral vectors have toxic side effect when expressed longer, a lentiviral vector and AAV expressing HA-tagged Hsp70 was evaluated for their capability to reduce the aggregate burden in A30PαSyn mice. Lentiviral vectors provided low neuronal transgene expression. AAV improved the neuronal transduction efficiency. However, Hsp70 overexpression was not sufficient to significantly reduce aggregate load in the infected brain area.

6. References

Abeliovich, A., Y. Schmitz, et al. (2000). "Mice lacking alpha-synuclein display functional deficits in the nigrostriatal dopamine system." Neuron 25(1): 239-52.

Aharon-Peretz, J., H. Rosenbaum, et al. (2004). "Mutations in the glucocerebrosidase gene and Parkinson's disease in Ashkenazi Jews." N Engl J Med 351(19): 1972-7.

Ahn, T. B. and B. S. Jeon (2006). "Protective role of heat shock and heat shock protein 70 in lactacystin-induced cell death both in the rat substantia nigra and PC12 cells." Brain Res 1087(1): 159-67.

Aisen, P., G. Cohen, et al. (1990). "Iron toxicosis." Int Rev Exp Pathol 31: 1-46.

Akli, S., C. Caillaud, et al. (1993). "Transfer of a foreign gene into the brain using adenovirus vectors." Nat Genet 3(3): 224-8.

Allen, K. L., A. Almeida, et al. (1995). "Changes of respiratory chain activity in mitochondrial and synaptosomal fractions isolated from the gerbil brain after graded ischaemia." J Neurochem 64(5): 2222-9.

Alvarez-Fischer, D., S. Guerreiro, et al. (2008). "Modelling Parkinson-like neurodegeneration via osmotic minipump delivery of MPTP and probenecid." J Neurochem 107(3): 701-11.

Amin, V., D. V. Cumming, et al. (1995). "The degree of protection provided to neuronal cells by a pre-conditioning stress correlates with the amount of heat shock protein 70 it induces and not with the similarity of the subsequent stress." Neurosci Lett 200(2): 85-8.

Ardley, H. C., G. B. Scott, et al. (2004). "UCH-L1 aggresome formation in response to proteasome impairment indicates a role in inclusion formation in Parkinson's disease." J Neurochem 90(2): 379-91.

Armstrong, R. C., T. J. Aja, et al. (1997). "Activation of the CED3/ICE-related protease CPP32 in cerebellar granule neurons undergoing apoptosis but not necrosis." J Neurosci 17(2): 553-62.

Artal-Sanz, M. and N. Tavernarakis (2005). "Proteolytic mechanisms in necrotic cell death and neurodegeneration." FEBS Lett 579(15): 3287-96.

Auluck, P. K., H. Y. Chan, et al. (2002). "Chaperone suppression of alpha-synuclein toxicity in a Drosophila model for Parkinson's disease." Science 295(5556): 865-8.

Auluck, P. K., M. C. Meulener, et al. (2005). "Mechanisms of Suppression of {alpha}-Synuclein Neurotoxicity by Geldanamycin in Drosophila." J Biol Chem 280(4): 2873-8.

Avraham, E., R. Szargel, et al. (2005). "Glycogen synthase kinase 3beta modulates synphilin-1 ubiquitylation and cellular inclusion formation by SIAH: implications for proteasomal function and Lewy body formation." J Biol Chem 280(52): 42877-86.

Azzouz, M., A. Hottinger, et al. (2000). "Increased motoneuron survival and improved neuromuscular function in transgenic ALS mice after intraspinal injection of an adeno-associated virus encoding Bcl-2." Hum Mol Genet 9(5): 803-11.

Ballinger, C. A., P. Connell, et al. (1999). "Identification of CHIP, a novel tetratricopeptide repeat-containing protein that interacts with heat shock proteins and negatively regulates chaperone functions." Mol Cell Biol 19(6): 4535-45.

Bankiewicz, K. S., M. Daadi, et al. (2006). "Focal striatal dopamine may potentiate dyskinesias in parkinsonian monkeys." Exp Neurol 197(2): 363-72.

Barkats, M., A. Bilang-Bleuel, et al. (1998). "Adenovirus in the brain: recent advances of gene therapy for neurodegenerative diseases." Prog Neurobiol 55(4): 333-41.

Beal, M. F. (2001). "Experimental models of Parkinson's disease." Nat Rev Neurosci 2(5): 325-34.

Beaucamp, N., T. C. Harding, et al. (1998). "Overexpression of hsp70i facilitates reactivation of intracellular proteins in neurones and protects them from denaturing stress." FEBS Lett 441(2): 215-9.

Beere, H. M. (2005). "Death versus survival: functional interaction between the apoptotic and stress-inducible heat shock protein pathways." J Clin Invest 115(10): 2633-9.

Beere, H. M., B. B. Wolf, et al. (2000). "Heat-shock protein 70 inhibits apoptosis by preventing recruitment of procaspase-9 to the Apaf-1 apoptosome." Nat Cell Biol 2(8): 469-75.

Bell, J. and A. J. Clark (1926). "A pedigree of paralysis agitans." Ann. Eugen(1): 455–462.

Bennett, M. C., J. F. Bishop, et al. (1999). "Degradation of alpha-synuclein by proteasome." J Biol Chem 274(48): 33855-8.

Bensadoun, J. C. and P. Aebischer (2006). "Viral vectors as a tool to model and treat Parkinson's disease." Wien Klin Wochenschr 118(19-20): 568-70.

Bensadoun, J. C., N. Deglon, et al. (2000). "Lentiviral vectors as a gene delivery system in the mouse midbrain: cellular and behavioral improvements in a 6-OHDA model of Parkinson's disease using GDNF." Exp Neurol 164(1): 15-24.

Berman, S. B. and T. G. Hastings (1997). "Inhibition of glutamate transport in synaptosomes by dopamine oxidation and reactive oxygen species." J Neurochem 69(3): 1185-95.

Bernheimer, H., W. Birkmayer, et al. (1973). "Brain dopamine and the syndromes of Parkinson and Huntington. Clinical, morphological and neurochemical correlations." J Neurol Sci 20(4): 415-55.

Betarbet, R., R. M. Canet-Aviles, et al. (2006). "Intersecting pathways to neurodegeneration in Parkinson's disease: effects of the pesticide rotenone on DJ-1, alpha-synuclein, and the ubiquitin-proteasome system." Neurobiol Dis 22(2): 404-20.

Bienemann, A. S., Y. B. Lee, et al. (2008). "Hsp70 suppresses apoptosis in sympathetic neurones by preventing the activation of c-Jun." J Neurochem 104(1): 271-8.

Bjorklund, A., D. Kirik, et al. (2000). "Towards a neuroprotective gene therapy for Parkinson's disease: use of adenovirus, AAV and lentivirus vectors for gene transfer of GDNF to the nigrostriatal system in the rat Parkinson model." Brain Res 886(1-2): 82-98.

Blandini, F., G. Nappi, et al. (2000). "Functional changes of the basal ganglia circuitry in Parkinson's disease." Prog Neurobiol 62(1): 63-88.

Blomer, U., L. Naldini, et al. (1997). "Highly efficient and sustained gene transfer in adult neurons with a lentivirus vector." J Virol 71(9): 6641-9.

Boatright, K. M. and G. S. Salvesen (2003). "Mechanisms of caspase activation." Curr Opin Cell Biol 15(6): 725-31.

Bohn, M. C., D. L. Choi-Lundberg, et al. (1999). "Adenovirus-mediated transgene expression in nonhuman primate brain." Hum Gene Ther 10(7): 1175-84.

Bonifati, V., P. Rizzu, et al. (2003). "Mutations in the DJ-1 gene associated with autosomal recessive early-onset parkinsonism." Science 299(5604): 256-9.

Bonin, M., F. P. Marx, et al. (2008). "Microarray expression analysis reveals genetic pathways implicated in C621 synphilin-1-mediated toxicity." J Neural Transm.

Bonini, N. M. (2002). "Chaperoning brain degeneration." Proc Natl Acad Sci U S A 99 Suppl 4: 16407-11.

Bove, J., D. Prou, et al. (2005). "Toxin-induced models of Parkinson's disease." NeuroRx 2(3): 484-94.

Bowling, A. C. and M. F. Beal (1995). "Bioenergetic and oxidative stress in neurodegenerative diseases." Life Sci 56(14): 1151-71.

Bowman, A. B., S. Y. Yoo, et al. (2005). "Neuronal dysfunction in a polyglutamine disease model occurs in the absence of ubiquitin-proteasome system impairment and inversely correlates with the degree of nuclear inclusion formation." Hum Mol Genet 14(5): 679-91.

Braak, H. and K. Del Tredici (2008). "Assessing fetal nerve cell grafts in Parkinson's disease." Nat Med 14(5): 483-5.

Brown, I. R. (2007). "Heat shock proteins and protection of the nervous system." Ann N Y Acad Sci 1113: 147-58.

Bruening, W., J. Roy, et al. (1999). "Up-regulation of protein chaperones preserves viability of cells expressing toxic Cu/Zn-superoxide dismutase mutants associated with amyotrophic lateral sclerosis." J Neurochem 72(2): 693-9.

Bukau, B., J. Weissman, et al. (2006). "Molecular chaperones and protein quality control." Cell 125(3): 443-51.

Burger, C., O. S. Gorbatyuk, et al. (2004). "Recombinant AAV viral vectors pseudotyped with viral capsids from serotypes 1, 2, and 5 display differential efficiency and cell tropism after delivery to different regions of the central nervous system." Mol Ther 10(2): 302-17.

Byrnes, A. P., M. J. Wood, et al. (1996). "Role of T cells in inflammation caused by adenovirus vectors in the brain." Gene Ther 3(7): 644-51.

Cao, L., Y. Liu, et al. (2000). "High-titer, wild-type free recombinant adeno-associated virus vector production using intron-containing helper plasmids." J Virol 74(24): 11456-63.

Carmichael, J., J. Chatellier, et al. (2000). "Bacterial and yeast chaperones reduce both aggregate formation and cell death in mammalian cell models of Huntington's disease." Proc Natl Acad Sci U S A 97(17): 9701-5.

Chai, Y., S. L. Koppenhafer, et al. (1999). "Analysis of the role of heat shock protein (Hsp) molecular chaperones in polyglutamine disease." J Neurosci 19(23): 10338-47.

Cheetham, M. E. and A. J. Caplan (1998). "Structure, function and evolution of DnaJ: conservation and adaptation of chaperone function." Cell Stress Chaperones 3(1): 28-36.

Cheng, H., J. P. Wu, et al. (2002). "Neuroprotection of glial cell line-derived neurotrophic factor in damaged spinal cords following contusive injury." J Neurosci Res 69(3): 397-405.

Choi-Lundberg, D. L., Q. Lin, et al. (1997). "Dopaminergic neurons protected from degeneration by GDNF gene therapy." Science 275(5301): 838-41.

Chowdhury, I., B. Tharakan, et al. (2006). "Current concepts in apoptosis: the physiological suicide program revisited." Cell Mol Biol Lett 11(4): 506-25.

Chung, K. K., Y. Zhang, et al. (2001). "Parkin ubiquitinates the alpha-synuclein-interacting protein, synphilin-1: implications for Lewy-body formation in Parkinson disease." Nat Med 7(10): 1144-50.

Connell, P., C. A. Ballinger, et al. (2001). "The co-chaperone CHIP regulates protein triage decisions mediated by heat-shock proteins." Nat Cell Biol 3(1): 93-6.

Conway, K. A., J. D. Harper, et al. (1998). "Accelerated in vitro fibril formation by a mutant alpha-synuclein linked to early-onset Parkinson disease." Nat Med 4(11): 1318-20.

Conway, K. A., S. J. Lee, et al. (2000). "Acceleration of oligomerization, not fibrillization, is a shared property of both alpha-synuclein mutations linked to early-onset Parkinson's disease: implications for pathogenesis and therapy." Proc Natl Acad Sci U S A 97(2): 571-6.

Conway, K. A., J. C. Rochet, et al. (2001). "Kinetic stabilization of the alpha-synuclein protofibril by a dopamine-alpha-synuclein adduct." Science 294(5545): 1346-9.

Cotzias, G. C. (1968). "L-Dopa for Parkinsonism." N Engl J Med 278(11): 630.

Coyle, J. T. and P. Puttfarcken (1993). "Oxidative stress, glutamate, and neurodegenerative disorders." Science 262(5134): 689-95.

Crews, C. M. (2003). "Feeding the machine: mechanisms of proteasome-catalyzed degradation of ubiquitinated proteins." Curr Opin Chem Biol 7(5): 534-9.

Csermely, P., T. Schnaider, et al. (1998). "The 90-kDa molecular chaperone family: structure, function, and clinical applications. A comprehensive review." Pharmacol Ther 79(2): 129-68.

Cuervo, A. M., L. Stefanis, et al. (2004). "Impaired degradation of mutant alpha-synuclein by chaperone-mediated autophagy." Science 305(5688): 1292-5.

Cummings, C. J., Y. Sun, et al. (2001). "Over-expression of inducible HSP70 chaperone suppresses neuropathology and improves motor function in SCA1 mice." Hum Mol Genet 10(14): 1511-8.

Cyr, D. M., X. Lu, et al. (1992). "Regulation of Hsp70 function by a eukaryotic DnaJ homolog." J Biol Chem 267(29): 20927-31.

Danthinne, X. and M. J. Imperiale (2000). "Production of first generation adenovirus vectors: a review." Gene Ther 7(20): 1707-14.

Dass, B., C. W. Olanow, et al. (2006). "Gene transfer of trophic factors and stem cell grafting as treatments for Parkinson's disease." Neurology 66(10 Suppl 4): S89-103.

Dauer, W. and S. Przedborski (2003). "Parkinson's disease: mechanisms and models." Neuron 39(6): 889-909.
Dawson, T. M. (2000a). "New animal models for Parkinson's disease." Cell 101(2): 115-8.
Dawson, V. L. (2000b). "Neurobiology. Of flies and mice." Science 288(5466): 631-2.
Dedmon, M. M., J. Christodoulou, et al. (2005). "Heat shock protein 70 inhibits alpha-synuclein fibril formation via preferential binding to prefibrillar species." J Biol Chem 280(15): 14733-40.
Demand, J., S. Alberti, et al. (2001). "Cooperation of a ubiquitin domain protein and an E3 ubiquitin ligase during chaperone/proteasome coupling." Curr Biol 11(20): 1569-77.
Deocaris, C. C., S. C. Kaul, et al. (2006). "On the brotherhood of the mitochondrial chaperones mortalin and heat shock protein 60." Cell Stress Chaperones 11(2): 116-28.
Dethy, S. and A. S. Hambye (2008). "[1231-FP-CIT (DaTSCAN) scintigraphy in the differential diagnosis of movement disorders]." Rev Med Brux 29(4): 238-47.
Deuschl, G. and C. Goddemeier (1998). "Spontaneous and reflex activity of facial muscles in dystonia, Parkinson's disease, and in normal subjects." J Neurol Neurosurg Psychiatry 64(3): 320-4.
Dewey, R. A., G. Morrissey, et al. (1999). "Chronic brain inflammation and persistent herpes simplex virus 1 thymidine kinase expression in survivors of syngeneic glioma treated by adenovirus-mediated gene therapy: implications for clinical trials." Nat Med 5(11): 1256-63.
Dexter, D. T., F. R. Wells, et al. (1989). "Increased nigral iron content and alterations in other metal ions occurring in brain in Parkinson's disease." J Neurochem 52(6): 1830-6.
Dickson, D. W. (2002). "Misfolded, protease-resistant proteins in animal models and human neurodegenerative disease." J Clin Invest 110(10): 1403-5.
Didelot, C., D. Lanneau, et al. (2007). "Anti-cancer therapeutic approaches based on intracellular and extracellular heat shock proteins." Curr Med Chem 14(27): 2839-47.
Do Thi, N. A., P. Saillour, et al. (2004). "Delivery of GDNF by an E1,E3/E4 deleted adenoviral vector and driven by a GFAP promoter prevents dopaminergic neuron degeneration in a rat model of Parkinson's disease." Gene Ther 11(9): 746-56.
Dodel, R. C., Y. Du, et al. (1998). "Peptide inhibitors of caspase-3-like proteases attenuate 1-methyl-4-phenylpyridinum-induced toxicity of cultured fetal rat mesencephalic dopamine neurons." Neuroscience 86(3): 701-7.
Donaire, V., M. Niso, et al. (2005). "Heat shock proteins protect both MPP(+) and paraquat neurotoxicity." Brain Res Bull 67(6): 509-14.
Dong, Z., B. Ferger, et al. (2002). "Overexpression of Parkinson's disease-associated alpha-synucleinA53T by recombinant adeno-associated virus in mice does not increase the vulnerability of dopaminergic neurons to MPTP." J Neurobiol 53(1): 1-10.
Dong, Z., D. P. Wolfer, et al. (2005). "Hsp70 gene transfer by adeno-associated virus inhibits MPTP-induced nigrostriatal degeneration in the mouse model of Parkinson disease." Mol Ther 11(1): 80-8.
Du, C., M. Fang, et al. (2000). "Smac, a mitochondrial protein that promotes cytochrome c-dependent caspase activation by eliminating IAP inhibition." Cell 102(1): 33-42.
Duan, D., P. Sharma, et al. (1998). "Circular intermediates of recombinant adeno-associated virus have defined structural characteristics responsible for long-term episomal persistence in muscle tissue." J Virol 72(11): 8568-77.
Duffy, P. E. and V. M. Tennyson (1965). "Phase and electron microscopic observations of Lewy bodies and melanin granules in the substantia nigra and locus coeruleus in Parkinson's disease." J Neuropathol Exp Neurol 24(3): 398-414.
Dull, T., R. Zufferey, et al. (1998). "A third-generation lentivirus vector with a conditional packaging system." J Virol 72(11): 8463-71.
Duvoisin, R. C. (1977). "Problems in the treatment of Parkinsonism." Adv Exp Med Biol 90: 131-55.
Dworniczak, B. and M. E. Mirault (1987). "Structure and expression of a human gene coding for a 71 kd heat shock 'cognate' protein." Nucleic Acids Res 15(13): 5181-97.

Eberhardt, O., R. V. Coelln, et al. (2000). "Protection by synergistic effects of adenovirus-mediated X-chromosome-linked inhibitor of apoptosis and glial cell line-derived neurotrophic factor gene transfer in the 1-methyl-4-phenyl-1,2,3,6-tetrahydropyridine model of Parkinson's disease." J Neurosci 20(24): 9126-34.

Eberling, J. L., W. J. Jagust, et al. (2008). "Results from a phase I safety trial of hAADC gene therapy for Parkinson disease." Neurology 70(21): 1980-3.

Ellis, R. J. and S. M. van der Vies (1991). "Molecular chaperones." Annu Rev Biochem 60: 321-47.

Emborg, M. E. (2004). "Evaluation of animal models of Parkinson's disease for neuroprotective strategies." J Neurosci Methods 139(2): 121-43.

Emborg, M. E., A. D. Ebert, et al. (2008). "GDNF-secreting human neural progenitor cells increase tyrosine hydroxylase and VMAT2 expression in MPTP-treated cynomolgus monkeys." Cell Transplant 17(4): 383-95.

Engelender, S., Z. Kaminsky, et al. (1999). "Synphilin-1 associates with alpha-synuclein and promotes the formation of cytosolic inclusions." Nat Genet 22(1): 110-4.

Eyal, A. and S. Engelender (2006). "Synphilin isoforms and the search for a cellular model of lewy body formation in Parkinson's disease." Cell Cycle 5(18): 2082-6.

Eyal, A., R. Szargel, et al. (2006). "Synphilin-1A: an aggregation-prone isoform of synphilin-1 that causes neuronal death and is present in aggregates from alpha-synucleinopathy patients." Proc Natl Acad Sci U S A 103(15): 5917-22.

Fahn, S. (1988). "Concept and classification of dystonia." Adv Neurol 50: 1-8.

Falkenburger, B. H. and J. B. Schulz (2006). "Limitations of cellular models in Parkinson's disease research." J Neural Transm Suppl(70): 261-8.

Fan, C. Y., S. Lee, et al. (2003). "Mechanisms for regulation of Hsp70 function by Hsp40." Cell Stress Chaperones 8(4): 309-16.

Fan, G. H., H. Y. Zhou, et al. (2006). "Heat shock proteins reduce alpha-synuclein aggregation induced by MPP+ in SK-N-SH cells." FEBS Lett 580(13): 3091-8.

Feany, M. B. and W. W. Bender (2000). "A Drosophila model of Parkinson's disease." Nature 404(6776): 394-8.

Fearnley, J. M. and A. J. Lees (1991). "Ageing and Parkinson's disease: substantia nigra regional selectivity." Brain 114 (Pt 5): 2283-301.

Fenton, W. A. and A. L. Horwich (2003). "Chaperonin-mediated protein folding: fate of substrate polypeptide." Q Rev Biophys 36(2): 229-56.

Floor, E. and M. G. Wetzel (1998). "Increased protein oxidation in human substantia nigra pars compacta in comparison with basal ganglia and prefrontal cortex measured with an improved dinitrophenylhydrazine assay." J Neurochem 70(1): 268-75.

Follenzi, A., L. Santambrogio, et al. (2007). "Immune responses to lentiviral vectors." Curr Gene Ther 7(5): 306-15.

Fornai, F., O. M. Schluter, et al. (2005). "Parkinson-like syndrome induced by continuous MPTP infusion: convergent roles of the ubiquitin-proteasome system and alpha-synuclein." Proc Natl Acad Sci U S A 102(9): 3413-8.

Fortin, D. L., M. D. Troyer, et al. (2004). "Lipid rafts mediate the synaptic localization of alpha-synuclein." J Neurosci 24(30): 6715-23.

Frank, M. J. (2005). "Dynamic dopamine modulation in the basal ganglia: a neurocomputational account of cognitive deficits in medicated and nonmedicated Parkinsonism." J Cogn Neurosci 17(1): 51-72.

Freyaldenhoven, T. E. and S. F. Ali (1997). "Role of heat shock proteins in MPTP-induced neurotoxicity." Ann N Y Acad Sci 825: 167-78.

Fujikake, N., Y. Nagai, et al. (2008). "Heat shock transcription factor 1-activating compounds suppress polyglutamine-induced neurodegeneration through induction of multiple molecular chaperones." J Biol Chem 283(38): 26188-97.

Gabai, V. L., K. Mabuchi, et al. (2002). "Hsp72 and stress kinase c-jun N-terminal kinase regulate the bid-dependent pathway in tumor necrosis factor-induced apoptosis." Mol Cell Biol 22(10): 3415-24.

Ganea, E. (2001). "Chaperone-like activity of alpha-crystallin and other small heat shock proteins." Curr Protein Pept Sci 2(3): 205-25.

Garcia-Mata, R., Z. Bebok, et al. (1999). "Characterization and dynamics of aggresome formation by a cytosolic GFP-chimera." J Cell Biol 146(6): 1239-54.
Garcia Ruiz, P. J. (2004). "[Prehistory of Parkinson's disease]." Neurologia 19(10): 735-7.
Gelb, D. J., E. Oliver, et al. (1999). "Diagnostic criteria for Parkinson disease." Arch Neurol 56(1): 33-9.
George, J. M. (2002). "The synucleins." Genome Biol 3(1): REVIEWS3002.
Gerdes, C. A., M. G. Castro, et al. (2000). "Strong promoters are the key to highly efficient, noninflammatory and noncytotoxic adenoviral-mediated transgene delivery into the brain in vivo." Mol Ther 2(4): 330-8.
Gething, M. J. and J. Sambrook (1992). "Protein folding in the cell." Nature 355(6355): 33-45.
Giaime, E., C. Sunyach, et al. (2006). "Caspase-3-derived C-terminal product of synphilin-1 displays antiapoptotic function via modulation of the p53-dependent cell death pathway." J Biol Chem 281(17): 11515-22.
Giasson, B. I., J. E. Duda, et al. (2000). "Oxidative damage linked to neurodegeneration by selective alpha-synuclein nitration in synucleinopathy lesions." Science 290(5493): 985-9.
Giasson, B. I. and V. M. Lee (2003). "Are ubiquitination pathways central to Parkinson's disease?" Cell 114(1): 1-8.
Gibb, W. R. (1997). "Functional neuropathology in Parkinson's disease." Eur Neurol 38 Suppl 2: 21-5.
Giffard, R. G., L. Xu, et al. (2004). "Chaperones, protein aggregation, and brain protection from hypoxic/ischemic injury." J Exp Biol 207(Pt 18): 3213-20.
Goldberg, M. S. and P. T. Lansbury, Jr. (2000). "Is there a cause-and-effect relationship between alpha-synuclein fibrillization and Parkinson's disease?" Nat Cell Biol 2(7): E115-9.
Goldfarb, S. B., O. B. Kashlan, et al. (2006). "Differential effects of Hsc70 and Hsp70 on the intracellular trafficking and functional expression of epithelial sodium channels." Proc Natl Acad Sci U S A 103(15): 5817-22.
Gunawardena, S., L. S. Her, et al. (2003). "Disruption of axonal transport by loss of huntingtin or expression of pathogenic polyQ proteins in Drosophila." Neuron 40(1): 25-40.
Gupta, A. K. and R. Bluhm (2004). "Seborrheic dermatitis." J Eur Acad Dermatol Venereol 18(1): 13-26; quiz 19-20.
Gupta, S. and A. A. Knowlton (2005). "HSP60, Bax, apoptosis and the heart." J Cell Mol Med 9(1): 51-8.
Haas, L. F. (2001). "Jean Martin Charcot (1825-93) and Jean Baptiste Charcot (1867-1936)." J Neurol Neurosurg Psychiatry 71(4): 524.
Halliwell, B. (1992). "Reactive oxygen species and the central nervous system." J Neurochem 59(5): 1609-23.
Hanna, J. and D. Finley (2007). "A proteasome for all occasions." FEBS Lett 581(15): 2854-61.
Hansson, O., J. Nylandsted, et al. (2003). "Overexpression of heat shock protein 70 in R6/2 Huntington's disease mice has only modest effects on disease progression." Brain Res 970(1-2): 47-57.
Hardy, S., M. Kitamura, et al. (1997). "Construction of adenovirus vectors through Cre-lox recombination." J Virol 71(3): 1842-9.
Harper, S. Q., P. D. Staber, et al. (2005). "RNA interference improves motor and neuropathological abnormalities in a Huntington's disease mouse model." Proc Natl Acad Sci U S A 102(16): 5820-5.
Hartl, F. U. (1996). "Molecular chaperones in cellular protein folding." Nature 381(6583): 571-9.
Harui, A., S. Suzuki, et al. (1999). "Frequency and stability of chromosomal integration of adenovirus vectors." J Virol 73(7): 6141-6.
Hasegawa, T., M. Matsuzaki, et al. (2004). "Accelerated alpha-synuclein aggregation after differentiation of SH-SY5Y neuroblastoma cells." Brain Res 1013(1): 51-9.

Haslbeck, M. (2002). "sHsps and their role in the chaperone network." Cell Mol Life Sci 59(10): 1649-57.
Haslbeck, M., T. Franzmann, et al. (2005). "Some like it hot: the structure and function of small heat-shock proteins." Nat Struct Mol Biol 12(10): 842-6.
Hauswirth, W. W., A. S. Lewin, et al. (2000). "Production and purification of recombinant adeno-associated virus." Methods Enzymol 316: 743-61.
Hengartner, M. O. (2001). "Apoptosis. DNA destroyers." Nature 412(6842): 27, 29.
Hermens, W. T., R. J. Giger, et al. (1997). "Transient gene transfer to neurons and glia: analysis of adenoviral vector performance in the CNS and PNS." J Neurosci Methods 71(1): 85-98.
Hillgenberg, M., H. Tonnies, et al. (2001). "Chromosomal integration pattern of a helper-dependent minimal adenovirus vector with a selectable marker inserted into a 27.4-kilobase genomic stuffer." J Virol 75(20): 9896-908.
Hohfeld, J., D. M. Cyr, et al. (2001). "From the cradle to the grave: molecular chaperones that may choose between folding and degradation." EMBO Rep 2(10): 885-90.
Hornykiewicz, O. (2002). "L-DOPA: from a biologically inactive amino acid to a successful therapeutic agent." Amino Acids 23(1-3): 65-70.
Horowski, R., L. Horowski, et al. (1995). "An essay on Wilhelm von Humboldt and the shaking palsy: first comprehensive description of Parkinson's disease by a patient." Neurology 45(3 Pt 1): 565-8.
Huang, B., J. Schiefer, et al. (2008). "Inducing huntingtin inclusion formation in primary neuronal cell culture and in vivo by high-capacity adenoviral vectors expressing truncated and full-length huntingtin with polyglutamine expansion." J Gene Med 10(3): 269-79.
Ihara, M., H. Tomimoto, et al. (2003). "Association of the cytoskeletal GTP-binding protein Sept4/H5 with cytoplasmic inclusions found in Parkinson's disease and other synucleinopathies." J Biol Chem 278(26): 24095-102.
Imaizumi, K., K. Miyoshi, et al. (2001). "The unfolded protein response and Alzheimer's disease." Biochim Biophys Acta 1536(2-3): 85-96.
Irizarry, M. C., T. W. Kim, et al. (1996). "Characterization of the precursor protein of the non-A beta component of senile plaques (NACP) in the human central nervous system." J Neuropathol Exp Neurol 55(8): 889-95.
Ishihara, L. and C. Brayne (2006). "A systematic review of depression and mental illness preceding Parkinson's disease." Acta Neurol Scand 113(4): 211-20.
Ito, T., J. Niwa, et al. (2003). "Dorfin localizes to Lewy bodies and ubiquitylates synphilin-1." J Biol Chem 278(31): 29106-14.
Itoh, H., A. Komatsuda, et al. (2002). "Mammalian HSP60 is quickly sorted into the mitochondria under conditions of dehydration." Eur J Biochem 269(23): 5931-8.
James, P., C. Pfund, et al. (1997). "Functional specificity among Hsp70 molecular chaperones." Science 275(5298): 387-9.
Jana, N. R., M. Tanaka, et al. (2000). "Polyglutamine length-dependent interaction of Hsp40 and Hsp70 family chaperones with truncated N-terminal huntingtin: their role in suppression of aggregation and cellular toxicity." Hum Mol Genet 9(13): 2009-18.
Jankovic, J. (2008). "Parkinson's disease: clinical features and diagnosis." J Neurol Neurosurg Psychiatry 79(4): 368-76.
Jankovic, J. and M. Stacy (2007). "Medical management of levodopa-associated motor complications in patients with Parkinson's disease." CNS Drugs 21(8): 677-92.
Jenner, P. (1998). "Oxidative mechanisms in nigral cell death in Parkinson's disease." Mov Disord 13 Suppl 1: 24-34.
Jenner, P. (2003). "Oxidative stress in Parkinson's disease." Ann Neurol 53 Suppl 3: S26-36; discussion S36-8.
Jensen, P. H., M. S. Nielsen, et al. (1998). "Binding of alpha-synuclein to brain vesicles is abolished by familial Parkinson's disease mutation." J Biol Chem 273(41): 26292-4.
Jiang, H., Y. C. Wu, et al. (2007). "Parkinson's disease genetic mutations increase cell susceptibility to stress: mutant alpha-synuclein enhances H2O2- and Sin-1-induced cell death." Neurobiol Aging 28(11): 1709-17.

Jin, H. G., H. Yamashita, et al. (2008). "Synphilin-1 transgenic mice exhibit mild motor impairments." Neurosci Lett.

Jindal, S., A. K. Dudani, et al. (1989). "Primary structure of a human mitochondrial protein homologous to the bacterial and plant chaperonins and to the 65-kilodalton mycobacterial antigen." Mol Cell Biol 9(5): 2279-83.

Jo, E., N. Fuller, et al. (2002). "Defective membrane interactions of familial Parkinson's disease mutant A30P alpha-synuclein." J Mol Biol 315(4): 799-807.

Johnston, J. A., C. L. Ward, et al. (1998). "Aggresomes: a cellular response to misfolded proteins." J Cell Biol 143(7): 1883-98.

Junn, E., S. S. Lee, et al. (2002). "Parkin accumulation in aggresomes due to proteasome impairment." J Biol Chem 277(49): 47870-7.

Kahle, P. J., M. Neumann, et al. (2000). "Subcellular localization of wild-type and Parkinson's disease-associated mutant alpha -synuclein in human and transgenic mouse brain." J Neurosci 20(17): 6365-73.

Kamen, A. and O. Henry (2004). "Development and optimization of an adenovirus production process." J Gene Med 6 Suppl 1: S184-92.

Kaplitt, M. G., A. Feigin, et al. (2007). "Safety and tolerability of gene therapy with an adeno-associated virus (AAV) borne GAD gene for Parkinson's disease: an open label, phase I trial." Lancet 369(9579): 2097-105.

Katsuse, O., E. Iseki, et al. (2003). "Developmental stages of cortical Lewy bodies and their relation to axonal transport blockage in brains of patients with dementia with Lewy bodies." J Neurol Sci 211(1-2): 29-35.

Kaufmann, S. H. and W. C. Earnshaw (2000). "Induction of apoptosis by cancer chemotherapy." Exp Cell Res 256(1): 42-9.

Kawamata, H., P. J. McLean, et al. (2001). "Interaction of alpha-synuclein and synphilin-1: effect of Parkinson's disease-associated mutations." J Neurochem 77(3): 929-34.

Kelly, S., J. McCulloch, et al. (2001). "Minimal ischaemic neuronal damage and HSP70 expression in MF1 strain mice following bilateral common carotid artery occlusion." Brain Res 914(1-2): 185-95.

Kelly, S., Z. J. Zhang, et al. (2002). "Gene transfer of HSP72 protects cornu ammonis 1 region of the hippocampus neurons from global ischemia: influence of Bcl-2." Ann Neurol 52(2): 160-7.

Kermer, P., N. Klocker, et al. (1999). "Long-term effect of inhibition of ced 3-like caspases on the survival of axotomized retinal ganglion cells in vivo." Exp Neurol 158(1): 202-5.

Kerr, J. F., A. H. Wyllie, et al. (1972). "Apoptosis: a basic biological phenomenon with wide-ranging implications in tissue kinetics." Br J Cancer 26(4): 239-57.

Kim, R. (2005). "Unknotting the roles of Bcl-2 and Bcl-xL in cell death." Biochem Biophys Res Commun 333(2): 336-43.

Kim, V. N., K. Mitrophanous, et al. (1998). "Minimal requirement for a lentivirus vector based on human immunodeficiency virus type 1." J Virol 72(1): 811-6.

Kirik, D., L. E. Annett, et al. (2003). "Nigrostriatal alpha-synucleinopathy induced by viral vector-mediated overexpression of human alpha-synuclein: a new primate model of Parkinson's disease." Proc Natl Acad Sci U S A 100(5): 2884-9.

Kirik, D., C. Rosenblad, et al. (1998). "Characterization of behavioral and neurodegenerative changes following partial lesions of the nigrostriatal dopamine system induced by intrastriatal 6-hydroxydopamine in the rat." Exp Neurol 152(2): 259-77.

Kirik, D., C. Rosenblad, et al. (2002). "Parkinson-like neurodegeneration induced by targeted overexpression of alpha-synuclein in the nigrostriatal system." J Neurosci 22(7): 2780-91.

Kitao, Y., Y. Imai, et al. (2007). "Pael receptor induces death of dopaminergic neurons in the substantia nigra via endoplasmic reticulum stress and dopamine toxicity, which is enhanced under condition of parkin inactivation." Hum Mol Genet 16(1): 50-60.

Klein, J. A. and S. L. Ackerman (2003). "Oxidative stress, cell cycle, and neurodegeneration." J Clin Invest 111(6): 785-93.

Kluck, R. M., E. Bossy-Wetzel, et al. (1997). "The release of cytochrome c from mitochondria: a primary site for Bcl-2 regulation of apoptosis." Science 275(5303): 1132-6.

Klucken, J., Y. Shin, et al. (2004a). "A single amino acid substitution differentiates Hsp70-dependent effects on alpha-synuclein degradation and toxicity." Biochem Biophys Res Commun 325(1): 367-73.

Klucken, J., Y. Shin, et al. (2004b). "Hsp70 reduces alpha-synuclein aggregation and toxicity." J Biol Chem.

Klucken, J., Y. Shin, et al. (2004c). "Hsp70 Reduces alpha-Synuclein Aggregation and Toxicity." J Biol Chem 279(24): 25497-502.

Kobayashi, Y. and G. Sobue (2001). "Protective effect of chaperones on polyglutamine diseases." Brain Res Bull 56(3-4): 165-8.

Kopecek, P., K. Altmannova, et al. (2001). "Stress proteins: nomenclature, division and functions." Biomed Pap Med Fac Univ Palacky Olomouc Czech Repub 145(2): 39-47.

Kopito, R. R. (2000). "Aggresomes, inclusion bodies and protein aggregation." Trends Cell Biol 10(12): 524-30.

Kordower, J. H., Y. Chu, et al. (2008). "Transplanted dopaminergic neurons develop PD pathologic changes: a second case report." Mov Disord 23(16): 2303-6.

Kowall, N. W., P. Hantraye, et al. (2000). "MPTP induces alpha-synuclein aggregation in the substantia nigra of baboons." Neuroreport 11(1): 211-3.

Kowsky, S., C. Poppelmeyer, et al. (2007). "RET signaling does not modulate MPTP toxicity but is required for regeneration of dopaminergic axon terminals." Proc Natl Acad Sci U S A 104(50): 20049-54.

Kremer, E. (2005). "Gene Transfer to the Central Nervous System: Current State of the Art of the Viral Vectors." Current Genomics 6(1): 13-37.

Krenz, A., B. H. Falkenburger, et al. (2009). "Aggregate formation and toxicity by wild-type and R621C synphilin-1 in the nigrostriatal system of mice using adenoviral vectors." J Neurochem 108(1): 139-46.

Kringelbach, M. L., N. Jenkinson, et al. (2007). "Translational principles of deep brain stimulation." Nat Rev Neurosci 8(8): 623-35.

Krobitsch, S. and S. Lindquist (2000). "Aggregation of huntingtin in yeast varies with the length of the polyglutamine expansion and the expression of chaperone proteins." Proc Natl Acad Sci U S A 97(4): 1589-94.

Kruger, R., W. Kuhn, et al. (1998). "Ala30Pro mutation in the gene encoding alpha-synuclein in Parkinson's disease." Nat Genet 18(2): 106-8.

Kugler, S., L. Meyn, et al. (2001). "Neuron-specific expression of therapeutic proteins: evaluation of different cellular promoters in recombinant adenoviral vectors." Mol Cell Neurosci 17(1): 78-96.

Kuhn, D. M., R. E. Arthur, Jr., et al. (1999). "Tyrosine hydroxylase is inactivated by catechol-quinones and converted to a redox-cycling quinoprotein: possible relevance to Parkinson's disease." J Neurochem 73(3): 1309-17.

Lai, H. C., T. J. Liu, et al. (2007). "Regulation of IGF-I receptor signaling in diabetic cardiac muscle: dysregulation of cytosolic and mitochondria HSP60." Am J Physiol Endocrinol Metab 292(1): E292-7.

Lai, Y., L. Du, et al. (2005). "Selectively increasing inducible heat shock protein 70 via TAT-protein transduction protects neurons from nitrosative stress and excitotoxicity." J Neurochem 94(2): 360-6.

Landry, J., H. Lambert, et al. (1992). "Human HSP27 is phosphorylated at serines 78 and 82 by heat shock and mitogen-activated kinases that recognize the same amino acid motif as S6 kinase II." J Biol Chem 267(2): 794-803.

Langer, T., C. Lu, et al. (1992). "Successive action of DnaK, DnaJ and GroEL along the pathway of chaperone-mediated protein folding." Nature 356(6371): 683-9.

Larkin, M. (1999). "Parkinson's disease research moves on briskly." Lancet 353(9152): 566.

Lashuel, H. A., D. Hartley, et al. (2002). "Neurodegenerative disease: amyloid pores from pathogenic mutations." Nature 418(6895): 291.

Lauwers, E., Z. Debyser, et al. (2003). "Neuropathology and neurodegeneration in rodent brain induced by lentiviral vector-mediated overexpression of alpha-synuclein." Brain Pathol 13(3): 364-72.

Lavoie, J. N., E. Hickey, et al. (1993). "Modulation of actin microfilament dynamics and fluid phase pinocytosis by phosphorylation of heat shock protein 27." J Biol Chem 268(32): 24210-4.

Le Gal La Salle, G., J. J. Robert, et al. (1993). "An adenovirus vector for gene transfer into neurons and glia in the brain." Science 259(5097): 988-90.

Lee, G., E. Junn, et al. (2002a). "Synphilin-1 degradation by the ubiquitin-proteasome pathway and effects on cell survival." J Neurochem 83(2): 346-52.

Lee, H. J., S. Y. Shin, et al. (2002b). "Formation and removal of alpha-synuclein aggregates in cells exposed to mitochondrial inhibitors." J Biol Chem 277(7): 5411-7.

Lee, M., D. Hyun, et al. (2001). "Effect of the overexpression of wild-type or mutant alpha-synuclein on cell susceptibility to insult." J Neurochem 76(4): 998-1009.

Leist, M. and M. Jaattela (2001). "Four deaths and a funeral: from caspases to alternative mechanisms." Nat Rev Mol Cell Biol 2(8): 589-98.

Lepoutre, A. C., D. Devos, et al. (2006). "A specific clinical pattern of camptocormia in Parkinson's disease." J Neurol Neurosurg Psychiatry 77(11): 1229-34.

Li, C. Y., J. S. Lee, et al. (2000). "Heat shock protein 70 inhibits apoptosis downstream of cytochrome c release and upstream of caspase-3 activation." J Biol Chem 275(33): 25665-71.

Li, J. Y., E. Englund, et al. (2008). "Lewy bodies in grafted neurons in subjects with Parkinson's disease suggest host-to-graft disease propagation." Nat Med 14(5): 501-3.

Li, Q. J., Y. M. Tang, et al. (2007). "Treatment of Parkinson disease with C17.2 neural stem cells overexpressing NURR1 with a recombined republic-deficit adenovirus containing the NURR1 gene." Synapse 61(12): 971-7.

Liani, E., A. Eyal, et al. (2004). "Ubiquitylation of synphilin-1 and alpha-synuclein by SIAH and its presence in cellular inclusions and Lewy bodies imply a role in Parkinson's disease." Proc Natl Acad Sci U S A 101(15): 5500-5.

Liberek, K., A. Lewandowska, et al. (2008). "Chaperones in control of protein disaggregation." Embo J 27(2): 328-35.

Liberek, K., J. Marszalek, et al. (1991). "Escherichia coli DnaJ and GrpE heat shock proteins jointly stimulate ATPase activity of DnaK." Proc Natl Acad Sci U S A 88(7): 2874-8.

Lieberman, A. (2006). "Depression in Parkinson's disease -- a review." Acta Neurol Scand 113(1): 1-8.

Lo Bianco, C., J. L. Ridet, et al. (2002). "alpha -Synucleinopathy and selective dopaminergic neuron loss in a rat lentiviral-based model of Parkinson's disease." Proc Natl Acad Sci U S A 99(16): 10813-8.

Lorincz, M. T. (2006). "Clinical implications of Parkinson's disease genetics." Semin Neurol 26(5): 492-8.

Lowe, J., A. Blanchard, et al. (1988). "Ubiquitin is a common factor in intermediate filament inclusion bodies of diverse type in man, including those of Parkinson's disease, Pick's disease, and Alzheimer's disease, as well as Rosenthal fibres in cerebellar astrocytomas, cytoplasmic bodies in muscle, and mallory bodies in alcoholic liver disease." J Pathol 155(1): 9-15.

Lowenstein, P. R. and M. G. Castro (2003). "Inflammation and adaptive immune responses to adenoviral vectors injected into the brain: peculiarities, mechanisms, and consequences." Gene Ther 10(11): 946-54.

Lowenstein, P. R., C. E. Thomas, et al. (2002). "High-capacity, helper-dependent, "gutless" adenoviral vectors for gene transfer into brain." Methods Enzymol 346: 292-311.

Lu, A., R. Ran, et al. (2002). "Geldanamycin induces heat shock proteins in brain and protects against focal cerebral ischemia." J Neurochem 81(2): 355-64.

Lu, L., C. Zhao, et al. (2005). "Therapeutic benefit of TH-engineered mesenchymal stem cells for Parkinson's disease." Brain Res Brain Res Protoc 15(1): 46-51.

Luo, J., Z. L. Deng, et al. (2007). "A protocol for rapid generation of recombinant adenoviruses using the AdEasy system." Nat Protoc 2(5): 1236-47.
Ma, Y. and L. M. Hendershot (2001). "The unfolding tale of the unfolded protein response." Cell 107(7): 827-30.
Magrane, J., R. C. Smith, et al. (2004). "Heat shock protein 70 participates in the neuroprotective response to intracellularly expressed beta-amyloid in neurons." J Neurosci 24(7): 1700-6.
Malik, J. M., Z. Shevtsova, et al. (2005). "Long-term in vivo inhibition of CNS neurodegeneration by Bcl-XL gene transfer." Mol Ther 11(3): 373-81.
Mandel, R. J., C. Burger, et al. (2008). "Viral vectors for in vivo gene transfer in Parkinson's disease: properties and clinical grade production." Exp Neurol 209(1): 58-71.
Mangiarini, L., K. Sathasivam, et al. (1996). "Exon 1 of the HD gene with an expanded CAG repeat is sufficient to cause a progressive neurological phenotype in transgenic mice." Cell 87(3): 493-506.
Marttila, R. J., J. Kaprio, et al. (1988). "Parkinson's disease in a nationwide twin cohort." Neurology 38(8): 1217-9.
Marx, F. P. (2004). Funktionelle Charakterisierung von Mutationen im Synphilin-1- und Parkin-Gen bei der Parkinson-Krankheit : Bedeutung von Proteinaggregation und des Ubiquitin-Proteasomen-Systems für die Pathogenese der Parkinson-Krankheit. Faculty of Chemistry and Pharmacy. Tuebingen, University of Tuebingen: 146.
Marx, F. P., C. Holzmann, et al. (2003). Identification and functional characterization of a novel R621C mutation in the synphilin-1 gene in Parkinson's disease. Hum Mol Genet. 12: 1223-31.
Marx, F. P., A. S. Soehn, et al. (2007). "The proteasomal subunit S6 ATPase is a novel synphilin-1 interacting protein--implications for Parkinson's disease." Faseb J 21(8): 1759-67.
Masliah, E., E. Rockenstein, et al. (2000). "Dopaminergic loss and inclusion body formation in alpha-synuclein mice: implications for neurodegenerative disorders." Science 287(5456): 1265-9.
Matsumori, Y., S. M. Hong, et al. (2005). "Hsp70 overexpression sequesters AIF and reduces neonatal hypoxic/ischemic brain injury." J Cereb Blood Flow Metab 25(7): 899-910.
Maurizi, M. R. and D. Xia (2004). "Protein binding and disruption by Clp/Hsp100 chaperones." Structure 12(2): 175-83.
Mayer, M. P. and B. Bukau (2005). "Hsp70 chaperones: cellular functions and molecular mechanism." Cell Mol Life Sci 62(6): 670-84.
McCormack, A. L., M. Thiruchelvam, et al. (2002). "Environmental risk factors and Parkinson's disease: selective degeneration of nigral dopaminergic neurons caused by the herbicide paraquat." Neurobiol Dis 10(2): 119-27.
McLean, P. J., H. Kawamata, et al. (2001). "Alpha-synuclein-enhanced green fluorescent protein fusion proteins form proteasome sensitive inclusions in primary neurons." Neuroscience 104(3): 901-12.
McLean, P. J., H. Kawamata, et al. (2002). "TorsinA and heat shock proteins act as molecular chaperones: suppression of alpha-synuclein aggregation." J Neurochem 83(4): 846-54.
McLean, P. J., J. Klucken, et al. (2004). "Geldanamycin induces Hsp70 and prevents alpha-synuclein aggregation and toxicity in vitro." Biochem Biophys Res Commun 321(3): 665-9.
McLear, J. A., D. Lebrecht, et al. (2008). "Combinational approach of intrabody with enhanced Hsp70 expression addresses multiple pathologies in a fly model of Huntington's disease." Faseb J 22(6): 2003-11.
McNaught, K. S., R. Belizaire, et al. (2003). "Altered proteasomal function in sporadic Parkinson's disease." Exp Neurol 179(1): 38-46.
McNaught, K. S. and P. Jenner (2001). "Proteasomal function is impaired in substantia nigra in Parkinson's disease." Neurosci Lett 297(3): 191-4.

McNaught, K. S., D. P. Perl, et al. (2004). "Systemic exposure to proteasome inhibitors causes a progressive model of Parkinson's disease." Ann Neurol 56(1): 149-62.
McNaught, K. S., P. Shashidharan, et al. (2002). "Aggresome-related biogenesis of Lewy bodies." Eur J Neurosci 16(11): 2136-48.
Meacham, G. C., C. Patterson, et al. (2001). "The Hsc70 co-chaperone CHIP targets immature CFTR for proteasomal degradation." Nat Cell Biol 3(1): 100-5.
Meehan, S., Y. Berry, et al. (2004). "Amyloid fibril formation by lens crystallin proteins and its implications for cataract formation." J Biol Chem 279(5): 3413-9.
Mendez, I., A. Vinuela, et al. (2008). "Dopamine neurons implanted into people with Parkinson's disease survive without pathology for 14 years." Nat Med 14(5): 507-9.
Meredith, G. E., S. Totterdell, et al. (2002). "Lysosomal malfunction accompanies alpha-synuclein aggregation in a progressive mouse model of Parkinson's disease." Brain Res 956(1): 156-65.
Meriin, A. B., X. Zhang, et al. (2002). "Huntington toxicity in yeast model depends on polyglutamine aggregation mediated by a prion-like protein Rnq1." J Cell Biol 157(6): 997-1004.
Miller, D. M., G. R. Buettner, et al. (1990). "Transition metals as catalysts of "autoxidation" reactions." Free Radic Biol Med 8(1): 95-108.
Mioduszewska, B., J. Jaworski, et al. (2008). "Inducible cAMP early repressor (ICER)-evoked delayed neuronal death in the organotypic hippocampal culture." J Neurosci Res 86(1): 61-70.
Mitchell, R. S., B. F. Beitzel, et al. (2004). "Retroviral DNA integration: ASLV, HIV, and MLV show distinct target site preferences." PLoS Biol 2(8): E234.
Miyoshi, H., U. Blomer, et al. (1998). "Development of a self-inactivating lentivirus vector." J Virol 72(10): 8150-7.
Mochizuki, H., H. Hayakawa, et al. (2001). "An AAV-derived Apaf-1 dominant negative inhibitor prevents MPTP toxicity as antiapoptotic gene therapy for Parkinson's disease." Proc Natl Acad Sci U S A 98(19): 10918-23.
Modrow, S. and D. Falke (1997). Molekulare Virologie. Heidelberg, Berlin.
Moore, D. J., V. L. Dawson, et al. (2003). "Role for the ubiquitin-proteasome system in Parkinson's disease and other neurodegenerative brain amyloidoses." Neuromolecular Med 4(1-2): 95-108.
Moore, D. J., A. B. West, et al. (2005). "Molecular pathophysiology of Parkinson's disease." Annu Rev Neurosci 28: 57-87.
Morgante, L., G. Salemi, et al. (2000). "Parkinson disease survival: a population-based study." Arch Neurol 57(4): 507-12.
Morimoto, R. I. (1998). "Regulation of the heat shock transcriptional response: cross talk between a family of heat shock factors, molecular chaperones, and negative regulators." Genes Dev 12(24): 3788-96.
Mosser, D. D., A. W. Caron, et al. (1997). "Role of the human heat shock protein hsp70 in protection against stress-induced apoptosis." Mol Cell Biol 17(9): 5317-27.
Mosser, D. D., A. W. Caron, et al. (2000). "The chaperone function of hsp70 is required for protection against stress-induced apoptosis." Mol Cell Biol 20(19): 7146-59.
Muchowski, P. J., G. Schaffar, et al. (2000a). "Hsp70 and hsp40 chaperones can inhibit self-assembly of polyglutamine proteins into amyloid-like fibrils." Proc Natl Acad Sci U S A 97(14): 7841-6.
Muchowski, P. J., G. Schaffar, et al. (2000b). "Hsp70 and hsp40 chaperones can inhibit self-assembly of polyglutamine proteins into amyloid-like fibrils." 97(14): 7841-7846.
Muchowski, P. J. and J. L. Wacker (2005). "Modulation of neurodegeneration by molecular chaperones." Nat Rev Neurosci 6(1): 11-22.
Mulholland, R. C. (1996). "Sir William Gowers 1845-1915." Spine 21(9): 1106-10.
Muller, T., E. Eising, et al. (1999). "Delayed motor response correlates with striatal degeneration in Parkinson's disease." Acta Neurol Scand 100(4): 227-30.
Muqit, M. M., P. M. Abou-Sleiman, et al. (2006). "Altered cleavage and localization of PINK1 to aggresomes in the presence of proteasomal stress." J Neurochem 98(1): 156-69.

Muruve, D. A. (2004). "The innate immune response to adenovirus vectors." Hum Gene Ther 15(12): 1157-66.
Myhre, R., H. Klungland, et al. (2008). "Genetic association study of synphilin-1 in idiopathic Parkinson's disease." BMC Med Genet 9: 19.
Nagano, Y., H. Yamashita, et al. (2003). "Siah-1 facilitates ubiquitination and degradation of synphilin-1." J Biol Chem 278(51): 51504-14.
Nagel, F., B. H. Falkenburger, et al. (2008). "Tat-Hsp70 protects dopaminergic neurons in midbrain cultures and in the substantia nigra in models of Parkinson's disease." J Neurochem.
Naldini, L., U. Blomer, et al. (1996a). "Efficient transfer, integration, and sustained long-term expression of the transgene in adult rat brains injected with a lentiviral vector." Proc Natl Acad Sci U S A 93(21): 11382-8.
Naldini, L., U. Blomer, et al. (1996b). "In vivo gene delivery and stable transduction of nondividing cells by a lentiviral vector." Science 272(5259): 263-7.
Naldini, L. and I. M. Verma (2000). "Lentiviral vectors." Adv Virus Res 55: 599-609.
Nandi, D., P. Tahiliani, et al. (2006). "The ubiquitin-proteasome system." J Biosci 31(1): 137-55.
Neumann, M., P. J. Kahle, et al. (2002). "Misfolded proteinase K-resistant hyperphosphorylated alpha-synuclein in aged transgenic mice with locomotor deterioration and in human alpha-synucleinopathies." J Clin Invest 110(10): 1429-39.
Nicklas, W. J., S. K. Youngster, et al. (1987). "MPTP, MPP+ and mitochondrial function." Life Sci 40(8): 721-9.
Nieto, M., F. J. Gil-Bea, et al. (2006). "Increased sensitivity to MPTP in human alpha-synuclein A30P transgenic mice." Neurobiol Aging 27(6): 848-56.
Nohl, H., V. Breuninger, et al. (1978). "Influence of mitochondrial radical formation on energy-linked respiration." Eur J Biochem 90(2): 385-90.
Nollen, E. A. and R. I. Morimoto (2002). "Chaperoning signaling pathways: molecular chaperones as stress-sensing 'heat shock' proteins." J Cell Sci 115(Pt 14): 2809-16.
Nylandsted, J., M. Gyrd-Hansen, et al. (2004). "Heat shock protein 70 promotes cell survival by inhibiting lysosomal membrane permeabilization." J Exp Med 200(4): 425-35.
O'Farrell, C., D. D. Murphy, et al. (2001). "Transfected synphilin-1 forms cytoplasmic inclusions in HEK293 cells." Brain Res Mol Brain Res 97(1): 94-102.
O'Neill, M. J., T. K. Murray, et al. (2004). "Neurotrophic actions of the novel AMPA receptor potentiator, LY404187, in rodent models of Parkinson's disease." Eur J Pharmacol 486(2): 163-74.
Ohtsuka, K. and M. Hata (2000). "Molecular chaperone function of mammalian Hsp70 and Hsp40--a review." Int J Hyperthermia 16(3): 231-45.
Opazo, F., A. Krenz, et al. (2008). "Accumulation and clearance of alpha-synuclein aggregates demonstrated by time-lapse imaging." J Neurochem 106(2): 529-40.
Ossowska, K., M. Smialowska, et al. (2006). "Degeneration of dopaminergic mesocortical neurons and activation of compensatory processes induced by a long-term paraquat administration in rats: implications for Parkinson's disease." Neuroscience 141(4): 2155-65.
Pappolla, M. A. (1986). "Lewy bodies of Parkinson's disease. Immune electron microscopic demonstration of neurofilament antigens in constituent filaments." Arch Pathol Lab Med 110(12): 1160-3.
Park, J. and A. Y. Liu (2001). "JNK phosphorylates the HSF1 transcriptional activation domain: role of JNK in the regulation of the heat shock response." J Cell Biochem 82(2): 326-38.
Parkinson, J. (2002). "An essay on the shaking palsy. 1817." J Neuropsychiatry Clin Neurosci 14(2): 223-36; discussion 222.
Parks, R. J., L. Chen, et al. (1996). "A helper-dependent adenovirus vector system: removal of helper virus by Cre-mediated excision of the viral packaging signal." Proc Natl Acad Sci U S A 93(24): 13565-70.

Paterna, J. C., J. Feldon, et al. (2004). "Transduction profiles of recombinant adeno-associated virus vectors derived from serotypes 2 and 5 in the nigrostriatal system of rats." J Virol 78(13): 6808-17.

Paxinou, E., Q. Chen, et al. (2001). "Induction of alpha-synuclein aggregation by intracellular nitrative insult." J Neurosci 21(20): 8053-61.

Peden, C. S., C. Burger, et al. (2004). "Circulating anti-wild-type adeno-associated virus type 2 (AAV2) antibodies inhibit recombinant AAV2 (rAAV2)-mediated, but not rAAV5-mediated, gene transfer in the brain." J Virol 78(12): 6344-59.

Peltekian, E., L. Garcia, et al. (2002). "Neurotropism and retrograde axonal transport of a canine adenoviral vector: a tool for targeting key structures undergoing neurodegenerative processes." Mol Ther 5(1): 25-32.

Perez, R. G., J. C. Waymire, et al. (2002). "A role for alpha-synuclein in the regulation of dopamine biosynthesis." J Neurosci 22(8): 3090-9.

Perrelet, D., A. Ferri, et al. (2000). "IAP family proteins delay motoneuron cell death in vivo." Eur J Neurosci 12(6): 2059-67.

Petrucelli, L., D. Dickson, et al. (2004). "CHIP and Hsp70 regulate tau ubiquitination, degradation and aggregation." Hum Mol Genet 13(7): 703-14.

Pickart, C. M. (2001). "Ubiquitin enters the new millennium." Mol Cell 8(3): 499-504.

Polymeropoulos, M. H., C. Lavedan, et al. (1997). "Mutation in the alpha-synuclein gene identified in families with Parkinson's disease." Science 276(5321): 2045-7.

Pratt, W. B. and D. O. Toft (2003). "Regulation of signaling protein function and trafficking by the hsp90/hsp70-based chaperone machinery." Exp Biol Med (Maywood) 228(2): 111-33.

Puntel, M., J. F. Curtin, et al. (2006). "Quantification of high-capacity helper-dependent adenoviral vector genomes in vitro and in vivo, using quantitative TaqMan real-time polymerase chain reaction." Hum Gene Ther 17(5): 531-44.

Quigney, D. J., A. M. Gorman, et al. (2003). "Heat shock protects PC12 cells against MPP+ toxicity." Brain Res 993(1-2): 133-9.

Rathke-Hartlieb, S., P. J. Kahle, et al. (2001). "Sensitivity to MPTP is not increased in Parkinson's disease-associated mutant alpha-synuclein transgenic mice." J Neurochem 77(4): 1181-4.

Ravagnan, L., S. Gurbuxani, et al. (2001). "Heat-shock protein 70 antagonizes apoptosis-inducing factor." Nat Cell Biol 3(9): 839-43.

Regulier, E., Y. Trottier, et al. (2003). "Early and reversible neuropathology induced by tetracycline-regulated lentiviral overexpression of mutant huntingtin in rat striatum." Hum Mol Genet 12(21): 2827-36.

Reich, A., C. Spering, et al. (2008). "Death receptor Fas (CD95) signaling in the central nervous system: tuning neuroplasticity?" Trends Neurosci 31(9): 478-86.

Ribeiro, C. S., K. Carneiro, et al. (2002). "Synphilin-1 is developmentally localized to synaptic terminals, and its association with synaptic vesicles is modulated by alpha-synuclein." J Biol Chem 277(26): 23927-33.

Rideout, H. J. and L. Stefanis (2001). "Caspase inhibition: a potential therapeutic strategy in neurological diseases." Histol Histopathol 16(3): 895-908.

Ridet, J. L., J. C. Bensadoun, et al. (2006). "Lentivirus-mediated expression of glutathione peroxidase: neuroprotection in murine models of Parkinson's disease." Neurobiol Dis 21(1): 29-34.

Ridoux, V., J. Robert, et al. (1995). "Adenovirus mediated gene transfer in organotypic brain slices." Neurobiol Dis 2(1): 49-54.

Riederer, P., J. Sian, et al. (2000). "Is there neuroprotection in Parkinson syndrome?" J Neurol 247 Suppl 4: IV/8-11.

Ritossa, F. (1996). "Discovery of the heat shock response." Cell Stress Chaperones 1(2): 97-8.

Roberti, M. J., C. W. Bertoncini, et al. (2007). "Fluorescence imaging of amyloid formation in living cells by a functional, tetracysteine-tagged alpha-synuclein." Nat Methods 4(4): 345-51.

Rogalla, T., M. Ehrnsperger, et al. (1999). "Regulation of Hsp27 oligomerization, chaperone function, and protective activity against oxidative stress/tumor necrosis factor alpha by phosphorylation." J Biol Chem 274(27): 18947-56.

Rott, R., R. Szargel, et al. (2008). "Monoubiquitylation of alpha-synuclein by seven in absentia homolog (SIAH) promotes its aggregation in dopaminergic cells." J Biol Chem 283(6): 3316-28.

Rouse, J., P. Cohen, et al. (1994). "A novel kinase cascade triggered by stress and heat shock that stimulates MAPKAP kinase-2 and phosphorylation of the small heat shock proteins." Cell 78(6): 1027-37.

Rousseau, S., F. Houle, et al. (1997). "p38 MAP kinase activation by vascular endothelial growth factor mediates actin reorganization and cell migration in human endothelial cells." Oncogene 15(18): 2169-77.

Sahara, N., M. Murayama, et al. (2008). "Active c-jun N-terminal kinase induces caspase cleavage of tau and additional phosphorylation by GSK-3beta is required for tau aggregation." Eur J Neurosci 27(11): 2897-906.

Saleh, A., S. M. Srinivasula, et al. (2000). "Negative regulation of the Apaf-1 apoptosome by Hsp70." Nat Cell Biol 2(8): 476-83.

Salmon, P. and D. Trono (2006). "Production and titration of lentiviral vectors." Curr Protoc Neurosci Chapter 4: Unit 4 21.

Sanftner, L. M., J. M. Sommer, et al. (2005). "AAV2-mediated gene delivery to monkey putamen: evaluation of an infusion device and delivery parameters." Exp Neurol 194(2): 476-83.

Sanftner, L. M., B. M. Suzuki, et al. (2004). "Striatal delivery of rAAV-hAADC to rats with preexisting immunity to AAV." Mol Ther 9(3): 403-9.

Schapira, A. H., J. M. Cooper, et al. (1989). "Mitochondrial complex I deficiency in Parkinson's disease." Lancet 1(8649): 1269.

Schmidt, M. L., J. Murray, et al. (1991). "Epitope map of neurofilament protein domains in cortical and peripheral nervous system Lewy bodies." Am J Pathol 139(1): 53-65.

Schober, A. (2004). "Classic toxin-induced animal models of Parkinson's disease: 6-OHDA and MPTP." Cell Tissue Res 318(1): 215-24.

Schober, A., H. Peterziel, et al. (2007). "GDNF applied to the MPTP-lesioned nigrostriatal system requires TGF-beta for its neuroprotective action." Neurobiol Dis 25(2): 378-91.

Schulz, J. B. (2006). "Anti-apoptotic gene therapy in Parkinson's disease." J Neural Transm Suppl(70): 467-76.

Schulz, J. B. (2008). "Update on the pathogenesis of Parkinson's disease." J Neurol 255 Suppl 5: 3-7.

Schulz, J. B., J. Lindenau, et al. (2000). "Glutathione, oxidative stress and neurodegeneration." Eur J Biochem 267(16): 4904-11.

Schulz, J. B., M. Weller, et al. (1999). "Caspases as treatment targets in stroke and neurodegenerative diseases." Ann Neurol 45(4): 421-9.

Sedelis, M., K. Hofele, et al. (2000). "MPTP susceptibility in the mouse: behavioral, neurochemical, and histological analysis of gender and strain differences." Behav Genet 30(3): 171-82.

Shen, H. Y., J. C. He, et al. (2005). "Geldanamycin induces heat shock protein 70 and protects against MPTP-induced dopaminergic neurotoxicity in mice." J Biol Chem 280(48): 39962-9.

Sherman, M. Y. and A. L. Goldberg (2001). "Cellular defenses against unfolded proteins: a cell biologist thinks about neurodegenerative diseases." Neuron 29(1): 15-32.

Shevtsova, Z. (2006). Development of Viral Tools for CNS Gene Transfer: Adeno-Associated Viral Vectors in Gene Therapy of Parkinson's Disease. Faculty of Biology. Göttingen, Georg August University Göttingen: 1-102.

Shi, M., J. Jin, et al. (2008). "Mortalin: a protein associated with progression of Parkinson disease?" J Neuropathol Exp Neurol 67(2): 117-24.

Shimoji, M., L. Zhang, et al. (2005). "Absence of inclusion body formation in the MPTP mouse model of Parkinson's disease." Brain Res Mol Brain Res 134(1): 103-8.

Shimura, H., Y. Miura-Shimura, et al. (2004). "Binding of tau to heat shock protein 27 leads to decreased concentration of hyperphosphorylated tau and enhanced cell survival." J Biol Chem 279(17): 17957-62.

Shimura, H., M. G. Schlossmacher, et al. (2001). "Ubiquitination of a new form of alpha-synuclein by parkin from human brain: implications for Parkinson's disease." Science 293(5528): 263-9.

Shin, Y., J. Klucken, et al. (2005). "The co-chaperone carboxyl terminus of Hsp70-interacting protein (CHIP) mediates alpha-synuclein degradation decisions between proteasomal and lysosomal pathways." J Biol Chem 280(25): 23727-34.

Sian, J., D. T. Dexter, et al. (1994). "Alterations in glutathione levels in Parkinson's disease and other neurodegenerative disorders affecting basal ganglia." Ann Neurol 36(3): 348-55.

Sian, J., M. Gerlach, et al. (1999). "Parkinson's disease: a major hypokinetic basal ganglia disorder." J Neural Transm 106(5-6): 443-76.

Simons, M., S. Beinroth, et al. (1999). "Adenovirus-mediated gene transfer of inhibitors of apoptosis protein delays apoptosis in cerebellar granule neurons." J Neurochem 72(1): 292-301.

Singleton, A. B., M. Farrer, et al. (2003). "alpha-Synuclein locus triplication causes Parkinson's disease." Science 302(5646): 841.

Sinn, P. L., S. L. Sauter, et al. (2005). "Gene therapy progress and prospects: development of improved lentiviral and retroviral vectors--design, biosafety, and production." Gene Ther 12(14): 1089-98.

Smith, W. W., Z. Pei, et al. (2006). "Kinase activity of mutant LRRK2 mediates neuronal toxicity." Nat Neurosci 9(10): 1231-3.

Snyder, H., K. Mensah, et al. (2003). "Aggregated and monomeric alpha-synuclein bind to the S6' proteasomal protein and inhibit proteasomal function." J Biol Chem 278(14): 11753-9.

Sofic, E., P. Riederer, et al. (1988). "Increased iron (III) and total iron content in post mortem substantia nigra of parkinsonian brain." J Neural Transm 74(3): 199-205.

Soudais, C., S. Boutin, et al. (2000). "Canine adenovirus type 2 attachment and internalization: coxsackievirus-adenovirus receptor, alternative receptors, and an RGD-independent pathway." J Virol 74(22): 10639-49.

Southgate, T., K. M. Kroeger, et al. (2008). "Gene transfer into neural cells in vitro using adenoviral vectors." Curr Protoc Neurosci Chapter 4: Unit 4 23.

Spillantini, M. G., M. L. Schmidt, et al. (1997). "Alpha-synuclein in Lewy bodies." Nature 388(6645): 839-40.

Srinivasula, S. M., M. Ahmad, et al. (1998). "Autoactivation of procaspase-9 by Apaf-1-mediated oligomerization." Mol Cell 1(7): 949-57.

St Martin, J. L., J. Klucken, et al. (2007). "Dopaminergic neuron loss and up-regulation of chaperone protein mRNA induced by targeted over-expression of alpha-synuclein in mouse substantia nigra." J Neurochem 100(6): 1449-57.

Stefanis, L., K. E. Larsen, et al. (2001). "Expression of A53T mutant but not wild-type alpha-synuclein in PC12 cells induces alterations of the ubiquitin-dependent degradation system, loss of dopamine release, and autophagic cell death." J Neurosci 21(24): 9549-60.

Stieger, K., G. Le Meur, et al. (2006). "Long-term doxycycline-regulated transgene expression in the retina of nonhuman primates following subretinal injection of recombinant AAV vectors." Mol Ther 13(5): 967-75.

Susin, S. A., E. Daugas, et al. (2000). "Two distinct pathways leading to nuclear apoptosis." J Exp Med 192(4): 571-80.

Susin, S. A., H. K. Lorenzo, et al. (1999). "Molecular characterization of mitochondrial apoptosis-inducing factor." Nature 397(6718): 441-6.

Szargel, R., R. Rott, et al. (2007). "Synphilin-1 isoforms in Parkinson's disease: regulation by phosphorylation and ubiquitylation." Cell Mol Life Sci.

Szelid, Z., P. Sinnaeve, et al. (2002). "Preexisting antiadenoviral immunity and regional myocardial gene transfer: modulation by nitric oxide." Hum Gene Ther 13(18): 2185-95.

Takahashi, T., H. Yamashita, et al. (2006). "Interactions of Synphilin-1 with phospholipids and lipid membranes." FEBS Lett 580(18): 4479-84.

Takeuchi, H., Y. Kobayashi, et al. (2002). "Hsp70 and Hsp40 improve neurite outgrowth and suppress intracytoplasmic aggregate formation in cultured neuronal cells expressing mutant SOD1." Brain Res 949(1-2): 11-22.

Tanaka, M., Y. M. Kim, et al. (2004). "Aggresomes formed by alpha-synuclein and synphilin-1 are cytoprotective." J Biol Chem 279(6): 4625-31.

Tanji, K., T. Tanaka, et al. (2006). "NUB1 suppresses the formation of Lewy body-like inclusions by proteasomal degradation of synphilin-1." Am J Pathol 169(2): 553-65.

Taylor, K. S., J. A. Cook, et al. (2007). "Heterogeneity in male to female risk for Parkinson's disease." J Neurol Neurosurg Psychiatry 78(8): 905-6.

Terzioglu, M. and D. Galter (2008). "Parkinson's disease: genetic versus toxin-induced rodent models." Febs J 275(7): 1384-91.

Thornberry, N. A. (1998). "Caspases: key mediators of apoptosis." Chem Biol 5(5): R97-103.

Tian, Y. Y., C. J. Tang, et al. (2007). "Favorable effects of VEGF gene transfer on a rat model of Parkinson disease using adeno-associated viral vectors." Neurosci Lett 421(3): 239-44.

Tofaris, G. K., P. Garcia Reitbock, et al. (2006). "Pathological changes in dopaminergic nerve cells of the substantia nigra and olfactory bulb in mice transgenic for truncated human alpha-synuclein(1-120): implications for Lewy body disorders." J Neurosci 26(15): 3942-50.

Ulusoy, A., T. Bjorklund, et al. (2008). "In vivo gene delivery for development of mammalian models for Parkinson's disease." Exp Neurol 209(1): 89-100.

Ungerstedt, U. (1968). "6-Hydroxy-dopamine induced degeneration of central monoamine neurons." Eur J Pharmacol 5(1): 107-10.

Uversky, V. N. (2003). "A protein-chameleon: conformational plasticity of alpha-synuclein, a disordered protein involved in neurodegenerative disorders." J Biomol Struct Dyn 21(2): 211-34.

Valente, E. M., P. M. Abou-Sleiman, et al. (2004). "Hereditary early-onset Parkinson's disease caused by mutations in PINK1." Science 304(5674): 1158-60.

Vallet, P. G., R. Guntern, et al. (1992). "A comparative study of histological and immunohistochemical methods for neurofibrillary tangles and senile plaques in Alzheimer's disease." Acta Neuropathol 83(2): 170-8.

van Adel, B. A., C. Kostic, et al. (2003). "Delivery of ciliary neurotrophic factor via lentiviral-mediated transfer protects axotomized retinal ganglion cells for an extended period of time." Hum Gene Ther 14(2): 103-15.

van der Putten, H., K. H. Wiederhold, et al. (2000). "Neuropathology in mice expressing human alpha-synuclein." J Neurosci 20(16): 6021-9.

Verhagen, A. M., P. G. Ekert, et al. (2000). "Identification of DIABLO, a mammalian protein that promotes apoptosis by binding to and antagonizing IAP proteins." Cell 102(1): 43-53.

Verma, I. M. and M. D. Weitzman (2005). "Gene therapy: twenty-first century medicine." Annu Rev Biochem 74: 711-38.

Voges, D., P. Zwickl, et al. (1999). "The 26S proteasome: a molecular machine designed for controlled proteolysis." Annu Rev Biochem 68: 1015-68.

von Coelln, R., S. Kugler, et al. (2001). "Rescue from death but not from functional impairment: caspase inhibition protects dopaminergic cells against 6-hydroxydopamine-induced apoptosis but not against the loss of their terminals." J Neurochem 77(1): 263-73.

Wajant, H. (2003). "Death receptors." Essays Biochem 39: 53-71.

Wakabayashi, K., S. Engelender, et al. (2000). "Synphilin-1 is present in Lewy bodies in Parkinson's disease." Ann Neurol 47(4): 521-3.

Wallace, D. C. (1992). "Mitochondrial genetics: a paradigm for aging and degenerative diseases?" Science 256(5057): 628-32.
Walter, B. L. and J. L. Vitek (2004). "Surgical treatment for Parkinson's disease." Lancet Neurol 3(12): 719-28.
Wang, C. E., H. Zhou, et al. (2008). "Suppression of neuropil aggregates and neurological symptoms by an intracellular antibody implicates the cytoplasmic toxicity of mutant huntingtin." J Cell Biol 181(5): 803-16.
Wang, J. J., D. B. Niu, et al. (2005). "A tetracycline-regulatable adeno-associated virus vector for double-gene transfer." Neurosci Lett 378(2): 106-10.
Wang, J. J., T. Zhang, et al. (2006). "Doxycycline-regulated co-expression of GDNF and TH in PC12 cells." Neurosci Lett 401(1-2): 142-5.
Wang, X. S., S. Ponnazhagan, et al. (1995). "Rescue and replication signals of the adeno-associated virus 2 genome." J Mol Biol 250(5): 573-80.
Ward, C. D., R. C. Duvoisin, et al. (1983). "Parkinson's disease in 65 pairs of twins and in a set of quadruplets." Neurology 33(7): 815-24.
Warrick, J. M., H. Y. Chan, et al. (1999). "Suppression of polyglutamine-mediated neurodegeneration in Drosophila by the molecular chaperone HSP70." Nat Genet 23(4): 425-8.
Warrick, J. M., H. L. Paulson, et al. (1998). "Expanded polyglutamine protein forms nuclear inclusions and causes neural degeneration in Drosophila." Cell 93(6): 939-49.
Webb, J. L., B. Ravikumar, et al. (2003). "Alpha-Synuclein is degraded by both autophagy and the proteasome." J Biol Chem 278(27): 25009-13.
Weitzman, M. D., S. R. Kyostio, et al. (1994). "Adeno-associated virus (AAV) Rep proteins mediate complex formation between AAV DNA and its integration site in human DNA." Proc Natl Acad Sci U S A 91(13): 5808-12.
Whitesell, L., E. G. Mimnaugh, et al. (1994). "Inhibition of heat shock protein HSP90-pp60v-src heteroprotein complex formation by benzoquinone ansamycins: essential role for stress proteins in oncogenic transformation." Proc Natl Acad Sci U S A 91(18): 8324-8.
Wichmann, T. and M. R. DeLong (1993). "Pathophysiology of parkinsonian motor abnormalities." Adv Neurol 60: 53-61.
Wong, H. R., R. J. Mannix, et al. (1996). "The heat-shock response attenuates lipopolysaccharide-mediated apoptosis in cultured sheep pulmonary artery endothelial cells." Am J Respir Cell Mol Biol 15(6): 745-51.
Wong, L. F., G. S. Ralph, et al. (2005). "Lentiviral-mediated delivery of Bcl-2 or GDNF protects against excitotoxicity in the rat hippocampus." Mol Ther 11(1): 89-95.
Woo, Y. J., J. C. Zhang, et al. (2005). "One year transgene expression with adeno-associated virus cardiac gene transfer." Int J Cardiol 100(3): 421-6.
Wu, C. (1995). "Heat shock transcription factors: structure and regulation." Annu Rev Cell Dev Biol 11: 441-69.
Wyttenbach, A. (2004). "Role of heat shock proteins during polyglutamine neurodegeneration: mechanisms and hypothesis." J Mol Neurosci 23(1-2): 69-96.
Xia, H., Q. Mao, et al. (2004). "RNAi suppresses polyglutamine-induced neurodegeneration in a model of spinocerebellar ataxia." Nat Med 10(8): 816-20.
Yaguchi, T., S. Aida, et al. (2007). "Involvement of mortalin in cellular senescence from the perspective of its mitochondrial import, chaperone, and oxidative stress management functions." Ann N Y Acad Sci 1100: 306-11.
Yamamoto, A., M. L. Cremona, et al. (2006). "Autophagy-mediated clearance of huntingtin aggregates triggered by the insulin-signaling pathway." J Cell Biol 172(5): 719-31.
Yamamoto, A., J. J. Lucas, et al. (2000). "Reversal of neuropathology and motor dysfunction in a conditional model of Huntington's disease." Cell 101(1): 57-66.
Yang, J., X. Liu, et al. (1997). "Prevention of apoptosis by Bcl-2: release of cytochrome c from mitochondria blocked." Science 275(5303): 1129-32.
Yang, Y., R. S. Turner, et al. (1998). "The chaperone BiP/GRP78 binds to amyloid precursor protein and decreases Abeta40 and Abeta42 secretion." J Biol Chem 273(40): 25552-5.

Yant, S. R., A. Ehrhardt, et al. (2002). "Transposition from a gutless adeno-transposon vector stabilizes transgene expression in vivo." Nat Biotechnol 20(10): 999-1005.

Yoritaka, A., N. Hattori, et al. (1996). "Immunohistochemical detection of 4-hydroxynonenal protein adducts in Parkinson disease." Proc Natl Acad Sci U S A 93(7): 2696-701.

Young, J. C., J. M. Barral, et al. (2003). "More than folding: localized functions of cytosolic chaperones." Trends Biochem Sci 28(10): 541-7.

Yu, W. H., Y. Matsuoka, et al. (2008). "Increased dopaminergic neuron sensitivity to 1-methyl-4-phenyl-1,2,3,6-tetrahydropyridine (MPTP) in transgenic mice expressing mutant A53T alpha-synuclein." Neurochem Res 33(5): 902-11.

Zaarur, N., A. B. Meriin, et al. (2008). "Triggering aggresome formation. Dissecting aggresome-targeting and aggregation signals in synphilin 1." J Biol Chem 283(41): 27575-84.

Zaiss, A. K. and D. A. Muruve (2008). "Immunity to adeno-associated virus vectors in animals and humans: a continued challenge." Gene Ther 15(11): 808-16.

Zarranz, J. J., J. Alegre, et al. (2004). "The new mutation, E46K, of alpha-synuclein causes Parkinson and Lewy body dementia." Ann Neurol 55(2): 164-73.

Zhou, H., S. H. Li, et al. (2001). "Chaperone suppression of cellular toxicity of huntingtin is independent of polyglutamine aggregation." J Biol Chem 276(51): 48417-24.

Zhou, P., N. Fernandes, et al. (2003). "ErbB2 degradation mediated by the co-chaperone protein CHIP." J Biol Chem 278(16): 13829-37.

Zhou, X. and N. Muzyczka (1998). "In vitro packaging of adeno-associated virus DNA." J Virol 72(4): 3241-7.

Zhu, Z. H., S. S. Chen, et al. (1990). "Phenotypic mixing between human immunodeficiency virus and vesicular stomatitis virus or herpes simplex virus." J Acquir Immune Defic Syndr 3(3): 215-9.

Zou, H., Y. Li, et al. (1999). "An APAF-1.cytochrome c multimeric complex is a functional apoptosome that activates procaspase-9." J Biol Chem 274(17): 11549-56.

Zou, J., Y. Guo, et al. (1998). "Repression of heat shock transcription factor HSF1 activation by HSP90 (HSP90 complex) that forms a stress-sensitive complex with HSF1." Cell 94(4): 471-80.

Zu, T., L. A. Duvick, et al. (2004). "Recovery from polyglutamine-induced neurodegeneration in conditional SCA1 transgenic mice." J Neurosci 24(40): 8853-61.

Zufferey, R., D. Nagy, et al. (1997). "Multiply attenuated lentiviral vector achieves efficient gene delivery in vivo." Nat Biotechnol 15(9): 871-5.

7. Appendix

7.1. Acknowledgements

I would like to thank all people who have supported me during the work on the PhD thesis.
Sincere thanks are given to Prof. Dr. Jörg B. Schulz, for his support, for closely following my progress on the project and for giving me the opportunity to work in his laboratory.
I am deeply grateful to my advisor Dr. Björn H. Falkenburger for his excellent supervision, for his strong support and encouragement, and for guiding me through all scientific challenges.
I would also like to thank Prof. Dr. Olaf Riess for agreeing to be the co-referee of my thesis.

Many thanks to…
… Dr. Björn H. Falkenburger and Dr. Felipe Opazo for letting me take part in the α-synuclein cell culture project.
… all my colleagues and friends in the laboratories in Waldweg in Göttingen and at the Hertie-Institute in Tübingen, especially to Dr. Ellen Gerhardt, Anja Drinkut, Dr. Felipe Opazo, Ute Neef, Caroline Herrmann, Sabine Kautzmann, Ana Pekanovic, and Christopher Spering for sharing their knowledge, for their friendship and honesty, for their care, their helping hands and open hearts, for constructive criticism and for just making my time in the lab.
… Ute Neef, Kirsten Fladung and Annette Bennemann for excellent technical help.
… Dr. S. Kügler and Dr. U. Naumann for providing AAV, respectively AdV-Hsp70 viral vector preparations.
… to Prof. Dr. P. Kahle (Hertie-Institut for Clinical Brain Researchf, Tübingen) for providing us with the A30PαSyn mouse line.
… Dr. Silke Nuber for teaching me to perform the PK-PET blot technique.
… the German Research Council (DFG) through the DFGResearch Center for Molecular Physiology of the Brain (CMPB), the Fortüne program (Medical Faculty, University of Tübingen) and the NGNF2 program of the Federal Ministry of Education and Research (BMBF) for funding this study.
… my dear friends Nicole, Tobi, Bianca, Marc, Steffi, Karsten, Ina, Carla and Alex for always being there, for believing in me and supporting me.

Thanks to all my family, my sister and her family, my parents in law and especially to my parents for their unconditional love and support and continuous encouragement.

Finally, I want to thank Björn for all the love and encouragement he gives to me. Thanks for your patients, for being with me and for sharing wonderful and bad moments with me.

7.2. Publications

Krenz, A., Falkenburger, B. H. Gerhardt, E., Drinkut, A., Schulz, J. B. (2009). "Aggregate formation and toxicity by wild-type and R621C synphilin-1 in the nigrostriatal system of mice using adenoviral vectors." J Neurochem 108(1): 139-46.

Opazo, F., **Krenz, A.**, Herrmann, S., Schulz, J. B., Falkenburger, B. H. (2008) “Accumulation and clearance of alpha-synuclein aggregates demonstrated by time-lapse imaging.” J Neurochem 106(2): 529-40

7.3. Abstracts/Posters

Antje Elstner, Björn H. Falkenburger, Jörg B. Schulz (2004): Molecular chaperone Hsp70 inhibits MPP^+ induced toxicity in neuroblastoma cells. *Society for Neuroscience Abstract 1013.8*

Antje Elstner, Björn H. Falkenburger, Jörg B. Schulz (2005): Chaperon-Therapie in Modellen der Parkinson-Krankheit. *Colloquium at Department of General Neurology, Center of Neurology and Hertie institute for clinical brain research, University of Tübingen and the fortüne program (Medical faculty at the University of Tuebingen)*

Antje Elstner, Björn H. Falkenburger, Jörg B. Schulz (2005): Synphilin-1 induced formation of PK-resistant alpha-synuclein inclusions in a mouse model Parkinson’s disease. *Proceedings FENS/Hertie Winter School in Kitzbühel*, *Austria,* 11-18.12.2005.

Antje Krenz, Björn H. Falkenburger, Jörg B. Schulz (2008): Aggregate Formation and Toxicity of WT and R621C Synphilin-1 *in vivo*. *4th training course of the Neurortrain project (Neuroscience training in Europe of the Federation of European Neuroscience Societies), Innsbruck, Ausstria,* 1-8.06.2008

Antje Krenz, Björn H. Falkenburger, Jörg B. Schulz (2008): Aggregate Formation and Toxicity of WT and R621C Synphilin-1 *in vivo*. *FENS Abstr., vol.4, 218.37, 2008, 6th Forum of European Neuroscience (FENS), Geneva, Switzerland*, 12-16.07.2008

Curriculum vitae

Personal details

Name:	Antje Krenz, née Elstner
Date of Birth:	October 11th 1977
Place of Birth:	Heilbad Heilgenstadt, Germany
Nationality:	German

Education

1998	General qualification of university entrance ("Abitur"), Berufliches Gymnasium Witzenhausen, Germany Main subject: Biotechnology, minor subjects: Chemistry, German
1998 - 2004	Undergraduate student at the University of Stuttgart
2004	Diploma, University of Stuttgart, Germany, Technical Biology Main subject: experimental biology, field: molecular biology (Exam: cell biology), Minor subjects: Microbiology, Genetics Thesis: Recombinant Akt expression in primary cortical neurons for induction of TNF mediated neuroprotective effects and expression analysis of NMDA receptor subunits
2004 – 2007	PhD student in the Department of Neurodegeneration and Restorative Research, DFG Center for Molecular Physiology of the Brain, supervised by Prof. Dr. J.B. Schulz and Dr. B.H. Falkenburger
2009	PhD thesis: The pathological role of synphilin-1 and the therapeutic potential of Hsp70 in models of Parkinson's disease using viral vectors